

**Holocene benthic foraminiferal assemblages from the SW Pacific:
implications for a high resolution.**

Diploma Thesis
at Aachen Technical University.

Completed at GEOMAR – Research Center for Marine Geosciences
of the Christian-Albrechts-University of Kiel.

Submitted by Sascha Überall

Kiel, April 2000

sueberall@geomar.de

ABSTRACT

The ocean between Australia / New Zealand and Antarctica is the major gateway for water mass exchange between the Indian and the Pacific Oceans. Thus, it is a key region of global oceanic circulation. As part of the paleoceanographical project TASQWA, this thesis presents a high-resolution study and interpretation of the Holocene oceanographic and ecological variability of this area. The investigation concentrates on the abundance and faunal association of deep-sea benthic foraminifera.

Short sediment cores were taken along two transects (South Tasman Rise and eastern Campbell Plateau) covering different water depths and water masses. The almost undisturbed sediments were continuously investigated in 1 cm intervals. The sediment record represents the entire Holocene period and is correlated to distinct climatic changes. However, evidence for erosional events and redepositional sedimentation is present.

Multiple environmental factors are reflected by the investigated foraminiferal assemblages:

- Early diagenesis diminishes the abundance of certain arenaceous species in the uppermost cm of the sediment.
- Variations of nutrient flux have the major impact on the living fauna. *Fursenkonia contemplata* indicates high productivity at the South Tasman Rise, lasting until ~7500 years before present. The enhanced productivity might reflect the position of the Subtropical Front.
- A correlation between climatic changes (indicated by planktic $\delta^{18}\text{O}$ isotope ratios) and benthic foraminifera species is described: *Uvigerina peregrina* is abundant in phases of warmer climate, *Melonis pompilioides* prefers phases of colder climate.
- Several distinct benthic foraminiferal assemblages, associated with certain water masses as published elsewhere, were found and described. A *Nuttalides umboinifer* association indicates strong influence of Antarctic Bottom Water (AABW). A *Globocassidolina subglobosa* association is described in samples recently bathed in the Circumpolar Deep Water (CPDW).

The variability in benthic foraminiferal assemblages indicates a change in bathymetric position of deep and bottom water masses:

The decreasing influence of the *N. umboinifer* association evolves into an abrupt change to the *G. subglobosa* association at the eastern Campbell Plateau at ~8000 years before present. This pattern is interpreted as a deepening of the water masses.

The trend of the faunal associations at the South Tasman Rise is reverse: the influence of the *N. umboinifer* association increases throughout the last ~7500 years before present, while the significance of the *G. subglobosa* association decreases. A shallowing of the water mass body structure is assumed.

KURZFASSUNG

Eine Schlüsselstelle globaler ozeanischer Zirkulation und für den Austausch von Wassermassen zwischen dem Indischen und Pazifischen Ozean liegt zwischen Australien und Neuseeland. Im Rahmen des paleoceanographischen TASQWA Projektes detailliert diese Arbeit hochauflösend die ozeanographischen und ökologischen Variationen im Holozän dieses Gebietes. Die Untersuchungen konzentrieren sich auf Häufigkeit und Zusammensetzung benthischer Foraminiferenvergesellschaftungen. Kurze Sedimentkerne wurden entlang zweier longitudinaler Profile (South Tasman Rise und östliches Campbell Plateau) aus verschiedenen Wassertiefen genommen. Obgleich Anzeichen für Schichtlücken und Erosion vorhanden sind, ist in den Sedimenten die Klimgeschichte des Holozäns kontinuierlich dokumentiert.

Variationen in den Artengemeinschaften benthischer Foraminiferen spiegeln die Einflüsse vielfältiger Umweltparameter wider:

- Frühdiagenetische Prozesse vermindern die Anzahl agglutinierender Foraminiferen in den obersten cm der Sedimentsäule.
- Die Zufuhr von Nährstoffen ist der wichtigste regulierende Faktor für die benthische Fauna. Das Vorkommen von *Fursenkonia contemplata* zeigt hohe Produktivität am South Tasman Rise bis ~7500 Jahren vor heute an.
- Eine Korrelation zwischen Klimaschwankungen und benthischer Fauna wird beschrieben. Die Häufigkeit von *Uvigerina peregrina* korreliert mit wärmerem Klima; die Häufigkeit von *Melonis pompilioides* zeigt einen gegenläufigen Trend.
- Das Vorkommen bestimmter Faunenassoziationen in Verbindung mit den Eigenschaften von Wassermassen wurde in früheren Studien beschrieben, und kann im Untersuchungsgebiet beobachtet werden. Eine *Nuttalides umbonifer* Vergesellschaftung zeigt Einfluss des Antarctic Bottom Water (AABW) an. Eine *Globocassidolina subglobosa* Vergesellschaftung kommt häufig im Bereich des Circumpolar Deep Water (CPDW) vor.

Die Änderungen in der Vergesellschaftung benthischer Foraminiferen zeigen Änderungen in der Verteilung der Tiefenwassermassen an:

Abnehmender Einfluss der *N. umbonifer* Vergesellschaftung wird am östlichen Campbell Plateau von zunehmendem Einfluss der *G. subglobosa* Vergesellschaftung begleitet. Eine Absenkung der Tiefenwassermassen seit ~8000 Jahren vor heute wird angezeigt.

Ein umgekehrter Trend ist am Süd Tasman Rücken zu beobachten: Der Einfluss der *N. umbonifer* Vergesellschaftung nimmt seit ~7500 Jahren vor heute zu. Die Bedeutung der *G. subglobosa* Vergesellschaftung nimmt ab. Ein Ansteigen der Wassermassen wird angezeigt.

Table of contents	page
--------------------------	-------------

1 INTRODUCTION	
1.1 The TASQWA project and objectives of this study	1
1.2 Previous studies	2
2 OCEANOGRAPHIC SETTINGS	4
3 METHODS AND MATERIAL	
3.1 Shipboard data	
3.1.1 Core locations	7
3.1.2 Coring methods	9
3.1.3 Visual core descriptions	9
3.2 Laboratory methods	
3.2.1 Sampling	9
3.2.2 Physical and physicochemical sediment properties	11
3.2.3 $\delta^{18}\text{O}$ and $\delta^{13}\text{C}$ stable isotope ratios, AMS ^{14}C radiocarbon dating	14
3.2.4 Analysis of benthic foraminiferal assemblages and data processing	16
4 RESULTS	
4.1 Cores from the eastern Campbell Plateau	
4.1.1 Physical and physicochemical sediment properties	18
4.1.2 $\delta^{18}\text{O}$ and $\delta^{13}\text{C}$ stable isotope ratios	25
4.1.3 Analysis of benthic foraminiferal assemblages	29
4.2 Cores from the South Tasman Rise	
4.2.1 Physical and physicochemical sediment properties	33
4.2.2 $\delta^{18}\text{O}$ and $\delta^{13}\text{C}$ stable isotope ratios, AMS ^{14}C radiocarbon dating	40
4.2.3 Analysis of benthic foraminiferal assemblages	46

Table of contents	page
--------------------------	-------------

5 DISCUSSION

5.1 Age model

5.1.1 General notes on the measured $\delta^{18}\text{O}$ stable isotope ratios	52
5.1.2 Core-correlation based on AMS ages	53
5.1.3 Correlation of Holocene climate changes	54
5.1.4 Erosional events and / or hiatuses at the South Tasman Rise	57

5.2 Benthic foraminiferal associations

5.2.1 Potential fossil associations	59
5.2.2 Cores from the eastern Campbell Plateau	62
5.2.3 Cores from the South Tasman Rise	68
5.2.4 Correlations of benthic fauna and Holocene climate changes	74
5.2.5 Definition of benthic foraminiferal associations	76

5.3 Paleoceanographical interpretation

5.3.1 Eastern Campbell Plateau	78
5.3.2 South Tasman Rise	79

5.4 Suggestions for further investigation

81

6 CONCLUSIONS

82

ACKNOWLEDGEMENTS

REFERENCES

ZUSAMMENFASSUNG IN DEUTSCH

Table of contents**page****APPENDIX**

A1	Taxonomy of benthic foraminifera species from the research area	I
A2	SEM photos of selected foraminiferal specimens	IX
A3	Paleontological data set	XII
A4	Data set of Q-mode Factor Analysis	XXVIII
A5	Data set of physical and physicochemical sediment properties	XL
A6	AMS ^{14}C radiocarbon data	XLV
A7	Photos of each core	XLVII
A8	Visual core descriptions	XLVIII
A9	Data CD	

1 INTRODUCTION

1.1 The TASQWA project and the objectives of this study

Benthic foraminifera are ubiquitous throughout the oceans. The reflection of distinct environmental settings by the abundance of certain species or species associations is commonly used for paleoceanographical interpretations. However, the indication of environmental settings is in many cases not transferable to other locations and periods. The ecology of benthic foraminifera reveals to be complex and cannot be generally described by a single or a few environmental parameters.

The objectives of the project TASQWA –Quaternary Variability of Water Masses in the Southern Tasman Sea and the Southern Ocean (SW Pacific Sector)- are to reconstruct the late Quaternary paleoceanographical variabilities of the SW Pacific and the southern Tasman Sea. The research area between Australia and New Zealand is the major gateway for water mass exchange and energy transfer between the Indian and the Pacific Ocean. Thus it is an essential location of global oceanic circulation, and the results of the project will be interpreted in the context of global climate changes.

This thesis describes the environmental variabilities of the entire Holocene period in the research area. Sediment samples from box cores taken of different water depths and water masses were investigated in high resolution (Fig. 3.1, Table 3.1, p. 7 and Fig. 2, p. 8). The investigation concentrates on species distribution and abundance of benthic foraminifera. Multivariate statistics are used to determine species or groups of species, which reflect the recent and subrecent environmental settings, i.e. the bottom water and pore water oxygen conditions, intensity of current and variability of primary production. Additionally, the physical and chemical sediment properties are used to support the investigations and interpretations. For stratigraphical purposes $\delta^{18}\text{O}$ and $\delta^{13}\text{C}$ isotope ratios and AMS ^{14}C radiocarbon ages are employed.

Aim of this thesis is to continuously document the Holocene variabilities of the benthic foraminiferal fauna at two locations and to correlate these with the recent and subrecent environmental settings, including paleoceanographical and paleoclimatological interpretations. Foraminiferal fauna associations will be defined, which reflect the recent and subrecent environmental and oceanographical settings. The defined standards will be used to calibrate the data from longer cores of this scarcely investigated area (Rüggeberg and Nees, 2000).

1.2 Previous studies

Paleoceanography of the research area:

On cruises of the USNS ELTANIN, South and West of New Zealand and Australia during the years 1965 to 1972 cores with a total length of over 2000 m were taken during the most extensive and systematic coring project in this region. Paleomagnetic and micropaleontological dating revealed the existence of hiatuses in the last 2.5 million years (Watkins and Kennett, 1976). In 1985 during the RV GLOMAR CHALLENGER cruise four holes were drilled on the South Tasman Rise in the current of the Deep-Sea Drilling Program (DSDP, Leg 29). In the same year the RV SONNE (SO36) visited the southern Tasman Plateau and off West Tasmania, where cores were taken for geophysical and geochemical studies (Hinz and party, 1985). During the cruise of the RV MARION DUFRENSE in 1988 short and long sediment cores were taken South of Tasmania. In 1994 the Australian Geological Survey Organisation (AGSO) undertook an expedition with the French R.V. L'ATALANTE (*Tasmanie* Cruise). Seismic investigations and a survey of the ocean floor on the western and southern side of Tasmania were done by means of Swath-Mapping and underway geophysics (Exon et al., 1994). Also in 1994 the Australian RV FRANKLIN went to the South Tasman Rise to retrieve several short sediment cores for paleoceanographical investigations. One year later numerous box cores and dredge samples were retrieved at the South Tasman Rise by researchers on board of the Australian RV RIG SEISMIC (Exon et al., 1995). On the research cruise of the RV MARION DUFRESNE (MD106) during the IMAGES III IPHIS expedition in 1997, sediment cores were taken from the South Tasman Rise. Paleoceanographic changes of the last 200,000 years were documented by investigation of the diatom and benthic foraminiferal record (Nees et al., 1999). Since only a few paleoceanographic studies have been conducted so far, further investigation by the project TASQWA will be done to fill this knowledge gap.

Studies on Holocene benthic foraminifera:

The reflection of specific oceanographic changes in the distribution of benthic foraminifera in sediment cores is described by e.g. Alavi (1988), Clark et al. (1994), Douglas and Woodruff (1981a, b), Harloff and Mackensen (1997), Mackensen (1990, 1992, 1997); Schnitker (1980), Streeter (1973) and Streeter and Lavery (1979). A review of the use of benthic foraminifera for paleoceanographical purposes is given by Corliss et al. (1986).

The relation of benthic foraminiferal abundance patterns to surface productivity is described for the equatorial Pacific in Herguera (1992). At oceanographic fronts the significantly increased sea-surface productivity leads to an important downward nutrient flux to deeper water

layers, which has been described by Altenbach and Sarnthein (1989), Loubere (1995, 1997) and Yoder et al. (1994). The abundance of benthic foraminifera is directly affected by the elevated supply of organic matter. To describe this process Graf (1989a, b) defined the term of "pelagic – benthic coupling". Van der Zwaan et al. (1999) presents a review of the use of benthic foraminifera for paleoceanographical means. Here the dependence of benthic foraminifera on nutrient fluxes rather than on water mass properties is emphasised. Especially infaunal foraminifera species are dependent on microhabitat preferences, as described by e.g. Corliss (1985), Jorissen et al. (1998) and are not directly influenced by conservative water mass properties. However, Mackensen (1992) and Schnitker (1994) concluded by the analysis of associations from the North and South Atlantic, that on the one hand benthic foraminifera are unequivocal indicators of productivity in areas of high productivity. On the other hand, benthic foraminiferal associations reveal the imprint of deep-water mass structures in areas of uniform productivity.

The effects of early diagenesis on agglutinating and certain calcareous species is described by e.g. Mackensen et al. (1990, 1993). Kuhnt et al. (1996) presents a review of the ecology of agglutinating foraminifera species. Corliss and Honjo (1981) give an experimental study on the effect of dissolution of calcium carbonate on foraminifera tests.

Studies on benthic foraminifera of the research area:

Only a few investigations based on interpretation of deep-sea benthic foraminiferal assemblages have been published from the research area. Examples are the qualitative reconstructions of paleoproduction of the Southern Tasman Sea by Corliss (1979a, b, c), Nees (1994, 1997) and Nees et al. (1999). Variabilities of oceanic productivity, exchange patterns of intermediate and deep-water masses, variabilities of bottom currents and oceanic frontal systems are reconstructed in these studies. The relation of species associations to distinct water masses in the vicinity of the research area is described by Corliss (1978a, b, 1982), Gupta (1994) and Mackensen (1990). Fenner et al. (1992) investigated planktic and benthic foraminifera in Holocene samples from the Chatham Rise, East of New Zealand.

Most of the studies on benthic foraminifera mentioned above are based on investigations of longer cores or on the analysis of surface samples for recent foraminifera. No studies on benthic foraminifera have been published covering the entire Holocene period of the research area in appropriate resolution. In this thesis a continuous documentation of the Holocene paleoceanographical situation and the variability of foraminifera fauna in the research area is presented.

2 OCEANOGRAPHIC SETTINGS

Surface Oceanography:

The surface oceanography of the SW Pacific and the southern Tasman Sea is characterised by the Antarctic Circumpolar Current (ACC) which connects all oceans of the Southern Hemisphere by its clockwise circulation. Here large portions of specific water masses flow from the main global ocean basins southward across the ACC. Thus deep waters, which originate from farther north enter the subpolar regime and mix with the Antarctic shelf waters. Due to the barotropic nature of the ACC, currents extend to a greater depth.

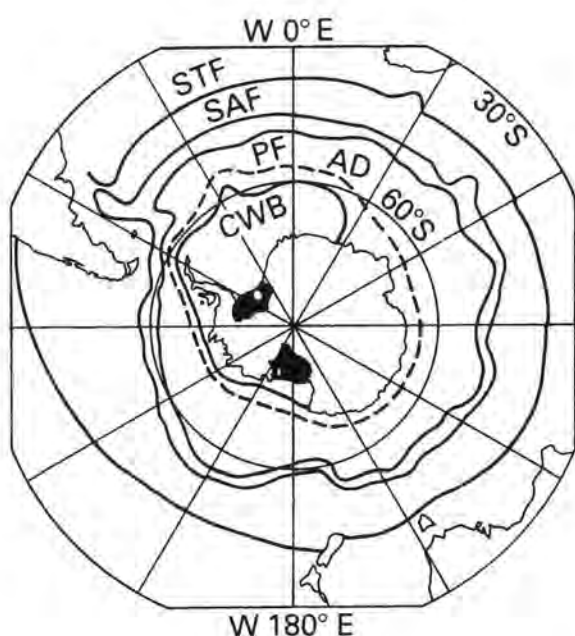


Figure 2.1 Convergences and divergences of the Southern Ocean. STF: Subtropical Front, SAF: Subantarctic Front, PF (Antarctic): Polar Front, AD: Antarctic Divergence (dashed line), CBW: Continental Water Boundary. The dark regions indicate the Weddell and Ross Sea ice sheets (Tomczak and Godfrey, 1994).

Two deep reaching major oceanic fronts occur in the ACC in the research area, as originally defined by Deacon (1937) and later by Emery and Meincke (1986) and Withworth (1980): The Polar Front (PF) and further North the Subantarctic Front (SAF). At the sharp delineated Polar Front the meeting of cold and warm waters leads to a sudden death of many planktic species. Later process leads to a higher flux of nutrients to the ocean floor. The protozoa of the mixing zone use the higher content of nutrients in the colder southern waters for enhanced primary production, which also leads to increased carbon fluxes to the sea floor. The southernmost extend of the warmer, high salinity (35.7 – 35.8) and nutrient poor waters of the Subtropical Surface Water (SASW) is defined by the Subtropical Front (STF), extending along 45° S (Garner, 1959; Hoffmann, 1985) (see Figs. 2.1 and 3.2, p. 8). The boundary follows the 15° C summer isotherm, the 10° C winter isotherm and the 34.7 – 34.8 salinity isoplethe (Garner, 1959). At the southern Campbell Plateau the SAF is forced in its direction by bathymetrical circumstances: the eastward flowing ACC is deflected northward by passing the southern edge

of the Campbell Plateau, forming a large permanent loop and continues eastward along the eastern slope of the Campbell Plateau (Bradford-Grieve et al., 1991; Gordon, 1972; Nees et al., 1999; Orsi et al., 1995), as outlined in Figure 3.2, p.8. Carter et al. (1996) proposes sediment transport by these strong currents along the slope.

Late Quaternary movement of oceanic fronts:

The late Quaternary movement of oceanic fronts in glacial and interglacial oscillations is controversy discussed for the research area. Fenner et al. (1992) and Weaver et al. (1998) report a constant position of the STF during the late Quaternary. Contrarily the STF is reported to have moved equatorwards during glacial times and southwards from its recent position during intergalcials by Howard and Prell (1992), Weaver et al. (1998), Wells and Conell (1997) and Wells and Okada (1996). Weaver et al. (1997) and Wells and Okada (1996) report the SAF and the PF as shifting equatorwards in glacial intervals.

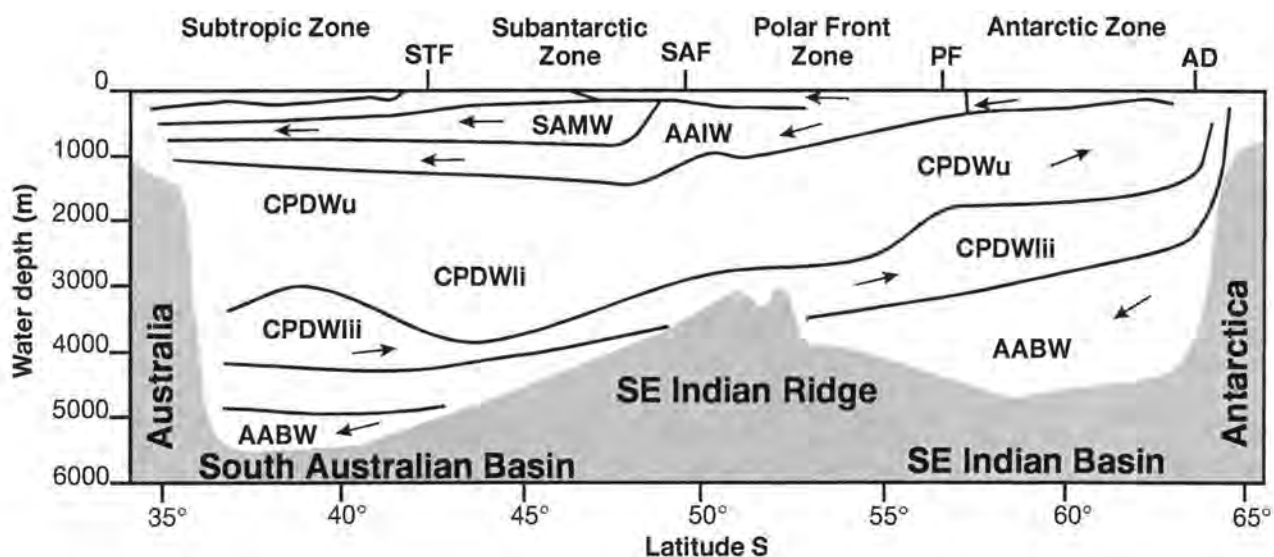


Fig. 2.2 Recent distribution of water masses and bathymetry in the Australian sector of the Southern Ocean at 135° E [after: Braatz and Corliss (1984), Dansie (1994), Gordon and Molinelli (1986), Orsi et al. (1995)].

STF:	Subtropic Front	SAMW:	South Australian Mode Water
SAF:	Subantarctic Front	AAIW:	Antarctic Intermediate Water
PF:	Polar Front	CPDWu:	Upper Circumpolar Deep Water
AD:	Antarctic Divergence	CPDWli:	Lower i Circumpolar Deep Water
		CPDWlii:	Lower ii Circumpolar Deep Water
		AABW:	Antarctic Bottom Water

Water masses:

Three different deep-water masses occur in the research area, besides various surface water masses: The Antarctic Intermediate Water (AAIW), the Circumpolar Deep Water (CPDW), and the Antarctic Bottom Water (AABW), as outlined in Fig. 2.2, p. 5. The physical properties of the specific water masses are given in Table 2.

The AAIW underlies various surface water masses, i.e. the Australian Subantarctic Water in the research area (see Fig. 3.2, p. 8). It is formed at about 55° to 60° S along the Polar Front and is forced to sink from ~600 to ~1450 m by downwelling.

The CPDW lies beneath the AAIW and flows northward. Due to differences in physical properties it is subdivided in Upper CPDW_u, Lower CPDW_{l1} and Lower CPDW_{l2}, which comprise the main body of CPDW flow (see Table 2). The CPDW is composed of ~45% Weddell Sea Water, 30% Pacific and Indian Ocean Intermediate Water and ~25% North Atlantic Deep Water (NADW).

The AABW originates in vertical convection along the Antarctic shelf from freezing of sea ice. The high salinity and cool water sinks and mixes with the ACC and NADW and flows northwards. It is, with few exceptions, the densest water in the ocean and thus sinks to the bottom of all great oceanic basins. Although the AABW mixes with the waters above along its path, its influence can be traced beyond the equator.

Table 2 Characteristics of major water masses of the research area, relevant for this study.

Water Mass	Abbr.	Depth (m)	Salinity	Temp. (°C)	Oxygen
Antarctic Intermediate Water	AAIW	600-1450	34.50-34.36	3.20-7.00	3.20-4.70
Circumpolar Deep Water (upper)	CPDW _u	1450-2900	34.67-34.71	1.60-1.80	3.03-3.45
Circumpolar Deep Water (lower i)	CPDW _{l1}	2900-3800	34.71-34.73	0.90-1.60	3.45-3.63
Circumpolar Deep Water (lower ii)	CPDW _{l2}	>3800	<34.71	0.55-0.90	4.70-4.80
North Atlantic Deep Water	NADW			← as for CPDW _{l2} →	
Antarctic Bottom Water*	AABW		34.66-34.69	-0.9-0.0	

*General term for cold northward flowing Antarctic waters

3 METHODS AND MATERIAL

3.1 Shipboard data

3.1.1 Core locations

Six cores were taken along two longitudinal transects at the eastern Campbell Plateau (~ NE to SW) and at the South Tasman Rise (~ N to S) from different water depths and water masses (see Figs. 3.1 and 3.2, p. 8, Table 3). The STF is cut perpendicular by a longitudinal transect, which is set by the three investigated cores from the South Tasman Rise. The SAF is cut by the longitudinal transect, set by the cores from the margin of the eastern Campbell Plateau.

Table 3 Core locations and data.

Core	Sampled depth (cm bsf)	Water-depth (m)	Latitude S	Longitude E	Station
<i>Campbell Plateau</i>					
SO136-019BX	0 – 36	4530	50°51.12'	176°53.18'	3
SO136-025BX	0 – 12	3440	50°38.99'	176°22.56'	4
SO136-037BX	0 – 19	1362	50°13.51'	175°19.07'	6
<i>South Tasman Rise</i>					
SO136-147BX	0 – 12	2175	48°30.13'	149°06.77'	30
SO136-161BX	0 – 27	3685	46°33.13'	149°04.88'	33
SO136-165BX	0 – 26	4060	45°17.84'	147°55.13'	35

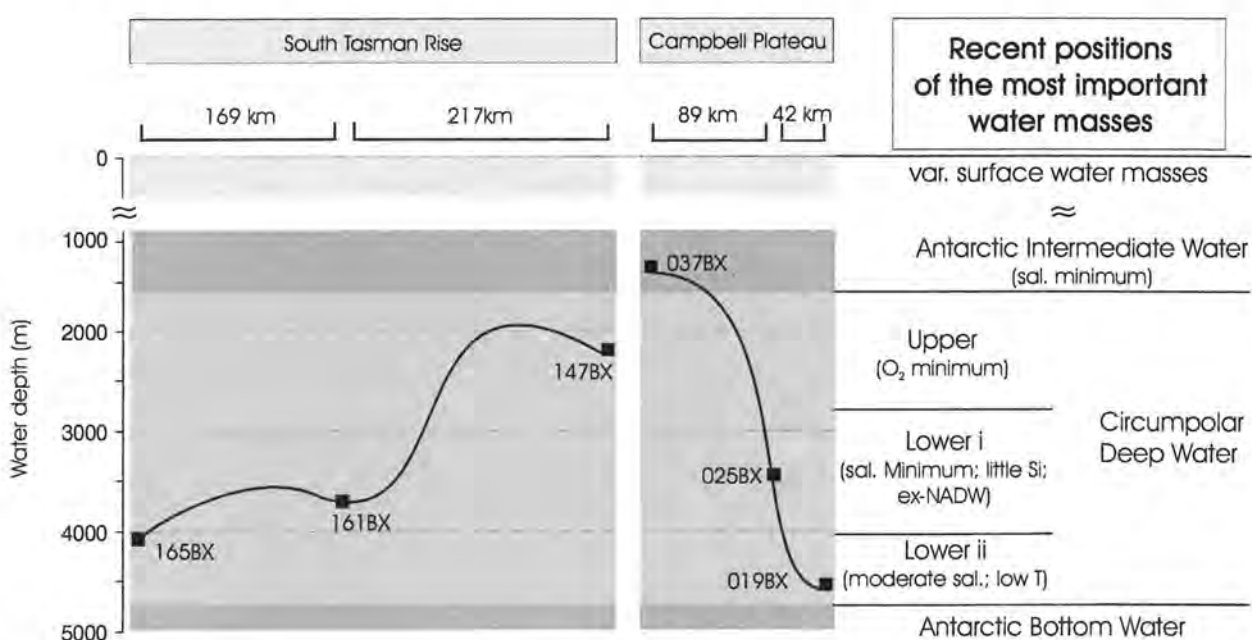


Fig. 3.1 The relative positions of the investigated sediment cores plotted versus water depth and the potential subsurface water masses, as listed in Table 2, p 6. The black line shows bathymetry (after: Scientific shipboard party: FS SONNE CRUISE REPORT SO 136, 1999).

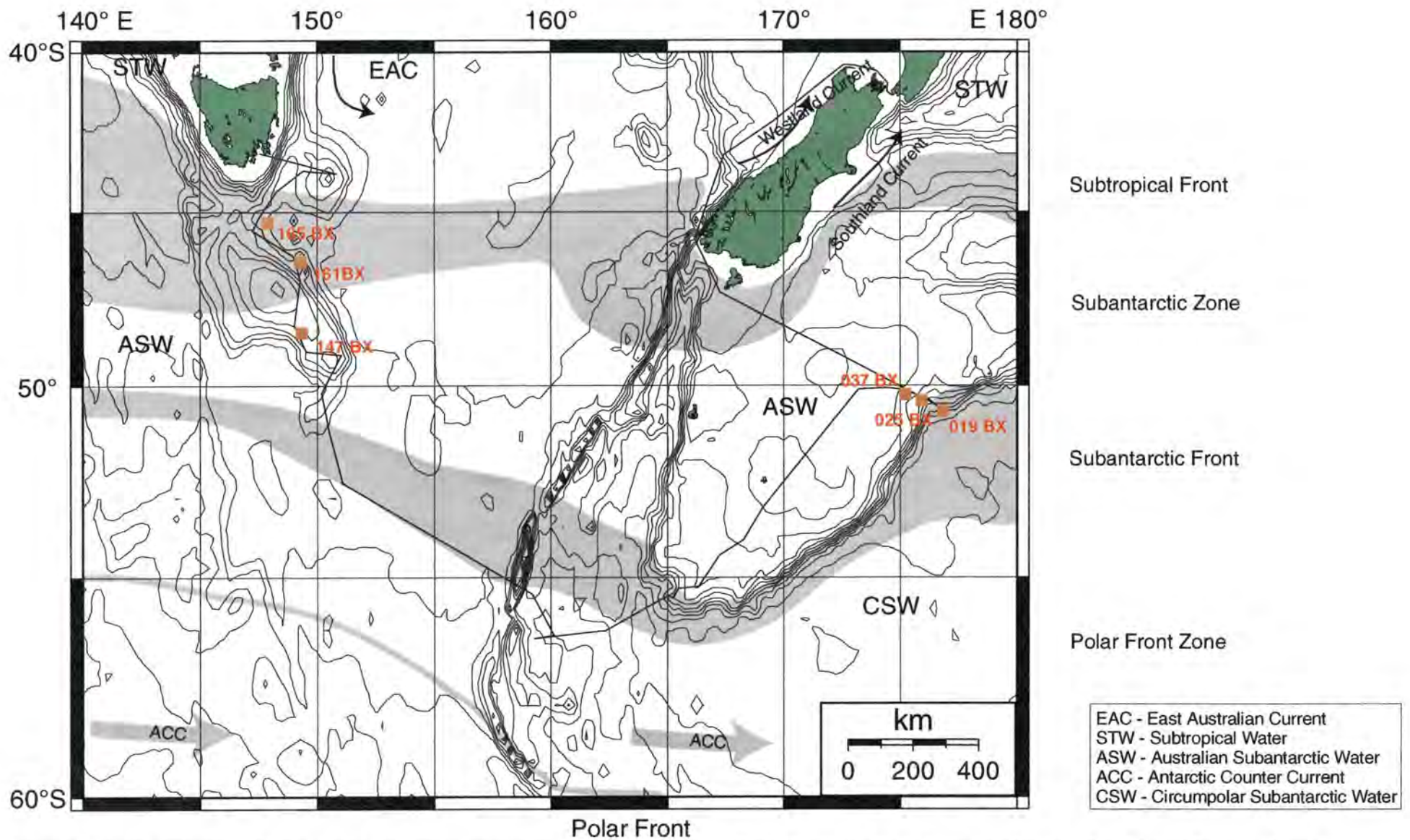


Figure 3.2 Core locations, bathymetry and surface oceanography of the research area. Shaded areas indicate the seasonal range of position of fronts and zones. Black squares mark core locations (after: Shipboard scientific party: FS SONNE CRUISE REPORT SO136, 1999). The frontal structure is taken from Orsi et al. (1995), and Belkin and Gordon (1996). The annual average position of the Subantarctic Front and Polar Front along 146°E longitude were reported further north by 6° and 4° respectively(Rintoul et al., 1997). Bathymetric follows ETOPO 5 (see references).)

EAC - East Australian Current
 STW - Subtropical Water
 ASW - Australian Subantarctic Water
 ACC - Antarctic Counter Current
 CSW - Circumpolar Subantarctic Water

3.1.2 Coring methods

All cores were taken with a box-core with an inner size of 50 x 50 x 50 centimetres; this enabled us to obtain almost undisturbed sediment. Plastic archive boxes were pushed from the side into the sediment of the opened box core to avoid shortening of a sediment core while sampling from the surface (see Photo 3[S.0.1]).



Photo 3 Sampling of box-core SO136-019BX on board. The arrow marks the position of the switch between the archive boxes at 25.5 cm bsf (see Chapter 4.1.1, p.18).

3.1.3 Visual core description

Core descriptions were done on board by Dr. J.J.G. Reimer (JR) and S. Roth (SR), GEOMAR, using the ODP (Ocean Drilling Program) visual core description forms for a systematic description of lithology, grain size, sedimentary structures and visual colour determination (via Munsell Colour Chart). The core description and photos are given in appendix A7, p. XLVII.

3.1 Laboratory methods

3.2.1 Sampling

A total of 136 samples was taken throughout six box-cores, listed in Table 3, p. 7. Every centimeter was sampled from top to bottom of each core. The sediment in the archive box was divided in two halves and cut in centimetre slices, using a spatula. The given sediment depth is the mean between upper and lower depth of the sampled slice (see inlet in Fig. 3.3, following page). All samples were collected in 100 ml NUNC plastic jars. The samples were prepared for further analysis (see Fig. 3.3, following page).

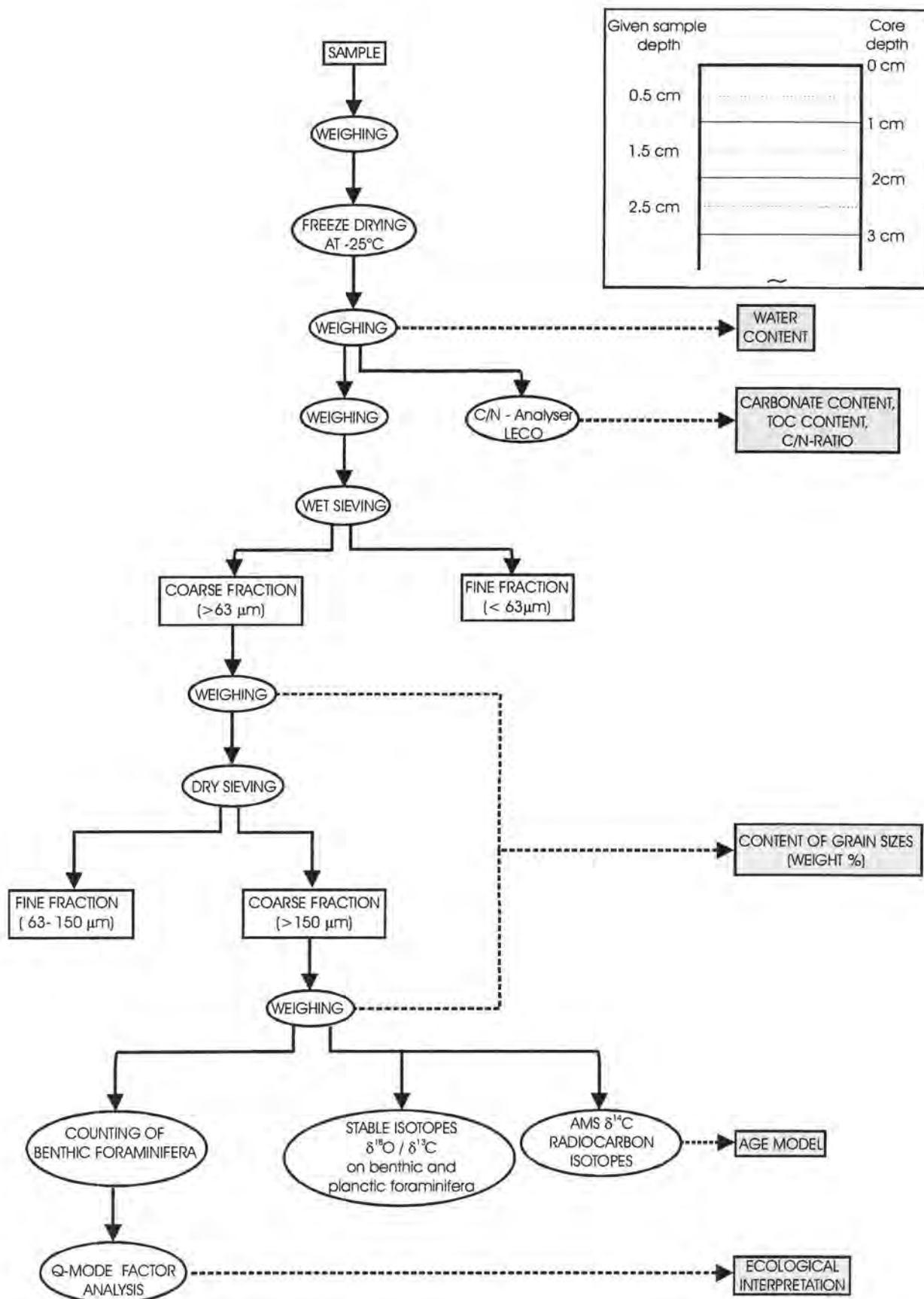


Figure 3.3 Sample processing.

In this scheme every single step of the laboratory preparation is given.

The figure in the inlet illustrates the position of the given sample depth in each sample slice.

3.2.2 Physical and physicochemical sediment properties

Water content:

Water content of each sample is calculated after Holler (1995) by subtracting the weight of the freeze-dried sample (at -25°C) from the weight of the wet sample. For salt-correction, the corresponding salinity values of the CTD - measurements from the TASQWA Cruise Report SO136 were used:

$$W = [(M_t - M_d) / (1 + r)] \cdot 100 \% \quad (1)$$

with: W = water content

M_t = weight of dry sample

M_d = weight of wet sample

r = salinity

Grain size distribution:

The samples were carefully washed through a 63 µm sieve for analysis of the grain size distribution. The fine fraction was collected in 5 l jars for further analysis. The coarse fraction was dried (at 50°C) and weighed. Afterwards the coarse fraction was dry sieved through a 150 µm sieve and the > 150µm subfraction was weighed again.

Dry bulk density:

Dry bulk density (DBD) was calculated after Holler (1995) by:

$$DBD = M_t / [(M_d - M_f) / 1.025 \text{ (g/cm}^3\text{)} 100\% / W] \quad (2)$$

with: 1.025 g/cm³ as density of seawater

Spectrophotometry:

For colour determination a Minolta CM 2002 spectral photometer was used, as described in Nagao and Nakashima (1992) and in Barranco et al. (1989). The sediments of all cores were scanned in original condition and only covered with clear plastic foil. The cores from the eastern Campbell Plateau (SO136-019BX, -025BX and -037BX) were scanned during the cruise by N. Andresen, GEOMAR. The cores from the Southern Tasman Rise (SO136-147BX, -161BX and -165BX) were scanned in the laboratory by the author. For comparison the three cores from the Campbell Plateau were scanned additionally in the laboratory. No difference between the shipboard and the laboratory data was found.

C/N ratio, organic carbon and carbonate content:

The C/N ratio and total organic carbon content (TOC) were measured with a Carlo Erba NA-1500 Elemental Analyser at GEOMAR, Kiel. The analytical operation of the Carlo Erba is based on flash combustion. The stationary phase in the combustion column is composed of a porous layer of the oxidation catalyst chromium trioxide, which is overlying silvered cobaltous cobaltic oxide granules. The sample is combusted at 1050°C in a temporarily enriched atmosphere of oxygen. The combustion products (CO_2 , NO_x and H_2O) are swept through the combustion reactor into a second column, the reduction reactor. In this column the excess oxygen is removed and NO_x reduced to N_2 . The N_2 , CO_2 and H_2O are separated on a Parapak QS chromatographic column maintained at 54°C. Detection is by thermal conductivity.

For a representative measurement, 3 to 4 g of each freeze-dried sample were thoroughly crushed and homogenised in a mortar, and 0.003 to 0.007 g were selected for measurement. Each run consisted of 19 samples (double measurements), four blank positions, one position of Acetanilide (as the National Bureau of Standards certified standard reference) and five positions of soil standard, which are taken from the same source throughout all measurements. Linear regressions of carbon and nitrogen versus area counts were computed (least-squares method) to evaluate the variations of each run.

In a first run the total carbon (TC) and total nitrogen content (TN) were measured. TOC content was measured in a second run, after in-situ dissolution of the samples carbonate content by addition of 15 % hydrochloric acid. The measured carbon is defined as TOC. The weight percentage (wt%) of inorganic carbon (calcium carbonate) is then calculated after Verardo et al. (1989) by:

$$\text{CaCO}_3 = 8.33 * (\text{TC} - \text{TOC}) \quad (3)$$

A total of 788 measurements were made for 134 samples (304 for TC/TN and 484 for TOC). The relative precision of the Carlo Erba is given in Verardo et al. (1989) as $\pm 0.3\%$ for organic carbon and $\pm 1.6\%$ for nitrogen. Samples that exceeded the standard deviation were measured again. The absolute detection limit is given as 0.62 µg carbon (Verardo et al., 1989).

In the runs for TC and TN 18 measurements required second measuring, in the runs for TOC (after treatment with acid) 108 measurements required second measuring. The main cause for the observed variations is probably loss of sample material due to microscopic explosions in the sediment during *in situ* treatment with acid. Drift of the analyser and the very low content of TOC in the samples (which is in the range of the relative precision) may be an additional source for analytical errors.

Double measurements:

Results of 12 samples did not show any trend out of up to six double-measurements. These samples and the core SO136-147BX were additionally measured with an LECO®-CS 125 infrared analyser at GEOMAR, Kiel. The LECO® burns 20 to 30 mg of the homogenised and freeze-dried sample in a high-frequency induction furnace. Carbon is oxidised to CO₂ and CO. In a catalyst furnace CO is oxidised to CO₂ and the entire CO₂ content is measured by absorption through an infrared cell. TOC and Carbonate content are determined by the same calculations as with the C/N-Analyser. Wolf (1991) calculated a variance of 8 % for the LECO®.

The double measurement of the samples of core SO136-147BX revealed an overall lower carbonate content of 89 to 92 wt%, against values of 90 to 97 wt% measured with the Carlo Erba. Thus a correction factor of 0.9543 was used in this study when adjusting measurements of the LECO® and the Carlo Erba. Although the overall variance of the LECO® is higher compared to the Carlo Erba, the higher amount of measured material and the larger dimension of the measuring cup suggests to diminish the influence of sample lost during treatment with acid.

In order to make the measurements of both methods comparable, TOC of the double measured samples was measured with the Carlo Erba with preceding dissolution of the carbonate content. This method avoids analytical errors due to sample loss during treatment with acid and due to too low amount of measured material. However, these values cannot be qualitatively compared with the previously measured, but they give ratio and trend of TOC in the samples compared to each other. About 0.5 g of the sample was treated for measurement with hydrochloric acid in a 50 ml jar, until no more development of gas could be detected. The jar was filled with distilled water and rotated in a centrifuge for 20 minutes. This forces the matter to settle and enables us to remove the water, in order to quicken the drying. Afterwards the sample was dried, grounded and treated with acid again. This procedure was repeated five times. Then the sample was weighed and measured in the Carlo Erba as described above. The measured values are given in appendix A5. The results of the LECO® have been found reliable by comparing ratio and trend of the measurements to the Carlo Erba.

Carbonate analysis:

During the cruise, the carbonate content of three to four samples from all cores (except the core SO136-165BX) was analysed using a "carbonate bomb" as described in Holler (1995). The carbonate bomb measures the CO₂ pressure following the reaction of hydrochloric acid with calcium carbonate. The data was used to check the results of the laboratory work, and is given in appendix A5, p. XXXIX.

After Nagao and Nakashima (1992) the L*-value of spectrophotometrical analysis (see Chapter 3.2.4) is supposed to correlate with the carbonate content of pelagic sediments with an organic carbon content of less than 0.6 wt% by a correlation factor of 0.91. Weber (1998) found a correlation factor of 0.95. Thus the L*-value was used as an additional proxy for the analytically derived carbonate content. The data for each core is given in Chapter 4.

3.2.3 $\delta^{18}\text{O}$ and $\delta^{13}\text{C}$ stable isotope ratios and AMS ^{14}C radiocarbon dating

$\delta^{18}\text{O}$ and $\delta^{13}\text{C}$ stable isotopes:

Clean tests of the epibenthic foraminifera *Cibicidoides wuellerstorfi* and the planktic foraminifera *Globigerina bulloides* were picked from the fraction >150 µm for measurement of $\delta^{18}\text{O}$ and $\delta^{13}\text{C}$ stable isotopes. Cleaning of the tests was not done. After Wefer and Berger (1991) and Tiedemann, GEOMAR (personal com.) uncleaned tests show no inconsistency in the measurement, as far as the tests are not filled or covered with nano plankton. The isotope ratios were detected by a FINNIGAN MAT 252 mass spectrometer (GEOMAR, Kiel). It contains a preceding carbonate preparation line ("Kiel CARBO 2 device"), where the tests are dissolved in 100% *ortho*-phosphoric acid at 70° C. The developing CO₂ is sampled in cooling traps and transferred into the mass spectrometer. The proportion of stable isotopes in the sample gas is measured relative to a laboratory intern standard gas (carbonic acid source from Burgbrohl, Germany). The adjustment of the standard gas to the international PDB-standard (Pee Dee Belemnite) is achieved through the carbonate standard NBS 19 of the National Bureau of Standards (Craig, 1957). The all over reproducibility of the measurements ($\pm \sigma_1$) is 0.03 ‰ for $\delta^{18}\text{O}$ and 0.01 ‰ for $\delta^{13}\text{C}$, concerning to a laboratory intern carbonate standard (Solnhofer carbonate rock). A minimum amount of 7 µg CO₂ (30 to 50 µg are ideal) is required to achieve reliable values. Therefore, 7 tests of *G. bulloides* and 3 tests of *C. wuellerstorfi* were selected for measuring. In 10 samples no sufficient numbers of *C. wuellerstorfi* were found. The position of the missing values is marked in the figures by a broken line.

AMS ^{14}C radiocarbon dating:

Two samples of each core from the South Tasman Rise were selected for ^{14}C radiocarbon dating with the Accelerator Mass Spectroscopic (AMS). The samples were selected from different sediment depth (see Table 4, p. 41), in order to enable a higher resolution by correlating the cores with each other, as discussed in Chapter 5.1.2, p. 54.

For measurement the AMS of the "Leibniz Labor für Altersbestimmung und Isotopenforschung" at the Christian-Albrechts-University of Kiel was used. Per sample a minimum of 1200 clean calcareous tests (~1.2 mg) of different planktic foraminiferal species were selected for measurement. The tests were cleaned with 15% H_2O_2 in an ultrasonic bath, in order to remove organic contents and contaminations like dust or carbonate fragments. In the AMS phosphoric acid at a concentration of 100% and at a temperature of 90°C is used for hydrolysis of CaCO_3 to CO_2 . The CO_2 is then reduced to elementary carbon by H_2 with support of an iron-catalyst. For AMS-measuring, the retrieved iron-graphite-mixture is pressed into a sample-holder.

The ^{14}C -measurements were corrected for isotope fractionation by the $^{13}\text{C}/^{12}\text{C}$ -ratio, which was measured by AMS. This $\delta^{13}\text{C}$ -ratio also reflects effects of graphitisation and isotopical fractionating in the AMS and thus is not comparable to the $\delta^{13}\text{C}$ -values measured in a Gas-mass spectrometer. Counting-statistics, stability of the AMS and uncertainties in the subtracted zero-effect are taken into account for the uncertainty of the ^{14}C -value. The counting-statistic and the observed scatter of the measuring intervals have been compared and the higher value was used in order to compensate the first two errors. The "Conventional Age" is defined after Stuiver and Polach (1977). For reservoir correction of the conventional ages the program "CALIB 4.1.2" was used (Stuiver et al., 1998a). The software can be downloaded at <http://radiocarbon.pa.qub.ac.uk>. The correction was done following the intercept method, which reveals one absolute age for each sample. It was assumed that the samples consist of 100 % marine carbon. For calibration the file "marine98.14c" from the same server was used. The correction is calibrated for samples from the Northern Hemisphere. Because of incomplete mixing between hemispheres, the age of the samples from the Southern Hemisphere was reduced by 24 years. By the program the calibrated ages and ranges are rounded to the nearest year, this may be too precise in many instances. Thus the computed results were rounded to the nearest 10 yr. for samples with standard deviation in the radiocarbon age greater than 50 yr. (Stuiver et al., 1998b). Due to the ^{14}C plateau in the range of 10000 yr. BP (Voelker et al., 1998), the reservoir correction of sample SO136-165BX at 22.5 cm bsf revealed three ages, which all have to be considered equally. For the attempt to correlate the three cores, the oldest age of the three has been used to be consistent with the age of the core SO136-165BX (see Chapter 5.1.2, p. 54).

3.2.4 Analysis of benthic foraminiferal assemblages and data processing

A total of 135 different species of benthic foraminifera was determined using a binocular. After carefully processing (see Fig. 3.3, p. 10) the $>150 \mu\text{m}$ subfraction was divided in appropriate amounts for examination using a micro sample-splitter. To obtain statistically significant results an amount of 300 specimens per sample is required and was achieved in most cases. The number of counted specimen per sample is given in appendix A 3, p. XII. The input of dropstones and pyroclastics was traced by counting clastic sediment grains parallel to the foraminiferal tests.

Q-mode Factor Analysis:

In order to arrange the high number of species found in a smaller number of species associations the paleontological data set was computed by means of multivariate Q-mode Factor Analysis with varimax rotation. The resulting varimax factor (VAR) is an indicator for species or groups of species, which show similar variations in abundance upcore, and thus should be related to similar environmental factors. Only species with an abundance of $>2\%$ in at least one sample of the core were considered for computing. This avoids mathematical effects and overrating of exotic species while computing an extensive data set. For the investigated samples, this method lead to a slightly higher Varimax Loading Factor in all cores compared to the computing of counted species. However, the values of significant and associative species were not affected by disregarding the species with a frequency lower than 2 %, of which none did show ecological significance (an exception is the species *Fursenkonia contemplata* in core SO136-165BX, see Chapter 5.2.3, p. 69). The program "PaleoToolBox" (Zielinski, 1998), written by Sieger at Bremen University and the program "CABFAC" of the program suite "WinTransfer" (Imbrie and Kipp, 1971) were used for data processing. The software can be downloaded from the server of the "PANGAEA - Network for Geological and Environmental Data" of Bremen University, at <http://www.pangaea.de>.

The Q-mode Factor Analysis results in two data sets:

1. The Varimax Factor (Loading) Matrix (VFM) indicates the weight of each factor of the data set. The loading of each factor varies between 0 and ± 1 . Loadings of $>\pm 0.4$ indicate a high significance of a factor (Backhaus et al., 1989; Malmgren and Haq, 1982). Additionally communality, variance and cumulative variance are calculated.

The communality indicates for each sample that part of the data, which is explained by the Q-Mode Factor model. Values reach from 0 to 1. For a representative factor communality should be >0.8 (personal com. Hüls, GEOMAR).

The variance of each factor defines the part of the factor on the model. The cumulative variance represents the quality of the model and increases with the number of factors, while the value of the variance decreases with the number of factors respectively. For better arrangement and to avoid mathematical effects, the number of factors should be as low as possible. However, the cumulative variance should cover a representative part of the core, for not loosing potential definitions of faunal associations. As a compromise four factors were used, which lead to a lowest cumulative variance of 92.682 % and an average of 94.297 %. All data sets were computed with the same number of factors to receive comparable results.

2. The Varimax Factor Score Matrix (VFSM) details the foraminiferal species within one factor and the extent of the influence of this species on the factor for each sample. The amount varies between ± 1 . Values of $>\pm 0.4$ indicate a significant influence, values of $>\pm 0.1$ indicate associative influence of a species (Niebler, 1995).

Different relations are detectable by comparing trends of foraminiferal species distribution with sediment properties as environmental parameters. However, the computing of the paleontological data set (spec./g) together with the physical and chemical sediment parameters (e.g. spectrophotometrical data, grain size contents, TOC contents and C/N ratios), by the means of Q-Mode Factor Analysis did not reveal significant correlations. This might be due to the limited environmental data set and the chosen analytical method, which computes canonical, not pair-wise correlation. More likely it reflects the fact, that many variations in benthic foraminiferal species distribution cannot be explained by correlation of a simple or few combined environmental parameters (Mackensen et al., 1990).

4 RESULTS

All core descriptions will be made from the base of the core to the top.

4.1 Cores from the eastern Campbell Plateau

4.1.1 Physical and physicochemical sediment properties

Description of core SO136-019BX

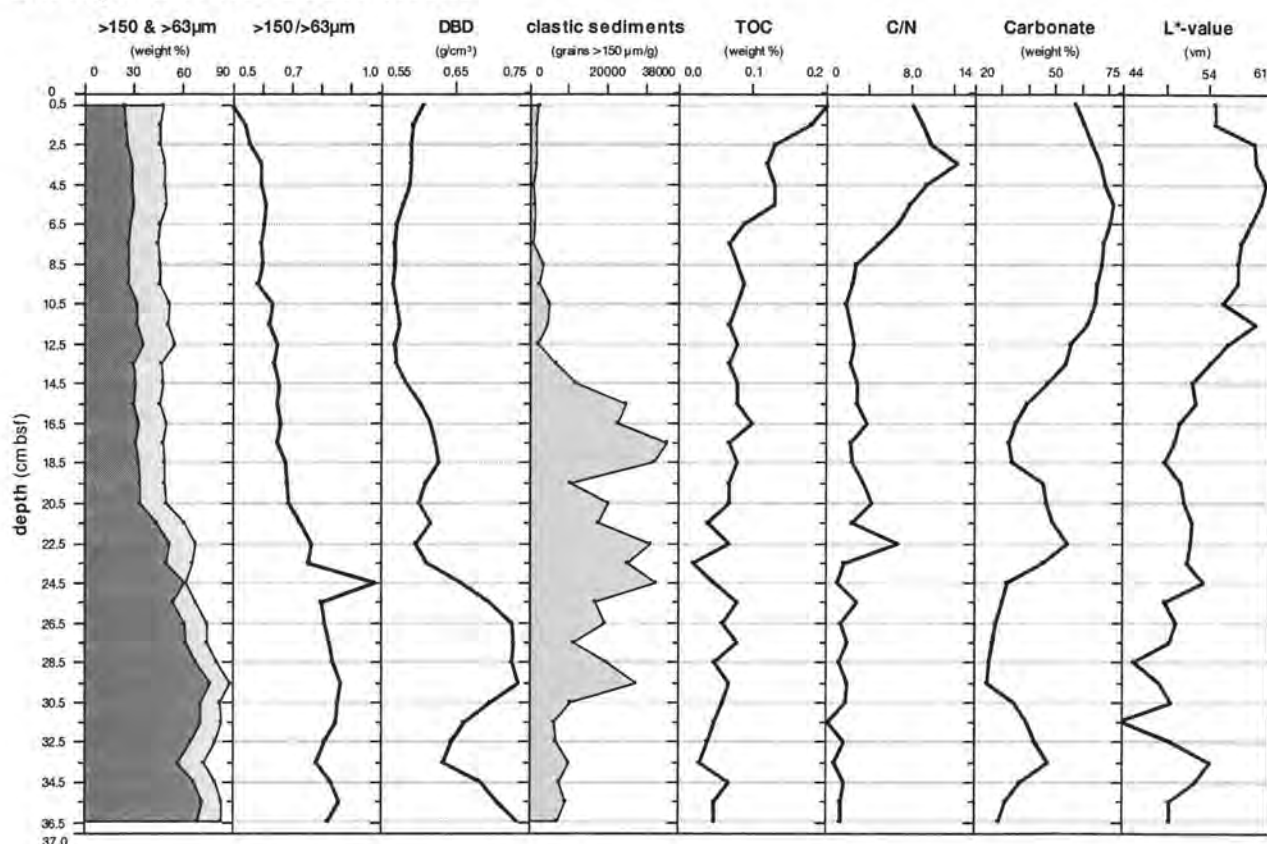


Fig. 4.1 Physical and physicochemical sediment properties of core SO136-019BX. In the first graph the dark grey area indicates $>150 \mu\text{m}$ grain size, the light grey area indicates $>63 \mu\text{m}$ grain size.

Grain size distribution and ratio of $>150 / >63 \mu\text{m}$ subfractions:

The weight percentage (wt%) of the fractions >63 (light grey) and $>150 \mu\text{m}$ (dark grey) decreases upcore. The absolute minima of 46 wt% for $>63 \mu\text{m}$ and of 24 wt% for $>150 \mu\text{m}$ are located at 1.5 cm below sea floor (bsf) and at 0.5 cm bsf respectively. The absolute maxima of 88 wt% for $>63 \mu\text{m}$ and of 77 wt% for $>150 \mu\text{m}$ are located at 29.5 cm bsf. The graphs of the coarser fractions trend almost parallel with an average difference of 22 wt%. An exception is the sample at 24.5 cm bsf where a local maximum of 60 wt% in the $>150 \mu\text{m}$ grain fraction occurs

in the same depth as a local minimum in the >63 µm grain fraction. At this depth the archive boxes were switched during sampling (see photo 3). This shifts the middle of the sampled parts for 6 cm sideways from the middle of the other part of the core. Two archive boxes were sampled overlapping in the laboratory. The sample at 25.5 cm bsf was taken out of the stratigraphy to correct the depth bsf throughout the core after processing all samples and comparing the measured values. A sudden decrease is located at 20.5 cm bsf, where the >63 µm fraction increases from 50 to 68 wt%. The >150 µm fraction increases from 34 to 52 wt% at 22.5 cm bsf respectively. Slight maxima of the coarser fractions are located between 3.5 to 6.5 cm bsf (49 wt% for >63 µm and 29 wt% for >150 µm) and in between 10.5 to 12.5 cm bsf (52 wt% for >63 µm and 33 wt% for >150 µm). In the middle of the two maxima a peak of abundance of big specimen (up to 4mm diameter) of the agglutinating foraminifera *Cyclamina cancellata* occurs, as described in Chapter 4.1.3, p. 29. The ratio of the grain sizes <150 / <63 µm decreases constantly to the absolute minimum of 24 at the top of the core. The absolute maximum consists of a single spike and is located at 24.5 cm bsf, with a value of 60. The next maximum besides this spike is located at 29.5 cm bsf.

Dry bulk density:

Dry bulk density (DBD) correlates with the trend of the content of the coarse grain sizes and anti-correlates with the carbonate content. A first maximum of 0.70 g/cm³ is located at 36.5 cm bsf. A first minimum is located at 33,5 cm bsf with 0.63 g/cm³. A second maximum reaches from 29,5 to 26,5 cm bsf with 0.73 g/cm³. After this maximum the DBD decreases to 0.59 g/cm³ at 22.5 cm bsf and varies only slightly to the top of the core. A peak of 0.63 g/cm³ is present at 18,5 cm bsf. A slight increase from 0.57 to 0.6 g/cm³ is present in the upper 6,5 cm bsf.

Clastic sediments:

The clastic sediments content in the grain-fraction >150 µm varies slightly between 36.5 and 30.5 cm bsf from 6500 to 10700 grains per gram dry sediment (grains/ g). A strong increase leads to a first maximum with 27500 grains/g at 29.5 cm depth, which correlates with the first maximum of the coarse grain fractions. A minimum is located at 27.5 cm bsf with 11500 grains/g. The next two maxima at 24.5 with 32000 and 22.5 cm bsf with 31000 grains/g correlate with a local minimum and a local maximum in the coarse grain fractions. A minimum is located at 19.5 cm bsf with 10600 grains/g. The absolute maximum is located at 17.5 cm depth with 35000 grains/g. After a strong decrease to 25000 grains/g at 12.5 cm bsf, the clastic sediment content slightly decreases to the top of the core. The absolute minimum is located at 4.5 cm bsf with 1090 grains/g.

TOC content and C/N ratio:

The TOC content increases from 0.05 wt% at the base of the core to 0.07 wt% at 7.5 cm bsf. The absolute minimum of 0.02 wt% is located at 23.5 cm bsf. At 22.5 cm bsf is a local maximum of 0.07 wt%, which correlates with local maxima in the C/N ratio and in the carbonate content. From 7.5 cm bsf upward the TOC content increases to the absolute maximum of 0.2 wt%, located at the top of the core. An interval of stable TOC content is present between 5.5 and 2.5 cm bsf. There the average content of TOC is 0.13 wt%. The C/N ratio trends mainly similar to the TOC content, except for the absolute maximum of 12.4 wt% at 3.5 cm bsf. The absolute minimum is located at 31.5 cm bsf with 0.19 wt%.

Carbonate content:

Carbonate content anti-correlates with the DBD. It shows increase from 29 wt% at the base of the core to 48 wt% at 33.5 cm bsf. This maximum anti correlates with the coarser grain sizes. Strong decrease guides to a local minimum of 25wt% at 29.5 cm bsf. Carbonate slightly increases to 32 wt% at 29.5 cm bsf. A strong increase leads to a local maximum of 54wt% at 22.5 cm bsf. This correlates with maxima in TOC and C/N. Slighter decrease leads to a local minimum of 33wt% at 17.5 cm bsf. The absolute maximum of 72 wt% is reached at 5.5 cm bsf.

Spectrophotometrical data:

The spectrophotometrical L*-value follows the trend of the carbonate content. A maximum of 54 vm at 33.5 cm bsf correlates with a maximum in the carbonate content. The absolute minimum of 44 vm is present at 31.5 cm bsf. The absolute maximum of 61 vm is located at 4.5 cm bsf. Both maxima are located one centimeter higher than the maxima in the carbonate content.

Description of core SO136-025BX

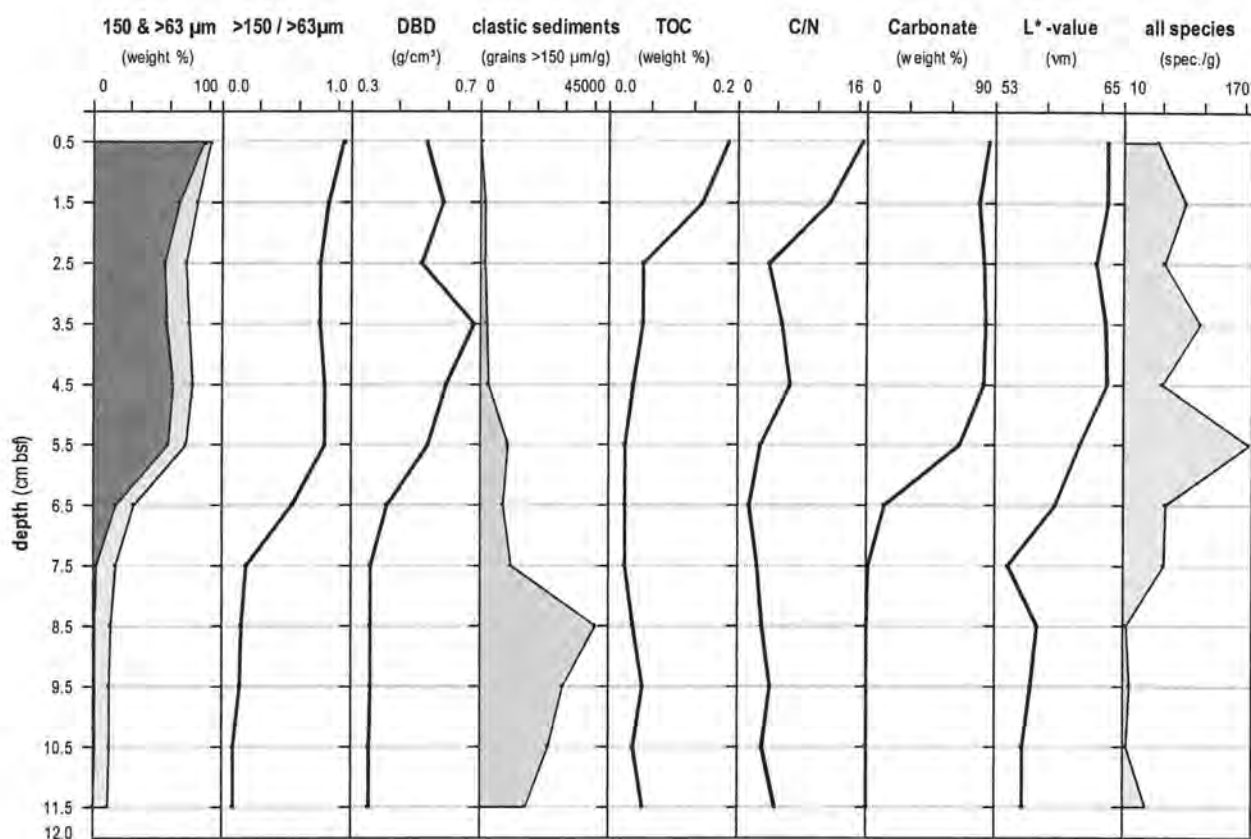


Fig. 4.2 Physical and physicochemical sediment properties and abundance of all benthic foraminifera species of core SO136-025BX. In the first graph the dark grey area indicates $>150 \mu\text{m}$, the light grey area indicates $>63 \mu\text{m}$.

Grain size distribution and ratio of $>150 / >63 \mu\text{m}$ subfractions:

The amount of the >150 (light grey) and the $>63 \mu\text{m}$ (dark grey) subfractions leads almost parallel upcore with an average difference of 14 wt%. The absolute minima of 2 wt% for $>63 \mu\text{m}$ and 1 wt% for $>150 \mu\text{m}$ are located at the base of the core. The content of the grain sizes decreases slightly from the base of the core to 18 wt% for $>63 \mu\text{m}$ and 3 wt% for $>150 \mu\text{m}$ at 7.5 cm bsf. A strong increase leads to a content of 73 wt% for $>63 \mu\text{m}$ and 59 wt% for $>150 \mu\text{m}$ at 5.5 cm bsf. A slight increase guides to the absolute maxima of 92 wt% at the top of the core for $>63 \mu\text{m}$ and of 87 wt% for $>150 \mu\text{m}$. The ratio of the grain size subfractions increases slightly from the absolute minimum of 0.1 at the base of the core to 0.19 at 7.5 cm bsf. Strong increase leads to 0.81 at 5.5 cm bsf. Slight increase leads to the absolute maximum of 0.94 at the top of the core.

Dry bulk density:

The DBD correlates with the content of the grain sizes. The absolute minimum of 0.36 g/cm^3 is located at the base of the core. The absolute maximum of 0.68 g/cm^3 is located at 0.3 cm bsf.

Clastic sediments:

The content of clastic sediment grains slightly decreases from the base of the core to the absolute maximum of 41000, to 16000 grains/g at 8.5 cm bsf. Strong decrease is present at a local maximum of 11000 grains/g at 7.5 cm bsf. Slight decrease leads to the absolute minimum of 203 grains/g at the top of the core.

TOC content and C/N ratio:

The organic carbon content decreases slightly from the base of the core to the absolute minimum of 0.02 wt% at 7.5 and to 0.04 wt% at 5.5 cm bsf. Slight decrease is present to 0.04 wt% at 2.5 cm bsf. Strong increase leads to the absolute maximum of 0.14 wt% at the top of the core. The trend of the C/N ratio follows the trend of TOC. An exception is a local maximum of 6.5 wt% at 4.5 cm bsf. The absolute minimum of 1.5 wt% is at 6.5 cm bsf. The absolute maximum of 15,5 wt% is at the top of the core.

Carbonate content:

Slight increase leads from the absolute minimum of 0.09 wt% at the base of the core to 1.3 wt% at 7.5 cm bsf. Strong increase leads to 83 wt% at 4.5 cm bsf. The carbonate content shows minor variations to the absolute maximum of 86 wt% at the top of the core.

Spectrophotometrical data:

The trend of the photospectrometrical data correlates with the carbonate content, except for a local minimum of 54 vm at 7.5 cm bsf. The values are almost constant from the base of the core to 8.5 cm bsf with 51 and 57 vm respectively. Steep increase leads from the local minimum at 7.5 cm bsf to 63 vm at 4.5 cm. The values show minor variations to the absolute maximum of 64 vm at the top of the core.

Abundance of all benthic foraminifera species:

The abundance of all benthic foraminifera species decreases slightly from 40 spec./g at the base of the core to the absolute minimum of 14 spec./g at 8.5 cm bsf to (see Fig. 4.1.2, p. 21). Following strong increase to the absolute maximum of 167 spec./g at 5.5 cm bsf. Slight decrease with minor variations leads to 40 spec./g at the top of the core.

Description of core SO136-037BX

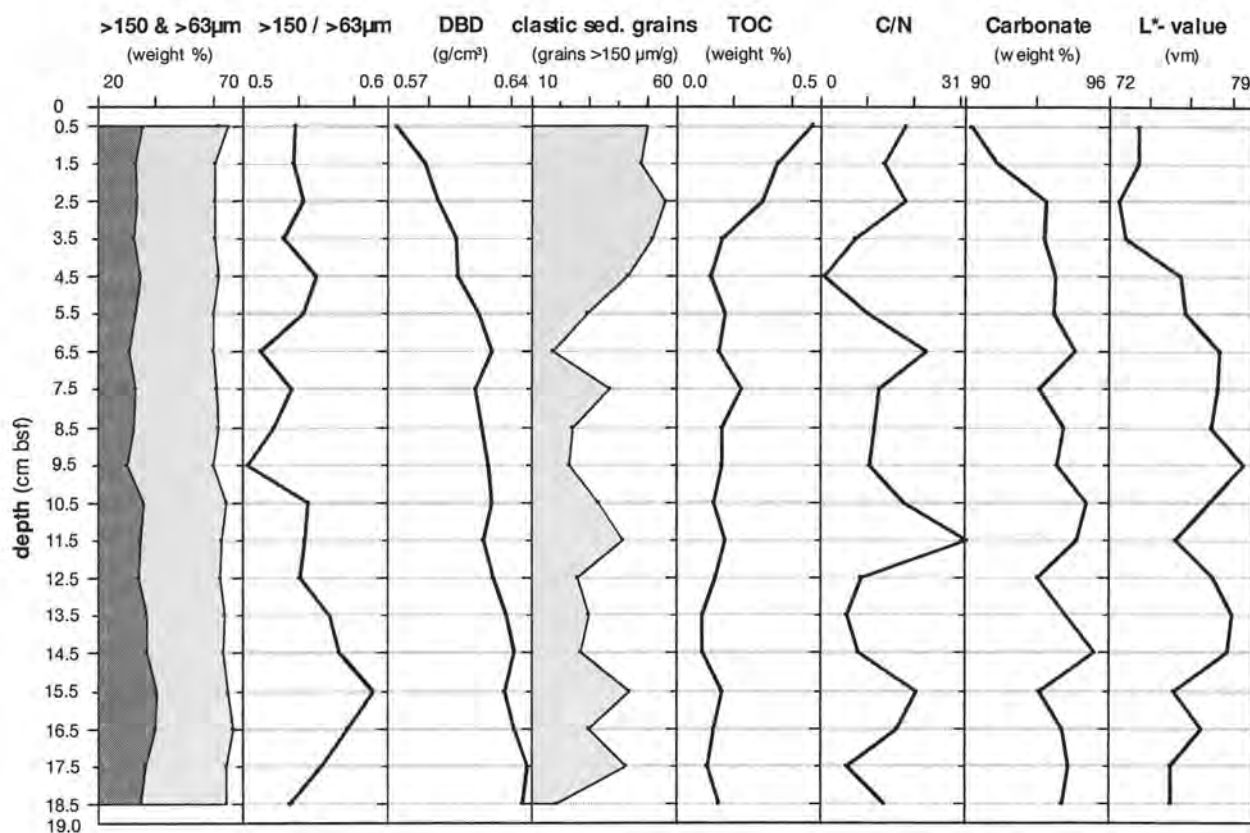


Fig. 4.3 Physical and physicochemical sediment properties of core SO136-037BX. In the first graph the dark grey area indicates $>150\text{ }\mu\text{m}$, the light grey area indicates $>63\text{ }\mu\text{m}$.

Grain size distribution and ratio of $>150 / >63\mu\text{m}$ subfractions:

The graphs of the two subfractions lead almost parallel and constant upcore. The amount of the $>150\text{ }\mu\text{m}$ fraction varies from 31 wt % at 6.5 cm bsf to 40 wt % at 15.5 cm bsf. The content of the $>63\text{ }\mu\text{m}$ fraction varies from 60 wt % at 5.5 cm bsf to 67 wt % at 16.5 cm bsf. The ratio shows coarsening up from 0.54 at the base of the core to the absolute maximum of 0.62 at 15.5 cm bsf. Slight decrease leads to the absolute minimum of 0.5 at 9.5 cm bsf. The ratio increases slightly to 0.55 at the top of the core.

Dry bulk density:

The DBD decreases constantly from the absolute maximum of 0.64 g/cm^3 at 17.5 cm bsf to the absolute minimum 0.57 g/cm^3 at the top of the core.

Clastic sediments:

The clastic sediments content increases upcore. A phase of slight variations is followed by strong increase from the absolute minimum of 18 grains/g dry sediment at 6.5 cm bsf to the absolute maximum of 56 grains/g dry sediment at 2.5 cm bsf.

TOC content and C/N ratio:

The organic carbon content stays almost constant from the base of the core to 4.5 cm bsf. The absolute minimum of 0.09 wt% is located at 13.5 and 14.5 cm bsf. A strong increase leads from 0.12 wt % at 4.5 cm bsf to the absolute maximum of 11.3 wt% at the top of the core. The C/N ratio shows four maxima, which follow the slight variations of the TOC content: 20.6 wt % at 15.5 cm bsf, the absolute maximum of 31.6 wt % at 11.5 cm bsf, 22.9 wt % at 6.5 cm bsf and 18.5 wt % at 2.5 cm bsf. Four minima of 5.9 wt %, 5.7 wt %, 10.7 wt % and 0.81 wt % are located at 17.5 cm bsf, at 13.5 cm bsf, at 9.5 cm bsf and at 4.5 cm bsf respectively.

Carbonate content:

The carbonate content stays constant in the lower 17 cm of the core. It varies between 95 wt % at the absolute maximum at 14.5 cm bsf and 93 wt % at three minima. The absolute minimum of 90 wt% is located at the top of the core.

Spectrophotometrical data:

The L*-value correlates in the lower 17 cm of the core with the carbonate content. The value increases from the base of the core to the absolute maximum of 77 vm at 9.5 cm bsf. Slight decrease with minor variations leads to the absolute minimum of 72 vm at 3.5 cm bsf. Slight increase leads to 73 vm at the top of the core.

4.1.2 $\delta^{18}\text{O}$ and $\delta^{13}\text{C}$ stable isotope ratios

Description of core SO136-019BX

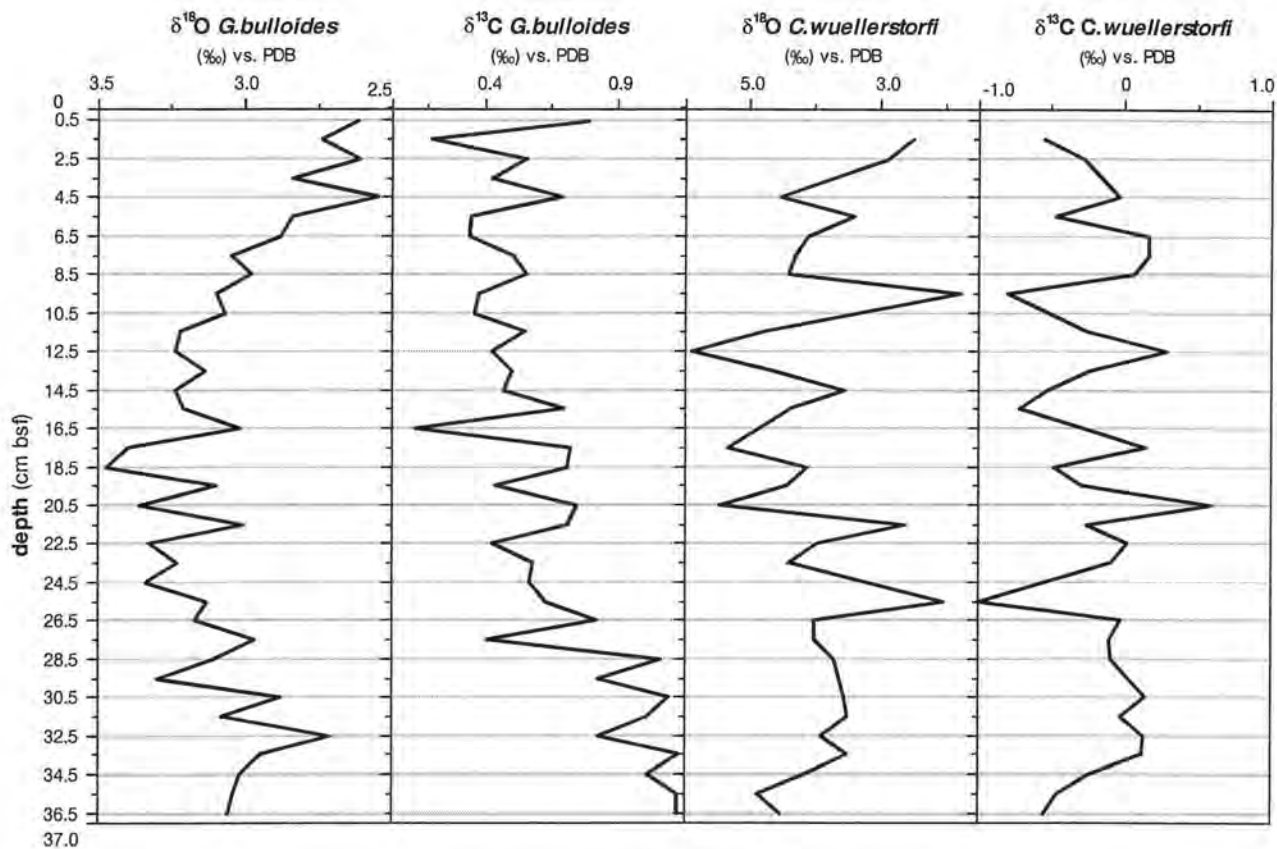


Fig. 4.4 Stable isotope ratios of benthic and planktic foraminifera tests in core SO136-019BX.

$\delta^{18}\text{O}$ and $\delta^{13}\text{C}$ stable isotope ratio of planktic foraminifera (*G. bulloides*):

The ratio shows an overall increase from 3.04 ‰ versus Pee Dee Belemnite (vs. PDB) at the base of the core to the absolute maximum of 3.45 ‰ vs. PDB at 18.5 cm bsf. The average variance throughout the core is 0.3 ‰ vs. PDB. Between 27.5 and 22.5 cm bsf the average variance is lower with 0.1 ‰ vs. PDB. The absolute maximum of 3.45 ‰ vs. PDB is located at 18.5 cm bsf. The ratio decreases to the top of the core with a variance of 0.2 ‰ vs. PDB. The variance is with 0.1 ‰ lower in-between 11.5 and 3.5 cm bsf. The absolute minimum of 2.53 ‰ vs. PDB is located at 4.5 cm bsf. The ratio of $\delta^{13}\text{C}$ shows slight decrease from the absolute maximum of 0.97 ‰ vs. PDB at the base of the core to 0.64 ‰ vs. PDB at the top of the core. The absolute minimum is located at 16.5 cm bsf with -0.01‰. The average variance upcore is 0.18 ‰ vs. PDB. At the same depths as in the $\delta^{18}\text{O}$ stable isotope ratio the variance is smaller, in this case it is 0.06 ‰ vs. PDB.

$\delta^{18}\text{O}$ and $\delta^{13}\text{C}$ stable isotope ratio of benthic foraminifera (*C. wuellerstorfi*):

The ratio decreases from 4.24 ‰ vs. PDB at 35.5 cm bsf to 3.35 ‰ vs. PDB at 26.5 cm bsf. The average variance is 0.4 ‰ vs. PDB. From the absolute minimum of 1.36 ‰ vs. PDB at 25.5 cm bsf the ratio increases with a variance of 1.1 ‰ to the absolute maximum of 5.23 ‰ vs. PDB at 12.5 cm bsf. Following decrease leads to 1.85 ‰ vs. PDB at 1.5 cm bsf. The value of the uppermost sample is missing due to a fault of the mass-spectrometer. The ratio of $\delta^{13}\text{C}$ correlates with the $\delta^{18}\text{O}$ stable isotope ratio, except for the depth between the base of the core and 33.5 cm bsf, where it increases from -0.55 to 0.12 ‰ vs. PDB. The absolute minimum is located at the same depth as in the $\delta^{13}\text{C}$ stable isotope ratio with -1 ‰ vs. PDB. The absolute maximum of 0.59 ‰ vs. PDB is located at 20.5 cm bsf.

Description of core SO136-025BX

The cores content of planktic foraminifera per sample increases from three yellowish and partly dissolved tests of uncertain genus at the base of the core to seven tests at 7.5 cm bsf. Further upcore a sufficient amount of tests was available for isotope measurements. A few benthic foraminifera of the species *C. wuellerstorfi* were available in the upper six samples of the core (except sample 5.5). No tests of this genus were found in the lower 6 samples.

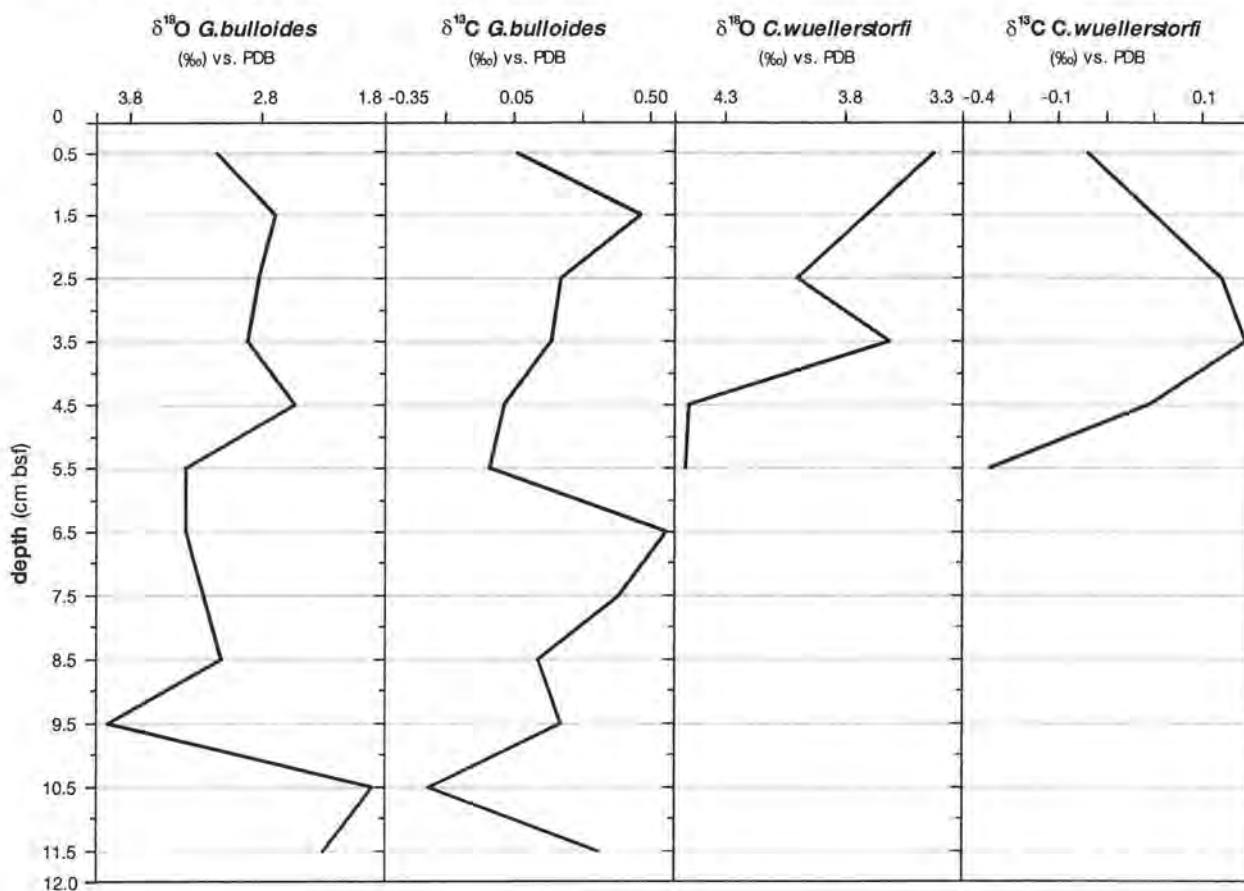


Fig. 4.5 Stable isotope ratios of benthic and planktic foraminifera tests in core SO136-025BX.

$\delta^{18}\text{O}$ and $\delta^{13}\text{C}$ stable isotope ratio of planktic foraminifera (*G. bulloides*):

The ratio of $\delta^{18}\text{O}$ shows stronger variations in the lower part of the core. Strong depletion leads from the base of the core to the absolute minimum of 1.89 ‰ vs. PDB at 10.5 cm bsf. Strong increase leads to the absolute maximum of 3.91 ‰ vs. PDB at 9.5 cm bsf. Further depletion guides to a local minimum of 2.48 ‰ vs. PDB at 4.5 cm bsf. Slight increase leads to 3.08 ‰ vs. PDB at the top of the core. Strong depletion in the ratio of $\delta^{13}\text{C}$ leads from the base of the core to the absolute minimum of -0.22 ‰ vs. PDB at 10.5 cm bsf. Slight increase leads to the absolute maximum of 0.48 ‰ vs. PDB at 10.5 cm bsf. The ratio shows strong depletion to a local minimum of -0.04 ‰ vs. PDB at 5.5 cm bsf. Slight increase leads to 0.4 ‰ vs. PDB at 1.5 cm bsf. Strong depletion leads to 0.04 ‰ vs. PDB at the top of the core.

$\delta^{18}\text{O}$ and $\delta^{13}\text{C}$ stable isotope ratio of benthic foraminifera (*C. wuellerstorfi*):

The first measured value of 4.38 ‰ vs. PDB at 5.5 cm bsf is the absolute maximum. The ratio depletes to 3.35 ‰ vs. PDB at 3.5 cm bsf, increases to 3.62 ‰ vs. PDB at 2.5 cm bsf and decreases to 3.35 ‰ vs. PDB at the top of the core. The ratio of $\delta^{13}\text{C}$ increases from the absolute minimum of -0.34 ‰ vs. PDB at 5.5 cm bsf to the absolute maximum of 0.19 ‰ vs. PDB at 3.5 cm bsf. Strong decrease leads to -0.14 ‰ vs. PDB at the top of the core.

Description of core SO136-037BX

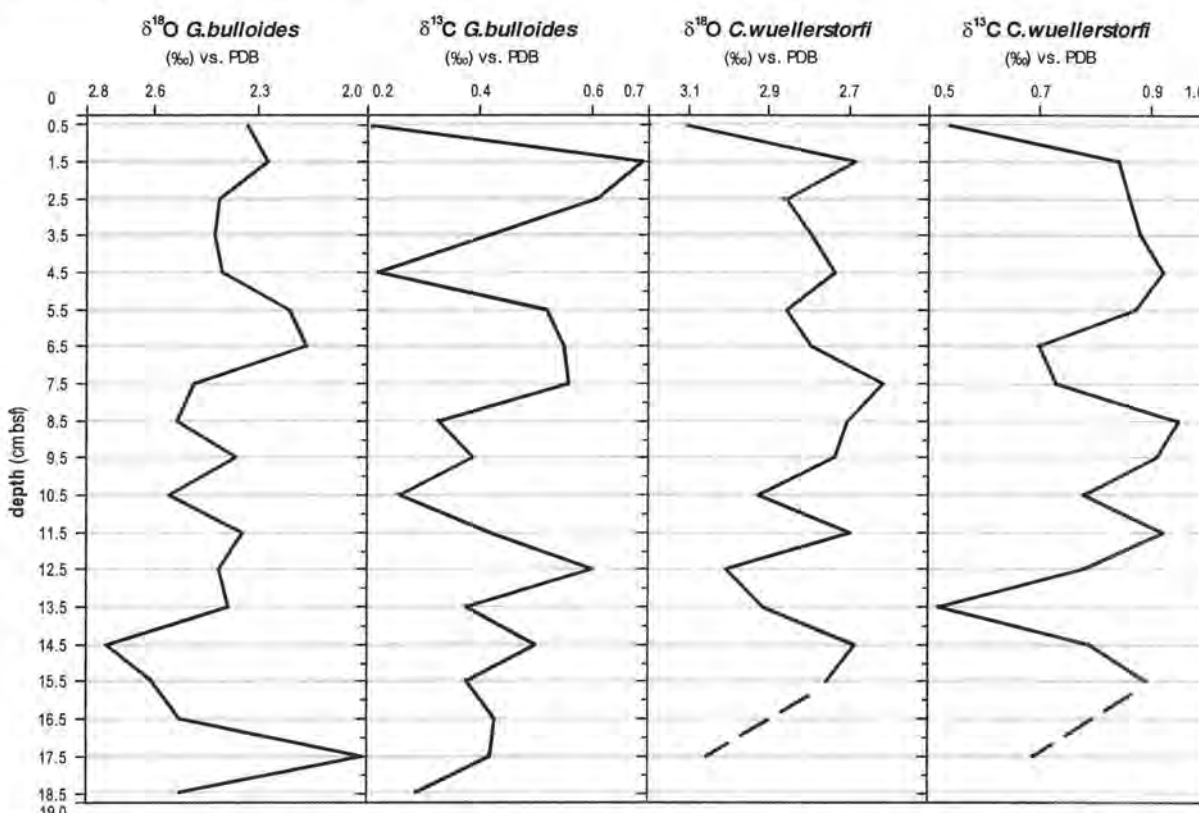


Fig. 4.6 Stable isotope ratios of benthic and planktic foraminifera tests in core SO136-037BX.

*$\delta^{18}\text{O}$ and $\delta^{13}\text{C}$ stable isotope ratio of planktic foraminifera (*G. bulloides*):*

Strong depletion of the $\delta^{18}\text{O}$ ratio leads from 2.58 ‰ vs. PDB at the base of the core to the absolute minimum of 2.06 ‰ vs. PDB at 17.5 cm bsf. A second measurement of this single spike revealed a value of 1.14 ‰ vs. PDB. Strong depletion leads to the absolute maximum of 2.79 ‰ vs. PDB at 14.5 cm bsf. A slight decrease with moderate variations leads to 2.39 ‰ vs. PDB at the top of the core. Two main local minima are located at 11.5 and at 6.5 cm bsf with 2.40 and 2.22 ‰ vs. PDB respectively. The $\delta^{13}\text{C}$ ratio shows slighter variations in the lower six centimeter of the core than the upper part. Slight increase leads from 0.29 ‰ vs. PDB at the base of the core to a local maximum of 0.60 ‰ vs. PDB at 12.5 cm bsf. Strong depletion leads to a local minimum of 0.26 ‰ vs. PDB at 10.5 cm bsf. Strong increase leads to 0.56 ‰ vs. PDB at 7.5 cm bsf. This value stays fairly constant, until strong depletion leads to a local minimum of 0.22 ‰ vs. PDB at 4.5 cm bsf. The double measurement of this spike revealed the same value. Strong increases leads to the absolute maximum of 0.69 ‰ vs. PDB at 1.5 cm bsf. Strong depletion leads to the absolute minimum of 0.21 ‰ vs. PDB at the top of the core. The double measurement of this spike revealed a value of 0.07 ‰ vs. PDB.

 *$\delta^{18}\text{O}$ and $\delta^{13}\text{C}$ stable isotope ratio of benthic foraminifera (*C. wuellerstorfi*):*

The values at the base of the core and at 16.5 cm bsf are missing due to an analyser failure, which destroyed the selected tests. A new selection was not possible in the given time, due to the low abundance of benthic foraminifera in the core. Strong depletion of the $\delta^{18}\text{O}$ ratio leads from 3.04 ‰ vs. PDB at 17.5 cm bsf to a local minimum of 2.67 ‰ vs. PDB at 14.5 cm bsf. Strong increase leads to a local maximum of 2.99 ‰ vs. PDB at 12.5 cm bsf. The ratio decreases to 2.60 ‰ vs. PDB at the absolute minimum at 7.5 cm bsf. A single local minimum of 2.68 ‰ vs. PDB is located at 11.5 cm bsf. Slight increase leads to 2.67 ‰ vs. PDB at 1.5 cm bsf. Strong increase leads to the absolute maximum of 3.09 ‰ vs. PDB at the top of the core. The first and third values of the $\delta^{13}\text{C}$ ratio are missing as explained above. Strong increase leads from 0.69 ‰ vs. PDB at 17.5 cm bsf to a local maximum of 0.89 ‰ vs. PDB at 15.5 cm bsf. Strong depletion leads to the absolute minimum of 0.52 ‰ vs. PDB at 13.5 cm bsf. Strong increase leads to 0.92 ‰ vs. PDB at 11.5 cm bsf. This value stays almost stable to 0.95 ‰ vs. PDB at 8.5 cm bsf, except a local minimum of 0.78 ‰ vs. PDB at 10.5 cm bsf. The ratio depletes to a local minimum of 0.70 ‰ vs. PDB at 6.5 cm bsf. Strong increase leads to a local maximum of 0.92 ‰ vs. PDB at 4.5 cm bsf. Slight depletion leads to 0.84 ‰ vs. PDB at 1.5 cm bsf, strong depletion to 0.54 at the top of the core.

4.1.3 Analysis of benthic foraminifera assemblages

The abundance of foraminifera species and the trend of varimax factors are described here which are discussed in Chapter 5.2. The complete paleontological data set is given in appendix A3, p. XII. The output of the Q-Mode Factor Analysis is given in appendix A4. Factor loadings of >0.4 are shown to outline the significance range of the factor.

Description of core SO136-019BX

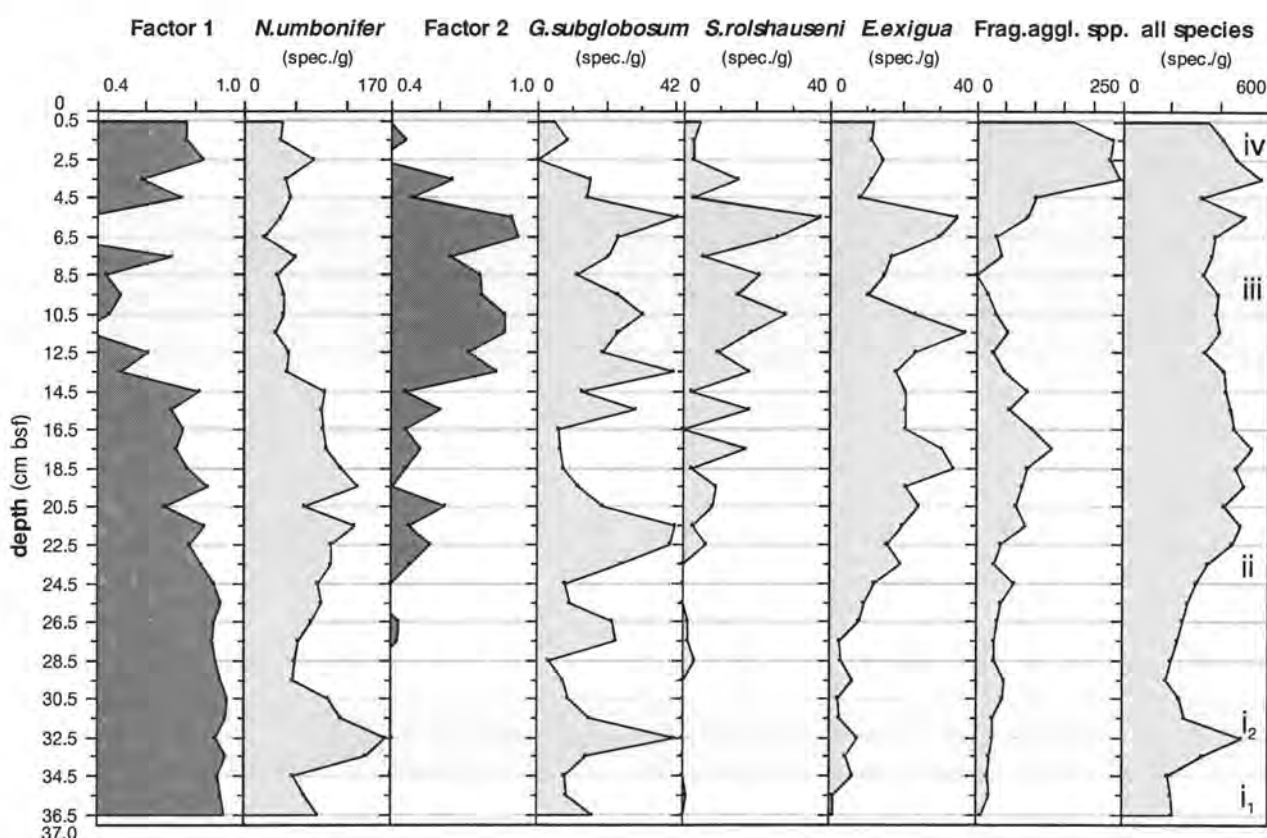


Fig. 4.7 VAR. factor 1 and 2 and abundances of resembling species in core SO136-019BX. The light grey squares indicate sections based on changes in foraminiferal fauna.

Factor 1 shows slightly decreasing factor loading from the absolute maximum of 0.920 at the base of the core to 0.495 at 13.5 cm bsf. A local minimum of 0.678 is located at 20.5 cm bsf. Strong decrease leads to a loading of 0.339 at 11.5 cm bsf. A peak of influence is located between 10.5 and 7.5 cm bsf with a maximal loading of 0.704. Strong increase introduces the next section of significance to 0.745 at 4.5 cm bsf. The loading shows slight variations to 0.765 at the top of the core. *Nuttalides umbonifer* has a factor score of 0.940 for factor 1. *Siphonotularia rolshauseni*, *Epistominella exigua* and *Ehrenbergina mestayeri* show associative influence with a factor score of -0.177, -0.139 and 0.128 respectively. The abundance of *N.*

umbonifer shows a distinct maximum from 34.5 to 29.5 cm bsf with the absolute maximum abundance of 164.99 spec./g at 32.5 cm bsf. Slight increase leads to a local maximum of 132.11 spec./g at 19.5 cm bsf. At 20.5 cm bsf, a local minimum of 71.05 spec./g exists. Strong decrease leads to 93.88 spec./g at 14.5 cm bsf. Slight decrease leads to the absolute minimum of 23.51 spec./g at 6.5 cm bsf. Slight increase leads to 45.74 spec./g at the top of the core.

The loading of factor 2 increases slightly from 0.401 at 24.5 cm bsf to 0.626 at 20.5 cm bsf. Strong decrease leads to 0.411 at 19.5 cm bsf. Slight increase leads to 0.607 at 15.5 cm bsf. Strong increase leads to 0.866 at 10.5 cm bsf. Slight decrease guides to a local minimum of 0.643 at 7.5 cm bsf. Strong increase leads to the absolute maximum of 0.924 at 5.5 cm bsf. Strong decrease leads to 0.467 at 1.5 cm bsf. *Globocassidolina subglobosa* has a factor score of 0.479. *Siphonostularia rolshauseni* has a factor score of 0.425. *Epistominella exigua* has a factor score of 0.408. *Pullenia bulloides* has a factor score of 0.294. *G. subglobosa* shows three single maxima in abundance in the lower 16.5 cm of the core: at 32.5 cm bsf with 16.42 spec./g, at 26.5 cm bsf with 21.93 spec./g and at 21.5 cm bsf with 40.07 spec./g. The minima in between have an average abundance of 8 spec./g. Strong increase leads from 6.22 spec./g at 16.5 cm bsf to a local maximum of 39.36 spec./g at 13.5 cm bsf. Strong decrease leads with slight variations to a local minimum of 11.45 spec./g at 8.5 cm bsf. Strong increase leads to the absolute maximum of 40.52 spec./g at 5.5 cm bsf. Strong decrease guides to 4.81 spec./g at the top of the core. *S. rolshauseni* shows slightly increasing abundance from 0 spec./g at 29.5 cm bsf to a local maximum of 28.04 spec./g at 10.5 cm bsf. Strong variations are present between 18.5 and 12.5 cm bsf. Strong decrease leads to a local minimum of 5.66 spec./g at 7.5 cm bsf. Strong increase leads to the absolute maximum of 37.63 spec./g at 5.5 cm bsf. Strong decrease guides to an abundance of 4.81 spec./g at the top of the core. *E. exigua* shows slight increase in abundance from the absolute minimum of 1.03 spec./g at the base of the core to 33.73 spec./g at 18.5 cm bsf. Steep decrease leads to a local minimum of 18.37 spec./g at 13.5 cm bsf. Strong increase guides to the absolute maximum of 37.10 spec./g at 11.5 cm bsf. Strong decrease leads to an abundance of 10.69 spec./g at 9.5 cm bsf. Strong increase leads to a local maximum of 34.73 spec./g at 5.5 cm bsf. Strong decrease leads to 8.52 spec./g at 4.5 cm bsf, and slight increase to 12.03 spec./g at the top of the core. The content of fragments of agglutinating foraminifera decreases slightly from 9.24 spec./g at the base of the core to a local maximum of 130.61 spec./g at 17.5 cm bsf. Slight decrease leads to the absolute minimum of 1.90 spec./g at 8.5 cm bsf. Strong increase leads to the absolute maximum of 244.39 spec./g at 3.5 cm bsf. Slight decrease leads to 166.39 spec./g at the top of the core. The abundance of all counted benthic foraminifera shows slight increase from 210.39 spec./g at the base of the core to a local maximum of 532.76 spec./g at 17.5 cm bsf. A peak of 492.31 spec./g is located at 32.5 cm bsf. Slight decrease leads from 17.5 cm bsf to the

absolute maximum of 568.97 spec./g at 3.5 cm bsf. Slighter decrease leads to 351.54 spec./g at the top of the core.

Description of core SO136-025BX

The core shows a sudden facies change at 6.5 cm bsf. Below this depth dark radiolarian mud is present. In this facies the number of present benthic foraminifera is not sufficient for a faunal analysis and was excluded from the statistical analysis. The data set of the upper 6.5 cm was computed. The agglutinating species *C. cancellata* and the group of fragments of agglutinating species were removed from the data set. The statistical analysis did not reveal satisfying results. The content of foraminifera per gram dry sediment resulted in a statistical not sufficient number of retrieved specimens, also in the upper 6.5 cm of the core. The abundance of all species is described in Chapter 4.1 and outlined in Figure 4.3, p. 23.

Description of core SO136-037BX

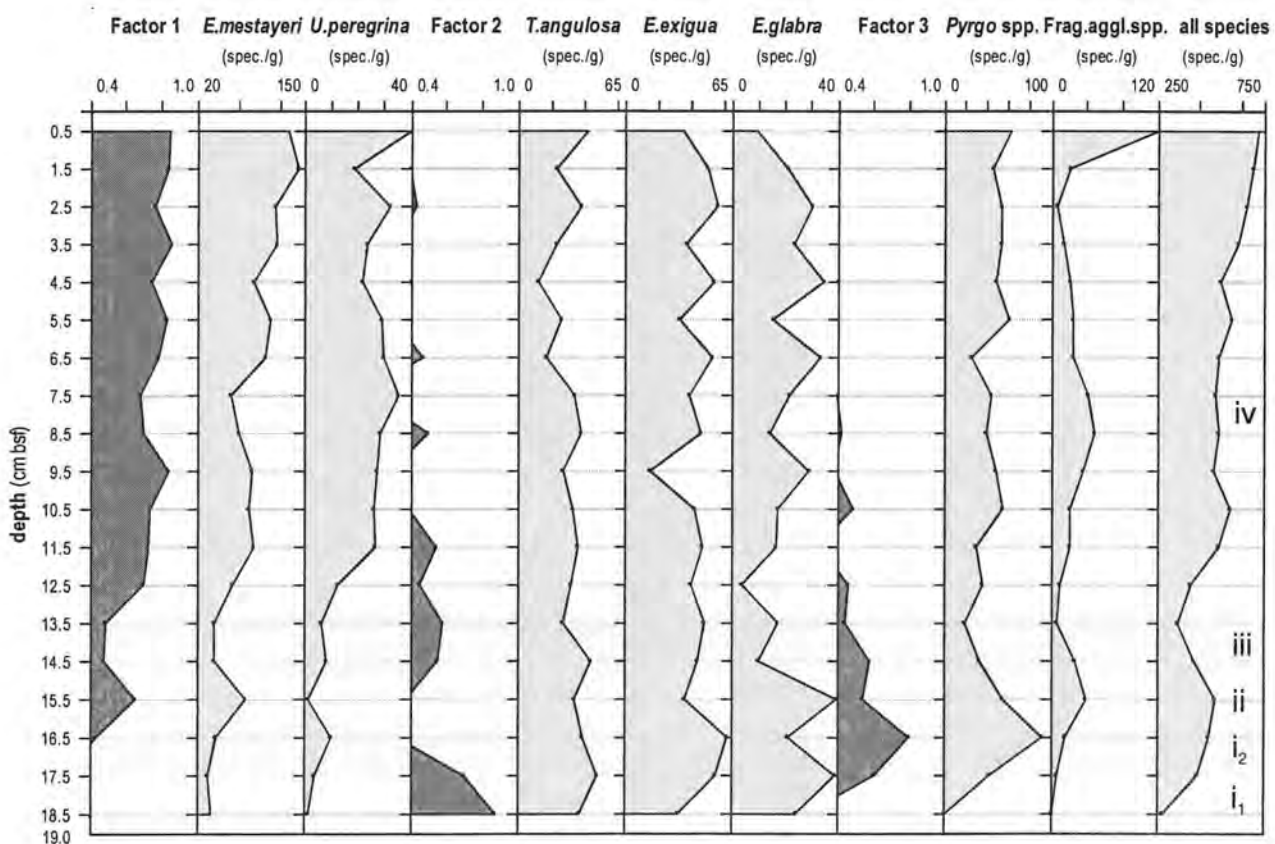


Fig. 4.8 VAR. factors 1 to 3 and abundances of resembling species in core SO136-037BX. The light grey squares indicate sections based on changes in foraminiferal fauna.

Factor 1 shows a first maximum of 0.653 at 15.5 cm bsf. Decrease leads to 0.486 at 13.5 cm bsf. Strong increase leads to 0.703 at 9.5 cm bsf. The loading varies to the absolute maximum of 0.846 at the top of the core. The abundance of *E. mestayeri* follows the trend of factor 1. A local maximum of 79.42 spec./g is located at 15.5 cm bsf. The absolute minimum of 33.56 spec./g is located at 17.5 cm bsf. The absolute maximum of 143.05 spec./g is located at 1.5 cm bsf. The abundance of *U. peregrina* also follows the trend of factor 1. Differences in this trend are local minima of 1.37 spec./g at 15.5 cm bsf and of 18.54 spec./g at 1.5 cm bsf respectively. The abundance increases to the absolute maximum of 40.48 spec./g at the top of the core. The absolute minimum of 1.44 spec./g is located at the base of the core. The loading of factor 2 decreases from the absolute maximum of 0.878 at the base of the core to 0.325 at 16.5 cm bsf. Slight increase leads to a local maximum of 0.581 at 13.5 cm bsf. Decrease with minor variations leads to 0.387 at 10.5 cm bsf. Small peaks are present at 8.5, 6.5 and 2.5 cm bsf. The abundance of *T. angulosa* is almost constant upcore. The absolute maximum of 48.32 spec./g is located at 17.5 cm bsf. Slight decrease leads to the absolute minimum of 12.72 spec./g at 4.5 cm bsf. Slight increase leads to 42.86 spec./g at the top of the core. The abundance of *E. exigua* is almost constant upcore. The absolute maximum of 62.84 spec./g is located at 16.5 cm bsf. Slight decrease leads to the absolute minimum of 15.54 spec./g at 9.5 cm bsf. Slight increase leads to 35.71 spec./g at the top of the core. The abundance of *E. glabra* shows strong variations upcore. The absolute maximum of 39.08 spec./g is located at 15.5 cm bsf. Strong decrease leads to the absolute minimum of 4.30 spec./g at 12.5 cm bsf. Slight increase leads to two local maxima of 33.63 and 34.50 spec./g at 6.5 and 4.5 cm bsf respectively. The local minimum of 15.70 spec./g between the two maxima is located at 5.5 cm bsf. Slight decrease leads to 9.52 spec./g at the top of the core. The loading of factor 3 increases from 0.225 at the base of the core to the absolute maximum of 0.789 at 16.5 cm bsf. Slight decrease leads to 0.239 at 11.5 cm bsf. Slight increase leads to 0.486 at 10.5 cm bsf. Slight decrease leads to 0.422 at 8.5 cm bsf. The factor shows no influence on the top of the core. The abundance of *Pyrgo* spp. increases strongly from 0.71 spec./g at the base of the core to the absolute maximum of 90.95 spec./g at 16.5 cm bsf. Strong decrease leads to a local minimum of 18.90 spec./g at 13.5 cm bsf. Minor variations leads to 61.90 spec./g at the top of the core. The number of fragments of agglutinating species per gram increases slightly from 6.71 spec./g at 17.5 cm bsf to 21.19 spec./g at 1.5 cm bsf. Strong increase leads to the absolute maximum of 123.80 spec./g at the top of the core. Local maxima of 14.88 and 48.76 spec./g are located at 15.5 and 8.5 cm bsf. The abundance of all counted species increases from the absolute minimum of 273.83 spec./g at the base of the core to 525.80 spec./g at 15.5 cm bsf. Slight decrease leads to a local minimum of 348.35 spec./g at 13.5 cm bsf. Slight increase leads to the absolute maximum of 723.81 spec./g at the top of the core.

4.2 CORES FROM THE SOUTH TASMAN RISE

4.2.1 Physical and physicochemical sediment properties

Description of core SO136-147BX

The length of core SO136-147BX was in the laboratory measured 2 cm shorter than noted on board.

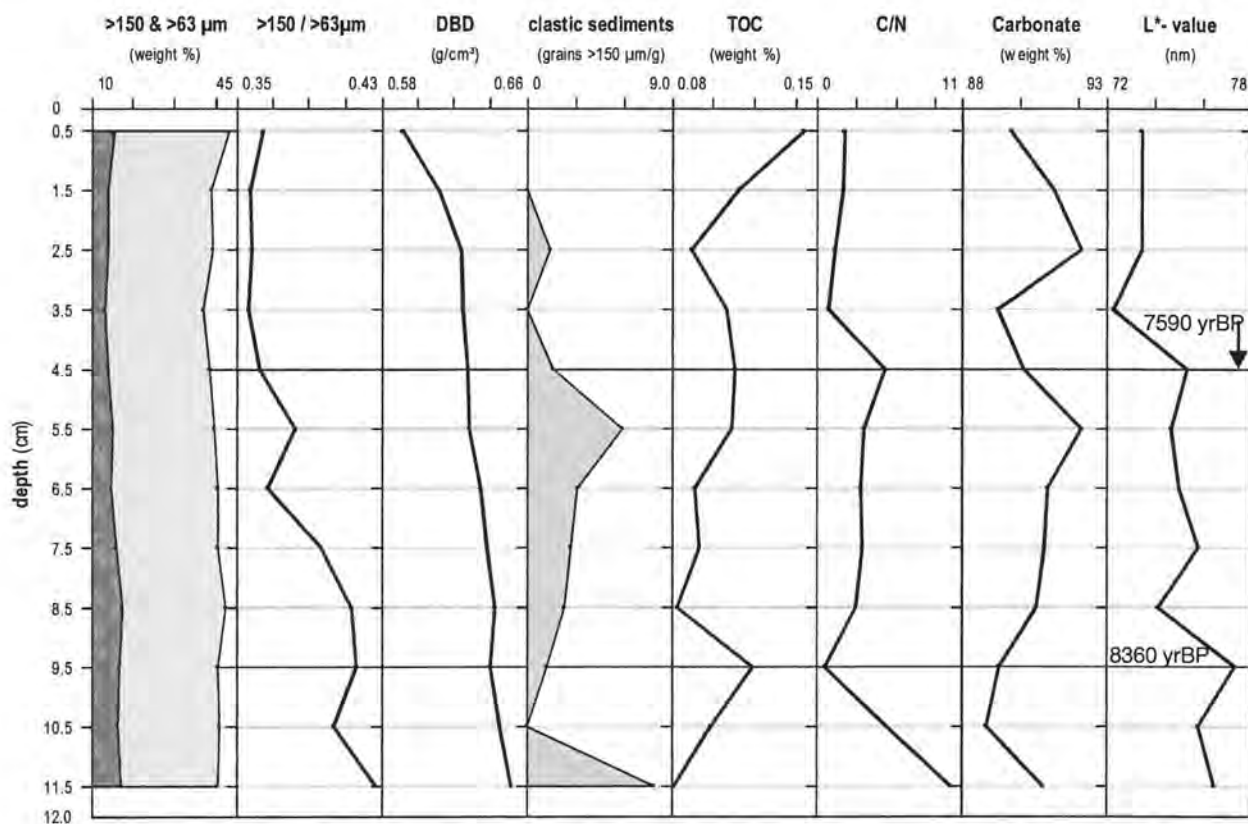


Fig. 4.9 Physical and physicochemical sediment properties of core SO136-147BX. In the first graph the dark grey area indicates $>150 \mu\text{m}$, the light grey area indicates $>63 \mu\text{m}$. The horizontal black line indicates AMS ^{14}C ages.

Grain size distribution and ratio of $>150 / >63\mu\text{m}$ subfractions:

The content of the grain fractions shows no strong variations upcore. The absolute maxima of 17.54 wt % for $>150 \mu\text{m}$ and 42.66 wt % for $>63 \mu\text{m}$ are located at 8.5 cm bsf. The absolute minima of 14 wt % and 39.14 wt % respectively are located at 1.5 cm bsf. The ratio of grain size leads to finer sizes from the absolute maximum of 0.43 at the base of the core to the absolute minimum of 0.36 at 2.5 cm bsf. Slight increase leads to 0.37 at the top of the core.

Dry bulk density:

Dry bulk density constantly decreases from the absolute maximum of 0.65 µm at the base of the base of the core to the absolute minimum of 0.52 µm at the top of the core.

Clastic sediments:

The content of clastic sediment grains decreases from the absolute maximum of 8 grains/g dry sediment at the base of the core to a first absolute minimum of 0 grains/g at 10.5 cm bsf. Slight increase leads to a content of 3 grains/g at 6.5 cm bsf. Strong increase leads to a local maximum of 6 grains/g at 5.5 cm bsf. The content decreases to 0 at 3.5 cm bsf. A small local maximum is located at 2.5 cm bsf with 1.5 grains/g. The content decreases versus 0 at 1.5 cm bsf and stays constant to the top of the core.

TOC content and C/N ratio:

The content of organic carbon shows strong increase from the absolute minimum of 0.08 wt % at the base of the core to 0.12 wt % at 9.5 cm bsf. Strong decrease leads to a local minimum of 0.09 wt % at 8.5 cm bsf. Slight increase leads to a local maximum of 0.11 at 4.5 cm bsf. Slight decrease leads to a local minimum of 0.09 wt % at 2.5 cm bsf. Strong increase leads to the absolute maximum of 0.14 wt % at the top of the core.

Strong decrease in the C/N ratio leads from the absolute maximum of 10.23 at the base of the core to the absolute minimum of 0.72 at 9.5 cm bsf. Slight increase leads to the only local maximum of 5.21 at 4.5 cm bsf. Slight decrease leads to a local minimum of 1.43 at 3.5 cm bsf. Slight increase leads to 2.11 at the top of the core.

Carbonate content:

Carbonate content decreases slightly from 90.78 wt % at the base of the core to the absolute minimum of 88.88 wt % at 10.5 cm bsf. Slight increase leads to the absolute maximum of 92.13 wt % at 5.5 cm bsf. Strong decrease leads to a local minimum of 89.24 wt % at 3.5 cm bsf. Strong increase leads to a local maximum of 92.13 wt % at 2.5 cm bsf. Slight decrease leads to 89.67 wt % at the top of the core.

Spectrophotometrical data:

The L*-value follows in the upper seven centimeter the trend of the carbonate content. Slight decrease leads from 76.49 vm at the base of the core to the absolute maximum of 77.36 vm, which is located at 9.5 cm bsf. Strong decrease leads to a local minimum of 74.17 vm at 8.5 cm bsf. Slight increase leads to a local maximum of 75.83 vm at 7.5 cm bsf. The variations are very

low to 75.35 vm at 4.5 cm bsf. Strong decrease leads to the absolute minimum of 72.33 vm at 3.5 cm bsf. Slight increase leads to 73.51 vm at the top of the core.

Description of core SO136-161BX

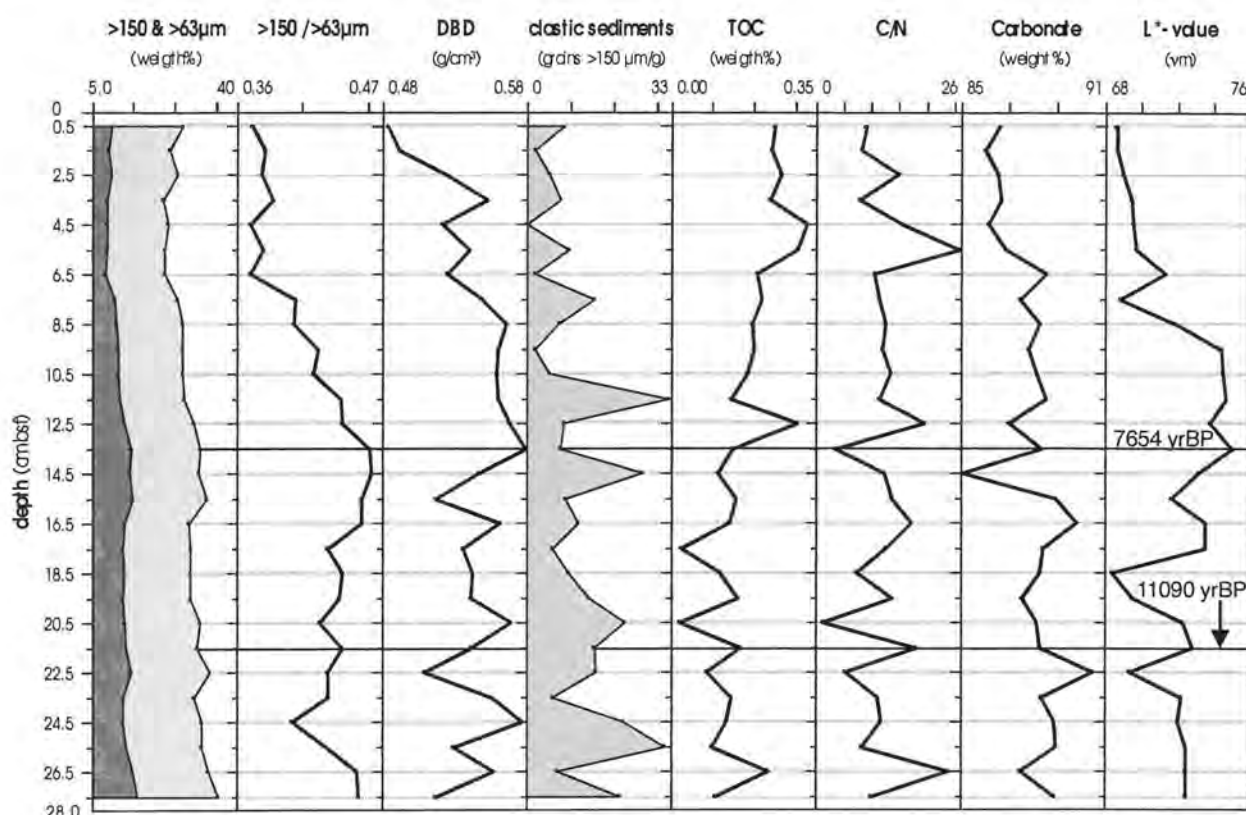


Fig. 4.10 Physical and physicochemical sediment properties of core SO136-161BX. In the first graph the dark grey area indicates $>150 \mu\text{m}$, the light grey area indicates $>63 \mu\text{m}$. The horizontal black line indicates AMS ^{14}C ages.

Grain size distribution and ratio of $>150 / >63\mu\text{m}$ subfractions:

The weight percentages of the grain fractions decrease upcore from the absolute maximum of 15.99 wt % for $>150 \mu\text{m}$ and 35.41 wt % for $>63 \mu\text{m}$ at the base of the core, to the absolute minimum of 8.69 and 22.43 wt % at 3.5 cm bsf respectively. Slight increase leads to 9.99 and 26.85 wt % at the top of the core respectively. Local maxima are located for both fractions at 22.5 cm bsf with 14.57 and 33.68 wt %, and at 15.5 cm bsf with 14.86 and 36.63 wt % respectively. The ratio leads to smaller sizes from 0.45 at the base of the core to a local minimum of 0.40 at 24.5 cm bsf. Slight increase leads to the absolute maximum of 0.46 at 14.5 cm bsf. Slight decrease leads to the absolute minimum of 0.37 at the top of the core.

Dry bulk density:

Dry bulk density shows strong variations in the lowest eight centimeter, from the absolute maximum of 0.58 g/cm^3 at 24.5 cm bsf to a local minimum of 0.51 g/cm^3 at 22.5 cm bsf. Lower variations between 0.57 and 0.56 g/cm^3 are present from 20.5 to 16.5 cm bsf. A local minimum of 0.52 g/cm^3 is at 15.5 cm bsf. Strong increase leads to a local maximum of 0.58 g/cm^3 at 13.5 cm bsf. Slight decrease leads to 0.56 g/cm^3 at 8.5 cm bsf. Strong decrease leads to the absolute minimum of 0.48 g/cm^3 at the top of the core.

Clastic sediments:

The content of clastic sediment grains per gram dry sediment shows an overall decrease upcore. The content strongly decreases from 21 grains/g at the base of the core to 7 grains/g at 26.5 cm bsf. Strong increase leads to a local maximum of 31 grains/g at 25.5 cm bsf. Strong decrease leads to a local minimum of 6 grains/g at 23.5 cm bsf. Slight increase leads to a local maximum of 23 grains/g at 20.5 cm bsf. Slight decrease leads to a local minimum of 6 grains/g at 17.5 cm bsf. Strong increase leads to a local maximum of 27 grains/g at 14.5 cm bsf. Strong decrease leads to a local minimum of 8 grains/g at 13.5 cm bsf. Strong increase leads to the absolute maximum of 32 grains/g at 11.5 cm bsf. Steep decrease leads to a local minimum of 2 grains/g at 9.5 cm bsf. Strong increase leads to a local maximum of 15 grains/g at 7.5 cm bsf. Strong decrease leads to the absolute minimum of 0 grains/g at 4.5 cm bsf. Slight increase leads to 9 grains/g at the top of the core.

TOC content and C/N ratio:

The organic carbon content slightly increases upcore. Strong increase leads from 0.10 wt % at the base of the core to a local maximum of 0.23 wt % at 26.5 cm bsf. Strong increase leads to the absolute minimum or 0.02 wt % at 20.5 cm bsf. Strong increase leads to a local maximum of 0.3 wt % at 12.5 cm bsf. Strong decrease leads to 0.15 wt % at 11.5 cm bsf. Slight increase leads to the absolute maximum of 0.33 wt % at 4.5 cm bsf. Slight decrease leads to 0.25 wt % at the top of the core.

The C/N ratio mainly follows the trend of the TOC content. An exception is a local minimum of 3.54 at 13.5 cm bsf. The absolute minimum of 1.20 is located at 20.5 cm bsf. The absolute maximum of 25.97 is located at 5.5 cm bsf.

Carbonate content:

Slight increase leads from a local minimum of 87.46 wt % at 26.5 cm bsf to the absolute maximum of 90.04 wt % at 21.5 cm bsf. Slight decrease leads to a local minimum of 87.57 wt %

at 19.5 cm bsf. Slight increase leads to a local maximum of 89.86 wt % at 16.5 cm bsf. Strong decrease leads to the absolute minimum of 85.10 wt % at 14.5 cm bsf. Strong increase leads to a local maximum of 87.04 wt % at 13.5 cm bsf. Strong increase leads to a local minimum of 87.04 wt % at 12.5 cm bsf. Slight increase leads to a local maximum of 88.56 wt % at 6.5 cm bsf. Slight decrease leads to 86.61 wt % at the top of the core.

Spectrophotometrical data:

The L*-value decreases from 72.49 vm at the base of the core to 69.37 vm at 21.5 cm bsf. Strong increase leads to a local maximum of 69.53 vm at 21.5 cm bsf. Strong decrease leads to the absolute minimum of 68.38 vm at 18.5 cm bsf. Strong increase leads to the absolute maximum of 75.10 vm at 13.5 cm bsf. Slight decrease leads to a local minimum of 68.88 vm at 7.5 cm bsf. Strong increase leads to a local maximum of 71.35 vm at 6.5 cm bsf. Slight decrease leads to 68.69 vm at the top of the core.

Description of core SO136-165BX

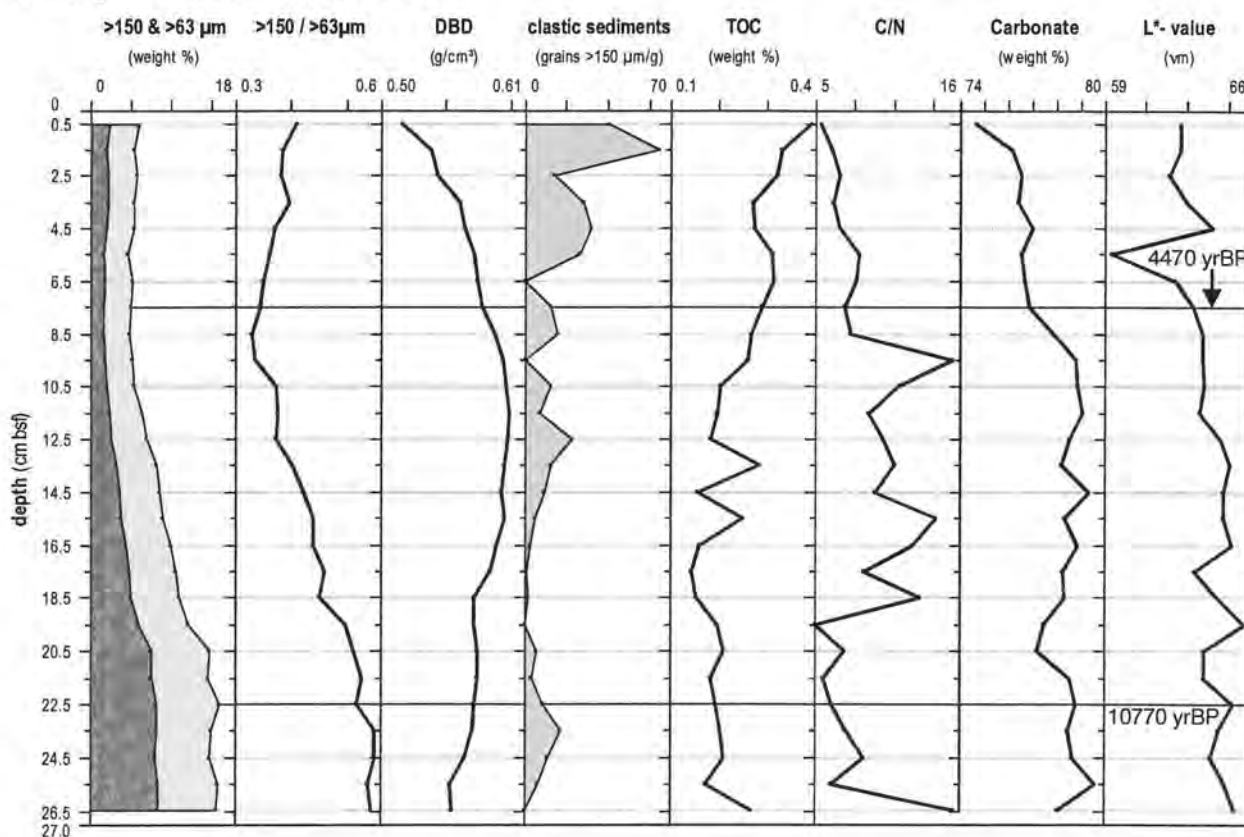


Fig. 4.11 Physical and physicochemical sediment properties of core SO136-165BX. In the first graph the dark grey area indicates >150 µm, the light grey area indicates >63 µm. The horizontal black line indicates AMS ¹⁴C ages.

Grain size distribution and ratio of >150 / >63 μ m subfractions:

The weight percentages of the coarse fractions decrease upcore. The absolute maximum is located at 25.5 cm bsf with 8.57 wt % for >150 and with 15.94 wt % for >63 μ m. The content stays almost constant to 7.60 and 14.87 wt % at 20.5 cm bsf respectively. Slight decrease leads to the absolute maximum of 1.72 and 4.77 wt % respectively at 5.5 cm bsf. The content stays almost constant to 2.45 and 6.01 wt % respectively at the top of the core. The ratio constantly decreases from the absolute maximum of 0.55 wt% at 23.5 cm bsf to the absolute minimum of 0.33 wt% at 8.5 cm bsf. Slight increase leads to 0.40 wt% at the top of the core.

Dry bulk density:

Dry bulk density constantly increases from 0.55 g/cm³ at the base of the core to the absolute maximum of 0.59 g/cm³ at 10.5 cm bsf. Constant decrease leads to the absolute minimum of 0.52 g/cm³ at the top of the core.

Clastic sediments:

The content of clastic sediment grains per gram dry sediment increases upcore. Slight increases leads from 0 to 17 grains/g at 23.5 cm bsf. Slight decrease leads to the next absolute minimum of 0 grains/g at 19.5 cm bsf. Slight increase followed by slight decrease leads to the next absolute minimum at 17.5 cm bsf. Slight increase leads to a local maximum of 23 grains/g at 12.5 cm bsf. Strong decrease leads to the next absolute minimum at 9.5 cm bsf. Strong increase leads to a local maximum of 16 grains/g at 8.5 cm bsf. Strong decrease leads to the next absolute minimum at 6.5 cm bsf. Strong increase leads to a local maximum of 32 grains/g at 4.5 cm bsf. Slight decrease leads to a local minimum of 14 grains/g at 2.5 cm bsf. Strong increase leads to the absolute maximum of 65 grains/g at 1.5 cm bsf. Strong decrease leads to 40 grains/g at the top of the core.

TOC content and C/N ratio:

The content of organic carbon increases upcore. Strong variations are present between 15.5 and 12.5 cm bsf. Strong decrease leads from 0.27 wt % at the base of the core to a local minimum of 0.17 wt % at 25.5 cm bsf. Slight increase leads to a local maximum of 0.21 wt % at 20.5 cm bsf. Slight decrease leads to the absolute maximum of 0.14 wt % at 17.5 cm bsf. Strong increase leads to a local maximum of 0.25 wt % at 15.5 cm bsf. Strong decrease leads to a local minimum of 0.16 wt % at 14.5 cm bsf. Strong increase leads to a local maximum of 0.28 wt % at 13.5 cm bsf. Strong decrease leads to a local minimum of 0.19 wt % at 12.5 cm bsf. Slight increase leads

to a local maximum of 0.31 wt % at 6.5 cm bsf. Slight decrease leads to a local minimum of 0.27 at 3.5 cm bsf. Slight increase leads to the absolute maximum of 0.39 wt % at the top of the core.

Strong decrease in the C/N ratio leads from the absolute maximum of 15.56 at the base of the core to a local minimum of 6.29 at 25.5 cm bsf. Strong increase leads to a local maximum of 8.74 at 24.5 cm bsf. Slight decrease leads to a local minimum of 5.12 at 19.5 cm bsf. Strong increase leads to a local maximum of 12.96 at 18.5 cm bsf. Strong decrease leads to a local minimum of 8.73 at 17.5 cm bsf. Strong increase leads to a local maximum of 14.28 at 15.5 cm bsf. Strong decrease leads to a local minimum of 9.62 at 14.5 cm bsf. The ratio stays almost constant to 9.12 at 11.5 cm bsf. Strong increases leads to a local maximum of 15.43 at 9.5 cm bsf. Strong decrease leads to a local minimum of 7.28 at 7.5 cm bsf. Slight decrease leads to the absolute minimum of 5.39 at the top of the core.

Carbonate content:

The carbonate content decreases upcore. Strong increase leads from 78.09 wt % at the base of the core to the absolute maximum of 79.66 wt % at 25.5 cm bsf. Slight decrease leads to a local minimum of 77.24 wt % at 20.5 cm bsf. Slight decrease leads to a local maximum of 79.37 wt % at 14.5 cm bsf. Slight decrease leads to the absolute minimum of 74.37 wt % at the top of the core.

Spectrophotometrical data:

The spectrophotometrical values show slight decrease upcore. Slight decrease leads from 65.31 vm at the base of the core to a local minimum of 63.85 vm at 21.5 and 20.5 cm bsf. Strong increase leads to a local maximum of 65.83 vm at 19.5 cm bsf. Strong decrease leads to a local minimum of 65.43 vm at 17.5 cm bsf. Strong increase leads to a local maximum of 65.17 vm at 16.5 cm bsf. Slight decrease leads to 62.5 vm at 6.5 cm bsf. Strong decrease leads to the absolute minimum of 59.36 vm at 5.5 cm bsf. Strong increase leads to a local maximum of 64.23 vm at 4.5 cm bsf. Slight decrease leads to 62.66 vm at the top of the core.

4.2.2 $\delta^{18}\text{O}$ and $\delta^{13}\text{C}$ stable isotope ratios, AMS ^{14}C radiocarbon dating

Table 4 Calibrated AMS ^{14}C ages of the cores from the South Tasman Rise.

Core number	Depth (cm bsf)	Conventional age (yr. BP)	Calibrated and corrected age(s) (calendar yr. BP)
SO136-147BX	4.5	7160 ± 55	7590
SO136-147BX	9.5	7950 ± 70	8360
SO136-161BX	7.5	4360 ± 40	7654
SO136-161BX	22.5	9925 ± 55	$11090, [10940], [10830]$
SO136-165BX	13.5	7240 ± 90	4470
SO136-165BX	21.5	10160 ± 55	10770

Description of core SO136-147BX

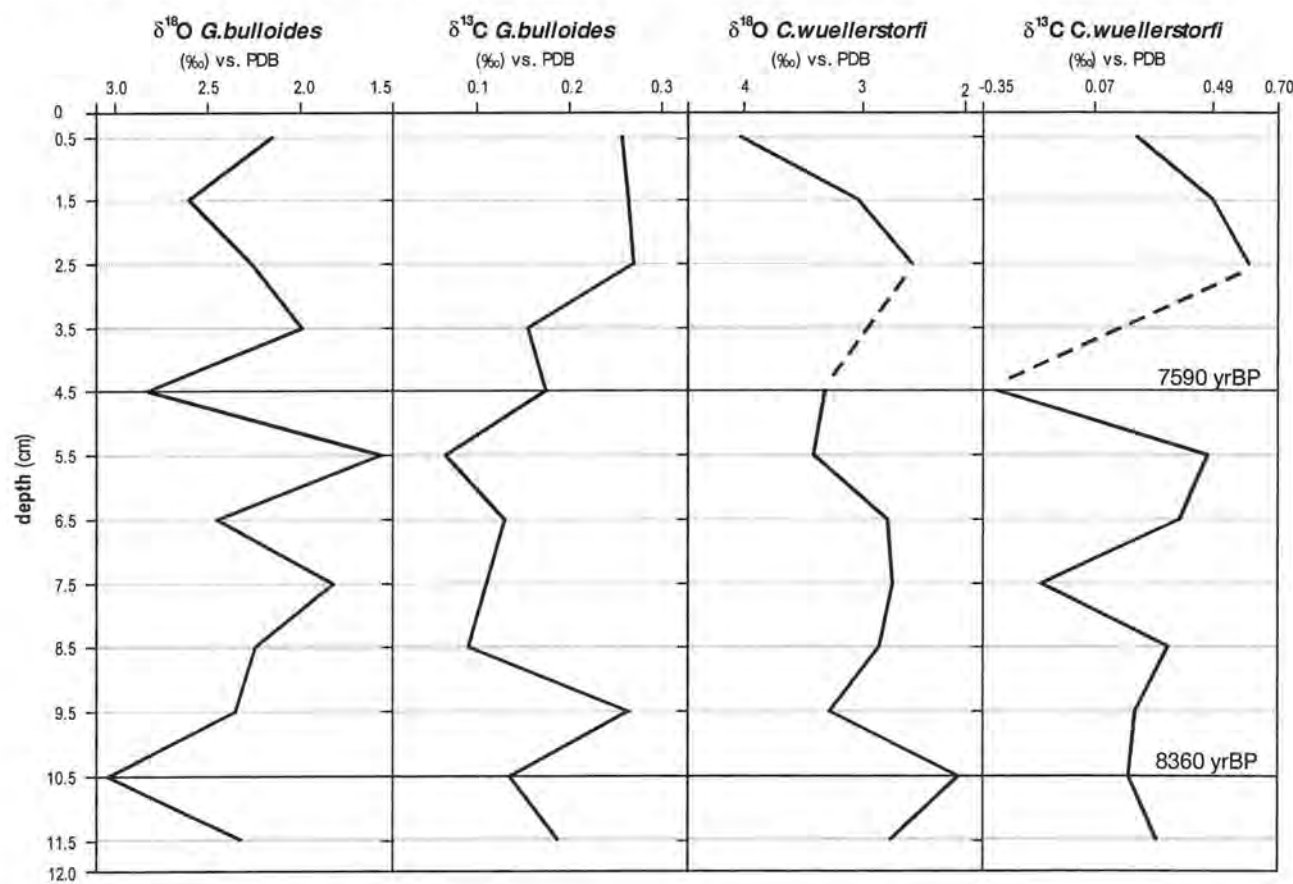


Fig. 4.12 Stable isotope ratios of benthic and planktic foraminifera tests in core SO136-147BX. The horizontal black line indicates AMS ^{14}C ages. The black line indicates AMS ^{14}C ages in years before present.

*δ^8O and $\delta^{13}C$ stable isotope ratio of planktic foraminifera (*G. bulloides*):*

The ratio shows strong variations with a general depleting trend upcore. Strong increase leads from 2.33 ‰ vs. PDB at the base of the core to the absolute maximum of 3.04 ‰ vs. PDB at 10.5 cm bsf. Strong depletion leads to a local minimum of 1.83 ‰ vs. PDB at 7.5 cm bsf. Strong increase leads to a local maximum of 2.45 ‰ vs. PDB at 6.5 cm bsf. Strong depletion leads to the absolute minimum of 1.57 ‰ vs. PDB at 5.5 cm bsf. Strong increase leads to a local maximum of 2.83 ‰ vs. PDB at 4.5 cm bsf. Strong depletion leads to a local minimum of 2.00 ‰ vs. PDB at 3.5 cm bsf. Slighter increase leads to a local maximum of 2.60 ‰ vs. PDB at 1.5 cm bsf. Strong depletion leads to 2.16 ‰ vs. PDB at the top of the core. Strong depletion in the $\delta^{13}C$ ratio leads from 0.18 ‰ vs. PDB at the base of the core to a local minimum of 0.10 ‰ vs. PDB at 10.5 cm bsf. Strong increase leads to a local maximum, which is a single spike of 0.30 ‰ vs. PDB at 9.5 cm bsf. Double measurement of this sample revealed a value of 0.37 ‰ vs. PDB. Strong depletion leads to a local minimum of 0.03 ‰ vs. PDB at 8.5 cm bsf. Slight increase leads to 0.09 ‰ vs. PDB at 6.5 cm bsf. Strong depletion leads to the absolute minimum of -0.01 ‰ vs. PDB at 5.5 cm bsf. Strong increase leads to the absolute maximum of 0.31 ‰ vs. PDB at 2.5 cm bsf. Slight decrease leads to 0.29 ‰ vs. PDB at the top of the core.

 *δ^8O and $\delta^{13}C$ stable isotope ratio of benthic foraminifera (*C. wuellerstorfi*):*

Strong depletion leads from 2.53 ‰ vs. PDB at the base of the core to the absolute minimum of 1.96 ‰ vs. PDB at 10.5 cm bsf. Strong increase leads to a local maximum of 3.04 ‰ vs. PDB at 9.5 cm bsf. Slight depletion leads to a local minimum of 2.56 ‰ vs. PDB at 6.5 cm bsf. Slight increase leads to a local maximum of 3.18 ‰ vs. PDB at 5.5 cm bsf. Slight depletion leads to a local minimum of 2.43 ‰ vs. PDB at 2.5 cm bsf. The value of 2.5 cm bsf is missing as the measurement revealed a value of -287.77 ‰ vs. PDB. Only one foraminifera specimen was found in this sample. The mass spectrometer reveals far too low values if the amount of carbonate is too low (see Chapter 3.2.3). Strong increase leads to 3.80 ‰ vs. PDB at the top of the core. Slight variations in the $\delta^{13}C$ ratio lead from 0.27 ‰ vs. PDB at the base of the core over a local minimum of 0.17 ‰ vs. PDB at 10.5 cm bsf to a local maximum of 0.31 ‰ vs. PDB at 8.5 cm bsf. Strong depletion leads to a local minimum of -0.14 ‰ vs. PDB at 7.5 cm bsf, which forms a single spike. Strong increase leads to a local maximum of 0.45 ‰ vs. PDB at 5.5 cm bsf. Strong depletion leads to the absolute minimum of -0.30 ‰ vs. PDB at 4.5 cm bsf. Strong increase leads to the absolute maximum of 0.60 ‰ vs. PDB at 2.5 cm bsf. Slight depletion leads to 0.20 ‰ vs. PDB at the top of the core.

Description of core SO136-161BX

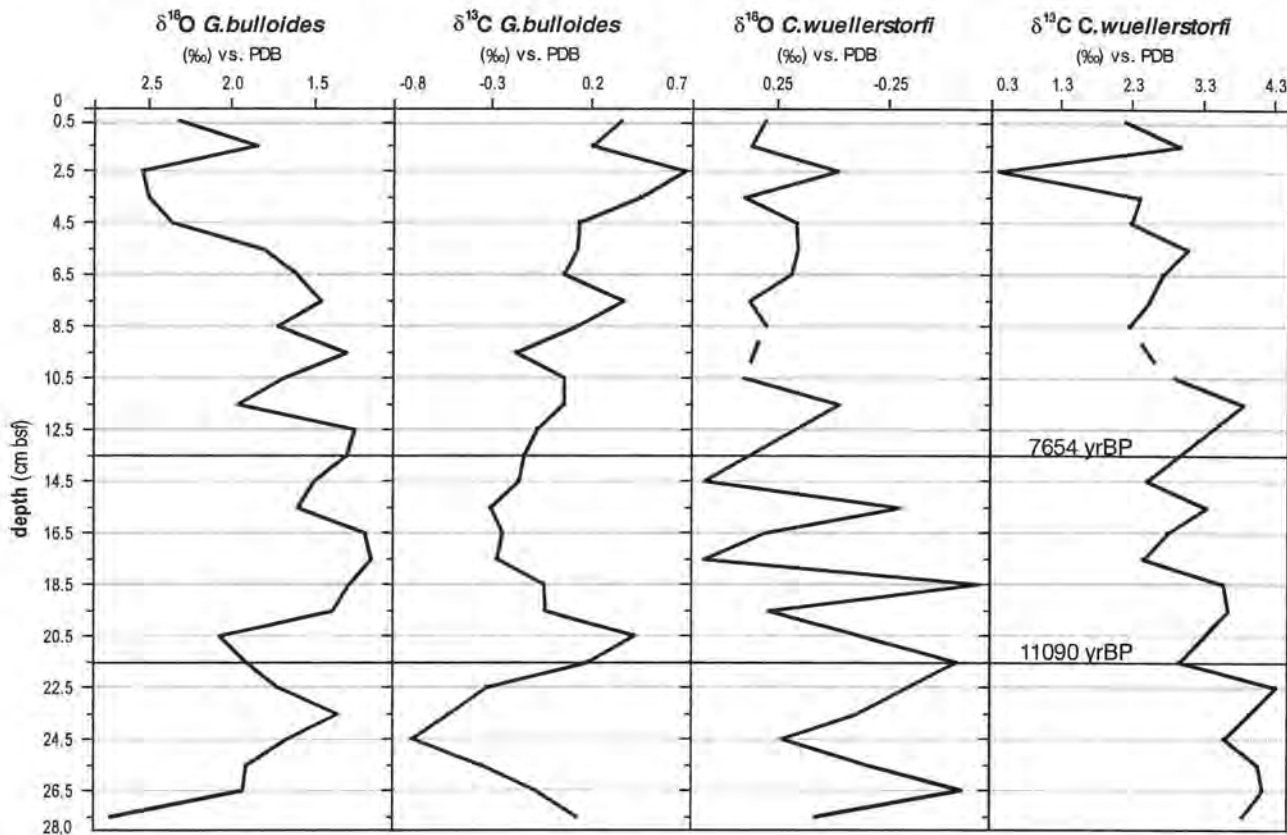


Fig. 4.13 Stable isotope ratios of benthic and planktic foraminifera tests in core SO136-161BX. The horizontal black line indicates AMS ¹⁴C ages in years before present.

$\delta^{18}\text{O}$ and $\delta^{13}\text{C}$ stable isotope ratio of planktic foraminifera (*G. bulloides*):

Strong depletion leads from the absolute maximum of 2.67 ‰ vs. PDB at the base of the core to a local minimum of 1.31 ‰ vs. PDB at 23.5 cm bsf. Strong increase leads to a local maximum of 2.02 ‰ vs. PDB at 20.5 cm bsf. Strong depletion leads to the absolute minimum of 1.10 ‰ vs. PDB at 17.5 cm bsf. Strong increase leads to a local maximum of 1.55 ‰ vs. PDB at 15.5 cm bsf. Slighter depletion leads to a local minimum of 1.20 ‰ vs. PDB at 12.5 cm bsf. Strong increase leads to a local maximum of 1.91 ‰ vs. PDB at 11.5 cm bsf. Strong depletion leads to a local minimum of 1.26 ‰ vs. PDB at 9.5 cm bsf. Strong increase leads to a local maximum of 1.67 ‰ vs. PDB at 8.5 cm bsf. Strong depletion leads to a local minimum of 1.41 ‰ vs. PDB at 7.5 cm bsf. Slighter increase leads to a local maximum of 2.48 ‰ vs. PDB at 2.5 cm bsf. Strong depletion leads to a local minimum of 1.80 ‰ vs. PDB at 1.5 cm bsf. Strong increase leads to 2.27 ‰ vs. PDB at the top of the core.

The trend of $\delta^{13}\text{C}$ follows mainly the trend of $\delta^{18}\text{O}$; exceptions are missing of local minima at 15.5 and 11.5 cm bsf. Strong depletion leads from 0.13 ‰ vs. PDB at the base of the core to the absolute minimum of -0.70 ‰ vs. PDB at 24.5 cm bsf. Slighter increase leads to a local maximum of 0.42 ‰ vs. PDB at 20.5 cm bsf. Slighter depletion leads to a local minimum

of -0.30 ‰ vs. PDB at 15.5 cm bsf. Slight variations lead to a local maximum of 0.06 ‰ vs. PDB at 11.5 and 10.5 cm bsf. Strong depletion leads to a minimum of -0.18 ‰ vs. PDB at 9.5 cm bsf. Strong increase leads to a local maximum of 0.36 ‰ vs. PDB at 7.5 cm bsf. Strong decrease leads to a local minimum of 0.06 ‰ vs. PDB at 6.5 cm bsf. Slight depletion leads to 0.14 ‰ vs. PDB at 4.5 cm bsf. Strong depletion leads to the absolute maximum of 0.67 ‰ vs. PDB at 2.5 cm bsf. Strong depletion leads to a local minimum of 0.20 ‰ vs. PDB at 1.5 cm bsf. Strong increase leads to 0.35 ‰ vs. PDB at the top of the core.

*δ^8O and $\delta^{13}C$ stable isotope ratio of benthic foraminifera (*C. wuellerstorfi*):*

The ratio increases upcore, with strong variations in the lower 11 cm before sea floor. Strong depletion leads from 0.05 ‰ vs. PDB at the base of the core to a local minimum of -0.61 ‰ vs. PDB at 26.5 cm bsf. Strong increase leads to a local maximum of 0.20 ‰ vs. PDB at 24.5 cm bsf. Slighter depletion leads to a local minimum of -0.59 ‰ vs. PDB at 21.5 cm bsf. Strong increase leads to a local maximum of 0.26 ‰ vs. PDB at 19.5 cm bsf. Strong depletion leads to the absolute minimum of -0.69 ‰ vs. PDB at 18.5 cm bsf. Strong increase leads to the first absolute maximum of 0.55 ‰ vs. PDB at 17.5 cm bsf. Strong decrease leads to a local minimum of -0.33 ‰ vs. PDB at 15.5 cm bsf. Strong increase leads to the second absolute maximum of 0.55 ‰ vs. PDB at 14.5 cm bsf. Slighter depletion leads to a local minimum of -0.06 ‰ vs. PDB at 11.5 cm bsf. Strong increase leads to a local maximum of 0.37 ‰ vs. PDB at 10.5 cm bsf. The value of 9.5 cm bsf is missing due to an analyser failure. A second measurement was not possible due to too less benthic foraminifera in the sample. Slight depletion leads to 0.14 ‰ vs. PDB at 4.5 cm bsf. Strong increase leads to a local maximum of 0.37 ‰ vs. PDB at 3.5 cm bsf. Strong depletion leads to a local minimum of -0.05 ‰ vs. PDB at 2.5 cm bsf. Strong increase leads to a local maximum of 0.34 ‰ vs. PDB at 1.5 cm bsf. Slight depletion leads to 0.28 ‰ vs. PDB at the top of the core. The ratio of $\delta^{13}C$ shows slight depletion upcore. Slight depletion leads from 3.88 ‰ vs. PDB at the base of the core to 2.52 ‰ vs. PDB at 14.5 cm bsf. The ratio varies between the absolute maximum of 4.43 ‰ vs. PDB at 22.5 cm bsf and 2.49 ‰ vs. PDB at 17.5 cm bsf. Strong increase leads to a local maximum of 3.87 ‰ vs. PDB at 11.5 cm bsf. Slighter depletion leads to a local minimum of 2.26 ‰ vs. PDB at 6.5 cm bsf. The value of 9.5 cm bsf is missing due to an analyser failure. A second measurement was not possible due to too less benthic foraminifera in the sample. Strong increase leads to a local maximum of 3.08 ‰ vs. PDB. The value of 9.5 cm bsf is missing due to an analyser failure. A second measurement was not possible due to too less benthic foraminifera in the sample at 5.5 cm bsf. Strong decrease leads to the absolute minimum of 0.42 ‰ vs. PDB at 2.5 cm bsf, which consists of a single

spike. Strong increase leads to a local maximum of 2.98 ‰ vs. PDB at 1.5 cm bsf. Strong decrease leads to 2.21 ‰ vs. PDB at the top of the core.

Description of core SO136-165BX

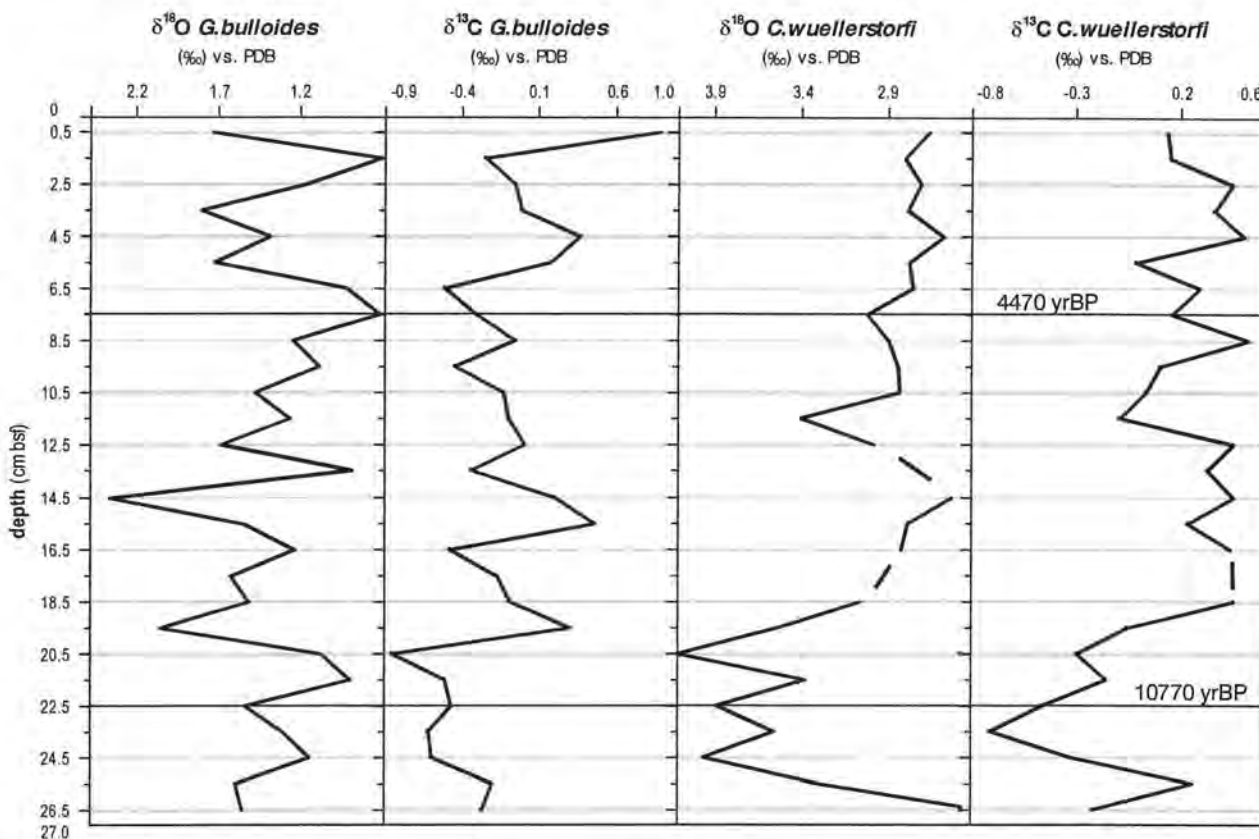


Fig. 4.14 Stable isotope ratios of benthic and planktic foraminiferal tests in core SO136-165BX. The horizontal black lines indicate AMS ^{14}C ages in years before present.

$\delta^{18}\text{O}$ and $\delta^{13}\text{C}$ stable isotope ratio of planktic foraminifera (*G. bulloides*):

Strong depletion leads from 1.68 ‰ vs. PDB at the base of the core to a local minimum of 1.26 ‰ vs. PDB at 24.5 cm bsf. Slighter increase leads to a local maximum of 1.66 ‰ vs. PDB at 22.5 cm bsf. Strong depletion leads to a local minimum of 1.01 ‰ vs. PDB at 21.5 cm bsf. Slighter increase leads to a local maximum of 2.17 ‰ vs. PDB at 19.5 cm bsf. Slight depletion with minor variations leads to a local minimum of 1.35 ‰ vs. PDB at 16.5 cm bsf. Strong increase leads to the absolute maximum of 2.48 ‰ vs. PDB at 14.5 cm bsf. Strong depletion leads to a local minimum of 1.00 ‰ vs. PDB at 13.5 cm bsf. Strong increase leads to a local maximum of 1.81 ‰ vs. PDB at 12.5 cm bsf. Slight depletion with minor variations leads to a local minimum of 0.84 ‰ vs. PDB at 7.5 cm bsf. Strong increase leads to two local maxima of 1.84 and 1.93 ‰ vs. PDB at 5.5 and 3.5 cm bsf respectively. The two maxima are parted by a local minimum of 1.04 ‰ vs. PDB at 4.5 cm bsf. Strong depletion leads to the absolute minimum of 0.83 ‰ vs. PDB at 1.5 cm bsf. Strong increase leads to 1.85 ‰ vs. PDB at the top

of the core. The ratio of $\delta^{13}\text{C}$ trends roughly parallel to the $\delta^{18}\text{O}$ curve. Strong depletion leads from -0.26 ‰ vs. PDB at the base of the core to a local minimum of -0.61 ‰ vs. PDB at 23.5 cm bsf. Slighter increase leads to a local maximum of -01.46 ‰ vs. PDB at 22.5 cm bsf. Strong depletion leads to the absolute minimum of -0.84 ‰ vs. PDB at 20.5 cm bsf. Strong increase leads to a local maximum of 0.31 ‰ vs. PDB at 19.5 cm bsf. Slight depletion with minor variations leads to a local minimum of -0.47 ‰ vs. PDB at 16.5 cm bsf. Strong increase leads to a local maximum of 2.48 at 15.5 cm bsf. Slighter depletion leads to a local minimum of -0.34 ‰ vs. PDB at 13.5 cm bsf. Strong increase leads to a local maximum of 0.01 ‰ vs. PDB at 12.5 cm bsf. Slight depletion with minor variations leads to a local minimum of -0.44 ‰ vs. PDB at 9.5 cm bsf. Strong increase leads to a local maximum of -0.05 ‰ vs. PDB at 8.5 cm bsf. Slighter decrease leads to a local minimum of -0.50 ‰ vs. PDB at 6.5 cm bsf. Slighter increase leads to a local maximum of 0.37 ‰ vs. PDB at 4.5 cm bsf. Slighter depletion leads to a local minimum of -0.24 ‰ vs. PDB at 1.5 cm bsf. Strong increase leads to 0.89 ‰ vs. PDB at the top of the core.

$\delta^{18}\text{O}$ and $\delta^{13}\text{C}$ stable isotope ratio of benthic foraminifera (*C. wuellerstorfi*):

The ratio of $\delta^{18}\text{O}$ shows three phases: strong increase from the absolute minimum of 2.29 ‰ vs. PDB at the base of the core to a local maximum of 3.90 ‰ vs. PDB at 24.5 cm bsf. The ratio stays relative constant to 20.5 cm bsf. Slight decrease leads with slight variations from 24.5 cm bsf to a local minimum of 3.31 ‰ vs. PDB at 19.5 cm bsf. Strong increase leads to the absolute maximum of 4.05 ‰ vs. PDB at 20.5 cm bsf. Strong depletion leads to 2.99 ‰ vs. PDB at 18.5 cm bsf, the ratio stays relative constant to top of the core. From 18.5 cm bsf, slight decrease leads to a local minimum of 2.46 ‰ vs. PDB at 14.5 cm bsf. The value of 17.5 cm bsf is missing due to an analyser failure. Slight increase leads to a local maximum of 3.34 ‰ vs. PDB at 11.5 cm bsf. Strong depletion leads to a local minimum of 2.76 ‰ vs. PDB at 10.5 cm bsf. Slight increase leads to a local maximum of 2.95 ‰ vs. PDB at 7.5 cm bsf. Slight depletion leads to a local minimum of 2.51 ‰ vs. PDB at 4.5 cm bsf. Slight increase leads with slight variations to 2.59 ‰ vs. PDB at the top of the core. The ratio of $\delta^{13}\text{C}$ mainly anticorrelates with the $\delta^{18}\text{O}$ ratio. An exception is the strong increase from -0.21 ‰ vs. PDB at the base of the core to a local maximum of 0.26 ‰ vs. PDB at 26.5 cm bsf. Strong depletion leads to the absolute minimum of -0.7 ‰ vs. PDB at 23.5 cm bsf. Strong increase leads to 0.46 ‰ vs. PDB at 18.5 cm bsf. The ratio stays almost constant to 0.46 ‰ vs. PDB at 12.5 cm bsf. Strong depletion leads to a local minimum of -0.09 ‰ vs. PDB at 11.5 cm bsf. Slighter increase leads to the absolute maximum of 0.53 ‰ vs. PDB at 8.5 cm bsf. Strong depletion leads with minor variations to a local minimum of -0.01 ‰ vs. PDB at 5.5 cm bsf. Strong increase leads to a local maximum of 0.50 ‰ vs. PDB at 4.5 cm bsf. Slight depletion leads to 0.14 ‰ vs. PDB at the top of the core.

4.2.3 Analysis of benthic foraminiferal assemblages

The abundance of foraminifera species and the trend of varimax factors, which are used in the discussion in Chapter 5.2, are described here. The complete paleontological data set is given in appendix A3. The output of the Q-mode Factor Analysis is given in appendix A4. Factor loadings of >0.4 are shown to outline the significance range of the factor.

Description of core SO136-147BX

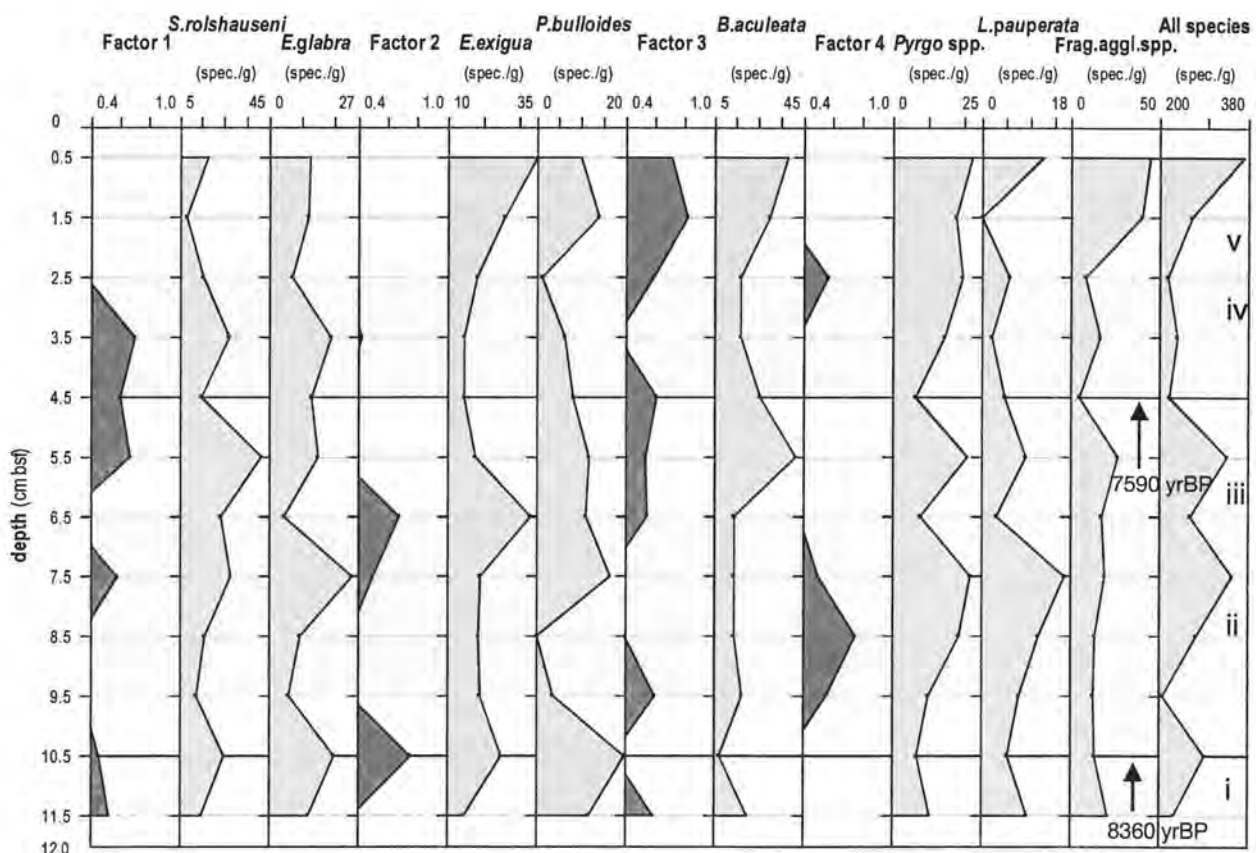


Fig. 4.15 VAR. factor 1 to 4 and abundances of resembling species in core SO136-147BX. The horizontal black lines indicate AMS ^{14}C ages in years before present. The light grey squares indicate sections based on changes in foraminiferal fauna.

The loading of factor 1 decreases from 0.542 at the base of the core to 0.338 at 9.5 cm bsf. Short influence of 0.580 is present at 7.5 cm bsf. Slight decrease leads to 0.230 at 6.5 cm bsf. Slight increase leads to the last phase of influence from 5.5 to 2.5 cm bsf. The absolute maximum of 01.702 is located at 3.5 cm bsf. The abundance of *S. rolshauseni* increases slightly with minor variations from 14.54 spec./g at the base of the core to the absolute maximum of 41.87 spec./g at 5.5 cm bsf. Slight decrease leads to the absolute minimum of 8.02 spec./g at 1.5 cm bsf. Slight increase leads to 17.60 spec./g at the top of the core. The abundance of *E. glabra* shows three

maxima: 19.81 spec./g at 10.5 cm bsf, the absolute maximum of 25.04 spec./g at 7.5 cm bsf and a slighter maximum of 18.99 spec./g at 3.5 cm bsf. Minima of 6.37 spec./g, 4.74 spec./g and 7.13 spec./g are located at 9.5 cm bsf, 6.5 cm bsf and 2.5 cm bsf respectively. The loading of factor 2 is significant for this core at 10.5 cm bsf and at 6.5 cm bsf with 0.757 and 0.677 respectively. Very slight influence of 0.430 is present at 3.5 cm. The abundance of *E. exigua* follows the trend of factor 2 and shows maxima of 25.22 spec./g at 10.5 cm bsf and of 33.20 spec./g at 6.5 cm bsf. Slight decrease leads to a local minimum of 14.63 spec./g at 3.5 cm bsf. Slight increase leads to 35.22 spec./g at the top of the core. The absolute minimum is located at the base of the core with 14.54 spec./g. The abundance of *P. bulloides* has the absolute maximum of 19.81 spec./g at 10.5 cm bsf. Strong decrease leads to the absolute minimum of 0 spec./g at 8.5 cm bsf. Strong increase leads to a local maximum of 16.69 spec./g at 7.5 cm bsf. Slight decrease leads to a local minimum of 1.42 spec./g at 2.5 cm bsf. Strong increase leads to a local maximum of 14.03 spec./g at 2.5 cm bsf. Slight decrease leads to 10.06 spec./g at the top of the core. The loading of factor 3 shows strong decrease from 0.591 at the top of the core to 0.321 at 10.5 cm bsf. Strong increase leads to 0.604 at 9.5 cm bsf. Slight decrease leads to 0.392 at 8.5 cm bsf. Slight increase leads to 0.615 at 4.5 cm bsf. Strong decrease leads to 0.344 at 3.5 cm bsf. Strong increase leads to 0.822 at 1.5 cm bsf. Slight decrease leads to 0.713 at the top of the core. The abundance of *B. aculeata* shows the absolute minimum of 7.21 spec./g at 10.5 cm bsf. Slight increase leads to 14.23 spec./g at 6.5 cm bsf. Strong increase leads to the absolute maximum of 41.87 spec./g at 5.5 cm bsf. Slight decrease leads to 17.11 spec./g at 2.5 cm bsf and slight increase to 37.73 spec./g at the top of the core. Factor 4 shows two phases of influence: Between 9.5 and 6.5 cm bsf with the absolute maximum of 0.733 at 8.5 cm bsf. The second influence is present at 2.5 cm bsf with a factor loading of 0.570. The abundance of the taxon *Pyrgo* spp. shows slight increase from 10.58 spec./g at the base of the core to 22.26 spec./g at 7.5 cm bsf. Slight decrease leads to a local minimum of 7.90 spec./g at 6.5 cm bsf. Strong increase leads to 20.93 spec./g at 5.5 cm bsf. Strong decrease leads to 6.50 at 4.5 cm bsf. Slight increase leads to 22.64 spec./g at the top of the core. The abundance of *L. pauperata* follows roughly the trend of the taxa *Pyrgo* spp. Slight increase leads to the absolute maximum of 16.69 spec./g at 7.5 cm bsf. Strong decrease leads to 3.16 spec./g at 6.5 cm bsf. Slight increase leads to a local maximum of 8.197 spec./g at 5.5 cm bsf. Slight decrease leads to the absolute minimum of 0 spec./g at 1.5 cm bsf. Strong increase leads to 12.57 spec./g at the top of the core. The number of fragments of agglutinating species increases slowly from 21.15 spec./g at the base of the core to 26.91 spec./g at 5.5 cm bsf. Slight decrease leads to the absolute minimum of 4.87 spec./g at 4.5 cm bsf. Strong increase leads to 45.28 spec./g at the top of the core. The abundance of all counted species increases from 230.08 spec./g at the base of the core to 291.89 spec./g at 10.5 cm bsf. Strong decrease leads to

207.64 spec./g at 10.5 cm bsf. Strong increase leads to 347.82 spec./g at 7.5 cm bsf. Strong decrease leads to 264.03 spec./g at 6.5 cm bsf. Strong increase leads to 337.94 spec./g at 5.5 cm bsf. Strong decrease leads to 221.13 spec./g at 4.5 cm bsf. Slight decrease leads to the absolute minimum of 218.18 spec./g at 2.5 cm bsf. Strong increase leads to the absolute maximum of 372.32 spec./g at the top of the core.

Description of core SO136-161BX

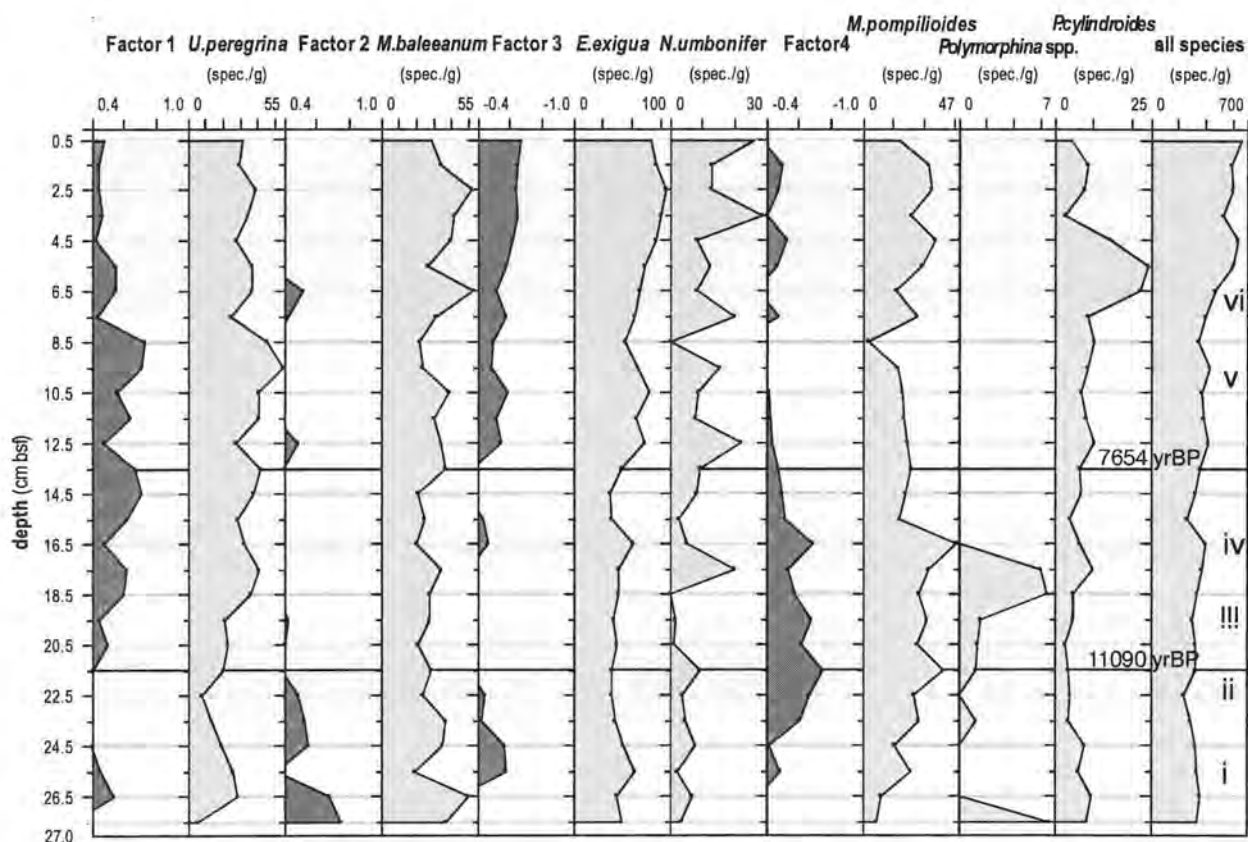


Fig. 4.16 VAR. factor 1 to 4 and abundances of resembling species in core SO136-161BX. The horizontal black lines indicate AMS ^{14}C ages in years before present. The light grey squares indicate sections based on changes in foraminiferal fauna.

The loading of factor 1 shows a small peak of 0.528 loading at 26.5 cm bsf. Slight increase leads with Strong variations from 0.401 at 21.5 cm bsf to the absolute maximum of 0.733 at 8.5 cm bsf. Slight decrease leads to 0.438 at 4.5 cm bsf. The loading stays almost constant to 0.477 at the top of the core. The abundance of *U. peregrina* follows roughly the trend of factor 1. The absolute minimum of 4.96 spec./g is located at the base of the core. Strong increase leads to a peak of 28.44 spec./g at 26.5 cm bsf. Slight decrease leads to 8.06 spec./g at 22.5 cm bsf. Slight increase with major variations leads to the absolute maximum of 54.64 spec./g at 9.5 cm bsf. Slight decrease leads to 30.78 spec./g at the top of the core. The loading of factor 2 decreases

from 0.733 at the base of the core to 0.360 at 25.5 cm bsf. Strong increase leads to 0.558 at 24.5 cm bsf. Slight decrease leads to 0.380 at 21.5 cm bsf. Slight influences of 0.403 and 0.510 are present at 13.5 and 6.5 cm bsf. The abundance of *M. baleeanum* is almost stable upcore. Maxima of 49.77, of 53.06 and of 51.94 spec./g are located at 26.5, 6.5 and 2.5 cm bsf respectively. The absolute minimum of 129.04 spec./g is located at 25.5 cm bsf. The loading of factor 3 shows a peak of -0.562 at 25.5 cm bsf. The next peak of -0.435 is located at 16.5 cm bsf. Slight increase lead from -0.366 at 13.5 cm bsf to -0.658 at the top of the core. The abundance of *E. exigua* shows a continuously increasing trend from 49.69 spec./g at the base of the core to 81.32 spec./g at the top of the core. Slight maxima of 63.49, 62.17 and the absolute maximum of 96.10 spec./g is located at 25.5, 16.5 and 2.5 cm bsf respectively. The abundance of *N. umbonifer* shows strong variations and a general increasing trend. Slight variations are present from 3.31 spec./g at the base of the core to 0 spec./g at the absolute minimum at 18.5 cm bsf. Slight increase to 26.37 spec./g at the top of the core is accompanied by strong variations. Maxima of 20.15, 22.13 and 28.66 spec./g are located at 17.5, 12.5 and 3.5 cm bsf respectively. A second absolute minimum is located at 8.5 cm bsf. The loading of factor 4 shows slight increase from -0.494 at 25.5 cm bsf to the absolute maximum of -0.751 at 21.5 cm bsf. Slight decrease with a local maximum of -0.692 at 16.5 cm bsf leads to -0.423 at 10.5 cm bsf. Slight peaks of -0.494, -0.536 and -0.512 are present at 7.5, 4.5 and 1.5 cm bsf respectively. The abundance of *M. pompiliooides* shows strong increase from 6.62 spec./g at the base of the core to the absolute maximum of 45.76 spec./g at 16.5 cm bsf. Strong decrease leads to 17.94 spec./g at 15.5 cm bsf. Slight decrease leads to the absolute minimum of 2.56 spec./g at 8.5 cm bsf. Strong increase leads to 17.58 spec./g at the top of the core. The abundance of *F. contemplata* shows strong variation upcore. Strong decrease leads from 6.62 spec./g at the base of the core to 0 spec./g at 26.5 cm bsf. Slight increase leads from 1.21 spec./g at 24.5 cm bsf to 1.59 at 19.5 cm bsf. Strong increase leads to the absolute maximum of 6.52 spec./g at 18.5 cm bsf. Strong decrease leads from 6.04 spec./g at 17.5 cm bsf to 0 spec./g at 16.5 cm bsf. The abundance of *P. cylindroides* stays constant upcore. It leads from 8.28 v at the base of the core to 8.84 spec./g at 7.5 cm bsf. Strong increase leads to the absolute maximum of 24.54 spec./g at 5.5 cm bsf. Strong decrease leads to the absolute minimum of 2.06 spec./g at 3.5 cm bsf. Slight increase leads to 4.39 spec./g at the top of the core. The abundance of all counted species shows a general increasing trend upcore. The abundance increases from 337.88 spec./g at the base of the core to the absolute maximum of 654.94 spec./g at the top of the core. The absolute minimum of 299.84 spec./g is located at 22.5 cm bsf.

Description of core SO136-165BX

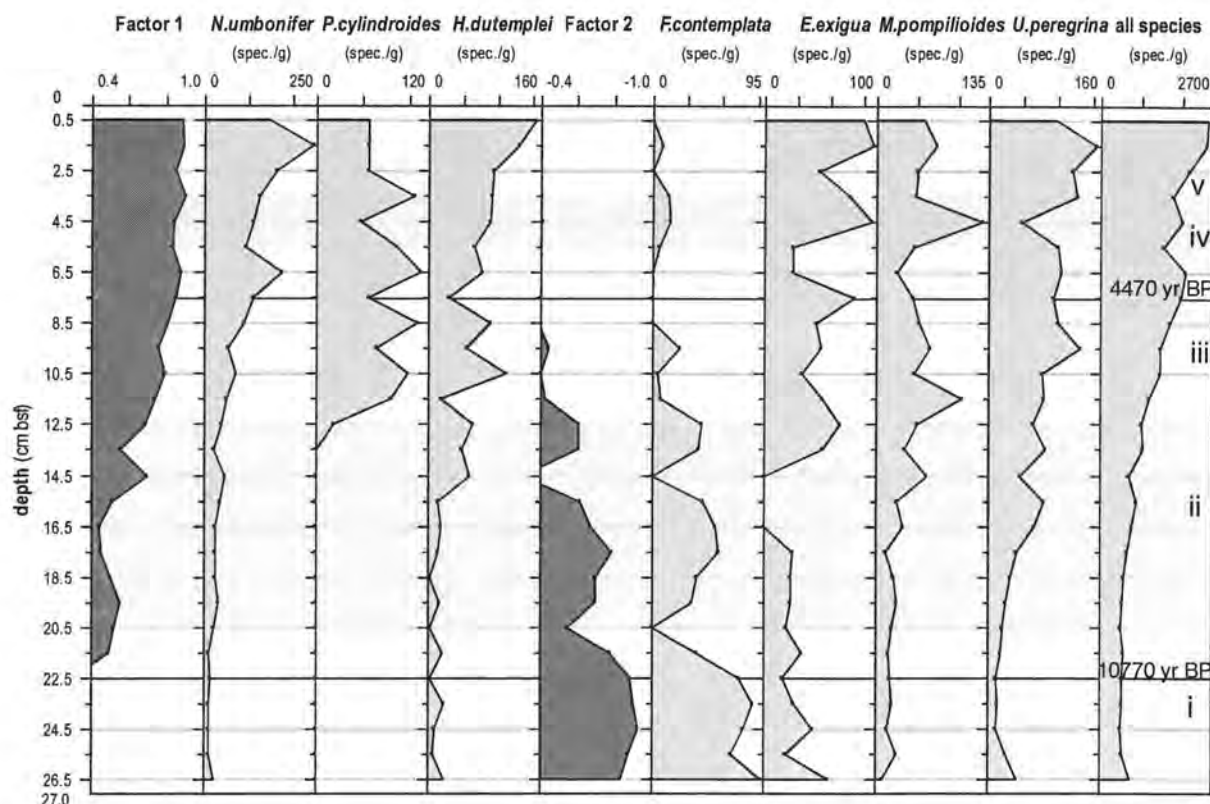


Fig. 4.17 VAR. factor 1 and 2 and abundances of resembling species in core SO136-165BX. The horizontal black lines indicate AMS ^{14}C ages in years before present. The light grey squares indicate sections based on changes in foraminiferal fauna.

The loading of factor 1 increases slightly from 0.489 at 21.5 cm bsf to 0.512 at 15.5 cm bsf. Strong increase leads to the absolute maximum of 0.898 at 1.5 cm bsf. The abundance of *N. umbonifer* follows roughly the trend of factor 1. Very slight increase leads from 23.30 spec./g at the base of the core to 56.14 spec./g at 9.5 cm bsf. Strong increase leads to a local maximum of 173.91 spec./g at 6.5 cm bsf. Strong decrease leads to 93.33 spec./g at 55. cm bsf. Strong increase leads to the absolute maximum of 244.89 spec./g at 1.5 cm bsf. Strong decrease leads to 146.93 spec./g at the top of the core. The abundance of *P. cylindroides* shows strong variations. It increases very steep from 19.04 spec./g at 13.5 cm bsf to 98.92 spec./g at 10.5 cm bsf. The abundance leads with strong variations to the absolute maximum of 113.04 at 6.5 cm bsf. Strong decrease leads from 105.26 spec./g at 3.5 cm bsf to 57.14 spec./g at 2.5 cm bsf. The abundance is constant to top of core. The abundance of *H. dutemplei* varies slightly from 23.30 spec./g at the base of the core to 15.38 spec./g at 15.5 cm bsf. Strong increase leads to a local maximum of 111.82 spec./g at 10.5 cm bsf. The rise in abundance is accompanied by a local minimum of 19.04 spec./g at 11.5 cm bsf. The abundance stays stable to 92.86 spec./g at 2.5 cm bsf. A local

minimum of 31.25 spec./g is present at 7.5 cm bsf. Strong increase leads to the absolute maximum of 155.10 spec./g at the top of the core. The loading of factor 1 decreases slightly from -0.838 at the base of the core to -0.605 at 12.5 cm bsf. The slight decrease is interrupted by minima of -0.548 and -0.294 at 20.5 and 14.5 cm bsf respectively. Strong decrease leads from 12.5 cm bsf to -0.430 at 11.5 cm bsf. The abundance of *F. contemplata* follows the trend of factor 2. The absolute maximum of 93.20 spec./g is located at the base of the core. Two minima of 0 spec./g are located at 20.5 and 14.5 cm bsf respectively. Small abundance is present between 5.5 and 1.5 cm bsf with a local maximum of 16.00 spec./g at 4.5 cm bsf. The abundance of *E. exigua* is slightly decreasing from 58.25 spec./g at the base of the core to 26.66 spec./g at 17.5 cm bsf. Strong increase leads from 0 spec./g at 14.5 cm bsf to 52.17 spec./g at 13.5 cm bsf. Slight decrease leads over a local maximum of 81.25 spec./g at 7.5 cm bsf to 26.66 spec./g at 5.5 cm bsf. Strong increase leads to a local maximum of 77.19 spec./g at 3.5 cm bsf. Strong decrease leads to a local minimum of 50.00 spec./g at 2.5 cm bsf. Strong increase leads to the absolute maximum of 97.96 spec./g at 1.5 cm bsf. Slight decrease leads to 89.79 spec./g at the top of the core. The abundance of *M. pompiliooides* increases slightly from 7.76 spec./g at the base of the core to 52.28 spec./g at 8.5 cm bsf. A single abundance peak of 65.49 spec./g is present at 9.5 cm bsf. Slight decrease leads to 26.08 spec./g at 6.5 cm bsf. Strong increase leads to the absolute maximum of 128.00 spec./g at 4.5 cm bsf. Strong decrease leads to 50.00 spec./g at 3.5 cm bsf. Slight increase leads to 57.14 spec./g at the top of the core. The abundance of *U. peregrina* increases slowly from the base of the core to a local maximum of 130.99 spec./g at 9.5 cm bsf. A local minimum of 45.90 spec./g at 14.5 cm bsf is anti-correlating with a local maximum of *M. pompiliooides*. Strong decrease leads from 99.35 spec./g at 8.5 cm bsf to a local minimum of 48.00 spec./g at 4.5 cm bsf. This minimum is anti-correlating with the absolute maximum of *M. pompiliooides*. Strong increase leads to the absolute maximum of 155.10 spec./g at 1.5 cm bsf. Strong decrease leads to 97.96 spec./g at the top of the core. The abundance of all counted species increases continuously from 737.86 spec./g at the base of the core to 2069.56 spec./g at 6.5 cm bsf. Slight decrease leads to a local minimum of 1540.00 spec./g at 4.5 cm bsf. Strong increase leads to the absolute maximum of 2595.92 spec./g at the top of the core.

5 DISCUSSION

5.1 Age model

5.1.1 General notes on the measured $\delta^{18}\text{O}$ stable isotope ratios.

The age model is based on the correlation of AMS ^{14}C ages and $\delta^{18}\text{O}$ stable isotope ratios. The carbonate tests of foraminifera reflect the isotopic ratio of their environment (Niebler, 1995). The $\delta^{18}\text{O}$ isotope ratio of seawater in the open ocean is dependent on the isotopic ratio of precipitation, which is influenced by storage of $\delta^{16}\text{O}$ in the waxing and waning global ice shields (Shackleton, 1973, 1987). Additionally it is dependent on regional temperature, which influences the amount of evaporation and isotopic fractionating of hydrogen and water (Epstein et al., 1953; McCrea, 1950; Urey, 1947). Vital effects cause variations in the ratio between different species.

A comparison of $\delta^{18}\text{O}$ isotope ratios from the Northern and Southern Hemisphere by Blunier et al. (1998) indicates a lag in the Greenland warming events of 1000 to 2500 yr. to the Antarctic counterparts for the period of 47000 to 23000 yr. before present (BP). Contrarily Steig et al. (1998) describes synchronous climate changes indicated by $\delta^{18}\text{O}$ isotope ratios from the North Atlantic and Antarctica. For the late Pleistocene and Holocene epoch Labracherie et al. (1989) shows the offset between the hemispheres as confined to the time span between 12000 to 10000 yr. before present. Tyson and Lindesay (1992) report counterparts of the northern hemispheres Little Ice Age and the Medieval Warm Period for southern Africa.

A correlation of the $\delta^{18}\text{O}$ stable isotope ratios of the investigated cores with $\delta^{18}\text{O}$ ratios from other high resolutional Holocene cores was not possible. A maximal correlation factor of 1.49 was achieved using the program AnalySeries by Paillard et al. (1996). The software was downloaded from <ftp://ftp-lmce.cea.fr/incoming/paillard/AnalySeries>. The investigated data included cores from the Southern Hemisphere (Ciais et al., 1992; Jouzel et al., 1995; Steig et al., 1998; Stuiver and Grootes, 1999), from the Southern Ocean in particular (Brathauer and Abelmann, 1999; Labracherie et al., 1989; McCorkle et al., 1998; Wells and Conell, 1997) and from the Northern Hemisphere (Alley et al., 1997; Pflaumann and Zhimini, 1999; von Grafenstein et al., 1999). The resolution of the cores investigated in this study turned out to be not sufficient, due to comparatively low overall sedimentation rates in the research area.

A correlation of the investigated cores with each other is presented in Fig. 5.1, p. 54 and discussed in the following chapter. Evidence for several erosional events and / or hiatuses is present in the investigated cores and discussed in Chapter 5.1.4, p. 58. No absolute radiocarbon ages are available for the cores from the eastern Campbell Plateau yet.

5.1.2 Core-correlation based on AMS ages

The objective of the model is to correlate patterns in the $\delta^{18}\text{O}$ ratio in the investigated cores with each other, with additional support of the AMS ^{14}C ages, as outlined in Fig. 5.1. The dashed lines indicate corresponding depths in the correlated cores. The model indicates only relative positions of the dated samples and does not imply the transfer of absolute ages from one core to another.

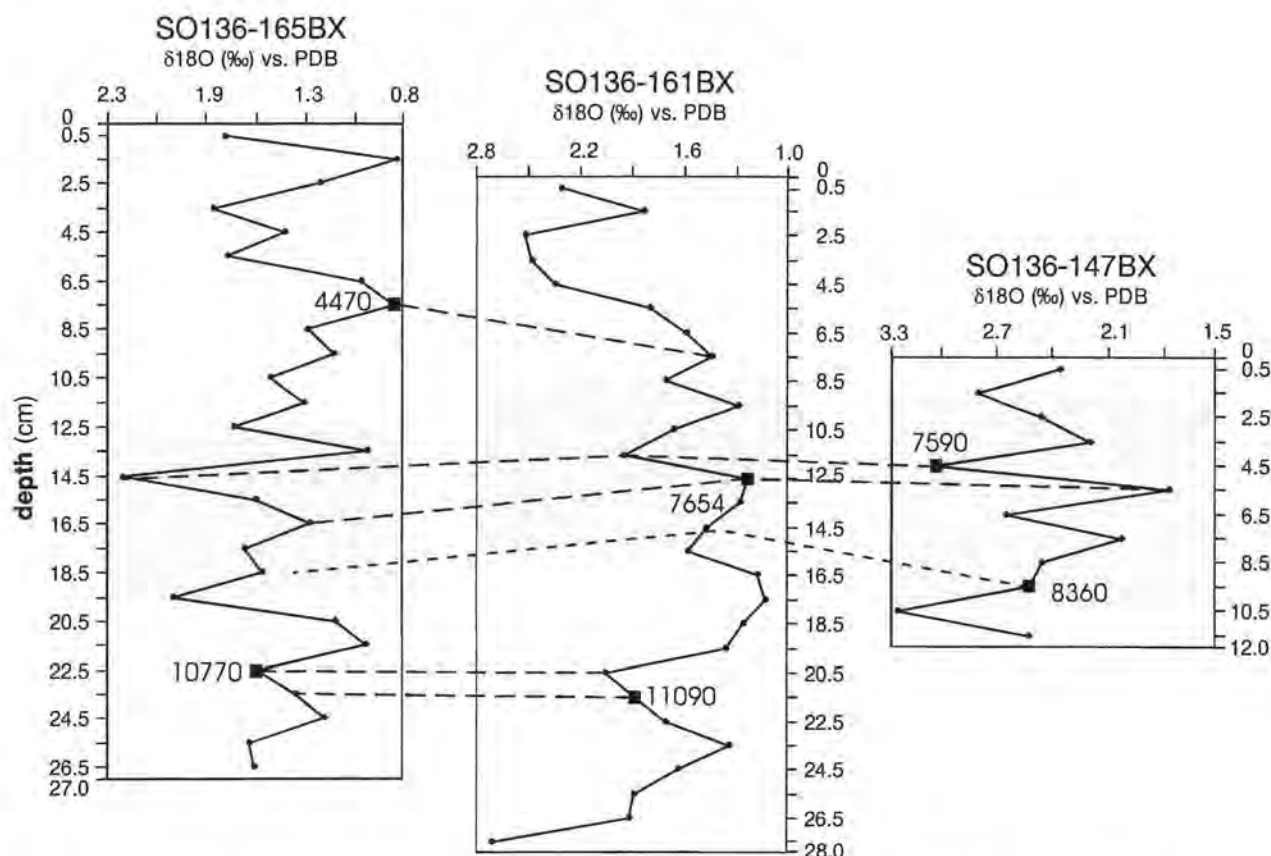


Fig. 5.1 Correlation of the cores from the South Tasman Rise with each other. The grey squares mark a similar pattern in the $\delta^{18}\text{O}$ values, which occurs in all cores. The dashed lines indicate other corresponding patterns.

The highest AMS ages in core SO136-165BX (10770 yr. BP) and SO136-161BX (11090 yr. BP) indicate a corresponding maximum in the isotopic ratios between 23.5 to 22.5 and 21.5 and 20.5 cm bsf respectively. The age of core SO136-161BX hits a ^{14}C plateau (see Chapter 4.2.2, p. 41 and Table 4, p. 41). The correlation of the highest age of core SO136-147BX (8360 yr. BP) with the two other cores is based on similar trends in the $\delta^{18}\text{O}$ ratios and on the position of a "Cold Event" as discussed in Chapter 5.1.3, following page. The correlation of the two youngest ages in the cores SO136-161BX (7654 yr. BP) and -147BX (7590 yr. BP) reveals a corresponding increase in the isotope ratio at 12.5 to 11.5 and 5.5 to 4.5 cm bsf respectively. The correlation with core SO136-165BX is based on similar patterns in the $\delta^{18}\text{O}$ ratio. To mention is the strong

variation in the $\delta^{18}\text{O}$ ratio of $\sim 1\text{‰}$ in 1 cm sediment depth, which might indicate sedimentary discontinuities and processes of redeposition at this depths. The correlations of the youngest age in core SO136-165BX (4470 yr. BP) with core SO136-161BX is based on a similar depletion in the $\delta^{18}\text{O}$ ratio.

5.1.3 Correlation of Holocene climate changes

The model is related to the core-correlation based on radiocarbon ages as outlined in Fig. 5.1 and Chapter 5.1.2 previous page. The timing of the climatic events follows mainly the correlation of the $\delta^{18}\text{O}$ ratios with the global average temperature variations (Folland et al., 1990) and the dating of certain events as discussed below.

The end of the last deglaciation in the Antarctic is described as a two-step process with two warming trends interrupted by a cold reversal. The maximum of the latter, the Antarctic Cold Reversal (ACR) is set to ~ 12500 yr. BP (Jouzel et al., 1995), indicating a lead in the Antarctic climate of ~ 1000 compared to the Northern Hemisphere. Such a lead has also been observed for this time span in the Southern Ocean by Labracherie et al. (1989). This event might correlate with the first increase of $\delta^{18}\text{O}$ after the end of depletion from the base of the core. However, the AMS measurements of the cores SO136-161BX and -165BX indicate younger ages for this phase. The phase corresponds with the global average temperature variations given by Folland et al. (1990) and with the timing of the Younger Dryas in the Northern Hemisphere, as recorded e.g. in the GRIP (Johnsen et al., 1992) and GISP 2 (Alley et al., 1993) Greenland ice cores. There the termination was set at 11550 ± 70 and 11640 ± 250 yr. BP respectively. This cooling event at ~ 11000 yr. BP is also documented by Weaver et al. (1998), by investigation of planktic foraminifera in cores from the Chatham Rise, east of New Zealand.

An early Holocene climate optimum from 10000 to 7500 yr. BP with a progressive return to colder climate at 6000 yr. BP is recorded in Antarctica's Vostok and Dome C ice cores (Ciais et al., 1992). The beginning of the Holocene climate optimum is also recorded in the Southern Ocean by Labracherie et al. (1989). This climate optimum can be traced in the investigated cores from the South Tasman Rise. Also the $\delta^{18}\text{O}$ stable isotope ratio of this phase is similar to the average global temperature curve, as outlined in Figure 5.2, p. 57. However, the Holocene climate optimum appears to be overprinted by several oscillations. The record in the sediments might be interrupted by erosional events and hiatuses or disturbed by redeposition and resuspension in the process of sedimentation. In the cores SO136-165BX and -161BX, the beginning of the climate optimum is set to 21.5 and 17.5 cm bsf respectively. Relying on the

youngest radiocarbon age, measured in core SO136-165BX at 7.5 cm bsf, the climate optimum follows the global average temperature variations and extends to 4470 yr. BP.

The longer extend of the climate optimum and an additional "Cold Event" at ~8000 yr. BP is described in ice cores from the Northern Hemisphere by von Grafenstein (1999) and in the ocean by Klitgaard-Kristensen et al. (1998). A "Cold Event" at 8000 to 8400 yr. BP is also documented in ice cores from Greenland and Antarctica and is correlated for both hemispheres by Alley et al. (1997). This event is in accordance with an increase in the $\delta^{18}\text{O}$ ratio in all cores: In core SO136-147BX the beginning of the "Cold Event" is indicated by depletion of the $\delta^{18}\text{O}$ ratio at 10.5 cm bsf and ends in the maximal depletion at 5.5 cm bsf. In core SO136-161BX, the increase of the $\delta^{18}\text{O}$ ratio starts at 10.5 cm bsf and ends at 5.5 cm bsf. An AMS age of 7654 yr. BP is available for the end of this event at 12.5 cm bsf. In core SO136-165BX a "Cold Event" is recorded in the sediment by depletion in the $\delta^{18}\text{O}$ ratio between 20.5 and 16.5 cm bsf, this observation is supported by the occurrence of dropstones (>4 mm diameter) at 17.5 cm bsf. No AMS ages are available for this phase.

All three cores show a next maximum in $\delta^{18}\text{O}$ ratio, which even surpasses the previously described "Cold Event". No resembling cold event has been found in the cited literature or in other isotope curves. This "Unconfirmed Cold Event" is dated with 7590 yr. BP at 4.5 cm bsf in core SO136-147BX.

This event is followed by a sudden depletion in $\delta^{18}\text{O}$, which leads to a local minima at 3.5 cm bsf in core SO136-147BX, at 9.5 cm bsf in core -161BX and 13.5 cm bsf in core SO136-165BX respectively. This trend is recorded in all three cores. However, the high variations in the $\delta^{18}\text{O}$ values (1.2 ‰ in core SO136-147BX, 1.6 ‰ in core -161BX and 1.3 ‰ in core -165BX) in this short time and depth interval might indicate a non-linear sedimentation rate and a disturbed $\delta^{18}\text{O}$ signal. The maximal depletion might resemble the warm event between 8000 and 6400 yr. BP, which is described by Weaver et al. (1998) in cores from New Zealand. This observation would be consistent with the description of the end of the cold event, described by Alley et al. (1997), if the maximum in between the two events would be not considered. However, the resolution of the cores is not sufficient to conclude if the variations are due to sedimentational discordances or due to climatical changes.

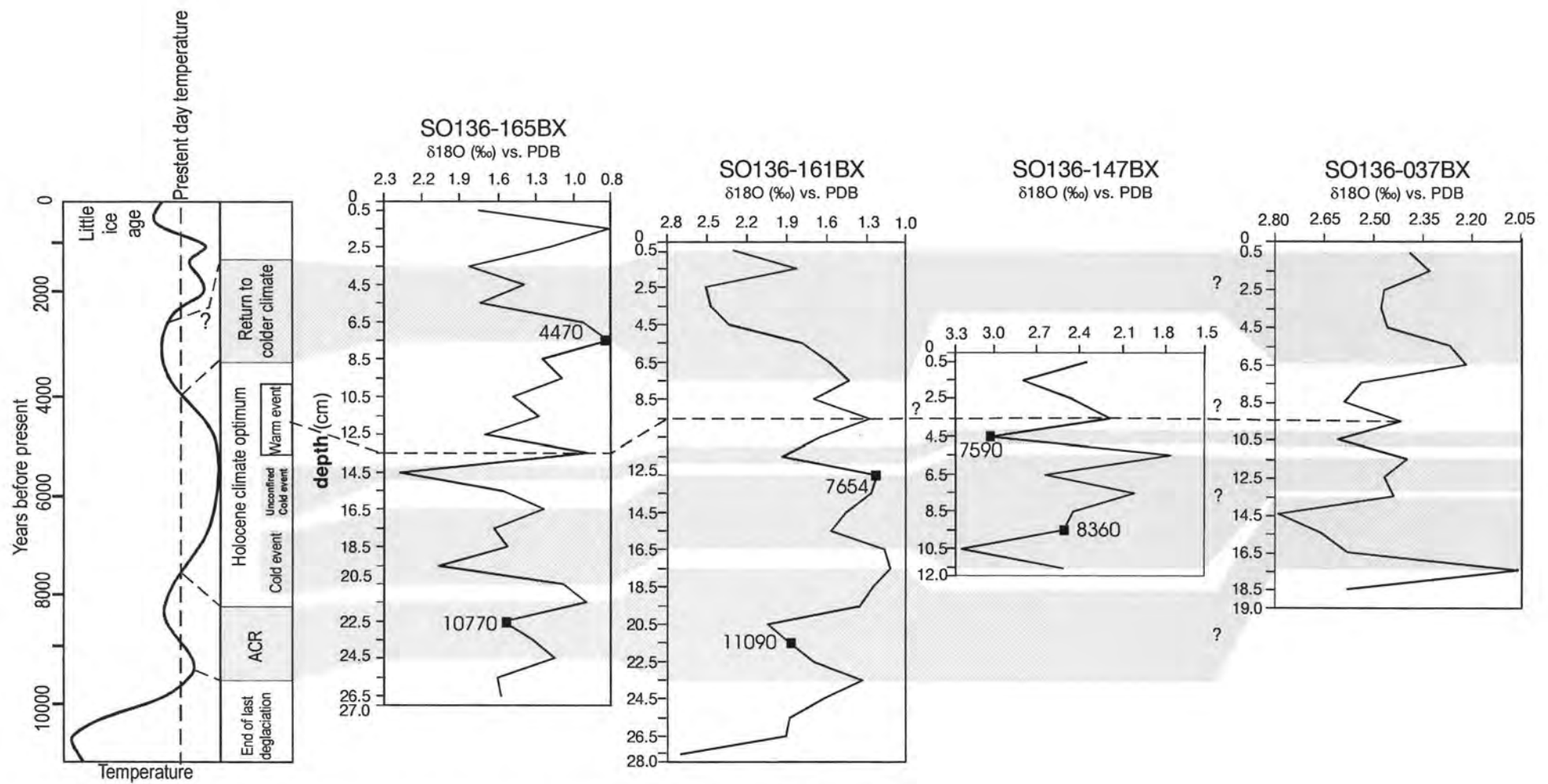


Fig. 5.2 Correlation of $\delta^{18}\text{O}$ isotope ratios of cores from the South Tasman Rise and the eastern Campbell Plateau with climate events reported in other locations. The left curve shows the global average temperature variations during the Holocene, after Folland (1990).

A sudden increase and gradual depletion towards the proposed end of the Holocene climate optimum follow this warm event. A progressive return to colder climate can be observed in the cores SO136-165BX and -161BX from 7.5 to 5.5 cm bsf and from 7.5 to 2.5 cm bsf respectively. The beginning of the increase is dated at the maximal depletion with 4470 yr. BP in core SO136-161BX. This peak might correlate with a maximum abundance of subtropical-tropical planktic species from ~6000 to 4000 yr. BP in samples from the east Chatham Rise (Fenner et al., 1992). However, in the Northern Hemisphere the warm middle Holocene is followed by a cooling in the last 4000 to 5000 years (Alm et al., 1996; Berger and Loutre, 1991; Johnsen et al., 1992). A late Holocene climate asynchrony might be indicated by these offsets.

The correlation of the $\delta^{18}\text{O}$ ratio in the upper part of the core SO136-161BX and especially of core -165BX is similar to the trend of the global average temperature. The uppermost two measured values in core SO136-165BX might resemble the Medieval Warm Period and the Little Ice Age in the Northern Hemisphere. Tyson and Lindesay (1992) traced these two events for the Southern Hemisphere in samples from South Africa. The Medieval Warm Period is set to extend from 1100 to 600 yr. BP. The Little Ice Age is correlated with a cooling period from 700 to 100 yr. BP. However, this assumption is based on only two measurements, which are not dated by AMS and additionally appear uncertain due to the mentioned sedimentary processes and erosional events. The surface of core SO136-165BX is a fluff layer of decomposing phytodetritus (see Chapter 3.1.3). This indicates a recent surface. On top of the cores SO136-147BX and -161BX, the fluff layer is not present.

5.1.4 Erosional events and hiatuses at the South Tasman Rise

Watkins and Kennett (1976) present a record of erosional events and hiatuses in the South Tasman Basin and at the Campbell Plateau for the last 0.7 million years. The average age of the sediment surface is given with 0.5 million years. A study of Wells and Conell (1997) describes multiple erosional events around 10000 yr. before present in cores from the South Tasman Rise. In five out of six investigated cores much of the Holocene sediment is missing. Fenner et al. (1992) reports a hiatus in cores from the Chatham Rise, east of New Zealand, where the last 900 to 1000 years are missing in the sediment record.

The AMS ^{14}C ages of core SO136-147BX indicate erosion of the cores upper few centimeters. This assumption is supported by the observation of difficulties during coring in the area, which were reported on the cruise (TASQWA, 1999): the seafloor consisted of foraminifera sands, which hint strong winnowing. However, the fine fraction <63 μm of the sediments amounts about 40 wt%. Phases of strong variation in the $\delta^{18}\text{O}$ values in short depth

intervals (see Chapter 4.2.2) additionally indicate that processes of resuspension and lateral advection of planktic foraminifera tests and / or downslope sediment transport might play a major role in the process of sedimentation. This is also supported by the frequent occurrence of the foraminifera *Uvigerina hollicki* in surface samples of the research area. The original type after Thalmann is occurring, which is referred to the Pliocene period (personal com., A. Altenbach, München University).

The correlation of the cores SO136-161BX and SO136-165BX in Figure 5.1 indicates that the upper 3 centimeters of core SO136-161BX are missing. This assumption is supported by the correlation of the trend of abundances of all benthic foraminifera in the two cores, as outlined in Figure 5.3, p. 71. The presence of a fluff layer on core SO136-165BX might hint a recent surface.

The planktic $\delta^{18}\text{O}$ ratio of core SO136-037BX can be correlated with the developed model, as outlined in Fig. 5.2, p. 57. However, no absolute ages are available to support the position of the core. No correlation was found for the cores SO136-019BX and -025BX. Core SO136-025BX appears to be sedimented by a high current event, a stratigraphical correlation is not possible. In core SO136-SO136-019BX the benthic $\delta^{18}\text{O}$ ratio trends astoundingly parallel to the $\delta^{13}\text{C}$ ratio. Additionally variations of 1.5 ‰ vs. PDB and measured values of -1.0 ‰ vs. PDB hint inconsistencies. The standards measured in the runs of the Mass-spectrometer revealed no variations, so failure of the device is unlikely. An explanation for the observed variation is strong redeposition of the benthic foraminifer test. The position of the core below the slope of the Campbell Plateau and the presence of the strong ACC support this explanation. It is to mention that the benthic foraminifera *C. wuellerstorfi* thrives in strong currents attached to protruding substrates. Its tests are of streamlined plan-convex shape, and enable the specimens to resist strong currents. Contrarily the tests of the planktic foraminifera *G. bulloides* is of round shape with an enhanced ratio of surface to mass, which enables the specimen to suspend in the water column. Consequently, redeposition of planktic foraminifera has to be considered, if redeposition of benthic foraminifera tests is assumed. The planktic $\delta^{18}\text{O}$ ratio of core SO136-019BX appears inconclusive.

5.2 Benthic foraminiferal associations

5.2.1 Potential fossil associations

Abundances in different grain size subfractions:

The deep-sea foraminiferal fauna is considered very diverse. However, a small number of species is dominant at depths greater than ~1000 m. This is probably due to the uniformity of water masses and substrate over large areas at great depth (Murray, 1991).

Big foraminiferal species occur mostly with a relatively small absolute number of specimens per gram. Since only the fraction $>150\mu\text{m}$ was examined, and not divided into subfractions, under-representation of big species has to be predicted during counting under the binocular (Timm, 1992). An example is a high abundance of very big (up to 4 mm in diameter) specimens of *Cyclammina cancellata* in core SO136-019BX between 3 and 6 cm depth. It was recognised while dry sieving, but does not appear any more after splitting the sample for counting.

A lower abundance of benthic foraminifera in the fraction $>150\mu\text{m}$ is supposed, if compared to the fraction $>125\mu\text{m}$. This assumption has to be drawn by the observation, that most benthic foraminifera were recognised to be abundant in the finer fraction of the examined samples; and by the overall higher abundance in the cores SO136-124GC and -155GC, in which the subfraction $>125\mu\text{m}$ was examined (Rüggeberg, 2000).

Abundance of benthic foraminifera and primary production:

As far as no sedimentation rates are available for the cores, all abundances are given in specimen per gram. This will result in overprinting patterns of benthic species with a low frequency by benthic species with a high frequency. This is frequent in the uppermost centimeters of all cores, where agglutinating species dominate the fauna. The occurrence pattern of agglutinating species in these depths is caused by diagenetic effects, rather than by paleoceanographical variabilities, as discussed in the following paragraph. Another effect is the flux of planktic foraminifera tests, which dilutes the fossil assemblage of benthic foraminifera: considering only the number of benthic foraminifera per gram, it is not conclusive if variations in abundance are due to variations of the benthic fauna, or to changes in the flux of planktic tests. An example is the higher number of benthic foraminifera in core SO136-165BX compared to core SO136-161BX (see Fig. 5.3, p. 71). The abundance patterns of all benthic foraminifera are very similar; contrarily is the higher frequency of benthic specimen in the deeper core. This effect is most

likely due to stronger dissolution of planktic specimen under the higher influence of the AABW in this core (see Chapter 5.3.2, p. 80).

Early diagenetic effects on agglutinating species:

In the modern ocean more than 50 %, often more than 90 % of the benthic meiofaunal biomass consists of agglutinated foraminifera (Kuhnt et al., 1996). The major part of these disintegrates soon after buring in the uppermost cm of the sediment. Consequently few specimens are present in the fossil record (Corliss, 1985; Goldstein et al., 1995; Loubere and Gary, 1990, 1993; Ozarko et al., 1997). The disintegration can be due to physical destruction of the test or due to bacterial destruction of the binding material (Mackensen et al., 1990). Fenner et al. (1992) describes a faunal change to higher abundance of agglutinating foraminifera in the upper parts of cores from the Chatham Rise, north of New Zealand. The near surface peak is assumed a preservational phenomenon. The same effect can be observed in all cores investigated in this study. The strong increase of abundance of agglutinating species in the uppermost 3 to 5 cm bsf of the core resulted in the calculation of a varimax factor, which showed a very high loading in the upper part of the core. This effect overprinted the faunal associations in the uppermost centimeters of the sediment. Mackensen et al. (1990) defined the concept of a potential fossil assemblage, and removed all agglutinating foraminifera species from the data set of the Q-mode Factor Analysis, except the species *Kariella* spp., *Martinotella nodulosa* and *Milliamina arenaca*, which are resistant against early diagenetic processes (Douglas and Woodruff, 1981a). Schmiedl (1995) enlarged the list of resistant species by including *Sigmoilopsis schlumbergeri* and *Siphonotularia catenata*. Mead and Kennet (1987) excluded all agglutinated foraminifera except *Eggerella bradyi*. Specimen of the genus *Reophax* spp. are considered to disintegrate rapidly below the bioturbated zone, specimen of the species *Cribostomoides subglobosus* and the genus *Cyclamina* spp. do not occur under 25 cm bsf. Following Harloff and Mackensen (1997), the listed species were removed from the data set for Q-mode Factor Analysis in this study: *Cribostomoides subglobosum*, *Cyclamina cancellata*, *Reophax miaceus*, *Reaphax spiriculifer* and the taxa of "fragments of agglutinating species". The agglutinating species which use calcearous binding material, e.g. *S. rolshauseni* and *E. bradyi* are not affected by the early diagenetic effects and were not removed from the data set.

Preservation of fragile foraminifera tests due to bioturbation:

The destruction of fragile foraminifera tests takes place at the oxic-anoxic interface in the sediment, which is in the uppermost centimeters (Tuominen et al., 1998). It is directly caused by decomposition of the organic cement of agglutinating species by microbiological activities, or

indirectly by the resulting change in pore water chemistry and dissolution of susceptible carbonate tests, e.g. *Bulimina aculeata* (Mackensen et al., 1990). However, in some investigated cores tests of these species are present in greater depths.

The amount of microbiological activity is mainly limited by the pore waters redox conditions, besides Fe content (Schröder, 1986). Hence in well-oxygenated conditions organic matter will decompose faster than in euxenic or anoxic conditions (Canfield, 1994). This assumption is based on the controversy discussed Remineralisation-Coefficient after Sun et al. (1993a): organic material of high quality will be oxygenated faster than material of lower quality under similar conditions. The degree of decomposition is beside other parameters dependent on the time of burial in the oxic sediment layer.

The C/N ratio can be used as an indicator of the lability or the refractory nature of the organic matter. The smaller the ratio, the higher is the content of protein in the organic matter. In fresh organic material, which has not been altered by microbial processes, a lower C/N ratio can be expected (personal com. C. Böttcher, IOW). A lower C/N ratio can also indicate anoxic conditions, which hinder the microbial alteration. However, in the deep-sea strong oxygen depletion on the sediment-water interface is rare due to comparatively small benthic and microbial communities (personal com. S. Papaspyro, University of Athens). The connection between C/N ratio and preservation of agglutinating foraminifera can be recognised e.g. in the upper 6.5 centimeter of core SO136-019BX, where the decrease of specimen per gram correlates with the decrease of the C/N ratio in the first centimeters from the top of the core downwards.

Bioturbation can cause different effects on the preservation of organic material in the sediment by mixing the oxic and euxenic sediment layers: On the one hand, deeper layers are oxygenated, which results in oxygenation of previously preserved organic matter. On the other hand fresh material can be transported in anoxic layers and preserved there (Henrichs, 1997; Kristensen and Blackburn, 1987). It is assumed that both mechanisms are present in bioturbated sediments. Local variations in pore water chemistry are assumed to cause the occurrence of agglutinating species and fragile calcareous species in deeper parts of the investigated cores. An example is core SO136-037BX, where high abundance of agglutinating species are present at 16.5 to 14.5 and 9.5 to 7.5 cm bsf. At the same depths, strong variations in the C/N ratio are present. Agglutinating foraminifera are frequent in greater depths in cores from the research area (Rüggeberg, 2000). However, the occurrences in longer cores cannot be compared to the short cores investigated in this study. Early diagenesis and bioturbation in the uppermost centimeters have a stronger impact on the results of high resolutional investigations at short cores than on long time studies, where such variations are equalised by greater sample intervals (Hayward et al., 1999).

5.2.2 Cores from the eastern Campbell Plateau

Discussion of core SO136-019BX

Ecology of the relevant benthic foraminifera species:

The faunal assemblage of factor 1 with *N. umbonifer*, *E. exigua* and *Pullenia bulloides* is similar to the "*Nuttalides umbonifer* association" defined for the Indian and Pacific Oceans in Murray (1991) after Corliss (1976, 1987, 1979b, c, 1982, 1984, 1987). In these studies the "*Nuttalides umboniferus* association" is indicating Antarctic Bottom Water (AABW). The same observations were made by Mackensen et al. (1990) in the eastern Weddell Sea, by Schnitker (1994) in the North and South Atlantic and by Lohmann (1978) for the SW Atlantic. Harloff and Mackensen (1997) found *N. umbonifer* associated with the AABW and the Lower Circumpolar Deep Water (Cowl) above the Calcite Compensation Depth (CDD) in the Argentine Basin. The AABW is under saturated with respect to calcite, dissolution of fossil foraminifera tests takes place (Corliss, 1976; Mackensen et al., 1990; Peterson, 1984). Corliss (1982) found *Nuttalides umbonifer* associated with deep cold waters and higher levels of carbonate undersaturation. He discussed the connection of *N. umbonifer* to carbonate aggressive waters: the occurrence can be due to either an ecological control on the living protozoa, or to preferentially concentration of the test due to lower affection by carbonate dissolution. An experimental study of Corliss and Honjo (1981) found tests of *N. umbonifer* as susceptible to carbonate dissolution as tests of other deep-sea foraminifera, as *Cibicidoides kullenbergi*, *Hoeglundina elegans* and *O. tener*, and less susceptible than *Planulina wuellerstorfi* (here *Cibicidoides wuellerstorfi*) and *Pyrgo murrhina*. It was concluded, that the relationship between the faunal pattern of *N. umbonifer* and carbonate undersaturation is a casual one, which results from the ecological influence on the living organisms, as also suggested by Bremer (1982). Although it was not possible to determine which ecological variable is controlling the fauna, Corliss confirmed the association of *N. umbonifera* and the AABW. Loubere (1991) found *N. umbonifer* as an indicator for low productivity in the eastern equatorial Pacific. Murray (1991) described it as an epifaunal species, living free of clinging at hard substrates. It thrives in marine environment in waters colder than 4°C and in the bathyal to abyssal zone.

The faunal assemblage of factor 2 with *G. subglobosa*, *S. rolshauseni*, *E. exigua*, *P. bulloides* and *N. umbonifer* is similar to the "*Globocassidolina subglobosa* association", defined in Murray (1991) after Burke (1981), Huges (1988), Nienstedt and Arnold (1988) and Resig (1981) for the Pacific Ocean. It is also similar to a "*Globocassidolina subglobosa* association" defined for the Indian Ocean by the same authors as for factor 1, except for the missing of *S. rolshauseni* in the assemblage. Both assemblages are associated with Deep Oxygen Minimum

Water and the Indian Deep Water (IDW). The physical properties of these water masses resemble the CPDW in the research area. The associated fauna of factor 2 indicates higher productivity: *Epistominella exigua* feeds on phytodetritus and lives semi-epifaunal in the fluff layer on top of sediment. The ability to quickly respond to food supply adapts *E. exigua* to a wide range of environmental conditions including strongly seasonal organic carbon fluxes and lower oxygen content (Mackensen et al., 1990, 1993; Perez-Cruz, 1990). *G. subglobosa* has been found in anoxic sediments (Bernhard, 1993) and is associated with the quantity of food supply to the seabed (Loubere et al., 1988). Little ecological information is available on *S. rolshauseni*, it is supposed to have an endo- to semi-endobenthic lifestyle (Bauch et al., 1999; Corliss, 1985) and may feed on organic particles delivered through the water column (Struck and Nees, 1991). *P. bulloides* is thought to live infaunal (Corliss, 1985; Murray, 1991) and is associated with high fluxes of organic carbon (Mackensen et al., 1994) and suboxic conditions (Kaiho, 1994).

Five core sections:

The core is divided in five sections, defined by abundances of benthic foraminifera: The lowest section i₁ reaches from 36.5 to 34.5 cm bsf and is dominated by factor 1. The loading of factor 1 decreases slightly throughout the entire core. The dominance of *N. umbonifer* in the faunal association indicates influence of a corrosive water mass, which might be the AABW. Section i₂ reaches from 34.5 to 30.5 cm bsf and is characterised by abundance peaks of *N. umbonifer* and *G. subglobosum* and in the abundance of all counted species. The peak occurs also in the species *Cibicidoides inawagaensis*, *Cibicidoides wuellerstorfi*, *Ehrenbergina mestayeri*, *Heteroplea dutemplei*, *Melonis pompilioides*, *Planulina ariminensis*, *P. bulloides*, *Pyrgo* spp. and *Trifarina angulosa*. This peak correlates with depletion in $\delta^{18}\text{O}$ of planktic foraminifera, which indicates conditions of warmer climate. Connections between climate variations and the composition of benthic foraminifera fauna are also described for the cores SO136-037BX, -161BX and 165BX. The peak correlates with carbonate content and anti-correlates with DBD. This pattern might be due to increased sedimentation of comparatively less dense planktic foraminifera tests.

A slightly higher abundance of *N. umbonifer*, *E. exigua* and the fragments of agglutinating species and of all counted species is present in section ii, which reaches from 26.5 to 18.5 cm bsf. The three mentioned species are resistant against carbonate dissolution (Mackensen et al., 1990) and comprise ~50% of the counted benthic foraminifera specimen. The pattern in foraminifera abundances correlate with higher content of clastic sediment grains and could be the result of increased carbonate dissolution. However, no correlation in the carbonate content can be observed. Unfortunately, the benthic $\delta^{18}\text{O}$ isotope ratio is not conclusive (see

Chapter 5.1.1). The benthic isotope ratios show strong variations in section ii. This might be due to redeposition or down-slope sediment transport, a disturbed stratigraphy is indicated.

Core section iii reaches from 13.5 to 4.5 cm bsf. Factor 2 and a faunal association, which might indicate influence of CPDW, dominates it. This trend is oscillating: the abundances of the associated foraminifera fauna is highest at 10.5 and at 5.5 cm bsf. In between these two peaks a short phase of influence of factor 1 occurs. The trend of factor 2 correlates with depletion in the planktic $\delta^{18}\text{O}$ isotope ratio. The depletion of $\delta^{18}\text{O}$ stagnates in the upper 4.5 cm of the core, correlating with the dropping influence of factor 2. This warming trend of the sea surface might have resulted in increasing primary production. Thus, factor 2 could also reflect a high productivity event. An abundance peak at the upper section supports this. This peak at 5.5 cm bsf is followed by a sudden decrease of the loading of factor 2. The peak could reflect movement of the sharp defined Subantarctic Front and the associated higher productivity (Tchernia, 1980). A less distinct abundance pattern is present at the lower border of this section. This pattern is in contradiction to the pattern of the abundance peak in section i₂: there is no increase in the abundance of all benthic species and the sudden change in faunal composition is not reflected in the carbonate no in the TOC content.

The upper section of the core is dominated by factor 1. However, only slightly higher abundance of *N. umbonifer* is present and the foraminifera fauna is dominated by the taxa of fragments of agglutinating species. Thus, the strong dominance of agglutinating species (42 % of the fauna) in the uppermost centimeters overprints the distribution patterns of other species. Diagenetic processes are reflected, rather than paleoceanographical changes. This assumption is supported by the observation, that factor 1 correlates in the lower section of the core with decreasing grain size, increasing carbonate content and roughly with the decreasing clastic sediment content. Although the upper section of the core is influenced by factor 1, nor the abundance of *N. umbonifer*, neither the sediment parameters show changes in trend. However, the abundance of the overprinting taxa should crosscut the abundance of the overprinted species. This is not the case; the change of factors is marked by a minimum abundance of all species besides the fragments of agglutinating species. This assumption supports the interpretation of factor 2 reflecting a temporal event, which finds its end at 4.5 cm bsf. The stratigraphical position of the core is problematic. No AMS¹⁴C ages are available and the $\delta^{18}\text{On}$ isotope ratio shows no apparent correlation with other cores or data in literature. The strong increase of agglutinating species in section iv indicates early diagenetic processes, which indicates the presence of a recent surface.

Discussion of core SO136-025BX

Two core sections:

The core was taken from a moderate steep (2°) slope. The core can be divided in two sections: The lower section reaches from the base of the core to an undulating erosional surface at 5.5 to 7.5 cm bsf (see Table A 7.2, p. XLVI). The sediment consists of fine silt with black streaks. Almost none benthic or planktic foraminifera tests are present. A statistical analysis was not computed for this part of the core. The upper section of the core consists almost entirely of planktic foraminifera tests of a grain size of $<150\text{ }\mu\text{m}$. The abundance of benthic foraminifera is very low. The Q-mode Factor Analysis did not reveal conclusive results. The upper part of the core is interpreted as the lower part of a turbidite, which eroded the upper part of the core. The upper part of the turbidite was eroded subsequently. Another possible interpretation is redeposition of these sediments due to winnowing. Hayward et al. (1999) gives winnowing as the cause for source faunas, which consist almost entirely of larger tests. The carbonate content of the sediments of the lower part of the core tends to zero. These sediments were deposited below the CCD, or represent the record of a strong algae bloom. As far as no similar sediments were found in the other cores from the eastern Campbell Plateau, it is obvious that much of these sediments were eroded prior to deposition of the upper section. Similar sediments were found in core SO136-124GC, which is also located in the range of the Subantarctic Front at $52^{\circ}59.71^{\prime}\text{S}$ and $151^{\circ}08.19^{\prime}\text{E}$ (Rüggeberg, 2000). The interpretation of core SO136-025BX merely reveals evidence for the existence of erosional events and the existence of radiolarian mud. A paleoceanographical interpretation of this core is not possible.

Discussion of core SO136-037BX

Ecology of the relevant benthic foraminifera species:

Factor 1 is strongly dominated by *Ehrenbergina mestayeri* with a factor score of 0.863. Unfortunately, little ecological information is available for this species. It is associated with fully marine, exposed and slightly sheltered environments and thrives at the outer- to deeper inner-shelf (Eade, 1967), and has not been recognised beyond the New Zealand region (Hayward et al., 1999). The species *Uvigerina peregrina* has an associative influence with a factor score of 0.236. It is a mainly infaunal form (Murray, 1991) associated with higher organic carbon concentrations. Therefore it is considered to be dependent on high nutrient fluxes (Altenbach, 1992) and an indicator for high productivity (Loubere, 1991). It is also described as an indicator for suboxic conditions (Kaiho, 1994; Mullins et al., 1985). However, Corliss et al. (1986) compared the abundance of *U. peregrina* in samples from the SE and SW Indian Ocean with the bottom-water dissolved oxygen. No apparent correlation with dissolved oxygen content was

found. Instead, a consistent relationship to high amount of organic carbon and fine-grained sediment was found. Contrarily Streeter (1979) traced the occurrence of *U. peregrina* for the entire length of the Atlantic Ocean, crossing areas of contrasting productivities. The distribution of *U. peregrina* shows no reaction to the changing nutrient fluxes, but was congruent to the distribution of waters with low oxygen content. The taxa *Pyrgo* spp. has a factor score of 0.218 and almost the same influence on factor 1 as *U. peregrina*. It is dominant in factor 3 and described there. The faunal assemblage of factor 2 is similar to the "*Trifarina angulosa / earlandi* association", which has been defined for the Southern Ocean in Murray (1991) after data from Anderson (1975) and Echols (1971). The "*Trifarina angulosa / earlandi* association" is associated with Fresh Shelf Water in the Southern Ocean. This resembles to the Australasian Subantarctic Water at the eastern Campbell Plateau. However, Mackensen (1985) and Mackensen et al. (1990, 1993) and Murray (1971) describe *T. angulosa* as not dependent on conservative water mass characteristics such as temperature and salinity, but as an indicator for strong bottom currents and sandy sediments. *Trifarina angulosa* is with a factor score of 0.572 significant for this factor. It is an indicator for suboxic conditions (Kaiho, 1994). In this core, *T. angulosa* shows no correlation with grain size distribution. *E. exigua* is with 0.512 factor score similar significant as *T. angulosa*. Little ecological information has been found for *Ehrenbergina glabra*, which is associative for the factor with a factor score of 0.310. In Murray (1991) an "*Ehrenbergina glabra* association" is defined, which was found in fine to coarse sands. Milam et al (1980) describes *E. glabra* as part of an assemblage occurring on the deep shelf in Saline Shelf Water (SSW) at East Antarctica. *Ehrenbergina glabra* is very similar to *Ehrenbergina pacifica* concerning test morphology. *Ehrenbergina pacifica* is associated with anoxic conditions (Kaiho, 1994). Factor 2 shows also associative influence of the taxa *Pyrgo* spp. with a factor score of -0.283. Factor 3 is dominated by the taxa *Pyrgo* spp. with a factor score of 0.830. This taxa contains fragments of the genus *Pyrgo*, which were disintegrated too strong to determine the species. The most frequent species of this genus in this core was *Pyrgo murrhina*, it is assumed, that most of the specimen of the taxa *Pyrgo* spp. belong to this species. A strong occurrence of these fragments could hint strong carbonate dissolution. Corliss and Honjo (1981) describe the process of carbonate dissolution on tests of nine different species. Tests of the porcelaneous, biloculine miliolid *P. murrhina* disintegrate in a sequence of steps: The test shows cracks, holes and dull surface textures. The chamber wall is removed subsequently and an earlier chamber in good condition is exposed. This process repeats itself, and results in decreasing grain size. No conclusive trend of correlation or anti-correlation can be observed in the core between the abundance of *Pyrgo* spp., the carbonate content and the ratio of the >150/>63 μm subfractions. However, the fragments of the genus *Pyrgo* examined under the binocular did not show a dull

surface, which should be expected if carbonate dissolution is taken into account. Furthermore, the fragments were marked with scratches, which might be traces of predating macro-fauna. *Pyrgo murrhina* lives epifaunal as a herbivore in marine environment (Murray, 1991). However, Altenbach (1992) describes it as a t-ubiquitous species with a broad range of nutrient preferences. Kaiho (1994) mentions *P. murrhina* as an indicator for oxic conditions. Factor 3 shows also associative influence of *T. angulosa* and *E. exigua* with factor scores of 0.278 and 0.276 respectively.

Four core sections:

The core can be divided in four sections: The lowest section is divided in sections i₁ and i₂. Section i₁ extends from the base of the core to 17.5 cm bsf and is dominated by factor 2. Although the species composition is similar to the "*Trifarina angulosa / earlandi* assemblage", an influence of the Australasian Surface Water seems not likely at the water depth of this core. The significant species of factor 2 indicate suboxic conditions. The factor might be associated with the CPDWu, which resembles low oxygen conditions. The occurrence of *T. angulosa* also indicates strong bottom currents. Section i₂ is characterised by factor 3 and reaches from 17.5 to in between 15.5 and 14.5 cm bsf. The taxa *Pyrgo* spp., or the species *P. murrhina* dominates factor 3 respectively. Beside this dominance, the faunal association is very similar to the faunal association of factor 2. The higher number *Pyrgo* spp. might be due to increased carbonate dissolution in this core section. Factor 3 is therefore considered to reflect mainly the same ecological circumstances as factor 2, with a higher level of carbonate undersaturation of the pore water. However, the carbonate content does not show signs of dissolution. In addition, the ratio of grain sizes shows no anti-correlation, which is to expect in phases of higher carbonate dissolution, due to fragmentation of foraminifera tests. A first short influence of factor 1 indicates section ii. In this phase the abundance of *E. mestayeri* and *E. exigua* increase slightly, while the abundances of *U. peregrina* decreases. Section iii shows weak influence of the factors 2 and 3. The abundance of all counted species decreases, with exception of *E. exigua*. Section iv is influenced by factor 1. While the abundances of the two significant species increases at the beginning, it stays stable in the upper part of the core. The same is valid for all other discussed species. Exceptions are the fragments of agglutinating species. The abundance pattern of these taxa depends on early diagenetic processes, as discussed in Chapter 5.2.1. The faunal assemblage of factor 1 is considered to indicate the salinity minimum Antarctic Intermediate Water (AIW), which the core is presently bathed in.

5.2.3 Cores from the southern Tasman Rise

Discussion of core SO136-147BX

Ecology of the relevant benthic foraminifera species:

The species assemblages defined by Q-mode Factor Analysis show similarities. Factor 1 is dominated by *S. rolshauseni* and *Ehrenbergina glabra*. Associative influence of *Bulimina aculeata* and *E. exigua* is present. Factor 2 contains almost the same species with different factor scores: *E. exigua* is the most dominant species. The species *Pullenia bulloides* has also significant influence and occurs not in factor 1. The preferences of this species to high fluxes of organic carbon and the high significance of *E. exigua* might characterise this factor as representing higher nutrient inputs compared to factor 1. The species *S. rolshauseni* and *B. aculeata* show associative influence as in factor 1. Factor 3 is dominated by *Bullimina aculeata*. Associative influence of *E. exigua* is present. *Bullimina aculeata* is described for the Weddell Sea by Mackensen et al. (1990) as an infaunal species, thriving under temperatures >0° C in TOC rich mud and consequently under lower bottom currents. Contrarily Lindberg and Auras (1984) found *B. aculeata* in the West of Heard Island on the Kerguelen Plateau consistently together with *Angulogerina earlandi* (here *T. angulosa*), which indicates sandy sediments and strong bottom currents. Close to the Polar Front in the southwestern Atlantic Mead and Kennet (1987) found a "B. aculeata assemblage" associated with the core of the warm Lower Circumpolar Deep Water between water depths of 1500 and 2600 m. Kaiho (1994) associated *B. aculeata* with suboxic conditions. Corliss (1982) reported a *B. aculeata* dominated assemblage overlaid by warm Antarctic Intermediate Water. He characterised *B. aculeata* as indicating the lower region of a mixture of AAIW and North Atlantic Deep Water (NADW). An important feature of fossil assemblages of *B. aculeata* is the effect of early diagenesis. Mackensen et al. (1990) found no specimen of *B. aculeata* under the sediment surface, few specimens in a sediment depth of >1 – 2 cm bsf were probably bioturbated. It was concluded, that destruction and dissolution of dead *B. aculeata* takes place in the uppermost sediment, where the decay of organic material leads to production of CO₂, which causes undersaturation of the interstitial water relative to calcite. However, in core SO136-147BX. *B. aculeata* is frequent throughout the core. The highest abundances correlate with higher abundance of the taxa of fragments of agglutinating species. At the same depth variations in C/N ratio occurs. It is concluded, that preservation of *B. aculeata* in greater depths is related to bioturbation. Factor 4 is dominated by the taxa *Pyrgo* spp, which indicates oxic conditions. Associative influence of *P. bulloides* and *Laticarinina pauperata* is present. *Laticarinina pauperata* is an indicator for oxic conditions.

(Kaiho, 1994) and resistant against carbonate dissolution (Mackensen et al., 1993). Considering the significant and associative species factor 4 indicates oxic conditions.

Five core sections:

The similar faunal associations in factor 1 to 3 and the short time span covered by the core leads to the assumption that relatively stable conditions are recorded in the sediment. However, evidence for a disturbed stratigraphy and redeposition are present, as discussed in Chapter 5.1.4.

Section i extends from the base of the core to 9.5 cm bsf, and is characterised by high loadings of the factors 1, 2 and 3. It is dominated by infaunal and semi-epifaunal species, which indicate high nutrient fluxes. The loading of factor 3 and *B. aculeata* anti-correlate to the loading of factors 1 and 2. This might be caused by dissolution of the tests of *B. aculeata* due to higher microbial activity and the resulting changes in pore water chemistry.

Section ii extends from 9.5 to 6.5 cm bsf and is characterised by a slight increase in the abundance of the species thriving under oxic conditions. However, *E. glabra* has its maximum abundance of the core and is reported to indicate suboxic conditions (Kaiho, 1994), as well as *P. bulloides*. This oscillating pattern might be explained by negative feedback. Increasing oxygen content provides better conditions for microbial activity, which again leads to depletion in oxygen content. However, oxygen is not considered to be a limiting factor with in the range discussed here (Belanger, 1980). A correlation of benthic fauna and climate variations indicated by the planktic $\delta^{18}\text{O}$ ratio can be observed: Variations of $\delta^{18}\text{O}$ ratio are followed by changes in abundance of benthic fauna. Especially the species *U. peregrina* and *Melonis pompilioides* shows an inverse trend, as discussed in Chapter 5.3 and outlined in Figure 5.3. In core SO136-147BX correlation of the taxa *Pyrgo* spp. to warmer climate is additionally present. According to the current understanding of the "pelagic-benthic coupling" (Graf, 1989a, b, Graf and Linke, 1992), primary productivity influences the benthic fauna.

Section iii reaches from 6.5 to 4.5 cm bsf and shows the same oscillations between oxic and anoxic fauna. Additionally the maximum abundance of *B. aculeata* and of the fragments of agglutinating species precedes a slight variation in C/N ratio. Incomplete degradation of organic material is supposed for this section. A high sedimentation rate and quick burring of the organic material might have enabled the preservation.

Section iv reaches from 4.5 to 2.5 cm bsf and is characterised by a generally low abundance of benthic foraminifera. This is announced by increasing loading of factor 1, which might represent the low production counterpart of factor 2.

Section vi reaches from 2.5 cm bsf to core top and shows increasing abundance of the species *E. exigua* and *P. bulloides*, which are dominant in factor 2. However, the section is

characterised by increasing loading of factor 3, for which *B. aculeata* is significant. This pattern is probably due to the effects of early diagenesis on tests of *B. aculeata*, which overprint the trend of the other fauna.

Discussion of core SO136-161BX

The abundance of benthic foraminifera of the cores SO136-161BX and -165BX shows similarities, as outlined in Figure 5.3. In order to make the results comparable, *Furciferia complanata* was added to the data set for the Q-mode Factor Analysis of core SO136-161BX, though it only reaches a significance of 1.95 % on all species.

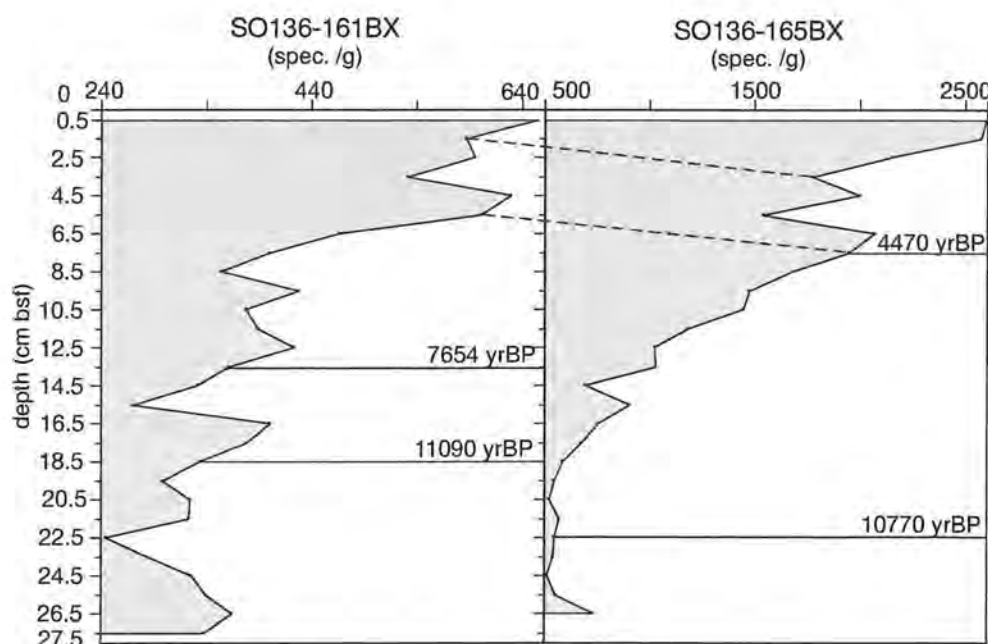


Figure 5.3 Similar trends in abundance of benthic foraminifera in the upper 7.5 cm bsf in the cores SO136-161BX and -165BX. The black lines indicate AMS ages. The dashed lines indicate similar patterns in abundance.

Ecology of the relevant benthic foraminifera species:

Factor 1 is strongly dominated by *U. peregrina*, with associative influence of *Tosaia hanzawai*, *S. rolshauseni* and *E. exigua*. In Murray (1991) an *Uvigerina* spp. association with similar faunal association is defined after Peterson (1984) for the SE Indian Ocean, this indicates Indian Bottom Water. Almost none ecological information is available on *T. hanzawai*. Kaiho (1994) mentions it as indicating suboxic conditions. Factor 2 shows strong significance of *Melonis baleeanum*, which is related to high input of organic matter and is therefore an indicator for high

productivity waters (Caralp, 1989; Loubere, 1991; Murray, 1973). Kaiho (1994) found *M. baleeanum* associated with low oxygen concentrations. After Linke and Lutze (1993) it is highly adaptable and can change between infaunal and epifaunal habitat, i.e. it is t-ubiquitous and migrates upward in the sediment in times of starvation. Mackensen (1987) suggested that the distribution of *M. baleeanum* is independent of water masses. Factor 3 is dominated by *E. exigua*, with a strong associative influence of *N. umbonifer*. Murray (1991) describes an "*E. exigua* association" after Peterson (1984) for the Indian Ocean, which appears to span the diffuse boundary between Indian Deep Water and Indian Bottom Water. These would resemble the NADW and the AABW in the research area. The "*E. exigua* association" was found best developed beneath the core of a cold and well-oxygenated geostrophic current. Factor 4 is clearly dominated by *Melonis pompilioides*. The ecological preferences of this species are similar to *M. baleeanum*; the more chubby shape indicates its preference to even higher nutrient fluxes where it outnumbers *M. baleeanum* (personal com. Schönenfeld, GEOMAR). This preference makes *M. pompilioides* less adaptable than *M. baleeanum*. No ecological information is available on the species *Pyrolina cylindroides*. *Furcikaria complanata* is described as living infaunal as a detritivore (Murray, 1991) under dysoxic conditions (Kaiho, 1994). *Furcikaria* spp. is an especially adapted high-productivity and low oxygen-tolerating genus. It is an indicator for areas of very high oceanic carbon fluxes, where it outnumbers opportunistic species like e.g. *E. exigua* (Mackensen et al., 1993).

Six core sections:

The abundances of the relevant species show little variations upcore. Concerning the loading of the Varimax Factors the core can be divided in four sections, which can be correlated to the climate variations outlined in Chapter 5.1.3. Section i reaches from the base of the core to 23.5 cm bsf. It is in the lower and upper parts characterised by factor 2. In between short influence of factors 1, 3 and 4 occurs. The associated species, *M. baleeanum*, *U. peregrina*, *E. exigua* and *M. pompilioides*, respectively indicate high nutrient fluxes and low oxygen conditions. At the base of the core high abundance of *P. cylindroides* is present. Section i is correlated with the end of the last deglaciation. Section ii is dominated by factor 4. It reaches from 23.5 to 19.5 cm bsf. The abundance of *M. pompilioides* tends to increase with decreasing surface temperatures. This assumption is supported by increasing abundance at the beginning of section ii, which is correlated with the ACR. Highest abundances precede the maximal $\delta^{18}\text{O}$ depletions at 20.5 cm bsf for the ACR and at 15.5 cm bsf for the described "Cold Event" (section iv) in the Holocene climate optimum. Additionally the abundance of *M. pompilioides* increases with the trend to colder climate from 7.5 to 1.5 cm bsf (section vi). *M. baleeanum* shows a less obvious, but still

apparent correlation to cold surface temperatures in this core. Section iii resembles the beginning of the Holocene climate optimum and reaches from 19.5 to 17.5 cm bsf. It is characterised by an abundance peak of *F. complanata*. Therefore, it represents a high-productivity event. Section iv represents the "Cold Event" in the Holocene climate optimum and reaches from 17.5 to 15.5 cm bsf. It is characterised by an abundance-peak of *M. pompilioides* and higher influence of factor 4. Section v reaches from 15.5 cm bsf to 7.5 cm bsf and is characterised by factor 1 and increasing influence of factor 3. *U. peregrina* is significant for this section and shows apparent correlation with surface temperature (see Fig. 5.4, p. 76). Section vi reaches from 7.5 to the top of the core and resembles the "Return to colder climate" and increasing influence of the "*Epistominella exigua* association". Increasing abundance of *M. pompilioides* and *M. baleeanum* indicates the climate trend. An abundance peak of *P. cylindroides* is present at the beginning of the section. A single peak of $\delta^{18}\text{O}$ depletion at 1.5 cm bsf might resemble decreasing abundance of these two species. The increasing influence of factor 3 continues from the middle of section v to the top of the core. It correlates with decreasing grain size, which also could hint strong dissolution of planktic foraminifera tests. Dissolution of planktic foraminifera tests, which resemble the biggest part of the sediment could also cause the overall increase of benthic foraminifera abundance upcore. An increased influence of AABW is indicated. The assumption of sinking water masses is supported by the increasing $\delta^{18}\text{C}$ ratio of *C. wuellerstorfi* and a colour change from light grey to very pale brown in the upper 10 cm of the core (see Table A 7.5, p. XLVI)

Discussion of core SO136-165BX

Ecology of the relevant benthic foraminifera species:

Nuttalides umbonifer, *P. cylindroides* and *Heteroplea dutemplei* dominate factor 1. Although *E. exigua* shows no influence on factor 1, it has a similar trend in abundance as factor 1 has in factor loading. The increasing abundance of *N. umbonifer* and *E. exigua* correlates with the increasing loading of factor 3 of core SO136-161BX. This observation is supported by the similar trends of abundance of all species as outlined in Figure 5.3, p. 71. There is little ecological information of *H. dutemplei*. After Murray (1991) species of the genus *Heteroplea* prefers an epifaunal lifestyle, attached to hard substrates and feeds as passive herbivore in marine environments. In the Pacific Ocean it has been associated with inner shelf environments. Factor 2 is dominated by *Fursenkonia complanata* and has significance influence of *M. baleeanum* and *E. exigua*. However, the abundance of *M. baleeanum* shows no apparent correlation to the loading of factor 2 and weak variations upcore. It is therefore not considered in the paleoecological interpretation.

Five core sections:

Section i is characterised by dominance of factor 2 and high abundance of *F. complanata*. It reaches from the base of the core to 20.5 cm bsf. The strong significance of *F. complanata* indicates very high nutrient fluxes and high surface productivity. The assemblage of benthic foraminifera species is governed by the food supply from the sea surface (Mackensen et al., 1993). In areas of high primary productivity, the supply of nutrients overprints the signal of the water mass and the surface temperature in the sediments (Mackensen et al., 1993; Schnitker, 1994). A decreased C/N ratio between 25.5 and 19.5 cm bsf accompany the high nutrient flux. This might indicate suboxic conditions in the sediment, which lead to incomplete degradation of organic material. The benthic $\delta^{13}\text{C}$ ratio trends to lighter values and supports the observation of a high productivity event in section v. The abundance of *F. contemplata* anti-correlates with warmer climate as indicated by $\delta^{18}\text{O}$ ratio. Very low abundance is present at the climate optimum end of the last deglaciation at 20.5 cm bsf. However, the minimum in abundance at 14.5 cm bsf correlates with a cold event indicated by $\delta^{18}\text{O}$ ratio. Section ii leads from 20.5 to 12.5 cm bsf. It characterises a phase of decreasing surface productivity and lower nutrient fluxes to the sea floor. Decreasing abundance of *F. contemplata* and a sudden increase in C/N ratio indicates this. Decreasing grain size and increasing abundance of benthic foraminifera supports the assumption, which indicates a reduced flux of planktic foraminifera tests to the sea floor. Section iii is characterised by quickly decreasing abundance of the infaunal *F. complanata* and sudden increase of abundance of the epifaunal species *P. cylindroides*, *H. dutemplei* and *E. exigua*. This is accompanied by slightly rising abundance of *N. umbonifer* to the end of the section. Section iv represents the imprint of the surface temperature, as increasing abundance of *M. pompilioides* and decreasing abundance of *U. peregrina* indicate the "return to colder climate", as outlined in Chapter 5.1.3 and Figure 5.3, p. 71. The high abundances of *N. umbonifer*, *H. dutemplei* and *E. exigua* in section v indicate increasing influence of carbonate aggressive waters, which leads to a rising of the water masses and increased influence of AABW. This is supported by the observation of strong dissolution of planktic foraminifera tests in the upper centimeters, which has been made while counting the benthic fauna. The increasing influence of factor 1 represents the water mass signal, which indicates sinking of the water mass. However, the increase is very slight and lies in the range of the overall increase of benthic foraminifera abundance. The high-productivity event in sections i and ii might be due to shifting of the Subtropical Front over the core location. The rising of water masses hints northward movement of the front system.

5.2.4 Correlations of benthic fauna and Holocene climate variations

A correlation of the abundance of *U. peregrina* and an anti-correlation of *M. pompiliooides* with the climate variations indicated by of $\delta^{18}\text{O}$ planktic isotope ratio can be recognised in the cores from the South Tasman Rise and core SO136-037BX from the eastern Campbell Plateau, as outlined in Fig. 5.4, p. 76. The benthic foraminifera fauna in core SO136-161BX is the lower part of the core overprinted in by the high productivity signal of *F. contemplata*. Good correlation of the $\delta^{18}\text{O}$ ratio and *M. pompiliooides* and anti-correlation of *U. peregrina* is present between 14.5 and 13.5 cm bsf and 4.5 and 1.5 cm bsf. Clear correlation is present between *U. peregrina* and the planktic $\delta^{18}\text{O}$ isotope ratio of core SO136-161BX between 20.5 and 5.5 cm bsf. The anti-correlation of *M. pompiliooides* is most obvious between 8.5 and 1.5 cm bsf.

The reasons for observed variations in the benthic fauna are probably due to changes in primary production. These might be caused by changes in mixing and stratification of the photic zone, which will affect the amount of light and nutrients available to the phytoplankton. The direct influence of the surface temperature on the amount of primary productivity is not essential. However, rising temperatures results in higher rate of metabolic turnover in organisms in general. The rate roughly doubles with a rise of 10°C in temperature (Rule of Q-10). Different species take different advantage out of changes in temperature. The changes in the climate will probably result in variations in the phytoplankton assemblages and different qualities of nutrients will reach the sea floor. This might be one reason for the observed variations in the benthic fauna.

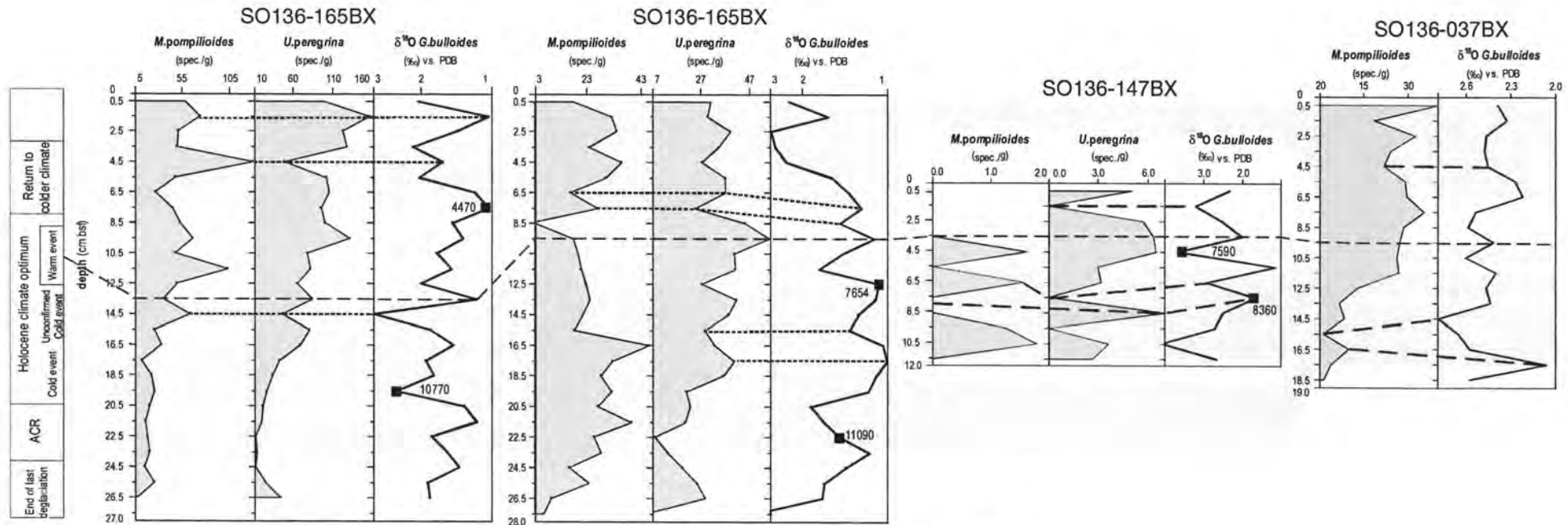


Fig. 5.4 Correlation of the abundances of *M. pompilioides* and *U. peregrina* with the climate trends recorded in the planktic $\delta^{18}\text{O}$ ratio. The dotted lines indicate apparent correlation and anti-correlation respectively. The black squares indicate AMS ^{14}C ages.

5.2.5 Definition of benthic foraminiferal associations and correlation to water masses

The association of benthic foraminiferal associations has to take into account that the benthic fauna is dependent on a variety of environmental factors. The conservative water mass properties represent only a part of these factors. Certain faunal associations, which are associated with distinct water masses, as described elsewhere, were recognised in the investigated cores. The available data is not sufficient to define certain foraminiferal associations, which can be correlated with the properties of distinct water masses. The low number of investigated cores is the main limitation of the data set. Every core is bathed in a different water mass, so the determined associations cannot be compared with other data. An exception are the cores SO136-161BX and -165BX, which are located close to each other, and provide similar patterns in foraminifera abundance and association in the upper parts of the cores (see Fig. 5.3, p. 71). However, the faunal associations of the two cores are overprinted by different ecological circumstances. In the following list, the water masses present in the research area and the associated faunal assemblages are discussed.

Antarctic Intermediate Water (AAIW):

Core SO136-037BX is the only investigated core bathed in the AAIW. The faunal association of the upper part of the core is supposed to represent the recent environmental conditions of the investigated sediment and is dominated by *E. mestayeri*. Associative influence of *U. peregrina* and *Pyrgo* spp. is present. The definition of this faunal association is based on the data of only one core location and requires verification by further investigation.

Circumpolar Deep Water (CPDW):

The faunal association of factor 2 in core SO136-019BX is with *G. subglobosum*, *S. rolshauseni*, *E. exigua* and *P. bulloides* similar to a "*Globocassidolina subglobosa* association" defined in Murray (1991), which indicates CPDW. A very similar faunal association is present in factor 2 of core SO136-037BX, differences are factor loadings of the single species. As far as the "*Globocassidolina subglobosa* association" is present in two cores of the research area and confirmed in literature, it is assigned to indicate CPDW in the research area. However, the two cores were bathed in the upper part of the Upper Circumpolar Deep Water and the lower part of the Lower Circumpolar Deep Water respectively.

Upper Circumpolar Deep Water (CPDWu):

Factor 2 and 3 in core SO136-037BX are supposed to represent the transition from CPDWu to AAIW. Core SO136-147BX is recently bathed in CPDWu. The only similarity between the

faunal associations of the two cores is the occurrence of *E. exigua*, which is a cosmopolitan species. The differences might be due to different environmental conditions. These are indicated by the different physical properties of the cores: The higher content of coarse grains in core SSO136-037BX and the lower content of TOC indicates higher current energy and higher oxygen levels than in core -147BX.

The faunal association of factors 1 to 3 in core SO136-147BX are very similar to each other and to the "*B. aculeata* association" defined by Mead and Kennet (1987). The ecological preferences of the fauna preserved in core SO136-147BX is more likely to indicate the physical properties of the CPDW_u (low oxygen, high T), and is therefore used to define a faunal association indicating the CPDW_u for the research area. The faunal association of the CPDW_u differs from the general faunal association for CPDW by the occurrence of *B. aculeata*, which reflects the low oxygen conditions of CPDW_u.

Lower Circumpolar Deep Water i (CPDWli):

Core SO136-161BX, which is bathed in the lower part of CPDWli shows the influence of primary productivity following the trend of sea surface temperature. A typical faunal association is present in factors 2 and 3: *H. dutemplei* occurs together with *P. bulloides*, *G. subglobosum* and *N. umbonifer*. It is frequently associated with *E. exigua*. This pattern is might be the signal of the water mass, which is overprinted by the effects of pelagic – benthic coupling. The same association is present in factors 1, 2 and 3 from core SO136-165BX, which is bathed in the upper part of CPDWlii. The described association is therefore interpreted as a variation of the "*G. subglobosum* association", which is defined in Murray (1991) and verified in this study as indicating the CPDW in general. The described variation might indicate the CPDWli. However, due to the limited data set this hypothesis is not verified at other locations in the research area.

Factor 3 is dominated by *E. exigua* and *N. umbonifer* and indicates increasing influence of the AABW. This signal overprints the signal of the surface temperature in the upper part of the core. Here *E. exigua* is dominating the factor. In factor 1 of core SO136-165BX this ranking is reversed: *Nuttalides umbonifer* shows a higher factor score than *E. exigua*. This pattern is explained by the ecological preferences of the two species: *E. exigua* becomes outnumbered with increasing carbonate undersaturation, as *N. umbonifer* is highly specialised to these environmental conditions (see description of core SO136-019BX in Chapter 5.2.2).

Lower Circumpolar Deep Water ii (CPDWlii):

The varimax Factors 1, 2 and 3 show similar faunal compositions, as discussed above with core SO136-161BX. A difference to the faunal assemblage indicating CPDWli is the occurrence of

M. baleeanum. It is present in the upper part of the core, as well as in the lower part, which is strongly overprinted by the occurrence of *F. contemplata*. Two further features are the occurrence of *P. cylindroides* and the lack of *S. rolshauseni* in the faunal association. Based on the observations a variation of the "G. subglobosum association" of Murray (1991) is defined for the CPDWlii (see Table 6). The increasing significance of *N. umbonifer* in the upper section of the core indicates rising influence of AABW, as discussed with core SO136-161BX.

The lower part of the core represents a high productivity event, and is characterised by high significance of *F. contemplata*. This species also occurs in core SO136-161BX. A high productivity association could be defined based on these observations. However, the available data set is limited and the faunal association stays the same, with the addition of strong significance of *F. contemplata*.

5.3 Paleoceanographical interpretation

5.3.1 Eastern Campbell Plateau:

Trends in Holocene bathymetry of deep-water masses

Core SO136-019BX

The slightly decreasing influence of factor 1, which resembles the "*Nuttalides umbonifer* association" indicates sinking of the AABW. Depletion of the planktic $\delta^{18}\text{O}$ isotope ratio from 18.5 cm bsf upwards is accompanied by slightly increasing loading of factor 2, which indicates increasing influence of CPDW. A sudden change from AABW to CPDW is located at 13.5 cm bsf. Considering rising surface temperatures and sinking of the upper border of the AABW, the Subpolar Front might have moved southward. The faunal associations of the upper 4.5 cm of the core are overprinted by dominance of agglutinating species. Therefore, the faunal associations are not conclusive. Early diagenetic processes cause the pattern of abundance of agglutinating species. This might indicate an undisturbed stratification of the upper part of the core. This assumption is supported by the observation, that the change of the water masses is located in the same sediment depth as in core SO136-037BX. However, these hints are not conclusive due to the lack of an age model. The variations in the planktic and especially in the benthic stable isotope ratio hints strong redeposition and probably sedimentation of down slope material.

Core SO136-037BX

The observed trend of sinking water masses recognised in core SO136-019BX is supported by results found in this core: The loadings of factors 2 and 3 increase in the lower sections of the core and indicate influence of the CPDWu. The rising influence of factor 1, which indicates the Antarctic Intermediate Water (AAIW) is accompanied by a short phase of increased carbonate dissolution. It is to mention that the beginning of the influence of the present water mass is located at the same depth as in core SO136-019BX. The correlation of the trend of planktic $\delta^{18}\text{O}$ isotope ratios with the ratios of the cores from the South Tasman Rise revealed an age of about ~12000 yr. for this core. Following this model, the change from CPDWu to AAIW should be located at the end of the ACR (see Figure 5.3. p. 71). However, as far as no absolute ages are available, this age model is not conclusive. Effects of early diagenesis on the foraminifera fauna are present and serve as evidence for a recent surface. As far as the composition of benthic foraminifera faunal varies only slightly in the upper 12.5 cm of the core, the faunal association of factor 1 should indicate the water mass the core is recently bathed in. It is to mention that no signs for redeposition are present in this core.

5.3.2 South Tasman Rise:

Trends in bathymetry of deep-water masses and ecological responses of benthic foraminiferal assemblages.

The faunal associations of the upper sections of all cores indicate rising influence of the water mass below. This is interpreted as a generally rising trend of the water masses, which might be accompanied with enhanced mixing of the water masses.

Core SO136-147BX

The core shows minor variations in paleoceanography. The observed patterns in benthic foraminifera fauna represent the normal variabilities of an ecosystem, which might be overprinted by bioturbation or erosional and redepositional processes. The benthic foraminiferal association mirrors the low oxygen conditions of the CPDWu. The short influences of species that indicate oxic conditions might indicate increased ventilation of the sediment due to strong currents.

Core SO136-161BX

The abundances of benthic foraminifera might mirror two trends:

- A general shallowing of the water mass body is indicated by increasing influence of the epifaunal "*Epistominella exigua* association" to the top of the core, and accompanied by increasing $\delta^{18}\text{O}$ isotope ratio of *C. wuellerstorfi*.
- The climate variations, which are indicated by the planktic $\delta^{18}\text{O}$ record can be traced in the infaunal benthic foraminiferal fauna. *M. pompiliooides* shows higher abundances in phases of decreased surface temperatures. *U. peregrina* is prevailing in the Holocene climate optimum, though it does not show as clear correlations as *M. pompiliooides* to colder temperatures. The ecological preferences of the described species differ only scarcely. All species prefer an infaunal lifestyle and indicate high nutrient fluxes and low oxygen conditions in the sediment. The variations in the faunal associations are probably due to slight changes in quantity (and quality ?) of food supply. These variations seem to be caused by changes in surface temperature and followed variation of primary production.

Core SO136-165BX

The core shows overprinting of three signals:

- The most dominant feature is a high productivity event in the lower two sections of the core, indicated by high abundance of *F. contemplata*. Movement of the Subtropical Front might have caused this high productivity event over the core position. The abundance of *F. contemplata* anti-correlates with sea surface temperature as indicated by $\delta^{18}\text{O}$ ratio.
- A second feature is the variation of sea surface temperature that can be traced in the benthic fauna, as described for core SO136-161BX.
- A general shallowing trend of the water mass body is indicated by increasing influence of *N. umbonifer* to the top of the core. The increasing influence of the carbonate aggressive AABW is supported by the counting of fragments of foraminifera tests in core SO136-164GC. The amount of fragments increases towards the upper centimeter of the core (personal com. A. Sturm, GEOMAR).

5.4 Suggestions for further investigation

- The sampling interval turned out to be not sufficient for a correlation of the $\delta^{18}\text{O}$ isotope ratios with other high resolution cores. It was not possible to set up a core stratigraphy. Higher resolution is recommended. Sampling intervals of 5 to 3 mm are suggested. The higher resolution would enhance the evidence of the observed climate variations.
- Additional AMS ^{14}C dating is recommended, especially at the following depths:
 - The top of the core SO136-165BX, which is covered by a fluff layer. The dating could reveal a recent surface and support the stratigraphical classification of all other cores.
 - The "Warm event", located at 13.5 cm bsf in core SO136-165BX, at 9.5 cm bsf in core SO136-161BX, at 3.5 cm bsf in core SO136-147BX and at 9.5 cm in core SO136-037BX. Additionally this would reveal the degree of resuspensional process, which is indicated by the high variations of the $\delta^{18}\text{O}$ ratio in core SO136-147BX.
 - The "Unconfirmed Cold Event" which is not described in the cited literature and present at 11.5 cm bsf in the cores SO136-165BX and -161BX and at 9.5 cm in core -037BX. This event is dated in core -147BX with 7590 yr. BP.
 - The changing of the bathymetrical position of the water mass body appears to synchronous in all investigated cores. AMS datings of these core depths would be useful to correlate the events (12.5 cm bsf in core SO136-019BX and -165BX, 13.5 cm bsf in core SO136-037BX and -161BX).
- Investigation of the foraminiferal fauna in the cores SO136-110BX or -116BX from the Emerald Basin might reveal more information about the bathymetrical variations in the water mass body. This might solve the question if the change in water mass depth is induced by enhanced current energy of the ACC.

6 CONCLUSIONS

Paleoclimatology

The entire Holocene climate record is preserved in the investigated sediments and can be correlated with climate variations described elsewhere. Table 6.2 outlines the timing of the climate variations.

An "Unconfirmed Cold Event", which is not described in literature, is present in the cores SO136-037BX, -147BX, -161BX and -165BX. AMS dating of core SO136-147BX indicates an age of ~ 7600 yr. BP for this event.

Benthic foraminifera fauna

Various environmental processes influence the composition of the benthic foraminifera fauna in the Holocene period. Five different processes are described and listed in decreasing intensity:

- (a) The tests of agglutinating foraminifera species disintegrate in the upper 2 to 6 centimeters of the sediment due to microbial destruction of the organic or Fe binding material. The agglutinating species dominate the fossil assemblage of the upper cm in such a way that all other fauna occurs in minor quantity. Resulting from diagenesis of the agglutinating species downcore the other species become relatively more important.
- (b) Variations in nutrient supply are the strongest influences on the living benthic foraminiferal fauna. These variations are reflected in the composition of the fossil assemblage.
- (c) Associations of foraminifera fauna, which are present in distinct water masses, are defined in Table 6.1.
- (d) Variations of the Holocene climate can be traced in the benthic foraminifera fauna. This is the weakest factor of influence.
 - *Uvigerina peregrina* shows higher abundance in periods of warmer climate.
 - *Melonis pompilioides* shows higher abundance in periods of colder climate.

Table 6.1 Faunal associations and resembling water masses of the Holocene period. Major associations are present in more than one core and confirmed in literature. Minor associations are present in only one core and not confirmation in literature.

Water mass	Significant species	Associative Species	Present in Core
Major associations:			
CPDW	<i>G. subglobosum</i> <i>S. rolshauseni</i> <i>E. exigua</i>	<i>P. bulloides</i> <i>N. umbonifer</i>	SO136-019BX -037BX, -147BX -161BX, -165BX
CPDWli	<i>H. dutemplei</i> <i>P. bulloides</i> <i>G. subglobosum</i>	<i>E. exigua</i> <i>N. umbonifer</i>	SO136-161BX -165BX
CPDWlii*	<i>M. baleeanum</i> <i>G. subglobosum</i> <i>E. exigua</i> <i>P. cylindroides</i>	<i>P. bulloides</i> <i>N. umbonifer</i>	SO136-019BX -165BX
AABW	<i>N. umbonifer</i>	<i>E. exigua</i>	SO136-019BX -161BX, -165BX
Minor associations:			
AAIW	<i>E. mestayeri</i>	<i>U. peregrina</i> <i>Pyrgo</i> spp.	SO136-037BX
CPDWu	<i>B. aculeata</i> <i>E. exigua</i> <i>S. rolshauseni</i>	<i>P. bulloides</i> <i>G. subglobosum</i>	SO136-147BX

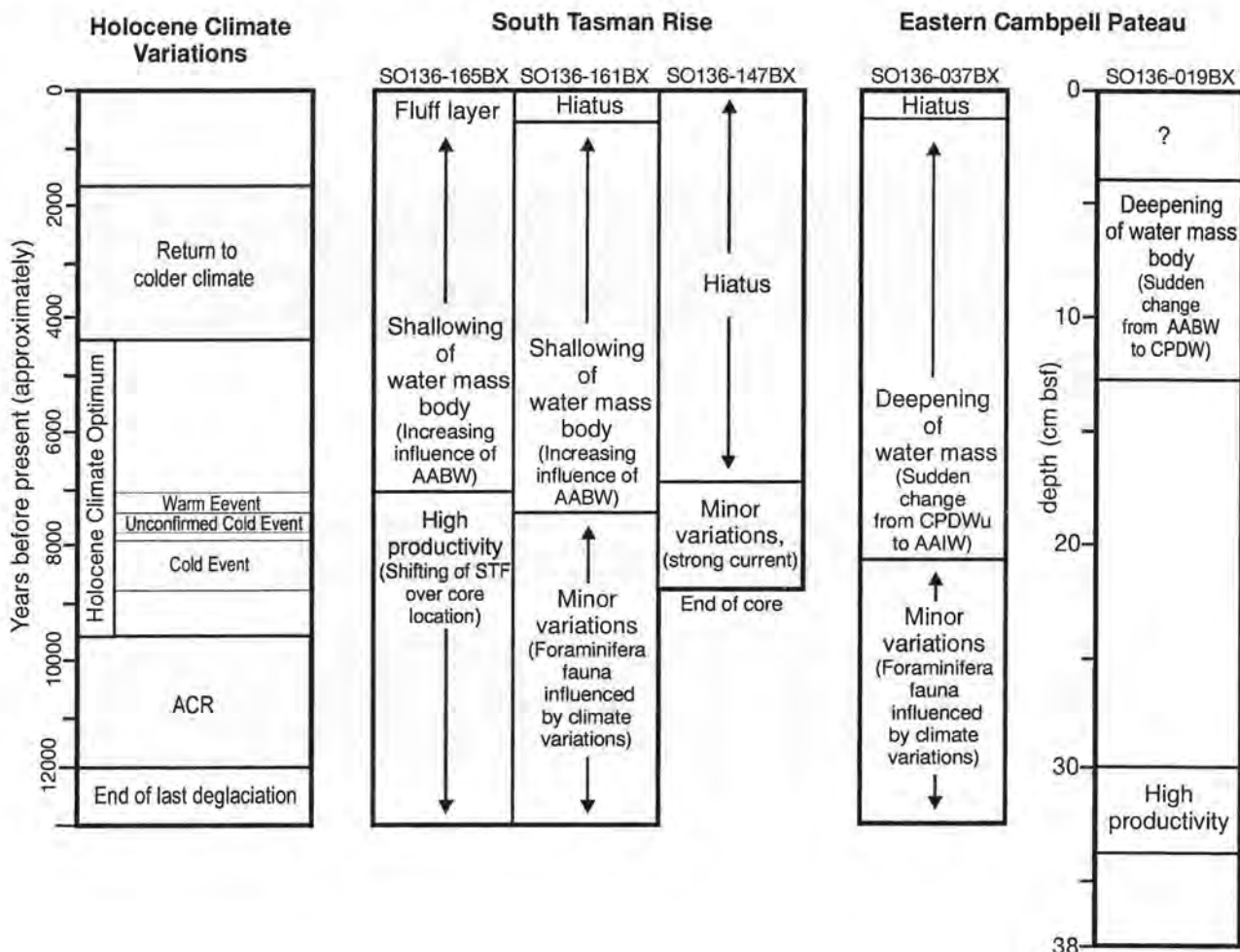
* Associated with *F. contemplata* in areas of high productivity.

Paleoceanography

- The analysis indicates deepening water masses at the eastern Campbell Plateau since the end of the Antarctic Cold Reversal, approximately since 8500 yr. BP until the present.
Sharp boundaries between the water masses are present.
- The water mass body at the South Tasman Rise rises since the end of the "Cold Event", approximately since 7500 yr. BP until the present.
Diffuse boundaries between the water masses are present.
- A high productivity fauna, dominated by *Furcifera complanata* indicates shifting of the Subtropical Front over the core location of SO136-165BX. The phase of high productivity extends until the beginning of the "Warm event" at ~7500 yr. BP.

- Processes of redeposition and resuspension play a major role in the process of sedimentation of the investigated box cores. Hiatuses and / or erosional events are a frequent feature at the South Tasman Rise.

Table 6.2 Oceanographic variations recorded in the investigated cores. The timing gives the approximated position of the single events and does not suggest absolute ages. No stratigraphical model is available for the core SO136-019BX.



ACKNOWLEDGEMENTS

I thank Professor Gerd Flajs from the Aachen Technical University and Professor Jörn Thiede from the AWI Bremerhaven for making the performance of this thesis possible.

For managing the project TASQWA and for suggesting this thesis I thank Dr. Stefan Nees from GEOMAR, Kiel.

Special thanks go again to Dr. Christian Bücker from the BGA Hannover, for introducing me to GEOMAR and to other proven contacts.

I want to thank Arne Sturm from GEOMAR for organising the stable isotope measurements in time, and most of all for being patient with almost any question. "Ask Arne!"

Dr. Joachim Schönfeld from GEOMAR I thank for valuable hints and Dr. Dorothee Spiegler for friendly help in the discrimination of certain foraminifera species.

Dr. John J.G. Reimer from GEOMAR deserves my thanks for reviewing this thesis.

Dr. Christian Samtleben and especially Miss Schuldt from the University of Kiel I thank for patience help with the SEM photos.

Professor Grootes from the Leibniz Labor für Altersbestimmung, Kiel contributed the AMS¹⁴C ages.

I want to thank Dr. Florian Böhm for listening and answering my questions about stable isotopes and especially for being the only always friendly face on the GEOMAR floor.

For long lessons about the fate of organic matter in the ocean and for voluntarily reviewing my thesis I want to thank Constanze Böttcher from the IOW, Warnemünde. Also my thank goes to Dr. Stefan Forster from the same institute for friendly suggestions about the same topic.

The comprehensive explanations on bioturbation and benthic fauna of Sokratis Papaspyro from the Department of Biology, University of Athens are preciated.

For patience in reviewing this thesis entirely, I want to thank Beatrice Neu from the Department of Geology and Palaeontology, Köln University. You will get it back very soon!

Last not least, I want to mention the co-operation of Sven Roth in the office and the co-endurance of Andres Rüggeberg on the binocular.

I appreciated the discussions with Lars Reuning. Thanks for reviewing my English.

Finally, I like to remember the entertaining companionship of Terry Mills, our guest from Bangor School of Ocean Sciences.

REFERENCES

- Alavi, S.N., 1988. Late Holocene deep-sea benthic foraminifera from the Sea of Marmara. *Marine Micropaleontology*, 13: 213-237.
- Alley, R.B. et al., 1997. Holocene climatic instability: A prominent widespread event 8200 yr. ago. *Geology*, 25(6): 483-486.
- Alley, R.B. et al., 1993. Abrupt increase in Greenland snow accumulation at the end of the Younger Dryas event. *Nature*, 362: 527-529.
- Alm, T., Vorren, K.D. and Morkved, B., 1996. Holocene Tree-Line Fluctuation and Climate in Central Troms, Northern Norway. *Historical Biology*, 12: 25-38.
- Altenbach, A.V., 1992. Verbreitungsmuster benthischer Foraminiferen im Arktischen Ozean und in glazialen und interglazialen Sedimenten des Europäischen Nordmeeres. *Habilitationsschrift*, Christian-Albrechts-Universität.
- Altenbach, A.V. and Sarnthein, M., 1989. Productivity record in benthic foraminifera. In: W.H. Berger, V.S. Smetacek and G. Wefer (Editors), *Productivity of the Oceans: Present and Past*, Dahlem Conferences, pp. 255-269.
- Anderson, J.B., 1975. Ecology and distribution of foraminifera in the Weddel Sea of Antarctica. *Micropaleontology*, 21: 69-96.
- Backhaus, K., Erichson, B., Plinke, W., Schuchard-Fischer, C. and Weiber, R., 1989. *Multivariate Analysemethoden*, 5. rev. Auflage, Berlin, Heidelberg, New York, London, Paris, Tokyo.
- Barker, R.W., 1960. Taxonomic Notes on the species figured by H. B. Brody in his report on the foraminifera dredged by H. M. S. Challenger during the years 1873-1876. *SEPM Spec. Publ.*, 9: 240.
- Barranco, F.T.J., Balsam, W.L. and Deaton, B.C., 1989. Quantitative reassessment of brick red lutites: evidence from reflectance spectrophotometry. *Marine Geology*, 89: 299-314.
- Bauch, H.A., Struck, U. and Thiede, J., 1999. Planktic and Benthic Foraminifera as Indicators of Past Ocean Changes in Surface and Deep Waters of the Nordic Seas. In: P. Schäfer, W. Ritzau, M. Schlüter and J. Thiede (Editors), *The Northern Atlantic: A changing environment*. Springer, Berlin, pp. 45 - 66.
- Belanger, P.E. and Streeter, S.S., 1980. Distribution and ecology of benthic foraminifera in the Norwegian-Greenland Sea., Mar. *Micropaleontol*, pp. 401-428.
- Berger, A. and Loutre, M.F., 1991. Insulation values for the climate of the last 10 million years. *Quaternary Sciences Review*, 117: 297 - 317.
- Bernhard, J.M., 1993. Experimental and field evidence of Antarctic foraminiferal tolerance to anoxia and hydrogen sulphide. *Marine Micropaleontology*, 20: 203-213.
- Blunier, T., Chappelaz, J., Schwander, A., Daumillenbach, B., Stauffer, B., Stocker, T.F., Raynaud, D., Jouzel, J., Clausen, H.B., Hammer, C.U., Johnsen, S.J. et al., 1998. Asynchrony of Antarctic and Greenland Climate Change During the Last Glacial Period. *Nature*, 394: 739-743.
- Braatz, B.V. and Corliss, B.H., 1984. Bottom water circulation in the South Australian Basin during the last 3.2 million years. *Antarctic Journal of the United States*, 19: 84-88.
- Bradford-Grieve, J.M., Lewis, K.B. and Stanton, B.R., 1991. Advances in New Zealand oceanography, 1967-91. *New Zealand Journal of Marine and Freshwater Research*, 25: 429-441.
- Brathauer, U. and Abelmann, A., 1999. Late Quaternary variations in sea surface temperatures and their relationship to orbital forcing recorded in the Southern Ocean (Atlantic sector). *Paleoceanography*, 14: 135-148.
- Bremer, M.L. and Lohmann, G.P., 1982. Evidence for primary control of the distribution of certain Atlantic Ocean benthonic foraminifera by degree of carbonate saturation. , 29: 987-998.
- Burke, S.C., 1981. Recent benthic foraminifera of the Ontong Java Plateau., *Journal of Foraminiferal Research*, pp. 1-19.

REFERENCES

- Canfield, D.E., 1994. Factors influencing organic carbon preservation in marine sediments. *Chemical Geology*, 114(3-4): 315-329.
- Caralp, M.H., 1989. Size and morphology of the benthic foraminifer *Melonis barleeanum*. Relationship with marine organic matter. *Journal of Foraminiferal Research*, 19(3): 235-245.
- Carter, R.M., Carter, L. and McCave, N., 1996. Current controlled sediment deposition from the shelf to the deep ocean: the Cenozoic evolution of circulation through the SW Pacific. *Geologische Rundschau*, 85(3): 438-451.
- Ciaia, P. et al., Petit, J.R., Jounzel, J., Loriaus, C., Barkov, N.I., Lipenkov, V., Nicolaiev, V 1992. Evidence for an early Holocene climatic optimum in the Arctic deep ice-core record. *Climate dynamics*, 6: 169-177.
- Clark, F.E., 1995. New species of unilocular calcareous foraminifera from the Holocene of the southwest Pacific Ocean. *Journal of Micropalaeontology*, 14(1): 1-5.
- Clark, F.E., Patterson, R.T. and Fishbein, E., 1994. Distribution of Holocene benthic foraminifera from the tropical southwest Pacific Ocean. *Journal of Foraminiferal Research*, 24(4): 241-267.
- Corliss, B., 1982. Distribution of Holocene deep-sea benthonic foraminifera in the Southwest Indian Ocean. , 30(2A): 95-117.
- Corliss, B.H., 1976. Recent deep-sea benthonic foraminiferal distributions in the southeast Indian Ocean. *Antarctic Journal*, 11: 165-167.
- Corliss, B.H., 1978a. Studies on deep-sea benthonic foraminifera in the southeast Indian Ocean. *Antarctic Journal*, 13: 116-118.
- Corliss, B.H., 1978b. Quaternary Antarctic Bottom-Water history: deep-sea benthonic foraminiferal evidence from the southeast Indian Ocean. *Quaternary Research*, 12: 271-289.
- Corliss, B.H., 1979b. Recent deep-sea benthonic foraminiferal distributions in the southeast Indian Ocean: inferred bottom-water routes and ecological implications. *Marine Geology*, 31: 115-138.
- Corliss, B.H., 1979c. Taxonomy of Recent deep-sea benthonic foraminifera from the Southeast Indian Ocean. *Micropaleontology*, 25: 1-19.
- Corliss, B.H., 1985. Microhabitats of benthic foraminifera within deep-sea sediments. *Nature*, 314: 435-438.
- Corliss, B.H. and Honjo, S., 1981. Dissolution of deep-sea benthonic foraminifera. *Micropaleontology*, 27: 356-378.
- Corliss, B.H., Martinson, D.G. and Keffer, T., 1986. Late Quaternary deep-ocean circulation. *Geological Society of America Bulletin*, 97: 1106-1121.
- Corliss, B.H. and Chen, C., 1988. Morphotype patterns of Norwegian Sea deep-sea benthic foraminifera and ecological implications., *Geology* (Boulder), pp. 716-719.
- Craig, H., 1957. The natural distribution of radiocarbon and the exchange time of carbon dioxide between the atmosphere and sea. *Tellus* (9): 1-17.
- Dansie, L., 1994. Reconstruction of Quaternary sea-surface temperatures for the Southeast Indian Ocean based on a Diatom Transfer Function, Geology Department, The Australian National University.
- Deacon, G.E.R., 1937. The hydrology of the Southern Ocean. *Discovery Reports*, 15: 1 - 24.
- Douglas, R. and Woodruff, F., 1981a. Deep-sea benthic foraminifera. In: C. Emiliani (Editor), *The oceanic lithosphere*. Univ. Miami, Dep. Geol., Miami, FL, United States. 7. John Wiley and Sons, New York, NY, United-States, pp. 1233-1327.
- Douglas, R.G. and Woodruff, F.C., 1981b. Miocene benthic foraminifera and bottom water evolution., Anonymous. *Geological Society of America*, 94th annual meeting. Abstracts with Programs Geological Society of America, pp. 441.
- Eade, J.V., 1967. New Zealand recent foraminifera of the families Islandiellidae and Cassidulinidae. *New Zealand Journal of marine and Freshwater Research*, 1: 421-454.

- Echols, R.J., 1971. Distribution of foraminifera in sediments of the Scotia Sea area, Antarctic waters. American Geophysical Union, Antarctic Research Series, 15: 93-168.
- Emery, W.J. and Meincke, J., 1986. Global water masses: summary and review. *Oceanologica Acta*, 9(4): 383-391.
- Epstein, S., Buchsbaum, R., Löwenstam, H.A. and Urey, H.C., 1953. Revised carbonate water isotopic temperature scale. *Bulletin of the Geological Society of America*, 64: 1315-1326.
- Exon, N.F. Hill, P.J., Royer, J.-Y., Müller, D., Whitmore, G., Belton, D., Dutkiewicz, A., Ramel, C., Rollet, N., Wellington, A., 1994. *Tasmante* swath-mapping and reflection seismic cruise off Tasmania using R.V. L'ATALANTE. AGSO Record, 1994/68: 72.
- Exon, N.F. Marshall, J.F., McCorkle, D.C., Alcock, M., Chaproniere, G.C.H., Connell, R., Dutton, S.J., Elmes, M., Findlay, C., Robertson, L., Rollet, N., Samson, C., Shafik, S., Whitmore, G.P., 1995. AGSO Cruise 147 Report - Tasman Rises Geological Sampling Cruise of Rig Seismic: stratigraphy, tectonic and palaeoclimate of the offshore Tasmanian Region. AGSO Record, 1995/56: 159.
- Fenner, J., Carter, L. and Stewart, R., 1992. Late Quaternary paleoclimatic and paleoceanographic change over northern Chatham Rise, New Zealand. *Marine Geology*, 108: 383-404.
- Feyling-Hanssen, R.W., Joergensen, J.A., Knudsen, K.L. and Andersen, A.-L.L., 1971. Late Quaternary Foraminifera from Vendysyssel, Denmark and Sandnes, Norway. *Bulletin of the Geological Society of Denmark*, 21(67-317).
- Folland, C.K., Karl, T.R. and Vinnikov, K.Y.A., 1990. Observed climate variations and change. In: J. T. Houghton, G.J. Jenkins and J.J. Ephraums (Editors), *Climate Change - The IPCC scientific assessment*. Cambridge University Press, New York, Port Chester, Melbourne, Sidney, pp. 195-238.
- Gabel, B., 1971. Die Foraminiferen der Nordsee. *Helgoländer wissenschaftliche Meeresuntersuchungen*, 22: 1-65.
- Garner, D.M., 1959. The subtropical convergence in New Zealand waters., 2: 315-337.
- Goldstein, S.T., Watkins, G.T. and Kuhn, R.M., 1995. Taphonomy of salt marsh foraminifera a case study from coastal Georgia. *Geological Society of America annual meeting abstracts*, 27(6): A29.
- Gordon, A.L., 1972. On the interaction of the Antarctic Circumpolar current and the Macquarie Ridge. In: D. E. Hayes (Editor), *Antarctic Oceanology II*, The Australian - New Zealand Sector. American Geophysical Union, Washington, pp. 71-78.
- Gordon, A.L. and Molinelli, E., 1986. *Southern Ocean Atlas: Thermohaline and chemical distributions*, Columbia University Press, New York.
- Graf, G., 1989a. Benthic-pelagic coupling in a deep-sea benthic community. *Nature*, 341: 437-439.
- Graf, G., 1989b. Die Reaktion des Benthals auf den saisonalen Partikelfluß und die laterale Advektion, sowie deren Bedeutung für Sauerstoff- und Kohlenstoffbilanzen. *Habilitation*, Christian-Albrechts-Universität.
- Graf, G. and Linke, P., 1992. Adenosine nucleotides as indicators of deep-sea benthic metabolism. In: G.T. Rowe and V. Pariente (Editors), *Deep-Sea Food Chains and the Global Carbon Cycle*. NATO ASI Series C: Mathematical and Physical Sciences. Kluwer Academic Publisher, Dordrecht/Boston/London, pp. 237-243.
- Gupta, A.K., 1994. Taxonomy and bathymetric distribution of Holocene deep-sea benthic foraminifera in the Indian Ocean and the Red Sea. *Micropaleontology*, 40(4): 351-367.
- Harloff, J. and Mackensen, A., 1997. Recent benthic foraminiferal associations and ecology of the Scotia Sea and Argentine Basin. *Marine Micropaleontology*, 31(1997): 1-29.
- Hayward, B.W., Grenfell, H. R., Reid, C. M. and Hayward, K. A., 1999. Recent New Zealand Shallow-Water Benthic Foraminifera. Monograph 21, New Zealand Geological Survey paleontological bulletin 75. Institute of Geological & Nuclear Sciences Limited, Levin, 258 pp.

- Henrichs, S.M., 1997. Preservation of organic matter in marine sediments; quantitative relationships between preservation and decomposition processes. Geological Society of America, 1997 annual meeting, 29(6): 16.
- Herguera, J.C., 1992. Deep-sea benthic foraminifera and biogenic opal: Glacial to postglacial productivity changes in the eastern equatorial Pacific. *Marine Micropaleontology*, 19(1/2): 79-98.
- Heß, S., 1998. Verteilungsmuster rezenter benthischer Foraminiferen im Südchinesischen Meer, Univ. Kiel, Kiel.
- Hinz, K. and shipboard party, 1985. Geophysical, geological and geochemical studies off West Tasmania and on the South Tasman Rise. Bundesanstalt für Geowissenschaften und Rohstoffe, Cruise Report SO 36B.
- Hoffmann, E. E., 1985. The large-scale horizontal structure of the Antarctic Circumpolar Current from FGGE drifters. *Journal of Geophysical Research*, 90(7087 - 7097).
- Holler, P., 1995. Arbeitsmethoden der marinen Geowissenschaften. Enke Verlag, Stuttgart, 150 pp.
- Howard, W.R. and Prell, W.L., 1992. Late Quaternary surface circulation of the southern Indian Ocean and its relationship to orbital variations. , 7(1): 79-117.
- Huges, G.W., 1988. Modern bathyal agglutinating foraminifera from the Vella Gulf and Balsche Channel, New Georgia, Solomon Islands, southwest Pacific. *Journal of Foraminiferal Research*, 18: 304 - 310.
- Imbrie, J. and Kipp, N. G., 1971. A new micropaleontological method for Quantitative Paleoclimatology: Application to a late Pleistocene Caribbean Core, in The Late Cenozoic Glacial Ages. Yale Univ. Press, New Haven, CT, 71-181 pp.
- Johnsen, S.J. et al., 1992. Irregular glacial interstadials recorded in a new Greenland ice core. *Nature*, 359: 311-313.
- Jorissen, F.J., Wittling, J.P., Rabouille, C. and Relexans, J.C., 1998. Live benthic foraminiferal faunas off Cape Blanc, NW-Africa: Community structure and microhabitats. *Deep-Sea Research*, 1(45): 2157 - 2188.
- Jouzel, J. et al., 1995. The two-step shape and timing of the last deglaciation in Antarctica. *Climate Dynamics*, 11: 151-161.
- Kaiho, K., 1994. Benthic foraminiferal dissolved-oxygen index and dissolved-oxygen levels in the modern ocean. *Geology*, 22: 719-722.
- Kitgaard-Kristensen, D. H., Seidrup, P., Halifdason, H., Johnsen, S. and Spurk, M., 1998. A regional 8200 cal. Yr. BP cooling event in Northwest Europe, induced by final stages of the Laurentide ice-sheet deglaciation? *Journal of Quaternary Science*, 13: 165-169.
- Kristensen, E. and Blackburn, H. T., 1987. The fate of organic carbon and nitrogen in experimental marine sediment systems: Influence of bioturbation and anoxia. *Journal of Marine Research*, 45: 231 - 257.
- Kuhnt, W., Moullade, M. and Kaminski, M.A., 1996. Ecological structuring and evolution of deep sea agglutinated foraminifera - a review. *Revue de Micropaléontologie*, 39(4): 27-281.
- Labracherie, M., Labeyrie, L.D., Duprat, J., Bard, E., Arnold, M., Pichon, J.-J., Duplessy, J.-C., 1989. The last deglaciation in the Southern Ocean. *Paleoceanography*, 4(6): 629-638.
- Lindberg, H.G. and Auras, A., 1984. Distribution of arenaceous foraminifera in depth profiles of the Southern Ocean (Kerguelen Plateau area). *Paleogeography, Paleoclimatology, Paleoecology*, 48: 61-106.
- Linke, P. and Lutze, G.F., 1993. Microhabitat preferences of benthic foraminifera - a static concept or a dynamic adaptation to optimise food acquisition? *Marine Micropaleontology*, 20: 215-234.
- Loeblich, A.R. and Tappan, J. and Tappan, H., 1964. Treatise on Invertebrate Paleontology, 1 and 2. The geological Society of America, Boulder.

- Lohmann, G. P., 1978. Abyssal benthonic foraminifera as hydrographic indicators in the Western South Atlantic Ocean. *Journal of Foraminiferal Research*, 8(1): 6-34.
- Loubere, P., 1991. Deep-sea benthic foraminiferal assemblage response to a surface ocean productivity gradient: a test. *Paleoceanography*, 6(2): 193-204.
- Loubere, P., 1995. The surface ocean productivity and bottom water oxygen signals in deep water benthic foraminiferal assemblages. *Marine Micropaleontology*, 28(1996): 247-261.
- Loubere, P., 1997. Benthic foraminiferal assemblage formation, organic carbon flux and oxygen concentrations on the outer continental shelf and slope. *Journal of Foraminiferal Research*, 27(2): 93-100.
- Loubere, P., Banonis, G. and Jakiel, R., 1988. *Globocassidulina subglobosa* (BRADY): environmental control of species abundance and specimen test size. *Journal of Foraminiferal Research*, 18(1): 6-15.
- Loubere, P. and Gary, A., 1990. Taphonomic process and species microhabitats in the living to fossil assemblage transition of deeper water benthic foraminifera. 5: 375-381.
- Loubere, P. and Gary, A., 1993. Generation of the benthic foraminiferal assemblage: theory and preliminary data. *Marine Micropaleontology*, 20: 165-181.
- Lutze, G.F., 1980. Depth distribution of benthic foraminifera on the continental margin off NW Africa. "Meteor" Forschungsergebnisse., Reihe C, 32: 31-80.
- Lutze, G.F. and Altenbach, A. V., 1988. *Rupertina stabilis* (Wallich), a highly adapted suspension feeding foraminifer. *Meyniana*, 40: 55-69.
- Mackensen, A., 1985. Verbreitung und Umwelt benthischer Foraminiferen in der Norwegischen See. Unveröffentlichte, PhD Thesis, Christian-Albrechts-Universität Kiel.
- Mackensen, A., 1987. Benthische Foraminiferen auf dem Island-Schottland Rücken: Umwelt-Anzeiger an der Grenze zweier ozeanischen Räume. *Paläontologische Zeitschrift*, 61(3/4): 149-179.
- Mackensen, A., 1997. Zur Paläoozeanographie hoher Breiten: Stellvertreterdaten aus Foraminiferen. *Berichte zur Polarforschung*, 243(1997): 0-146.
- Mackensen, A., Barrera, E. and Hubberten, H.-W., 1992. Neogen circulation in the Southern Indian Ocean: evidence from benthic foraminifers, carbonate data, and stable isotope analyses (Site 751). *Proceedings of the Ocean Drilling Program, Scientific Results*, Vol. 120: 867-878.
- Mackensen, A., Fütterer, D.K., Grobe, H. and Schmiedl, G., 1993. Benthic foraminiferal assemblages from the eastern South Atlantic Polar Front region between 35° and 57°S: Distribution, ecology and fossilisation potential. *Marine Micropaleontology*, 22(1993): 33-69.
- Mackensen, A., Grobe, H., Hubberten, H.-W. and Kuhn, G., 1994. Benthic foraminiferal assemblages and the $\delta^{13}\text{C}$ -signal in the Atlantic sector of the Southern Ocean: glacial-to-interglacial contrasts. In: R. Zahn, T.F. Pedersen, M. A. Kaminski and L. Labeyrie (Editors), *Carbon Cycling in the Glacial Ocean: Constraints on the Ocean's Role in Global Change. Global Environmental Change*. Springer, Berlin Heidelberg New York, pp. 105-144.
- Mackensen, A., Grobe, H., Kuhn, G. and Fütterer, D.K., 1990. Benthic foraminiferal assemblages from the eastern Weddell Sea between 68° and 73° S: Distribution, ecology and fossilisation potential. *Marine Micropaleontology*, 16(1990): 241-283.
- Malmgren, B. A. and Haq, B. U., 1982. Assessment of quantitative techniques in paleobiography. , 7: 213-236.
- McCorkle, D.C., Heggie, D. T. and Veeh, H.H., 1998. Glacial and Holocene stable isotope distributions in the southeastern Indian Ocean. *Paleoceanography*, 13(1): 20-34.
- McCrea, J.M., 1950. On the isotopic chemistry of carbonates and a paleotemperature scale. *Journal of Chemistry and Physics*, 18: 849-857.
- Mead, G.A. and Kennet, J.P., 1987. The disintegration of recent benthic foraminifera in the Polar Front region, southwest Atlantic. *Marine Micropaleontology*, 11: 343-360.

- Milam, R.W. and Anderson, J.B., 1981. Distribution and ecology of recent benthonic foraminifera of the Adelie-George continental shelf and slope, Antarctica. *Marine Micropaleontology*, 6(1981): 297-325.
- Morkhoven, F. P. C. M. v., Berggren, W.A. and Edwards, A. S., 1986. Cenozoic cosmopolitan deep-water benthic foraminifera. *Bulletin des Centres de Recherches Exploration Production Elf Aquitaine. Memoire*, pp. 650.
- Mullins, H. T., Thompson, J.B., McDougall, K. and Vercoutere, T.L., 1985. Oxygen-minimum one edge effect: evidence from the central California coastal upwelling system. *Geology*, 13: 491-494.
- Murray, J.W., 1971. An Atlas of Recent Foraminiferids. Heinemann Educational Books, London, U.K., 244 pp.
- Murray, J.W., 1973. Distribution and ecology of living benthonic Foraminiferids. Heineman Educational Books, London, 274 pp.
- Murray, J.W., 1991. Ecology and Palaeoecology of Benthic Foraminifera. Longman Scientific & Technical, Essex.
- Nagao, S. and Nakashima, S., 1992. The factors controlling vertical colour variations of North Atlantic Madeira Abyssal Plain sediments. *Marine Geology*, 109: 83-94.
- Nees, S., 1994. The benthic foraminiferal record of Late Quaternary glacial/interglacial cycles in core E 36-23, East Tasman Plateau. In: G.J. van der Lingen, K. M. Swanson and R. J. Muir (Editors), *The Evolution of the Tasman Sea Basin. Proceedings of the Tasman Sea Conference (November 1992, Christchurch, New Zealand)*. Balkema, Rotterdam, pp. 203-214.
- Nees, S., 1997. Late Quaternary palaeoceanography of the Tasman Sea: the benthic foraminiferal view. *Paleogeography, Paleoclimatology, Paleoecology*, 131(3/4): 365-390.
- Nees, S., Armand, L., De Decker, P., Labracherie, M. and Passlow, V., 1999. A diatom and benthic foraminiferal record from the South Tasman Rise (southeastern Indian Ocean): implications for palaeoceanographic changes for the last 200,000 years. *Marine Micropaleontology*, 38: 69-89.
- Niebler, H.-S., 1995. Reconstruction of paleo-environmental parameters using stable isotopes and faunal assemblages of planktonic foraminifera in the South Atlantic Ocean. 167, Alfred Wegener Institut für Polar und Meeresforschung, Bremerhaven.
- Nienstedt, J.C. and Arnold, A.J., 1988. The distribution of benthic foraminifera on seamounts near the East Pacific Rise. *Journal of Foraminiferal Research*, pp. 237-29.
- Ohkushi, K. I., Thomas, E. and Kawahata, H., 1999. Abyssal benthic foraminifera from the northwestern Pacific (Shatsky Rise) during the last 298kyr. *Marine Micropaleontology*, 38: 119-147.
- Oki, K., 1989. Ecological Analysis of Benthonic Foraminifera in Kagoshima Bay, South Kyushu, Japan. *South Pacific Studies*, 10(1): 1-191.
- Orsi, A.H., Whitworth III, T. and Nowlin Jr., W. D., 1995. On the meridional extent and fronts of the Antarctic Circumpolar Current. *Deep Sea Research*, 42(5): 641-673.
- Ozarko, D. L., Patterson, R.T. and Williams, H.F.L., 1997. Marsh foraminifera from Nanaimo, British Columbia (Canada): implications of infaunal habitat and taphonomic biasing. *Journal of Foraminiferal Research*, 27(51): 451.
- Paillard, D., Labeyrie, L. and Yiou, P., 1996. Macintosh Program Performs Time-Series Analysis. *Eos Trans. AGU*, 77: 379.
- Perez-Cruz, L. L. and Machain-Castillo, M. L., 1990. Benthic foraminifera of the oxygen minimum zone, continental shelf of the gulf of Tehuantepec, Mexico. *Journal of Foraminiferal Research*, 20(4): 312-325.
- Peterson, L.C., 1984. Recent abyssal benthic foraminiferal biofacies of the eastern equatorial Indian Ocean. *Marine Micropaleontology*, 8(6): 479-515.

- Pflaumann, U. and Zhimini, J., 1999. Modern distribution patterns of planktonic foraminifera in the South China Sea and western Pacific: a new transfer technique to estimate regional sea-surface temperatures. *Marine Geology*, 156: 41 - 83.
- Resig, J.M., 1981. Biogeography of benthic foraminifera of the northern Nazca Plate and adjacent continental margin., Kulm, LaVerne D., Dymond, Jack, Dasch, E. Julius, Hussong, Donald M., Roderick, Roxanne. Nazca Plate; crustal formation and Andean convergence. *Memoir Geological Society of America*.
- Rüggeberg, A. and Nees, S., 2000. Late Quaternary Paleoceanography in the South Tasman Region: Implications of Benthic Foraminifers and Grain Size Analysis. *in prep.*
- Schiebel, R., 1992. Rezente benthische Foraminiferen in Sedimenten des Schelfes und oberen Kontinentalhängen im Golf von Guinea (Westafrika). 51, GEOMAR - Research Center for Marine Geosciences, Kiel.
- Schmiedl, G., 1995. Rekonstruktion der spätquartären Tiefenwasserzirkulation und Produktivität im östlichen Südatlantik anhand von benthischen Foraminiferenvergesellschaftungen. *Reports on Polar Research*, 160: 207.
- Schnitker, D., 1980. Quaternary deep-sea benthic foraminifers and bottom water masses. *Annual Review of Earth and Planetary Sciences*, 8: 343-370.
- Schnitker, D., 1994. Deep-sea benthic foraminifers: food and bottom water masses. In: R. Zahn, T.F. Pedersen, M. A. Kaminski and L. Labeyrie (Editors), *Carbon Cycling in the glacial ocean: constraints on the ocean's role in Global Change*. NATO ASI Series I: Global Environmental Change. Springer Verlag, Berlin/Heidelberg/New York, pp. 539-554.
- Schröder, C. J., 1986. Deep-water arenaceous foraminifera in the northwest Atlantic Ocean. *Ocean Science*, 71: 191.
- Shackleton, N.J., 1987. Oxygen isotopes, ice volume and sea level. *Quaternary Science Reviews*, 6: 183-190.
- Shackleton, N.J. and Opdyke, N.D., 1973. Oxygen-isotope and paleomagnetic stratigraphy of the equatorial Pacific core V28-238: oxygen-isotope temperatures and ice volumes on an 10 5 year to 10 6 year scale. *Quaternary Research*, 3: 39 - 55.
- Steig, E. et al., 1998. Synchronous climate changes in Antarctica and the North Atlantic. *Science*, 282: 92-95.
- Streeter, S. S., 1973. Bottom water and benthonic foraminifera in the North Atlantic - glacial/interglacial contrasts. *Quaternary Research*, 3: 131- 141.
- Streeter, S. S. and Lavery, S. A., 1979. Holocene benthic foraminifera from the continental slope and rise off eastern North America; reconnaissance study., *Geol. Soc. Am., Abstr. Programs*, pp. 525.
- Struck, U., 1992. Zur Paläo-Ökologie benthischer Foraminiferen im Europäischen Nordmeer während der letzten 600.000 Jahre. *Berichte aus dem Sonderforschungsbereich* 313, 38: 1-89.
- Struck, U. and Nees, S., 1991. Die stratigraphische Verbreitung von *Siphonostularia rolshauseni* (Phleger & Parker) in Sedimentkernen aus dem Europäischen Nordmeer. *Geol. Jb., A* 128: 243-249.
- Stuiver and Polach, 1977. Discussion: Reporting of 14C data. *Radiocarbon*, 19/3: 355.
- Stuiver, M. and Grootes, P., 1999. GISP2-Taylor Dome oxygen isotope ratios. *Quaternary Research*, (in press).
- Stuiver, M., Reimer, P.J., Stuiver, M., Reimer, P.J., Bard, E., Beck, J.W., Burr, G.S., Hughen, K.A., Kromer, B., McCormac, F.G., v.d. Plicht, J., Spurk, M., 1998a. RADIOCARBON CALIBRATION PROGRAM REV 4.1.2. *Radiocarbon*, 40: 1041-1083.
- Stuiver, M., Reimer, P.J. and Braziunas, T.F., 1998b. High-precision radiocarbon age calibration for terrestrial and marine samples. *Radiocarbon*, 40: 1127-1151.
- Sun, M. Y., Lee, C. and Aller, R. C., 1993a. Laboratory studies of oxic and anoxic degradation of chlorophyll-a in Long Island Sound sediments. *Geochimica et Cosmochimica Acta.*, 57: 147 - 157.

REFERENCES

- Sverdrup, H.U. and Johnson, M. W., 1942. The oceans: their physics, chemistry and general biology. Prentice-Hall, Englewood Cliffs.
- TASQWA, S. Nees and the shipboard scientific party of TASQWA, 1999. Cruise Report SO136 - TASQWA. 89, GEOMAR - Research Center for Marine Geosciences, Kiel.
- Tchernia, P., 1980. Descriptive Regional Oceanography, 1. Pergamon Press, Paris.
- Thies, A., 1991. Die Benthosforaminiferen im Europäischen Nordmeer. Berichte aus dem Sonderforschungsbereich 313, 31: 1-97.
- Tilzer, M. M., 1995. Primärproduktion im Südpolarmeer: Die Bedeutung tiefer Wassertemperaturen für Produktivität und Wachstum des Phytoplanktons. In: I.G. Hempel (Editor), Biologie der Polarmeere. Gustav Fischer Verlag, Jena, pp. 147 - 154.
- Timm, S., 1992. Rezente Tiefsee-Benthosforaminiferen aus Oberflächensedimenten des Golfs von Guinea (Westafrika) - Taxonomie, Verbreitung, Ökologie und Korngrößenfraktionen. 59, Geologisches-Paläontologisches Institut und Museum.
- Tomczak, M. and Godfrey, J. S., 1994. Regional Oceanography: an introduction. Pergamon, Oxford, 422 pp.
- Tuominen, L., Heinänen, A., Kuparinen, J. and Nielsen, L. P., 1998. Spatial and temporal variability of denitrification in the sediments of the northern Baltic Proper. *Marine Ecology Progress Series*, 172: 13-24.
- Tyson, P. D. and Lindesay, J.A., 1992. The climate of the last 2000 years in southern Africa. *The Holocene*, 2(3): 271-278.
- Urey, H. C., 1947. The thermodynamic properties of isotopic substances. *Journal of the Chemical Society*, ?: 526-581.
- Van der Zwaan, G. et al., 1999. Benthic foraminifers: proxies or problems? A review of paleoecological concepts. *Earth-Science Reviews*, 46: 213-236.
- Vella, P., 1957. Studies in New Zealand Foraminifera. *New Zealand Geological Survey Paleontological Bulletin*, 28: 1-64.
- Verardo, D. J., Froelich, P.N. and McIntyre, A., 1989. Determination of organic carbon and nitrogen in marine sediments using the Carlo Erba NA-1500 Analyser. *Deep-Sea Research*.
- Voelker, A.H.L. et al., 1998. Correlation of marine ^{14}C ages from the Nordic sea with the GISP2 isotope record: Implications for radiocarbon calibration beyond 25 ka BP. *Radiocarbon*, 20.
- von Grafenstein, U., Erlenkeuser, H., Brauer, A., Jouzel, J. and Johnsen, S.J., 1999. A Mid-European Decadal Isotope-Climate Record from 15,500 to 5000 Years B. P. *Science*, 284(June): 1654-1657.
- Watkins, N.D. and Kennett, J.P., 1976. Erosion of deep-sea sediments in the southern ocean between longitudes 70° E and 190° E and contrasts in manganese nodule development. *Marine Geology*, 23(1/2): 103-111.
- Weaver, P.P.E., Carter, L. and Neil, H. L., 1998. Response of surface water masses and circulation to late Quaternary climate changes east of New Zealand. *Paleoceanography*, 13(1): 70-83.
- Weaver, P.P.E., Neil, H. and Carter, L., 1997. Sea surface temperature estimates from the Southwest Pacific based on planktonic foraminifera and oxygen isotopes. *Paleogeography, Paleoceanography, Paleoecology*, 131(1997): 241-256.
- Weber, M. E., 1998. Estimation of biogenic carbonate and opal by continuous non-destructive measurements in deep-sea sediments: application to the eastern Equatorial Pacific. *Deep-Sea Research I*, 45: 1955-1975.
- Wefer, G. and Berger, W.H., 1991. Isotope paleontology: growth and composition of extant calcareous species. *Marine Geology*, Vol. 100: 207-248.
- Wells, P. E. and Conell, R., 1997. Movement of hydrological fronts and widespread erosional events in the southwestern Tasman Sea during the Late Quaternary. *Australian Journal of Earth Sciences*, 44: 105-112.

REFERENCES

- Wells, P. E. and Okada, H., 1996. Holocene and Pleistocene glacial Paleoceanography of Southeastern Australia, based on Foraminifers and Nanofossils in Vema Cored Hole V 18-222. *Australian Journal of Earth Sciences*, 43: 509 - 523.
- Withworth, T., 1980. Zonation and geostrophic flow of the Antarctic Circumpolar Current at Drake Passage. *Deep Sea Research*, 27(497 - 507).
- Wolf, T.C., 1991. Paläo-ozeanographisch-klimatische Entwicklung des nördlichen Nordatlantiks seit dem späten Neogen (ODP Legs 105 und 104, DSDP Leg 81). *GEOMAR Report*, 5: 92.
- Yoder, J.A., Ackleson, S.G., Barber, R.T., Flament, P. and Balch, W.M., 1994. A line in the sea. *Nature*, 371(20 October 1994): 689-692.
- Zielinski, U., Gersonde, R., Sieger, R. and Fütterer, D., 1998. Quaternary surface water temperature estimations: Calibration of a diatom transfer function for the Southern Ocean. *Paleoceanography*, 13 (4): 365 - 383.

ZUSAMMENFASSUNG IN DEUTSCH

Benthische Foraminiferen aus dem Holozän des SW Pazifik: Ergebnisse hochauflösender Untersuchungen

Einleitung

Das Untersuchungsgebiet des TASQWA Projektes zwischen Australien und Neu Seeland ist eine Passage für den Austausch von Wassermassen zwischen dem Indischen und Pazifischen Ozean; Und somit eine Schlüsselstelle globaler ozeanischer Zirkulation. Erstaunlicherweise ist die Paläozeanographie dieses Gebiet bislang nur wenig erforscht.

Die rezente Ozeanographie des Untersuchungsgebietes wird im wesentlichen durch den Antarktischen Zirkumpolaren Strom geprägt. Im Untersuchungsgebiet kommen verschiedene ozeanische Fronten vor: Die Subantarktische Front (SAF) wird durch ein longitudinales Profil von drei Kastengreifern am östlichen Campbell Plateau geschnitten. Die Subtropische Front (STF) schneidet ein longitudinales Profil von drei Kastengreifern am Südlichen Tasman Rücken (siehe Fig. 3.1, S. 7 und 3.2, S. 8). Die sechs untersuchten Kerne stammen aus verschiedenen Wassertiefen und Wassermassen. Die tiefsten Kerne zeigen Einfluss des Antarktischen Bodenwassers (AABW) und des Antarktischen Tiefenwassers (CPDW). Der flachste Kern liegt im Bereich des Antarktischen Mittelwassers (AAIW) (siehe Table 2, S. 6 und 3, S. 7 und Fig. 3.1, S. 7).

Das allgegenwärtige Vorkommen und die große Artenvielfalt benthische Foraminiferen in den Ozeanen machen diese Einzeller zu idealen Anzeigern für paläoceanographische Veränderungen. Die Untersuchungen an benthischen Foraminiferen im allgemeinen und im Untersuchungsgebiet im speziellen beruhen in den meisten Fällen auf Untersuchungen langer Kerne. Holozäne Foraminiferen wurden meist an Oberflächenproben untersucht. In der vorliegenden Arbeit wird eine kontinuierliche und hochauflösende (1 cm Probenabstand) Dokumentation der holozänen ozeanographischen und ökologischen Veränderlichkeiten des Untersuchungsgebietes präsentiert.

Methodik und Material

Jeweils drei Kerne wurden von Süd Tasman Rücken und vom östlichen Campbell Plateau aus verschiedenen Wassertiefen gezogen. Um eine möglichst ungestörte Probe des Ozeanbodens zu erhalten wurde ein Großkastengreifer benutzt (siehe Foto 3, S. 9). Die erhaltenen Proben wurden im Labor nach in die Kornfraktionen $>63\mu\text{m}$ und $>150\mu\text{m}$ unterteilt und gewogen. Darüber hinaus wurde der Gehalt organischen Kohlenstoffs (TOC) und Stickstoffs (TN) bestimmt, sowie

der Karbonatgehalt errechnet (siehe Fig. 3.3, S. 10). Des weiteren wurden Helligkeit und Farbe des Sedimentes mit einem Photospektrometer gemessen. Die so erhaltenen physischen und physikchemischen Sedimentparameter wurden zur Unterstützung der Faunenanalyse der benthischen Foraminiferen herangezogen. Um eine Kernstratigraphie zu erstellen wurden stabile $\delta^{18}\text{O}$ und $\delta^{13}\text{C}$ Isotope an planktischen und benthischen Foraminiferen gemessen, sowie an jeweils zwei Proben der Kerne vom Süd Tasman Rücken absolute AMS ^{14}C Alter bestimmt. Zur Analyse der benthischen Foraminiferenfauna wurde die Kornfraktion $>150\mu\text{m}$ mit einem Binokular untersucht. Es wurden 112 Arten und 20 Gattungen benthischer Foraminiferen bestimmt. Der so gewonnene Datensatz wurde mit Hilfe multivariater Statistik (Q-Modus Faktor Analyse) in überschaubare Gruppen von Arten eingeteilt. Die Q-Modus Faktor Analyse quantifiziert Arten mit ähnlichen Trends in der Verteilung der Häufigkeit in dem jeweiligen Kern. Arten mit ähnlichen ökologischen Präferenzen sollen so in Faktoren zusammengefasst werden. Durch Vergleich der Arten und Gruppen von Arten mit Literaturdaten und den physikalischen und physikchemischen Sedimentparametern wird der jeweilige Faktor bestimmten Umweltbedingungen zugeordnet. Diese Umweltbedingungen können durch die Verteilung der Wassermassen bestimmt sein, so dass bestimmten Faunenassoziationen bestimmte Wassermassen zugeordnet werden können. Die Umweltbedingungen der Tiefsee werden aber nur in geringem Maße durch die umgebende Wassermasse bestimmt. In Gebieten höherer primärer Produktivität entsteht ein erhöhter Fluss von Nährstoffen zum Ozeanboden. Dieser Umweltfaktor überprägt das Signal der Wassermasse in der Foraminiferenfauna.

Diskussion und Interpretation der Ergebnisse

Um eine Stratigraphie aufzustellen wurde versucht die $\delta^{18}\text{O}$ Werte der untersuchten Kerne mit anderen hochauflösenden Kernen zu korrelieren. Eine Korrelation war nicht möglich, da die Auflösung der untersuchten Kerne zu gering war. Es wurden die untersuchten Kerne mit Hilfe der AMS Alter untereinander korreliert (siehe Fig. 5.1, S. 53) und mit Klimadaten aus der Literatur verglichen (siehe Fig. 5.2, S. 56).

Östliches Campbell Plateau:

Der tiefste Kern am östlichen Campbell Plateau (SO136-019BX) liegt heute im Bereich des unteren Zirkumpolaren Tiefenwassers (CPDWlii) (siehe Fig. 4.7). Der untere Teil des Kerns ist durch die *N. umbonifer* Vergesellschaftung dominiert, die Einfluss des AABW anzeigt. Ein schneller Wechsel von AABW zu CPDWlii wird durch das plötzliche Auftreten der *G. subglobosa* Vergesellschaftung in 12.5 cm Teufe angezeigt. Der oberste Teil des Kerns des Kern ist durch die Taxa "Fragmente agglutinierender Arten" dominiert. Das organische oder

ferrytische Bindemittel dieser Taxa wird in den obersten cm des Sediments durch mikrobiologische Aktivität zersetzt. Die Abnahme der Häufigkeit dieser Arten beruht auf diagenetischen Prozessen. Da aufgrund der fehlenden Zeitskala keine Akkumulationsraten bestimmt werden konnten, ist die Individuenzahl in den untersuchten Kernen in Individuen pro Gramm Sediment gegeben. Eine große Zahl an agglutinierenden Foraminiferen wird die Individuenzahlen aller anderen Arten beeinflussen und überprägen. Der oberste Teil des Kerns entzieht sich daher einer Interpretation der Faunenvergesellschaftung. Eine zeitliche Einordnung des Kerns ist nicht möglich: Es fehlen absolute Datierungen. Zusätzlich sind die $\delta^{18}\text{O}$ Werte des Kerns durch sehr starke Schwankungen gekennzeichnet, was als ein Zeichen für Umlagerung und möglicherweise für Schüttungen gedeutet wird. Eine Korrelation mit den anderen untersuchten Kernen war nicht möglich. Die Auswertung des Kerns ergibt lediglich den Trend sinkender Wassermassen, der durch die Interpretation des flacheren Kerns bestätigt werden wird.

Der Kern aus mittlerer Wassertiefe (SO136-025BX) zeigt einen deutlichen Fazieswechsel: Diatomeen Schlamm wechselt zu sehr grobkörnigem Foraminiferensand. Sedimente die dem unteren Teil des Kerns ähnlich sind wurden in keinem Anderen der untersuchten Kerne gefunden. Der Wechsel zeigt ein Erosionsereignis an. Die Oberfläche des unteren Teils wurde durch einen Turbidit, oder ein Ereignis hoher Strömungsenergie erodiert. Der Obere Teil wurde vermutlich durch dieses Ereignis sedimentiert. Im unteren Tel des Kerns finden sich zu wenige Foraminiferen, um verlässliche Isotopenmessungen durchzuführen. Im oberen Teil des Kerns ist der Gehalt an benthischen Foraminiferen pro Gramm Sediment so gering, dass keine ausreichende Anzahl an Individuen für eine statistische Analyse gefunden wurde. Der Kern zeigt lediglich das Vorhandensein des feinkörnigen Diatomeenschlamm am Campbell Plateau an. Die Sedimente könnten aus einer Planktonblüte des Opalgürtels südlich der Polaren Front Zone entstammen. Ähnliche Sedimente sind im unteren Teil des Kerns SO136-124GC vom südlichen Tasman Rücken vorhanden.

Der obere Kern des östlichen Campbell Plateaus (SO136-037BX) liegt heute im Bereich des AAIW. Der Kern wurde mit den Kernen vom Süd Tasman Rücken korreliert (siehe Figs. 5.1, S. 53 und 5.2, S. 56). Allerdings ist die Korrelation nicht durch absolute Datierungen bestätigt. Die Foraminiferenfauna zeigt einen Wechsel von einer Modifikation der *G. subglobosa* Vergesellschaftung zu einer Vergesellschaftung an, die heute im AAIW vorkommt. Dieser Kern bestätigt den Trend der sinkenden Wassermassen aus dem tiefen Kern SO136-019BX. Der Wechsel liegt in der gleichen Sediment-Teufe wie in Kern SO136-019BX. Nach der Korrelation

mit den Kernen vom Süd Tasman Rücken entspricht dies dem Ende des Antarctic Cold Reversal (ACR) (siehe Fig. 5.2, S. 56).

Süd Tasman Rücken:

Der tiefste Kern vom Süd Tasman Rücken ist im unteren Teil charakterisiert von einer Hochproduktionsfauna, die von *Furcifera contemplata* dominiert wird. Die hohe Produktivität ist vermutlich durch Versatz der Subtropischen Front über die Kernlokation verursacht. Der mittlere Teil des Kerns ist charakterisiert durch eine modifizierte *G. subglobosa* Vergesellschaftung, die das untere zirkumpolare Tiefenwasser anzeigt (CPDWli). Der Kern zeigt Anzeichen eines Einflusses der Temperatur der Meeresoberfläche auf die benthische Fauna. Diese Einflüsse sind klarer zu erkennen in Kern SO136-161BX. Im oberen Teil des Kerns wird das Signal der Oberflächentemperatur durch zunehmenden Einfluss des darunter liegenden AABW überprägt. Der Einfluss zeigt sich durch eine Zunahme der *N. umbonifer* Vergesellschaftung. Ein Ansteigen der Wassermassen wird angezeigt.

Der mittlere Kern (SO136-161BX) vom Süd Tasman Rücken zeigt eine deutliche Korrelation der benthischen Fauna mit der Temperatur der Meeresoberfläche. Die Verteilungsmuster der benthischen Fauna folgen den Variationen des Klimas (siehe Fig. 5.3, S. 75) besonders deutliche Korrelation mit wärmerem Klima zeigt *Uvigerina peregrina*. Die Art *Melonis pompilioides* dagegen zeigt deutliche Antikorrelation. Die Einflüsse der Oberflächentemperatur überprägen eine modifizierte *G. subglobosa* Vergesellschaftung. Im Oberen Teil des Kerns zeigt sich eine Änderung im Signal der Wassermasse. Steigender Einfluss des AABW zeigt sich durch eine Zunahme der *N. umbonifer* Vergesellschaftung, die in dieser Wassertiefe noch durch *Epistominella exigua* dominiert wird. Ein Ansteigen der Wassermassen wird angezeigt.

Der flachste Kern (SO136-147BX) stammt aus einer Zone sehr hoher Strömungsenergie. Der obere Teil des Kerns wurde erodiert. Der Kern zeigt keine Veränderung in der ozeanographischen Situation an. Die Faunengemeinschaft benthischer Foraminiferen zeigt eine modifizierte Vergesellschaftung der *G. subglobosa* Vergesellschaftung an.

Schlussfolgerungen

Paleoklimatologie:

Die untersuchten Sedimente spiegeln die gesamte Klimageschichte des Holozän wider. In allen Kernen finden sich Anzeichen für eine Kälteperiode (Unconfirmed Cold Event), die nicht in der aufgeführten Literatur erwähnt wird.

Benthische Foraminiferenfauna:

Die benthische Foraminiferenfauna wird durch vielfältige Umwelteinflüsse geprägt. In dieser Arbeit werden fünf verschiedene Faktoren unterschieden. Die verschiedenen Faktoren sind in abnehmender Intensität aufgelistet:

- (a) Frühdiagenetische Prozesse führen zu einer starken Abnahme an agglutinierenden Foraminiferen in den obersten 2 bis 6 Zentimetern des Sediments. Die Schalen werden durch Abbau des organischen Zements durch mikrobiologische Aktivität zerstört. Durch den hohen Anteil agglutinierender Arten an der Lebendfauna überprägt dieser Prozess die fossile Vergesellschaftung der obersten Zentimeter des Sediments.
- (b) Variationen in der Nährstoffzufuhr haben den stärksten Einfluss auf die Zusammensetzung der Lebendgemeinschaften der benthischen Foraminiferenfauna.
- (c) In Tabelle 1 werden Faunenvergesellschaftungen definiert, die in Zusammenhang mit der Verteilung der jeweiligen Wassermasse in Zusammenhang gesetzt werden können. Bestätigte Vergesellschaftungen sind in mehreren Kernen präsent und durch Literaturzitate bestätigt.
Vermutete Vergesellschaftungen sind lediglich in einem Kerne vorhanden und nicht durch Literaturzitate bestätigt.
- (d) Variationen in der Temperatur der Meeresoberfläche verursachen Veränderungen in der benthischen Foraminiferenfauna.
 - Die Häufigkeit von *Uvigerina peregrina* korreliert mit wärmerem Klima.
 - Die Häufigkeit von *Melonis pompilioides* korreliert mit kälterem Klima.

Paläozeanographie:

Die Paläozeanographie des Untersuchungsgebietes ist durch folgende Variationen charakterisiert:

- Absenkung der Wassermassen findet am östlichen Campbell Plateau seit etwa 8000 Jahren statt. Der Beginn der Absenkung entspricht dem Ende des Antarctic Cold Reversal. Der Übergang der Wassermassen ist scharf abgegrenzt.
- Die Wassermassen am Süd Tasman Rücken zeigen einen gegensätzlichen, ansteigenden Trend seit dem Ende des "Cold Event", ~7500 Jahre vor heute. Der Übergang der einzelnen Wassermassen ist diffus.
- Umlagerung und Resuspension sind wesentliche Prozesse für die Sedimentation aller untersuchten Kerne, mit Ausnahme von SO136-0337BX. Hiatusse und Phasen der Erosion sind häufig am Süd Tasman Rücken.

Tabelle 1 Vergesellschaftungen benthischer Foraminiferen in den untersuchten Kernen aus dem Holozän des Arbeitsgebietes.

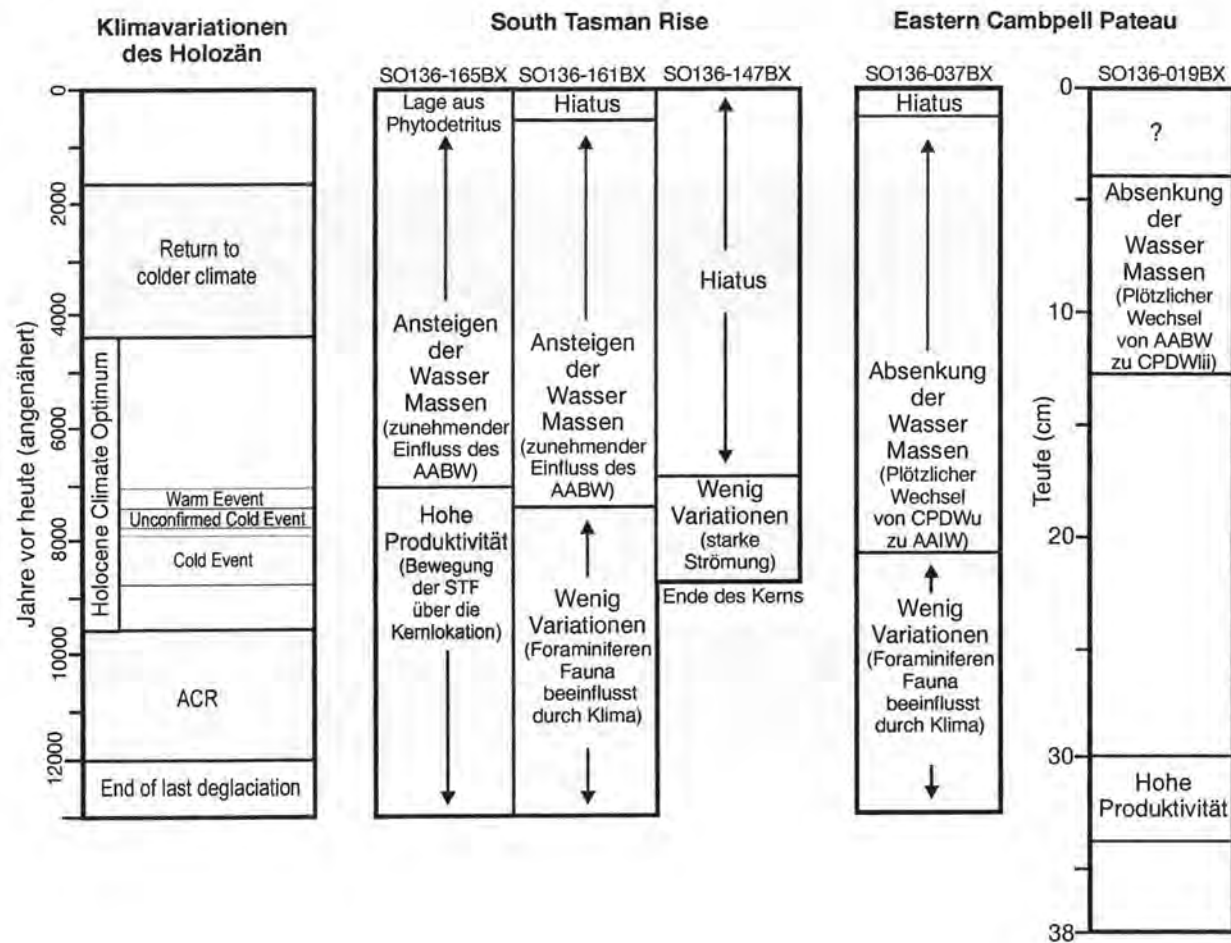
Wasser Masse	Signifikante Arten	Assoziierte Arten	Vorhanden in Kern
Bestätigte Vergesellschaftungen:			
CPDW	<i>G. subglobosum</i> <i>S. rolshauseni</i> <i>E. exigua</i>	<i>P. bulloides</i> <i>N. umbonifer</i>	SO136-019BX -037BX, -147BX -161BX, -165BX
CPDWli	<i>H. dutemplei</i> <i>P. bulloides</i> <i>G. subglobosum</i>	<i>E. exigua</i> N. umbonifer	SO136-161BX -165BX
CPDWlii*	<i>M. baleeanum</i> <i>G. subglobosum</i> <i>E. exigua</i> <i>P. cylindroides</i>	<i>P. bulloides</i> <i>N. umbonifer</i>	SO136-019BX -165BX
AABW	<i>N. umbonifer</i>	<i>E. exigua</i>	SO136-019BX -161BX, -165BX

Unbestätigte Vergesellschaftungen:

AAIW	<i>E. mestayeri</i>	<i>U. peregrina</i> <i>Pyrgo</i> spp.	SO136-037BX
CPDWu	<i>B. aculeata</i> <i>E. exigua</i> <i>S. rolshauseni</i>	<i>P. bulloides</i> <i>G. subglobosum</i>	SO136-147BX

* Assoziiert mit *F. contemplata* in Gebieten hoher Primärproduktion.

Tabelle 2 Die pläoceanographischen Veränderungen im Holozän des Untersuchungsgebietes. Die Altersangaben sind ungefähre Werte. Für den Kern SO136-019BX existiert keine Stratigraphie.



APPENDIX

A1	Taxonomy of benthic foraminifera species from the research area	I
A2	SEM photos of selected foraminiferal specimens	IX
A3	Paleontological data set	XII
A4	Data set of Q-mode Factor Analysis	XXVIII
A5	Data set of physical and physicochemical sediment properties	XL
A6	AMS ^{14}C radiocarbon data	XLV
A7	Photos of each core	XLVII
A8	Visual core descriptions	XLVIII
A9	Data CD	

APPENDIX

A1 Taxonomy

List of 112 identified benthic foraminiferal species and 20 taxa, which have not been determined to the species level. All specimens originate from the six investigated sediment cores samples from the eastern Campbell Plateau and the South Tasman Rise in alphabetical order. Reference cells of each specimen are deposited at GEOMAR Research Center for Marine Geosciences, Kiel. Photos of certain taxa are shown in Appendix A5, especially of those, which could not be determined to the species level.

Fragments of agglutinating spp.: fragments of agglutinating species, which were too weakly preserved to determine the species.

Amphicoryna separians (Brady) (former: *Nodosaria scalaris* Batsch var. *sperans*: Gabel (1971) Plate 9, Fig. 24.

Amphicoryna scalaris (Batsch): Loeblich and Tappan (1964) Plate 401, Fig. 1; Oki (1989) Plate 6, Fig. 3.

Amphicoryna sp.: Genus level was determined after Loeblich and Tappan (1964) Plate 401; Gabel (1971) Plate 9.

Bagatella inconspicua Howe: Loeblich and Tappan (1964) Plate 427, Fig. 1.

Baggina californica Cushman: Loeblich and Tappan (1964) Plate 462, Fig. 1.

Bolivina pacifica (Cushman & McCulloch): Oki (1989) p. 109, Plate 9, Fig. 6; Timm (1992) Plate 5, Fig. 5.

Bulimina alazanensis (Cushman): Gupta (1994) Plate 3, Fig. 7.

Bulimina aceluata (d'Orbigny): Mackensen et al. (1990) Plate 2, Fig. 1 – 3; Gabel (1971) Plate 14, Fig. 10 – 11; Morkhoven et al. (1986) Plate 7, Fig. 1 – 3; Gupta (1994) Plate 3, Fig. 5 – 6; Mackensen (1992) Plate 1, Fig. 1 - 2.

Bulimina alazanensis: Gupta (1994) Plate 3, Fig. 7; Mackensen (1992) Plate 1, Fig. 3 - 4.

Caribbeanella polystoma Bermúdez: Loeblich and Tappan (1964) Plate 555, Fig. 2; Oki (1989) Plate 18, Fig. 3.

Cibicidoides sp.: Genus level was determined after Loeblich and Tappan (1964) Plate 612.

Cassidella tegulata (Reuss): Loeblich and Tappan (1964) Plate 600, Fig. 5 – 7.

Cassidulina crassa (d'Orbigny): Feyling-Hanssen et al. (1971) Plate 7, Fig. 18 – 19; Timm (1992) Plate 6, Fig. 16; Heß (1998), Plate 13, Fig. 6 - 7.

- Cassidulina laevigata* (d'Orbigny): Schiebel (1992) Plate 2, Fig. 11;
 Feyling-Hanssen et al. (1971) Plate 7, Fig. 20 - 21, Plate 18, Fig. 12;
 Heß (1998) Plate 13, Fig. 8,
 Gabel (1971) Plate 17, Fig. 7 - 9.
- Cibicidoides fletcheri* (Galloway & Wissler): Lutze and Altenbach (1988) Plate 32, Fig. 11;
 = *Cibicidoides teretis*: Nees (1989) Plate 2, Fig. 2;
 Lutze (1980) Plate 12, Fig. 11.
- Cibicidoides hyalinus* (Hofker): Loeblich and Tappan (1964) Plate 621, Fig. 2 a - c.
- Cibicidoides lobatulus* (Walker & Jacob): Struck (1992) Plate 5, Fig. 1;
 Feyling-Hanssen et al. (1971) Plate 9, figs. 9 - 14;
 Thies (1991) Plate 17, Fig. 4, Plate 18, Fig. 1 - 20;
 Struck (1992) Plate 5, Fig. 1;
 Milam et al. (1980) Plate 9, Fig. 4;
 = *Cibicides lobatulus* (Walter & Jako): Gabel (1971) Plate 18, Fig. 32 - 34.
- Cibicidoides mundulus* (Brady, Parker & Jones): Ohkushi et al. (1999) Plate 4, Fig. 3;
 Gupta (1994) Plate 5, Fig. 7;
 Morkhoven et al. (1986) Plate 21, Fig. 1;
 Loeblich and Tappan (1964) Plate 621, Fig. 1;
 Clark et al. (1994) pl 1, Fig. 4 - 6;
 Mackensen (1992) Plate 3, Fig. 5 - 7..
- Cibicidoides inawagaensis*: Oki (1989) Plate 18, Fig. 2 a - c.
- Cibicidoides wuellerstorfi* (Schwager): Struck (1992) Plate 1, figs. 3-4;
 Heß (1998) Plate 16, Fig. 5 - 7;
 = *Planulina wuellerstorfi* (Schwager): Gabel (1971) Plate 19, Fig. 7 - 9;
 Corliss (1988) Plate 1, Fig. 3 - 4;
 Corliss (1979c) Plate 2, Fig. 13 - 16;
 Morkhoven et al. (1986) pl 14, Fig. 1 - 2;
 Gupta (1994) Plate 5, Fig. 8 - 9;
 Mackensen (1992) Plate 3, Fig. 1 - 3;
 Corliss and Honjo (1981) Plate 8; Fig. 1 - 16;
 = *Fontbiota wuellerstorfi*: Loeblich & Tappan (1988) Plate 2, Fig. 4 - 5.
- Cribostomoides subglobosus* (Sars): Mackensen et al. (1990) Plate 4, Fig. 7 - 9,
 Gabel (1971) Plate 4, Fig. 1 - 2;
 = *Cribostomoides subglobosum* (Sars): Milam et al. (1980) Plate 3, Fig. 1.
- Cribostomoides weddellensis* (Earland): Mackensen et al. (1990) Plate 4, Fig. 4 - 5.
- Cruciloculina triangularis* (d'Orbigny): Loeblich and Tappan (1964) Plate 349, Fig. 5 - 6.
- Cyclammina cancellata* (Brady): Loeblich and Tappan (1964) Plate 142, Fig. 1 - 4.
- Cyclammina trussilita* (Brady): Mackensen et al. (1990) Plate 8, Fig. 4 - 5.
- Dentalina baggi* (Galloway & Wissler): Feyling-Hanssen et al. (1971) Plate 3, Fig. 1.
- Dentalina communis* (d'Orbigny): Heß (1998) Plate 11, Fig. 13.
- Dentalina inorta* (d'Orbigny): Heß (1998) Plate 11, Fig. 12;
 var. *bradyensis* (Deriveus) Gabel (1971) Plate 2, Fig. 1 - 2.
- Dentalina* sp 1: Genus level was determined after Loeblich and Tappan (1964) Plate 403.
- Dentalina* sp. 2: Genus level was determined after Loeblich and Tappan (1964) Plate 403.

Eggerellina brevis (d'Orbigny): Loeblich and Tappan (1964) Plate 186, Fig. 6.

Eggerella scabra (Williamson): Gabel (1971) Plate 5, Fig. 8 – 10;
Oki (1989) Plate 4, Fig. 7.

Ehrenbergina mestayeri (Cushman): Hayward et al. (1999) Plate 8, Fig. 26 – 27;
Eade (1967): Plate 8, Fig. 3 – 5.

Ehrenbergina glabra Heron-Allen & Earland: Mackensen et al. (1990) Plate 1, Fig. 5 – 6;
Mackensen (1992) Plate 4, Fig. 13 – 14;
Milam et al. (1980) Plate 9, Fig. 7.

Epistominella exigua (Brady): Mackensen et al. (1990) Plate 7, Fig. 1 – 2.
Heß (1998) Plate 14, Fig. 15 – 16;
Timm (1992) Plate 7, Fig. 6;
Ohkushi et al. (1999) Plate 3, Fig. 1;
Gupta (1994) Plate 4, Fig. 18 – 19;
Corliss (1979c) Plate 2, Fig. 7 – 9;
Mackensen (1992) Plate 4, Fig. 7 - 8.

Fissurina abyssicola (Jones): Ohkushi (1999) Plate 1, Fig. 7.

Fissurina agassizi (Todd & Bronnimann): Oki (1989) Plate 8, Fig. 1.

Fissurina daniza (Madsen): Feyling-Hanssen et al. (1971) Plate 6, Fig. 6-7, Plate 18, Fig. 3;
Gabel (1971) Plate 9, Fig. 42 – 43.

Fissurina laevigata (Reuss): Oki (1989), Plate 8, Fig. 2;
Gabel (1971) Plate 15, Fig. 32 – 33.

Fissurina marginata (Montagu): Gabel (1971) Plate 15, Fig. 35 – 36;
Loeblich and Tappan (1964) Plate 425, Fig. 7.

Fissurina orbignyana (Seguenza): Oki (1989) Plate 8, Fig. 3;
Gabel (1971) Plate 15, Fig. 40 – 41.

Fissurina serrata (Schlumberger): Feyling-Hanssen et al. (1971) Plate 6, Fig. 9.

Fissurina sp.2: Genus level was determined after Loeblich and Tappan (1964) Plate 425.

Fissurina sp.3: Genus level was determined after Loeblich and Tappan (1964) Plate 425.

Florius asterisans: Loeblich and Tappan (1964) Plate 612, Fig. 4.

Fursenkonia complanata (Egger): Jones (1994) Plate 52, Fig. 1 – 3.

Globocassidolina subglobosa (Brady)
= *Cassidulina subglobosa*: Brady (1884) Plate 2, Fig. 17 -18;
Gabel (1971) Plate 12, Fig. 16 – 17;
Struck (1992) Plate 3, Fig. 2;
Mackensen (1992) Plate 3, Fig. 8 – 9;
Timm (1992) Plate 6, Fig. 20;
Ohkushi et al. (1999) Plate 2, Fig. 8;
Heß (1998) Plate 13, Fig. 14;
Gupta (1994) Plate 2, Fig. 17 – 18;
Corliss (1979c) Plate 3, Fig. 12 - 13.

Globorotalites multisepta (Brotzen): Loeblich and Tappan (1964) Plate 615, Fig. 8.

Grigelis orrectus: Heß (1998) Plate 11, Fig. 15.

Gyroidina neosoldanii: Nees (1994) Plate 1, Fig. 7.

Gyroidinoides nipponicus (Ishizaki): Oki (1989) Plate 21, Fig. 3.

Gyroidinoides orbicularis (d'Orbigny)

= *Gyroidina orbicularis*: d'Orbigny (1826) Plate 6, Fig. 15;
Gupta (1994) Plate 6, Fig. 15.

Haplofragmoides canariensis (d'Orbigny): Mackensen et al. (1990) Plate 8, Fig. 3 – 6;

Gabel (1971) Plate 3, Fig. 28 – 29;

Milam et al. (1980) Plate 2, Fig. 7.

Heteroplea dutemplei (d'Orbigny): Loeblich and Tappan (1964) Plate 623, Fig. 3 a – c;

= *Cibicidoides dutemplei* (d'Orbigny): Morkhoven et al. (1986) Plate 35, Fig. 1 - 2.

Kariella siphonella (Cushman): Loeblich and Tappan (1964) Plate 186, Fig. 2 – 3.

Lagena amphora (Reuss): Oki (1989) Plate 6, Fig. 7.

Lagena gracillima (Seguenza): Gabel (1971) Plate 10, Fig. 1 – 2.

Lagena gracillis (Williamson)

= *Amphorina costai* (Anderson): Gabel (1971) Plate 10, Fig. 7 – 8.

Lagena hispidula (Cushman): Oki (1989) Plate 6, Fig. 10;

Gabel (1971) Plate 10, Fig. 10.

Lagena semilineata: Feyling-Hanssen et al. (1971) Plate 4, Fig. 3.

Lagena setigera: Oki (1989), Plate 6, Fig. 11.

Lagena sp.1: Genus level was determined after Loeblich and Tappan (1964) Plate 402.

Lagena sp.2: Genus level was determined after Loeblich and Tappan (1964) Plate 402.

Lagena striata (d'Orbigny): Feyling-Hanssen et al. (1971) Plate 16, Fig. 3 – 4;

Gabel (1971) Plate 10, Fig. 12.

Lagena substriata: Gabel (1964) Plate 10, Fig. 11 – 16.

Lagena sulcata laevicostata (Cushman & Gray): Feyling-Hanssen et al. (1971),

Plate 16, Fig. 7 – 9;

Loeblich and Tappan (1964) Plate 404, Fig. 11.

Laticarinina pauperata (Parker & Jones): Heß (1998) Plate 9, Fig. 13;

Mackensen et al. (1990) Plate 7, Fig. 3;

Morkhoven et al. (1986) Plate 26, Fig. 1;

Loeblich and Tappan (1964) Plate 457, Fig. 2 – 3;

Timm (1992) Plate 7, Fig. 13;

Gupta (1994) Plate 5, Fig. 1 – 2;

Mackensen (1992) Plate 3, Fig. 1 - 2.

Lenticulina rotulata (Lamarck): Loeblich and Tappan (1964) Plate 406, Fig. 1;

Gabel (1971) Plate 9, Fig. 3 – 4.

Martinottiella nodulosa (Cushman): Mackensen et al. (1990) Plate 2, Fig. 8 – 9;

Mackensen (1992) Plate 3, Fig. 4;

= *Multifidella nodulosa* in Mackensen (1993).

Melonis baleeanum (Williamson): Ohkushi et al. (1999) Plate 5, Fig. 6;
 Gupta (1994) Plate 6, Fig. 1;
 Struck (1992) Plate 4, Fig. 6;
 Ohkushi et al. (1999), Plate 5, Fig. 6;
 Timm (1992) Plate 6, Fig. 6;
 Heß (1998) Plate 13, Fig. 5;
 Gabel (1971) Plate 12, Fig. 18 – 19;
 Corliss (1979c) Plate 5, Fig. 7 – 8
 = *Melonis baleeanus*: Mackensen (1992) Plate 5, Fig. 2.

Melonis pompiliooides (Fichtel & Moll): Morkhoven et al. (1986) Plate 23A, Fig. 1 – 2;
 = *Nautilus pompiliooides*: Gupta (1994) Plate 6, Fig. 2 – 3;
 Gabel (1971) Plate 12, Fig. 8 – 9;
 Corliss (1979c) Plate 5, Fig. 9 – 10;
 Mackensen (1992) Plate 3, Fig. 11 - 12.

Melonis zaandami (Van Voorthuysen): Loeblich and Tappan (1964) Plate 627, Fig. 2-3;
 Gabel (1971) Plate 12, Fig. 20 – 21;
 Corliss (1988) Plate 1, Fig. 8 - 9.

Milliammina arenaca (Chapman): Mackensen et al. (1990) Plate 2, Fig. 4 – 5;
 Gabel (1971) Plate 5, Fig. 25 – 26.

Nonionella iridea Heron-Allend & Earland: Mackensen et al. (1990) Plate 1, Fig. 7 – 9.

Nonionella labradoricus Volsoshina: Loeblich and Tappan (1964) Plate 613, Fig. 2 – 5.

Nodophthalmidium tibia (Jones & Parker): Oki (1989) Plate 4, Fig. 13.

Nuttallides umbonifer (Cushman): Mackensen et al. (1990) Plate 7, Fig. 7 – 9;
 Gupta (1994) Plate 5, Fig. 14 – 16;
 Mackensen (1993) Plate 2, Fig. 1 – 2;
 = *Nuttallides umboniferus* in (Murray, 1991);
 = *Epistominella umbonifera* in (Corliss, 1985);
 Corliss (1979c) Plate 2, Fig. 10 – 12;
 Corliss and Honjo (1981) Plate 3, Fig. 1 – 5;
 Clark et al. (1994) Plate 2, Fig. 8 – 17;
 Mackensen (1992) Plate 4, Fig. 1 - 3.

Oolina borealis (Loeblich & Tappan): Feyling-Hanssen et al. (1971) Plate 6, Fig. 2.

Oolina caudigera (Wiesner): Feyling-Hanssen et al. (1971) Plate 6, Fig. 3.

Oolina globosa (Montagu): Ohkushi et al. (1999) Plate 1, Fig. 11 a - b.

Oolina hexagona (Williamson): Oki (1989) Plate 7, Fig. 10;
 Feyling-Hanssen et al. (1971) Plate 17, Fig. 6;
 Gabel (1971) Plate 10, Fig. 23.

Oolina melo (d'Orbigny): Feyling-Hanssen et al. (1971) Plate 6, Fig. 5;
 Feyling-Hanssen et al. (1971) Plate 17, Fig. 6;
 Oki (1989) Plate 7, Fig. 10;
 Gabel (1971) Plate 10, Fig. 24.

Oolina sp.: Genus level was determined after Loeblich and Tappan (1964) Plate 425;

Oolina lineata (Williamson): Feyling-Hanssen et al. (1971) Plate 17, Fig. 7 – 8;
 Loeblich and Tappan (1964) Plate 425, Fig. 2.

Oridosalis umbonatus (Reuss): Mackensen et al. (1990) Plate 7, Fig. 4 – 6;
 Heß (1998) Plate 14, Fig. 9 – 10;
 Timm (1992) Plate 7, Fig. 7;
 Struck (1992) Plate 1, Fig. 1 – 2;
 Ohkushi et al. (1999) Plate 5, Fig. 1;
 Gupta (1994) Plate 6, Fig. 11;
 Corliss (1988) Plate 1, Fig. 6 – 7;
 Clark et al. (1994) pl 1, Fig. 7 – 10;
 Mackensen (1992) Plate 3, Fig. 10 – 12..

Oridosalis sp.: Genus level was determined after Loeblich and Tappan (1964) Plate 614.

Osangularia culter (Parker & Jones)

= *Planorbulina culter*: Parker & Jones (1865) Plate 6, figs. 9, 10;
 Gupta (1994) Plate 6, Fig. 9 – 10.

Osangularia sp.: Genus level was determined after Loeblich and Tappan (1964) Plate 615;

Parafissurina lateralis (Cushman): Ohkushi et al. (1999) Plate 1, Fig. 12;
 Gabel (1971) Plate 15, Fig. 42 – 43.

Parafissurina ovata (Wiesner): Struck (1992) Plate 4, Fig. 4.

Parafissurina ventricosa (Silvestris): Loeblich and Tappan (1964) Plate 425, Fig. 9 – 10.

Parvicarinina alto (Finlay) = *Laticarinina altocamerata* (Heron-Allen & Earland):
 Loeblich and Tappan (1964), Plate 457, Fig. 4.

Planulina arimensis: Loeblich and Tappan (1964) Plate 552, Fig. 1, Plate 553;
 Morkhoven et al. (1986) Plate 10 Fig. 1 - 4.

Polymorphina sp.: The genus level was determined after Loeblich and Tappan (1964) Plate 415;
 Feyling-Hanssen et al. (1971) Plate 4 – 5,
 Gabel (1971) Plate 2, Plate 11.

Psammosphera fusca (Schulze): Gabel (1971) Plate 2, Fig. 1 – 2.

Pseudorotalia garmadii (d'Orbigny): Oki (1989) Plate 16, Fig. 1 a – b.

Pullenia bulloides (d'Orbigny): Feyling-Hanssen et al. (1971) Plate 10, Fig. 13 – 14,
 Heß (1998) Plate 13, Fig. 9 – 10;
 Gupta (1994) Plate 6, Fig. 4;
 Ohkushi et al. (1999) Plate 5, Fig. 9;
 Mackensen et al. (1990) Plate 7, Fig. 6;
 Struck (1992) Plate 2, Fig. 1 – 2;
 Gabel (1971) Plate 17, Fig. 39 – 40;
 Corliss (1988) Plate 1, Fig. 14 – 15;
 Mackensen (1992) Plate 2, Fig. 1 – 2;
 Corliss (1979c) Plate 4, Fig. 1 – 2;
 Clark et al. (1994) Plate 2, Fig. 18 – 19;
 = *Nonionina bulloides*: d'Orbigny (1846) Plate 6, Fig. 4.

Pullenia quinqueloba (Reuss): Struck (1992) Plate 2, Fig. 3,
 Ohkushi et al. (1999) Plate 5, Fig. 2;
 Heß (1998) Plate 13, Fig. 11 – 12;
 Gupta (1994) Plate 6, Fig. 7;
 Oki (1989) Plate 20, Fig. 7;
 Clark et al. (1994) Plate 1, Fig. 15 - 16.

Puleniella asymmetrica (Uijie): Ohkushi et al. (1999) Plate 4, Fig. 7a – 7b
 = *Pullenia osloensis*: Gupta (1994) Plate 6, Fig. 5 – 6.

Pyrgo murrhina (Schwager): Heß (1998) Plate 9, Fig. 1;
 Gabel (1971) Plate 7, Fig. 21 – 22;
 Ohkushi et al. (1999) Plate 1, Fig. 5;
 Morkhoven et al. (1986) Plate 15, Fig. 1 – 2;
 Gupta (1994) Plate 1, Fig. 14;
 Corliss (1988) Plate 1, Fig. 5;
 Corliss (1979c) Plate 1, Fig. 15 – 18;
 Corliss and Honjo (1981) Plate 9, Fig. 1 – 12;
 Mackensen (1992) Plate 4, Fig. 4.

Pyrgo oblonga (d'Orbigny): Phleger (1953) Plate 5, Fig. 25 – 26;
 Barker (1960) Plate 2, Fig. 9;
 Gabel (1971) Plate 7, Fig. 1 – 2.

Pyrgo rotalia Loeblich & Tappan: Theis (1991) Plate 14, Fig. 4;
 Struck (1992) Plate 3, Fig. 1.

Pyrgo serrata: Cushman (1921) Plate 95, Fig. 3.

Pyrgo sp.: Genus level was determined after Theis (1991) Plate 14.

Pyrgo spp.: Genus level was determined after Theis (1991) Plate 14, this genus contains fragments which could not be assigned to a certain species.

Pyrgo tasmanensis (Vella): (Vella, 1957) Plate 7, Fig. 141 – 142.

Pyrgo williamsoni (Silvestri): Hess (1998) Plate 9, Fig. 2;
 Loeblich and Tappan (1964) Plate 352, Fig. 4;
 Feyling-Hanssen et al. (1971) Plate 2, Fig. 8 – 9;
 Hess (1998) Plate 9, Fig. 2.

Pyrolina cylindroides (Roemer): Feyling-Hanssen et al. (1971) Plate 5, Fig. 10 – 11.

Quinqueloculina spp.: Genus level was determined after Loeblich and Tappan (1964) Plate 349.

Reophax miceata (Cushman): Gabel (1971) Plate 2, Fig. 9;
 = *Reophax miaceus* (Earland): Timm (1992) Plate 6, Fig. 6 a - c.

Reophax spiculifer (Brady): Mackensen et al. (1990) Plate 6, Fig. 7 – 8.

Reussela spinulosa (Reuss): Oki (1989) Plate 11, Fig. 10;
 Loeblich and Tappan (1964) Plate 445, Fig. 3 – 5.

Rutherfordis sp.: Genus level was determined after Heß (1998) Plate 11, Fig. 9.

Sigmoilopsis schlumbergi (Silvestri): Oki (1989) Plate 5, Fig. 7,
 Gabel (1971) Plate 5, Fig. 27 – 28;
 Morkhoven et al. (1986) Plate 17, Fig. 1 – 3;
 Loeblich and Tappan (1964) Plate 353, Fig. 2;
 Feyling-Hanssen et al. (1971) Plate 2, Fig. 17 – 18;
 Oki (1989), Plate 5, Fig. 7;
 Struck (1992), Plate 3, Fig. 6;
 Gupta (1994) Plate 1, Fig. 7.

Stilostomella lepidula (Schwager) = *Nodosaria lepidula*: Schwager (1866) Plate 1, Fig. 5;
 Gupta (1994) Plate 4, Fig. 5.

Siphotextularia rolshauseni (Phleger & Parker): Struck (1992) Plate 2, Fig. 5 – 7,
 Gabel (1971) Plate 4, Fig. 39 – 41;
 Oki (1989) Plate 3, Fig. 6.

Spiroloculina disparilis Terquem: Vella (1957) Plate 6, Fig. 122 – 123.

Suggrunda porosa Hoffmeister & Bery: Loeblich and Tappan (1964) Plate 600, Fig. 10.

Textularia truncata (Höglund): Gabel (1971) Plate 4, Fig. 20 – 21.

Textularia porrecta (Brady): Heß (1998) Plate 8, Fig. 10.

Textularia wiesneri Earland: Mackensen (1990) Plate 5, Fig. 4 – 9.

Tosaia hanzawai (Takayanagi): Loeblich and Tappan (1964) Plate 429, Fig. 1 a - c.

Trifarina angulosa (Williamson): Mackensen et al. (1990) Plate 1, Fig. 1 – 3;
 Oki (1989) Plate 12, Fig. 10;
 Loeblich and Tappan (1964) Plate 450, Fig. 1 – 3;
 Timm (1992) Plate 6, Fig. 5;
 Mackensen (1992) Plate 1, Fig. 6 – 8;
 Gabel (1971) Plate 15, Fig. 15 – 16;
 = *Angulogerina angulosa* (Williamson): Mackensen (1993) Plate 1, Fig. 1 – 2.

Triloculina sp.: Genus level was determined after (Loeblich et al, 1964) Plate 353.

Triloculina tricarinata: Thies (1991) Plate 14, Fig. 6, Plate 16, Fig. 1 - 12;
 Struck (1992) Plate 1, Fig. 8;
 Heß (1998) Plate 9, Fig. 10;
 Gabel (1971) Plate 7, Fig. 1 – 2;
 Gupta (1994) Plate 2, Fig. 1.

Trochammina montagui (Brönnimann & Whittaker): Timm (1992) Plate 4, Fig. 4a.

Uvigerina auberiana Cushman: Timm (1992) Plate 6, Fig. 2.

Uvigerina peregrina (Cushman): Ohkushi et al. (1999) Plate 2, Fig. 4;
 Gupta (1994) Plate 3, Fig. 14 - 15;
 Feyling-Hanssen et al. (1971) Plate 7, Fig. 9 – 11;
 Timm (1992) Plate 6, Fig. 2;
 Heß (1998) Plate 11, Fig. 2 – 3;
 Corliss (1988) Plate 1, Fig. 13.

Uvigerina pigmea (d'Orbigny): Timm (1992) Plate 6, Fig. 1;
 Loeblich and Tappan (1964) Plate 446, Fig. 1 – 2.

Uvigerina spp.: Genus level was determined after Loeblich and Tappan (1964) Plate 446,
 this genus contains fragments which could not be assigned to a certain species;

Uvigerina sp.: Genus level was determined after Loeblich and Tappan (1964) Plate 446.

Uvigerina schwageri Brady: H.B. Report on the foraminifera dredged by H.M.S. Challenger,
 during the years 1873-1876, <http://www.sstar.com/paleo/Uschlag.html>.

Vasicostella cranimorpha sp. nov., holotype: Clark (1995) Plate 1, Fig. 1 – 3.

A2 SEM PHOTOS OF CERTAIN FORAMINIFERA SPECIMEN**PLATE 1:**

(Figs. 1 to 3 and 5 to 12: upper scale bar = 100 µm)

- Fig. 1 *Nuttalides umbonifer* (Cushman), SO136-019BX, 13.5 cm bsf.
 Fig. 2 *Heteroplea dutemplei* (d'Orbigny), SO136-037BX, 8.5 cm bsf.
 Fig. 3 *Pullenia bulloides* (d'Orbigny), SO136-161BX, 4.5 cm bsf.
 Fig. 4 *Uvigerina peregrina* (Cushman), SO136-161BX, 22.5 cm bsf (lower scale bar).
 Fig. 5 *Fursenkonia complanata* (Egger), SO165BX, 26.5 cm bsf.
 Fig. 6 *Textularia wiesneri* Earland, SO136-161BX, 17.5 cm bsf.
 Fig. 7 *Siphonotextularia rolshauseni* (Phleger & Parker), SO136-161BX, 11.5 cm bsf.
 Fig. 8 – 9 *Melonis baleeanum* (Williamson), side and edge view, SO136-037BX, 3.5 cm bsf.
 Fig. 10 *Epistominella exigua* (Brady), SO136-019BX, 4.5 cm bsf.
 Fig. 11 *Bulimina aceluata* (d'Orbigny), SO136-147BX, 7.5 cm bsf.
 Fig. 12 – 13 *Globocassidolina subglogosa* (Brady), SO136-019BX, 2.5 cm bsf,

Scale bar of close up = 10 µm (not the toothed aperture).

PLATE 2:

(Figs. 14 – 19: upper scale bar = 100µm)

- Fig. 14 *Pyrolina cylindroides* (Roemer), SO136-161BX, 23.5 cm bsf.
 Fig. 15 – 16 *Melonis pompilioides* (Fichtel & Moll), edge and side view,
 SO136-161BX, 1.5 cm bsf.
 Fig. 17 *Pyrgo* sp. 2, SO136-037BX, 11.5 cm bsf.
 Fig. 18 *Rutherfordis* sp., SO136-165BX, 14.5 cm bsf.
 Fig. 19 *Reusella* sp., SO136-165BX, 23.5 cm bsf.

(Figs. 20 – 26: lower scale bar = 100 µm)

- Fig. 20 *Oridosalis* sp., SO136-161BX, 12.5 cm bsf.
 Fig. 21 *Pyrgo rotalia* Loeblich & Tappan, SO136-037BX, 14.5 cm bsf.
 Fig. 22 *Ehrenbergina mestayeri* (Cushman), SO136-037BX, 12.5 cm bsf.
 Fig. 23 *Vasicostella cranimorpha* sp. nov., holotype, SO136-147BX, 4.5 cm bsf.
 Fig. 24 - 25 *Tosaiia hanzawai* (Takayanagi), SO136-037BX, 8.5 cm bsf, side and top view.

PLATE 1

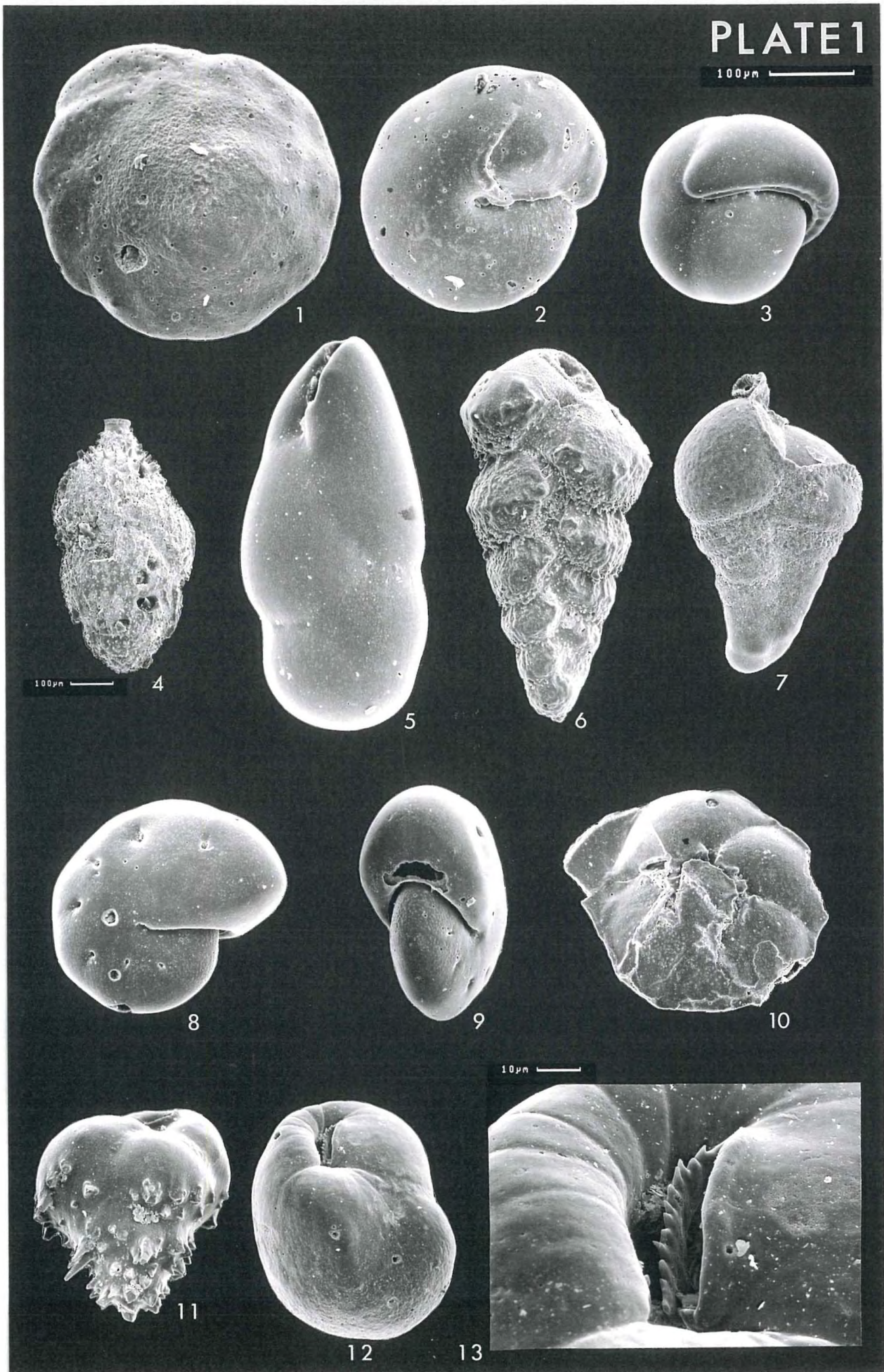
100 μ m —

PLATE 2

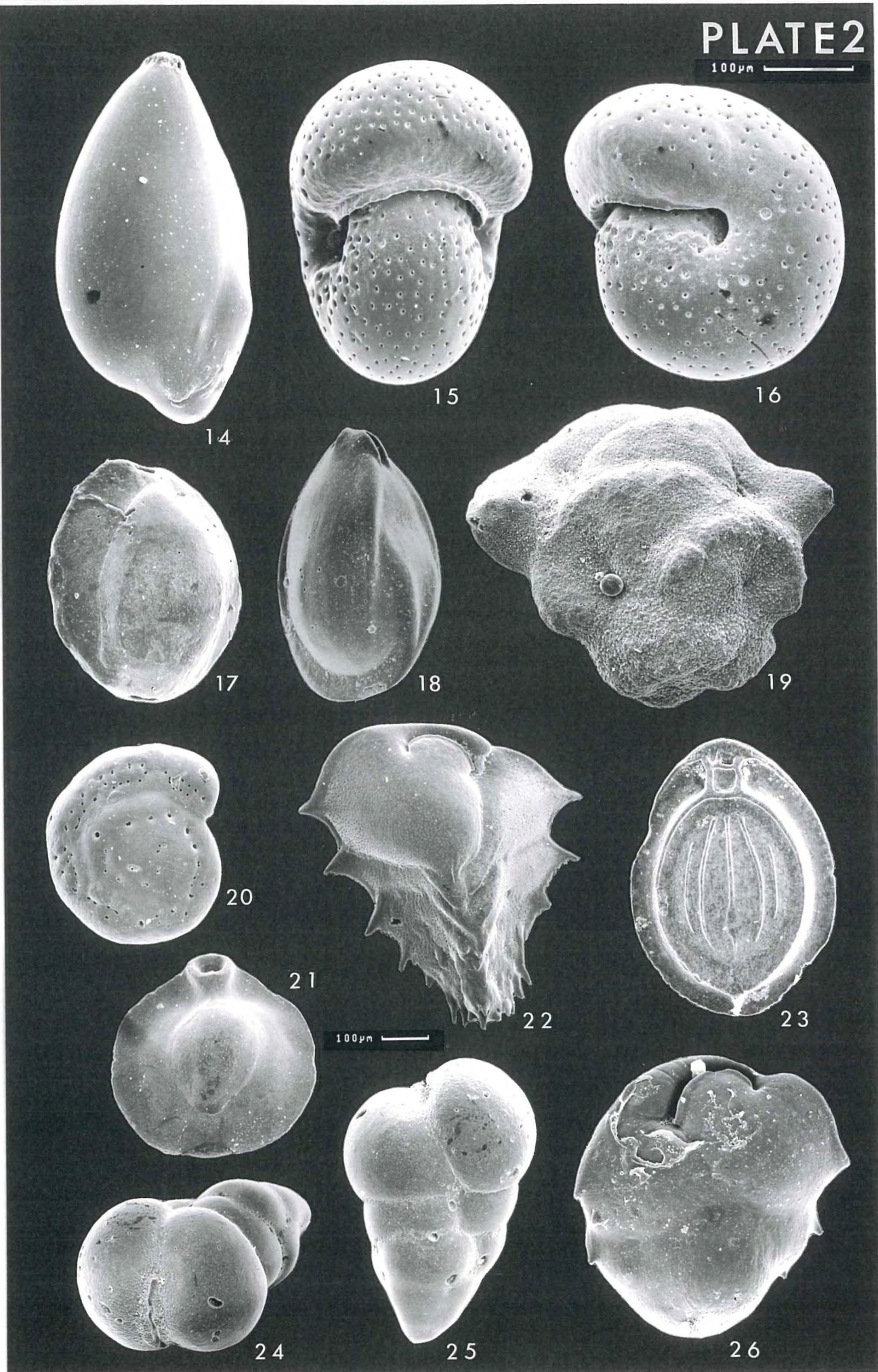
100 μ m

Table A 3.1 Paleontological data set of core SO136-019BX (continued). All species are given in spec./g.

depth (cm bsf)	<i>Globocassidolima subglobosa</i>	<i>Gyroidina neosoldanii</i>	<i>Gyroidinoides orbicularis</i>	<i>Gyronoides nipponicus</i>	<i>Haplophragmoides canariensis</i>	<i>Heteroplea dulempeleri</i>	<i>Lagena distoma</i>	<i>Lagena globosa</i>	<i>Lagena gracilima</i>	<i>Lagena hispidula</i>	<i>Lagena semilineata</i>	<i>Lagena gracilis</i>	<i>Lagena seifgesae</i>	<i>Lagena sp1</i>	<i>Lagena substriata</i>	<i>Lenticulina rotulata</i>	<i>Melonis baileeanum</i>	<i>Melonis pomphiloides</i>	<i>Melonis zandami</i>	<i>Miliammina arenacea</i>	<i>Nonionellina labradoricus</i>	<i>Nuttallides umbonifer</i>	<i>Oolina borealis</i>	<i>Oolina caudigera</i>	<i>Oolina hexagona</i>	<i>Oolina melo</i>	<i>Oridosalis umbonatus</i>	<i>Osangularia culta</i>	<i>Osangularia sp</i>	<i>Parafissurina ovata</i>	<i>Planulina ariminensis</i>												
0.5	4.82	4.82	0.00	0.00	2.41	0.00	0.00	0.00	0.00	0.00	0.00	7.22	0.00	0.00	2.41	0.00	2.91	0.00	0.00	0.00	2.41	45.75	0.00	0.00	0.00	2.41	0.00	0.00	2.41	0.00													
1.5	8.74	0.00	0.00	2.91	0.00	0.00	0.00	0.00	0.00	0.00	0.00	5.83	8.74	0.00	0.00	2.91	2.91	2.91	2.91	0.00	0.00	0.00	43.72	0.00	0.00	0.00	0.00	0.00	0.00	2.91	0.00												
2.5	0.00	0.00	0.00	0.00	0.00	0.00	0.00	0.00	0.00	0.00	0.00	8.76	5.84	0.00	0.00	8.76	0.00	3.82	0.00	3.82	3.82	3.82	0.00	0.00	0.00	0.00	0.00	0.00	0.00	0.00	0.00												
3.5	15.27	7.64	0.00	3.82	0.00	0.00	0.00	0.00	7.64	15.27	3.82	0.00	0.00	0.00	0.00	2.84	11.36	5.68	2.84	11.36	0.00	0.00	2.84	0.00	0.00	0.00	0.00	0.00	0.00	0.00	0.00												
4.5	14.20	0.00	0.00	0.00	0.00	2.84	0.00	0.00	0.00	11.36	5.68	2.84	11.36	0.00	0.00	2.84	2.84	5.68	0.00	0.00	0.00	5.68	53.97	0.00	0.00	0.00	8.52	0.00	0.00	2.84	0.00												
5.5	40.52	0.00	0.00	0.00	2.89	5.79	0.00	0.00	0.00	11.58	2.89	0.00	5.79	0.00	11.58	0.00	14.47	0.00	2.89	0.00	5.79	43.42	0.00	0.00	0.00	0.00	0.00	0.00	0.00	0.00	0.00												
6.5	23.51	0.00	0.00	6.41	0.00	8.55	0.00	0.00	0.00	6.41	8.55	4.28	8.55	0.00	0.00	0.00	0.00	0.00	0.00	5.85	2.14	4.28	0.00	2.14	23.51	2.14	0.00	0.00	6.41	0.00	0.00	2.14	6.41	0.00									
7.5	20.75	0.00	0.00	3.77	0.00	5.66	0.00	0.00	3.77	1.89	0.00	1.89	0.00	5.66	1.89	3.77	3.77	3.77	3.77	0.00	0.00	0.00	0.00	0.00	0.00	0.00	0.00	0.00	0.00	0.00	0.00	0.00	0.00										
8.5	11.46	0.00	0.00	7.64	0.00	26.73	0.00	0.00	9.55	1.91	3.82	3.82	1.91	1.91	1.91	1.91	1.91	1.91	3.82	9.55	3.82	40.10	1.91	0.00	0.00	1.91	9.55	0.00	0.00	5.73	0.00	0.00	5.73	0.00									
9.5	23.53	0.00	0.00	2.14	0.00	23.53	0.00	0.00	0.00	12.83	4.28	2.14	2.14	0.00	2.14	0.00	0.00	4.28	6.42	0.00	6.42	4.28	47.06	0.00	0.00	0.00	0.00	0.00	0.00	2.14	0.00	0.00	6.42	2.14	0.00	0.00	0.00	0.00					
10.5	30.39	0.00	0.00	7.01	0.00	7.01	0.00	0.00	0.00	11.69	0.00	0.00	7.01	2.34	2.34	2.34	2.34	9.35	0.00	0.00	0.00	0.00	0.00	0.00	46.75	0.00	0.00	0.00	0.00	0.00	0.00	11.69	0.00	0.00	11.69	0.00							
11.5	23.19	2.32	0.00	0.00	18.55	2.32	0.00	0.00	2.32	0.00	0.00	0.00	0.00	0.00	0.00	0.00	0.00	2.32	2.32	11.59	6.96	0.00	6.96	2.32	37.10	6.96	2.32	0.00	2.32	9.28	0.00	0.00	11.59	2.32	0.00	0.00	0.00	0.00					
12.5	19.03	0.00	2.38	4.76	0.00	19.03	0.00	0.00	2.38	16.65	0.00	0.00	2.38	4.76	2.38	0.00	2.38	7.14	0.00	2.38	2.38	52.34	4.76	0.00	0.00	0.00	9.52	0.00	0.00	7.14	4.76	0.00	0.00	0.00	0.00								
13.5	39.36	0.00	2.62	2.62	0.00	10.50	0.00	0.00	0.00	13.12	2.62	0.00	5.25	0.00	13.12	5.25	0.00	5.25	0.00	0.00	0.00	5.25	49.86	0.00	0.00	0.00	0.00	0.00	0.00	10.50	0.00	0.00	2.62	2.62	0.00	0.00	0.00	0.00					
14.5	13.04	0.00	0.00	0.00	0.00	5.22	0.00	0.00	0.00	18.26	2.61	5.22	7.82	0.00	2.61	2.61	0.00	10.43	0.00	5.22	0.00	93.89	0.00	7.82	0.00	0.00	0.00	0.00	0.00	0.00	0.00	0.00	5.22	0.00	0.00	0.00	0.00	0.00	0.00				
15.5	28.51	2.59	0.00	0.00	0.00	36.29	0.00	0.00	0.00	0.00	12.96	5.18	2.59	2.59	0.00	10.37	10.37	7.78	5.18	0.00	0.00	0.00	0.00	90.72	0.00	0.00	0.00	0.00	0.00	0.00	2.59	0.00	0.00	7.78	0.00	0.00	0.00	0.00	0.00	0.00			
16.5	6.22	0.00	0.00	0.00	0.00	12.44	0.00	0.00	0.00	20.73	12.44	0.00	0.00	0.00	0.00	0.00	0.00	2.07	0.00	14.51	6.22	0.00	2.07	93.26	0.00	0.00	0.00	0.00	0.00	0.00	6.22	0.00	0.00	0.00	0.00	0.00	0.00	0.00	0.00	0.00	0.00		
17.5	6.87	0.00	0.00	0.00	0.00	10.31	0.00	6.87	6.87	3.44	0.00	6.87	20.62	0.00	3.44	0.00	13.75	6.87	3.44	0.00	0.00	0.00	96.24	0.00	0.00	0.00	0.00	0.00	0.00	3.44	6.87	0.00	0.00	0.00	0.00	0.00	0.00	0.00	0.00	0.00			
18.5	7.79	0.00	0.00	0.00	0.00	15.57	0.00	12.98	0.00	5.19	5.19	0.00	2.60	0.00	0.00	0.00	12.98	10.38	0.00	2.60	0.00	114.19	2.60	0.00	0.00	0.00	0.00	0.00	0.00	2.60	0.00	0.00	0.00	0.00	0.00	0.00	0.00	0.00	0.00	0.00			
19.5	12.01	0.00	0.00	0.00	3.00	0.00	12.01	0.00	3.00	0.00	15.01	3.00	0.00	0.00	0.00	0.00	3.00	6.01	0.00	3.00	0.00	132.11	6.01	18.02	0.00	0.00	0.00	0.00	0.00	0.00	15.01	0.00	0.00	0.00	0.00	0.00	0.00	0.00	0.00	0.00	0.00		
20.5	19.13	0.00	0.00	0.00	0.00	0.00	24.59	0.00	5.47	0.00	2.73	0.00	0.00	2.73	0.00	0.00	0.00	8.20	8.20	2.73	0.00	2.73	71.05	0.00	19.13	0.00	0.00	0.00	10.93	0.00	0.00	0.00	13.66	0.00	0.00	0.00	0.00	0.00	0.00	0.00	0.00	0.00	0.00
21.5	40.07	0.00	0.00	0.00	0.00	5.72	0.00	2.86	2.86	0.00	0.00	0.00	5.72	0.00	2.86	0.00	5.72	17.17	0.00	2.86	0.00	128.80	2.86	11.45	0.00	0.00	0.00	17.17	0.00	0.00	0.00	0.00	0.00	0.00	0.00	0.00	0.00	0.00	0.00				
22.5	38.30	0.00	0.00	0.00	0.00	12.77	0.00	0.00	0.00	3.19	0.00	0.00	3.19	0.00	0.00	0.00	0.00	9.58	19.15	0.00	0.00	9.58	0.00	102.14	0.00	9.58	3.19	0.00	19.15	0.00	0.00	6.38	6.38	0.00	0.00	0.00	0.00	0.00	0.00	0.00	0.00	0.00	0.00
23.5	24.20	0.00	0.00	0.00	0.00	2.42	0.00	4.84	0.00	2.42	0.00	0.00	0.00	0.00	0.00	0.00	2.42	4.84	16.94	0.00	0.00	0.00	101.64	2.42	2.42	0.00	0.00	0.00	7.26	0.00	0.00	16.94	4.84	0.00	0.00	0.00	0.00	0.00	0.00	0.00	0.00	0.00	
24.5	8.34	0.00	0.00	0.00	0.00	4.17	0.00	2.09	2.09	0.00	4.17	2.09	0.00	4.17	0.00	0.00	4.17	6.26	6.26	0.00	0.00	0.00	87.59	0.00	2.09	0.00	0.00	0.00	8.34	0.00	0.00	0.00	0.00	0.00	0.00	0.00	0.00	0.00	0.00				
25.5	9.85	0.00	0.00	0.00	0.00	4.92	0.00	0.00	2.46	4.92	4.92	0.00	0.00	0.00	4.92	0.00	0.00	0.00	0.00	0.00	0.00	0.00	91.08	0.00	2.46	0.00	0.00	0.00	2.46	0.00	0.00	0.00	0.00	0.00	0.00	0.00	0.00	0.00	0.00	0.00			
26.5	21.93	0.00	0.00	0.00	0.00	10.12	0.00	0.00	6.75	0.00	3.37	3.37	0.00	3.37	0.00	0.00	5.11	0.00	1.69	0.00	0.00	0.00	79.28	1.69	5.06	0.00	0.00	0.00	0.00	0.00	0.00	0.00	0.00	0.00	0.00	0.00	0.00	0.00	0.00	0.00	0.00		
27.5	22.96	0.00	0.00	0.00	0.00	4.59	0.00	7.65	1.53	0.00	0.00	1.53	0.00	0.00	1.53	0.00	0.00	4.59	0.00	0.00	0.00	64.28	0.00	6.12	0.00	0.00	0.00	4.59	0.00	0.00	4.59	0.00	0.00	0.00	0.00	0.00	0.00	0.00	0.00	0.00			
28.5	3.41	0.00	0.00	0.00	0.00	5.11	0.																																				

Table A 3.1 Paleontological data set of core SO136-019BX (continued). All species are given in spec./g.

Table A 3.2 Paleontological data set of core SO136-025BX. All species are given in spec./g.

depth (cm bs)	<i>Bolivina pacifica</i>	<i>Cibicidoides fletcheri</i>	<i>Cibicidoides inawagensis</i>	<i>Cibicidoides lobatulus</i>	<i>Cibicidoides mundulus</i>	<i>Cibicidoides sp</i>	<i>Cibicidoides williersiorum</i>	<i>Cribrostomoides subglobosum</i>	<i>Cnicalculina triangulana</i>	<i>Cyclammina cancellata</i>	<i>Dentalina baggi</i>	<i>Tosia hanzawai</i>	<i>Ehrenbergina pacifica</i>	<i>Epistominella exigua</i>	<i>Fissurina laevigata</i>	<i>Fissurina marginata</i>	<i>Globocassidolina subglobosa</i>	<i>Gyroidinoides orbicularis</i>	<i>Gyrinoides nipponicus</i>	<i>Heteroplea dutemplei</i>	<i>Lagenaria gracilis</i>	<i>Lagenaria hispida</i>	<i>Lagenaria substriata</i>	<i>Leniculina rotulata</i>	<i>Melonis baileanum</i>	<i>Nuttallides umbonifer</i>
0.5	0.00	0.00	3.15	0.00	0.00	0.00	0.00	0.00	0.00	0.00	0.00	0.00	0.00	0.00	0.00	0.00	0.00	0.00	0.00	0.00	0.00	0.00	0.00	0.00	0.00	0.00
1.5	0.00	0.00	0.00	0.00	0.00	0.00	0.00	7.48	2.49	0.00	0.00	0.00	0.00	0.00	0.00	0.00	0.00	0.00	0.00	0.00	0.00	0.00	0.00	0.00	0.00	0.00
2.5	0.00	0.00	0.00	4.27	0.00	0.00	0.00	2.13	0.00	0.00	0.00	0.00	0.00	0.00	0.00	0.00	0.00	0.00	0.00	0.00	0.00	0.00	0.00	0.00	0.00	0.00
3.5	1.77	0.00	7.07	3.54	0.00	0.00	1.77	1.77	3.54	0.00	0.00	0.00	0.00	0.00	0.00	0.00	0.00	0.00	0.00	0.00	0.00	0.00	0.00	0.00	0.00	0.00
4.5	0.00	2.04	0.00	0.00	2.04	0.00	2.04	0.00	0.00	0.00	0.00	0.00	0.00	0.00	0.00	0.00	0.00	0.00	0.00	0.00	0.00	0.00	0.00	0.00	0.00	0.00
5.5	0.00	0.00	3.55	0.00	0.00	17.74	10.64	0.00	3.55	0.00	3.55	0.00	0.00	0.00	0.00	0.00	0.00	0.00	0.00	0.00	0.00	0.00	0.00	0.00	0.00	0.00
6.5	0.00	0.00	0.00	0.00	0.00	0.00	5.84	0.00	0.00	2.92	0.00	8.76	0.00	0.00	0.00	0.00	0.00	0.00	0.00	0.00	0.00	0.00	0.00	0.00	0.00	0.00
7.5	0.00	0.00	0.00	0.00	0.00	0.00	8.89	0.00	0.00	0.00	0.00	0.00	0.00	0.00	0.00	0.00	0.00	0.00	0.00	0.00	0.00	0.00	0.00	0.00	0.00	0.00
8.5	0.00	0.00	0.00	0.00	0.00	0.00	0.00	0.00	0.00	0.00	0.00	0.00	0.00	0.00	0.00	0.00	0.00	0.00	0.00	0.00	0.00	0.00	0.00	0.00	0.00	0.00
9.5	0.00	0.00	0.00	0.00	0.00	0.00	0.00	0.00	0.00	0.00	0.00	0.00	0.00	0.00	0.00	0.00	0.00	0.00	0.00	0.00	0.00	0.00	0.00	0.00	0.00	0.00
10.5	0.00	0.00	0.00	0.00	0.00	0.00	0.00	0.00	0.00	0.00	0.00	0.00	0.00	0.00	0.00	0.00	0.00	0.00	0.00	0.00	0.00	0.00	0.00	0.00	0.00	0.00
11.5	0.00	0.00	0.00	0.00	0.00	0.00	0.00	0.00	0.00	0.00	0.00	0.00	0.00	0.00	0.00	0.00	0.00	0.00	0.00	0.00	0.00	0.00	0.00	0.00	0.00	0.00

Table A 3.2 Paleontological data set of core SO136-025BX (continued). All species are given in spec./g.

depth (cm bs)	<i>Orbitalis umbonatus</i>	<i>Parafissurina ventricosa</i>	<i>Planulina ariminensis</i>	<i>Pulenia bullidies</i>	<i>Pyrgo murchina</i>	<i>Pyrgo oblonga</i>	<i>Pyrgo rotalaria</i>	<i>Pyrgo serrata</i>	<i>Pyrgo spp</i>	<i>Pyrgo tasmania</i>	<i>Quinqueloculina spp</i>	<i>Ehrenbergina mestayeri</i>	<i>Siphonotextularia rolshauseni</i>	<i>Spiraloculina disparilis</i>	<i>Siliostomella lepidula</i>	<i>Trifarina angulosa</i>	<i>Uvigerina auberiana</i>	<i>Uvigerina peregrina</i>	<i>Uvigerina pigmea</i>	<i>Fragments of agglutinating spp.</i>	All species / g	Clastic sediments / g	Σ (counts)	Weight of sample [g]	Factor of split	
0.5	0.00	0.00	0.00	0.00	0.00	0.00	6.31	0.00	3.15	3.15	0.00	0.00	0.00	0.00	0.00	0.00	0.00	0.00	0.00	53.60	203.35	34	10.15	1/16		
1.5	0.00	0.00	2.49	0.00	0.00	4.98	0.00	9.97	0.00	0.00	0.00	0.00	0.00	0.00	0.00	0.00	0.00	0.00	87.23	2218.07	35	12.84	1/32			
2.5	0.00	0.00	0.00	2.13	0.00	2.13	0.00	4.27	0.00	4.27	0.00	2.13	2.13	0.00	0.00	4.27	2.13	0.00	0.00	10.67	61.87	1798.40	29	15.00	1/32	
3.5	1.77	0.00	3.54	0.00	0.00	0.00	0.00	0.00	7.07	3.54	10.61	12.38	0.00	0.00	0.00	0.00	0.00	5.30	0.00	0.00	22.98	106.08	2743.87	60	18.10	1/32
4.5	0.00	0.00	4.08	0.00	2.04	2.04	0.00	0.00	2.04	0.00	4.08	0.00	0.00	0.00	0.00	0.00	0.00	0.00	0.00	2.04	59.15	3401.91	29	20.92	3/128	
5.5	3.55	0.00	3.55	3.55	17.74	0.00	0.00	3.55	7.10	0.00	0.00	7.10	0.00	0.00	0.00	10.64	0.00	0.00	0.00	24.83	166.74	9770.29	47	9.02	1/32	
6.5	8.76	2.92	0.00	0.00	0.00	0.00	0.00	0.00	0.00	0.00	2.92	0.00	0.00	0.00	0.00	0.00	0.00	0.00	0.00	2.92	64.23	8058.39	22	2.74	1/8	
7.5	0.00	0.00	0.00	0.00	0.00	0.00	0.00	0.00	0.00	0.00	17.78	0.00	0.00	0.00	0.00	0.00	0.00	0.00	0.00	35.56	62.22	11333.33	7	0.45	1/4	
8.5	0.00	0.00	0.00	0.00	0.00	0.00	0.00	0.00	0.00	0.00	0.00	0.00	0.00	0.00	0.00	0.00	0.00	0.00	0.00	14.29	14.29	40928.57	1	0.28	1/4	
9.5	0.00	0.00	0.00	0.00	0.00	0.00	0.00	0.00	0.00	0.00	0.00	0.00	0.00	0.00	0.00	0.00	0.00	0.00	0.00	0.00	18.18	29236.36	1	0.11	1/2	
10.5	0.00	0.00	0.00	0.00	0.00	0.00	0.00	0.00	0.00	0.00	0.00	0.00	0.00	0.00	0.00	0.00	0.00	0.00	0.00	0.00	15.38	24061.54	1	0.13	1/2	
11.5	0.00	0.00	0.00	0.00	0.00	0.00	0.00	0.00	0.00	0.00	0.00	0.00	0.00	0.00	0.00	0.00	0.00	0.00	0.00	40.00	16080.00	3	0.15	1/2		

Table A 3.3 Paleontological data set of core SO136-037BX. All species are given in spec./g.

0.5	0.00	0.00	0.00	4.76	2.38	2.38	0.00	0.00	0.00	2.38	14.29	0.00	2.38	0.00	7.14	11.90	0.00	0.00	0.00	0.00	7.14	52.38	0.00	9.52	130.95	35.71	
1.5	0.00	0.00	0.00	5.30	0.00	7.95	0.00	0.00	0.00	2.65	15.89	0.00	2.65	2.65	2.65	31.79	0.00	0.00	0.00	0.00	2.65	47.68	0.00	21.19	143.05	50.33	
2.5	2.02	0.00	0.00	0.00	0.00	10.08	4.03	0.00	0.00	2.02	14.11	0.00	6.05	4.03	0.00	22.17	0.00	0.00	0.00	2.02	0.00	50.38	0.00	30.23	114.88	56.43	
3.5	0.00	0.00	0.00	5.98	1.99	7.98	0.00	0.00	0.00	11.96	13.96	1.99	21.93	0.00	1.99	17.94	0.00	0.00	0.00	0.00	0.00	39.88	1.99	23.93	117.63	37.88	
4.5	1.82	0.00	0.00	9.08	1.82	3.63	0.00	0.00	0.00	1.82	25.43	0.00	7.26	10.90	0.00	7.26	0.00	0.00	0.00	0.00	0.00	25.43	0.00	34.51	88.99	54.48	
5.5	0.00	0.00	0.00	8.97	0.00	6.73	0.00	2.24	0.00	0.00	20.19	0.00	22.43	11.22	0.00	15.70	0.00	4.49	0.00	0.00	0.00	40.38	0.00	15.70	109.92	33.65	
6.5	0.00	0.00	0.00	0.00	1.98	1.98	0.00	0.00	0.00	0.00	19.78	0.00	0.00	5.94	0.00	17.81	0.00	0.00	9.89	0.00	0.00	35.61	0.00	33.63	102.87	53.42	
7.5	1.97	0.00	0.00	1.97	0.00	11.83	1.97	0.00	0.00	0.00	7.89	0.00	5.92	9.86	1.97	21.69	0.00	0.00	0.00	0.00	0.00	67.06	0.00	21.69	61.14	39.45	
8.5	0.00	0.00	0.00	8.13	0.00	4.06	0.00	0.00	0.00	0.00	18.29	0.00	0.00	10.16	0.00	10.16	0.00	2.03	4.06	0.00	0.00	28.44	0.00	14.22	71.11	46.73	
9.5	0.00	0.00	0.00	3.89	0.00	0.00	0.00	0.00	0.00	0.00	21.37	0.00	0.00	13.60	1.94	11.66	0.00	0.00	0.00	0.00	0.00	33.03	0.00	29.14	87.43	15.54	
10.5	1.76	0.00	0.00	10.55	0.00	8.79	3.52	0.00	0.00	0.00	21.10	0.00	0.00	17.58	3.52	14.07	1.76	3.52	0.00	0.00	0.00	0.00	31.65	0.00	17.58	82.64	42.20
11.5	0.00	1.91	0.00	5.73	0.00	0.00	1.91	0.00	0.00	0.00	7.64	0.00	0.00	3.82	19.10	11.46	0.00	0.00	1.91	0.00	0.00	17.19	0.00	17.19	89.76	47.75	
12.5	0.00	0.00	0.00	5.73	0.00	2.86	0.00	0.00	0.00	0.00	10.03	4.30	10.03	0.00	10.03	10.03	0.00	0.00	2.86	0.00	0.00	25.78	0.00	4.30	63.03	40.11	
13.5	0.00	0.00	0.00	6.75	2.70	0.00	0.00	0.00	0.00	5.40	0.00	6.75	6.75	0.00	8.10	0.00	0.00	1.35	0.00	0.00	31.05	0.00	17.55	41.86	48.61		
14.5	0.00	0.00	0.00	1.71	5.13	1.71	0.00	0.00	0.00	1.71	11.97	0.00	1.71	6.84	1.71	1.71	0.00	0.00	3.42	0.00	0.00	30.77	3.42	10.26	41.03	44.44	
15.5	0.00	0.00	0.00	0.00	0.00	1.37	0.00	0.00	2.74	0.00	5.48	0.00	0.00	5.48	1.37	15.06	0.00	0.00	0.00	41.08	0.00	41.08	0.00	39.71	79.42	36.97	
16.5	0.00	1.65	0.00	1.65	1.65	3.31	0.00	1.65	3.31	0.00	9.92	0.00	0.00	8.27	0.00	8.27	0.00	0.00	0.00	0.00	0.00	36.38	0.00	21.50	43.00	62.84	
17.5	0.00	1.34	1.34	5.37	2.68	0.00	0.00	0.00	1.34	1.34	5.37	1.34	0.00	9.40	9.40	16.11	9.40	0.00	0.00	0.00	1.34	17.45	38.93	33.56	55.03		
18.5	0.00	1.43	0.00	1.43	0.72	0.00	0.00	0.00	0.00	0.00	7.17	0.00	0.00	2.15	0.72	10.75	0.72	0.00	0.72	0.72	0.00	0.00	6.45	24.37	36.56	32.26	

Table A 3.3 Paleontological data set of core SO136-037BX (continued). All species are given in spec./g.

depth (cm bsf)		<i>Fissurina danica</i>	<i>Fissurina laevigata</i>	<i>Fissurina marginata</i>	<i>Fissurina orbignyana</i>	<i>Fissurina serrata</i>	<i>Fissurina wieśni</i>	<i>Florius astensisans</i>	<i>Globocassidolina subglobosa</i>	<i>Globorotalites multisepia</i>	<i>Grigolis orectus</i>	<i>Gyroldinoides orbicularis</i>	<i>Gyroldinoides nipponicus</i>	<i>Heteroplea dumtemplei</i>	<i>Karitella siphonella</i>	<i>Lagena distoma</i>	<i>Lagena gracillima</i>	<i>Lagena gracilis</i>	<i>Lagena hispidula</i>	<i>Lagena semilineata</i>	<i>Lagena setigera</i>	<i>Lagena sp1</i>	<i>Lagena striata</i>	<i>Lagena substrata</i>	<i>Lagenaria sulcata laevicostata</i>	<i>Laticarinina pauperata</i>
0.5	0.00	0.00	11.90	9.52	4.76	0.00	0.00	0.00	0.00	0.00	0.00	0.00	0.00	2.38	0.00	0.00	0.00	0.00	0.00	2.38	0.00	0.00	0.00	0.00	0.00	
1.5	2.65	0.00	5.30	15.89	5.30	0.00	0.00	0.00	5.30	0.00	0.00	0.00	0.00	13.25	5.30	0.00	7.95	0.00	0.00	2.65	0.00	0.00	0.00	7.95	0.00	
2.5	4.03	0.00	12.09	12.09	0.00	0.00	0.00	10.08	0.00	0.00	0.00	0.00	0.00	6.05	0.00	0.00	1.99	0.00	0.00	4.03	0.00	0.00	0.00	4.03	0.00	
3.5	3.99	0.00	7.98	9.97	1.99	0.00	1.99	5.98	0.00	0.00	0.00	0.00	0.00	0.00	0.00	0.00	0.00	0.00	0.00	1.99	0.00	0.00	0.00	0.00	3.99	
4.5	5.45	0.00	10.90	5.45	1.82	0.00	0.00	1.82	6.73	0.00	0.00	0.00	0.00	0.00	2.24	8.97	0.00	0.00	0.00	0.00	1.82	0.00	0.00	3.63	0.00	1.82
5.5	2.24	0.00	4.49	4.49	0.00	2.24	6.73	0.00	0.00	0.00	0.00	0.00	0.00	0.00	0.00	0.00	0.00	0.00	0.00	2.24	0.00	0.00	2.24	0.00	0.00	
6.5	0.00	0.00	7.91	3.96	0.00	0.00	1.98	5.94	0.00	0.00	0.00	0.00	0.00	9.89	1.98	0.00	1.98	0.00	0.00	1.98	0.00	0.00	1.98	0.00	0.00	
7.5	3.94	0.00	7.89	3.94	1.97	0.00	0.00	7.89	0.00	0.00	0.00	1.97	0.00	0.00	0.00	0.00	0.00	0.00	0.00	0.00	0.00	0.00	0.00	0.00	0.00	
8.5	2.03	0.00	6.10	4.06	2.03	0.00	0.00	2.03	0.00	0.00	0.00	6.10	10.16	4.06	0.00	0.00	0.00	0.00	0.00	8.13	0.00	0.00	6.10	0.00	0.00	
9.5	0.00	0.00	9.71	13.60	0.00	0.00	0.00	3.89	0.00	0.00	0.00	0.00	0.00	0.00	5.83	1.94	0.00	1.94	0.00	0.00	0.00	0.00	0.00	0.00	1.94	
10.5	7.03	0.00	8.79	17.58	0.00	0.00	0.00	3.52	0.00	0.00	0.00	1.76	0.00	3.52	0.00	1.76	3.52	3.52	0.00	7.03	0.00	1.76	1.76	0.00	0.00	
11.5	1.91	0.00	5.73	5.73	0.00	1.91	1.91	3.82	0.00	0.00	0.00	1.91	1.91	3.82	1.91	1.91	1.91	1.91	0.00	0.00	5.73	0.00	0.00	0.00	7.64	1.91
12.5	1.43	0.00	7.16	12.89	1.43	1.43	0.00	1.43	0.00	1.43	0.00	0.00	0.00	0.00	4.30	1.43	0.00	0.00	0.00	0.00	1.43	0.00	0.00	5.73	2.86	0.00
13.5	0.00	0.00	1.35	0.00	0.00	6.75	0.00	0.00	0.00	0.00	0.00	1.35	8.10	8.10	0.00	0.00	0.00	0.00	0.00	5.40	0.00	1.35	5.40	0.00	1.35	
14.5	1.71	0.00	0.00	1.71	0.00	8.55	0.00	3.42	0.00	0.00	0.00	0.00	0.00	0.00	1.71	0.00	0.00	0.00	1.71	0.00	0.00	0.00	0.00	5.13	3.42	
15.5	4.11	1.37	10.95	4.11	0.00	0.00	0.00	0.00	0.00	0.00	1.37	4.11	1.37	0.00	0.00	1.37	2.74	0.00	0.00	2.74	1.37	0.00	2.74	0.00	4.11	
16.5	1.65	1.65	4.96	1.65	0.00	0.00	0.00	0.00	1.65	0.00	0.00	0.00	0.00	0.00	3.31	0.00	0.00	0.00	0.00	0.00	1.65	1.65	1.65	3.31	0.00	0.00
17.5	1.34	0.00	4.03	8.05	0.00	1.34	0.00	12.08	0.00	0.00	1.34	0.00	2.68	0.00	0.00	0.00	0.00	0.00	0.00	0.00	0.00	1.34	0.00	2.68	1.34	4.03
18.5	0.00	0.72	0.72	2.87	0.00	10.04	0.00	1.43	0.00	0.72	0.00	0.00	4.30	0.00	0.00	0.00	0.00	0.00	0.00	0.00	0.72	0.00	0.00	3.58	0.00	0.72

Table A 3.3 Paleontological data set of core SO136-037BX (continued). All species are given in spec./g.

depth (cm bsf)	2.38	21.43	2.38	Melonis baleanum	Melonis zandami	0.00	7.14	Nonionellina labradoricus	Oolina borealis	Oolina caudigera	Oolina hexagona	2.38	Oolina melo	4.76	Oridosalis umbonatus	Osangularia culta	Parafissurina lateralis	Parafissurina ovata	Parafissurina ventricosa	Planulina ariminensis	Polymorphina luceta	Pseudorotalia gaimardi	Pulenia bulloides	Pulenia quinqueloba	Pyrgo murrinha	Pyrgo oblonga	Pyrgo notalania	Pyrgo serrata	Pyrgo sp2	Pyrgo spp	Pyrgo tasmania
0.5	2.38	29.14	0.00	0.00	2.65	0.00	0.00	0.00	2.65	15.89	0.00	0.00	10.60	0.00	0.00	0.00	0.00	15.89	7.95	0.00	31.79	0.00	7.95	0.00	45.03	5.30					
1.5	7.95	26.20	0.00	0.00	10.08	2.02	0.00	0.00	4.03	6.05	2.02	0.00	10.08	0.00	4.03	0.00	0.00	6.05	2.02	0.00	32.25	0.00	2.02	0.00	52.40	6.05					
2.5	2.02	19.94	3.99	0.00	3.99	0.00	0.00	0.00	5.98	9.97	0.00	0.00	9.97	0.00	0.00	0.00	0.00	15.95	1.99	0.00	5.98	0.00	7.98	0.00	53.83	1.99					
3.5	0.00	9.08	0.00	0.00	3.63	0.00	0.00	0.00	3.63	9.08	3.63	0.00	3.63	0.00	0.00	0.00	0.00	5.45	0.00	19.98	0.00	5.45	0.00	49.04	1.82						
4.5	7.26	17.95	0.00	0.00	2.24	0.00	0.00	0.00	4.49	2.24	2.24	0.00	8.97	0.00	0.00	0.00	0.00	4.49	11.22	0.00	31.41	0.00	4.49	0.00	60.57	0.00					
5.5	4.49	9.89	0.00	0.00	1.98	0.00	0.00	0.00	3.96	9.89	1.98	0.00	17.81	0.00	1.98	0.00	0.00	7.91	3.96	0.00	21.76	0.00	1.98	0.00	25.72	0.00					
6.5	1.98	11.83	0.00	0.00	9.86	0.00	0.00	1.97	0.00	1.97	0.00	0.00	7.89	0.00	0.00	0.00	0.00	5.92	0.00	41.42	0.00	0.00	0.00	43.39	1.97						
7.5	0.00	14.22	0.00	0.00	0.00	2.03	0.00	2.03	6.10	4.06	0.00	0.00	12.19	0.00	0.00	0.00	0.00	6.10	10.16	0.00	18.29	0.00	6.10	0.00	38.60	0.00					
8.5	3.89	13.60	0.00	0.00	0.00	0.00	1.94	0.00	3.89	1.94	0.00	0.00	9.71	0.00	0.00	0.00	1.94	3.89	0.00	0.00	13.60	13.60	3.89	0.00	48.57	0.00					
9.5	5.27	12.31	0.00	0.00	0.00	0.00	0.00	3.52	0.00	12.31	1.76	0.00	5.27	1.76	0.00	0.00	0.00	3.52	5.27	0.00	19.34	8.79	0.00	0.00	54.51	0.00					
10.5	0.00	11.46	0.00	0.00	1.91	0.00	0.00	0.00	3.82	0.00	0.00	0.00	17.19	0.00	0.00	0.00	0.00	9.55	1.91	0.00	26.74	3.82	9.55	0.00	30.56	0.00					
11.5	5.73	12.89	0.00	0.00	4.30	0.00	0.00	1.43	1.43	0.00	1.43	0.00	4.30	1.43	0.00	0.00	0.00	2.86	2.86	4.30	7.16	10.03	0.00	0.00	35.81	0.00					
12.5	0.00	4.05	1.35	1.35	1.35	6.75	1.35	1.35	0.00	0.00	0.00	5.40	4.05	1.35	0.00	0.00	1.35	0.00	1.35	1.35	18.90	0.00	0.00	0.00	18.90	0.00					
13.5	0.00	13.68	0.00	0.00	3.42	0.00	0.00	6.84	0.00	1.71	0.00	3.42	1.71	6.84	1.71	0.00	5.13	8.55	6.84	0.00	18.80	1.71	0.00	0.00	32.48	0.00					
14.5	1.37	13.69	1.37	0.00	2.74	1.37	0.00	1.37	1.37	2.74	4.11	5.48	0.00	2.74	0.00	0.00	0.00	1.37	2.74	0.00	13.69	0.00	0.00	1.37	54.77	0.00					
15.5	3.31	8.27	0.00	0.00	0.00	0.00	0.00	0.00	6.61	1.65	0.00	8.27	0.00	3.31	0.00	1.65	8.27	9.92	3.31	0.00	23.15	0.00	0.00	0.00	90.96	0.00					
16.5	0.00	13.42	0.00	0.00	0.00	0.00	1.34	4.03	4.03	5.37	0.00	2.68	1.34	0.00	0.00	0.00	1.34	1.34	2.68	1.34	21.48	0.00	0.00	0.00	42.95	0.00					
17.5	0.72	11.47	0.00	0.72	2.87	2.15	0.00	1.43	7.17	4.30	0.00	7.89	2.87	0.00	0.72	0.00	2.15	5.02	0.72	0.72	14.34	0.00	0.00	0.72	0.72	0.00					

Table A 3.3 Paleontological data set of core SO136-037BX (continued). All species are given in spec./g.

depth (cm bsf)	<i>Quinqueloculina</i> spp	<i>Reophax micaceus</i>	<i>Rutherfordia</i> sp	<i>Sigmoilopsis schlumbergerii</i>	<i>Siphonotextularia rolshauseni</i>	<i>Spiroloculina disparilis</i>	<i>Suggrunda porosa</i>	<i>Textularia porrecta</i>	<i>Textularia truncata</i>	<i>Trifarina angulosa</i>	<i>Triloculina</i> sp	<i>Triloculina tricarinata</i>	<i>Trochammina montagui</i>	<i>Uvigerina auberiana</i>	<i>Uvigerina peregrina</i>	<i>Uvigerina pygmaea</i>	<i>Uvigerina schwageri</i>	<i>Vasicostella craniomorpha</i>	Fragments of agglutinating spp.	All species (spec./g)	Clastic sediments / g	Σ (counts)	Weight of sample [g]	Factor of split	
0.5	0.00	0.00	0.00	7.14	2.38	0.00	0.00	0.00	16.67	42.86	0.00	0.00	0.00	40.48	2.38	0.00	11.90	0.00	123.81	723.81	50.00	304	7.68	7/128	
1.5	2.65	0.00	0.00	7.95	0.00	0.00	2.65	0.00	13.25	23.84	0.00	0.00	0.00	18.54	2.65	2.65	5.30	2.65	21.19	696.69	47.68	263	6.04	1/16	
2.5	2.02	0.00	0.00	0.00	6.05	0.00	2.02	0.00	10.08	38.29	0.00	0.00	0.00	32.25	6.05	4.03	10.08	4.03	6.05	671.11	56.43	333	10.42	3/63	
3.5	29.91	0.00	0.00	1.99	3.99	0.00	0.00	0.00	9.97	23.93	0.00	1.99	0.00	9.97	23.93	3.99	1.99	5.98	3.99	13.96	632.02	51.84	317	5.35	3/32
4.5	5.45	0.00	1.82	5.45	0.00	0.00	0.00	0.00	12.71	12.71	0.00	0.00	0.00	5.45	21.79	7.26	5.45	9.08	3.63	21.79	546.65	43.59	301	8.81	1/16
5.5	6.73	0.00	0.00	2.24	2.24	0.00	2.24	0.00	6.73	26.92	0.00	0.00	0.00	29.16	0.00	0.00	8.97	4.49	24.68	601.19	29.16	268	9.51	3/64	
6.5	0.00	0.00	0.00	9.89	1.98	0.00	1.98	0.00	13.85	17.81	0.00	0.00	0.00	29.68	1.98	0.00	3.96	0.00	25.72	542.07	17.81	274	6.47	5/64	
7.5	3.94	0.00	0.00	1.97	0.00	0.00	1.97	0.00	19.72	33.53	0.00	0.00	0.00	1.97	35.50	0.00	0.00	1.97	0.00	41.42	554.21	37.47	281	12.98	5/128
8.5	0.00	0.00	0.00	2.03	2.03	0.00	4.06	0.00	6.10	38.60	0.00	0.00	0.00	4.06	28.44	4.06	2.03	4.06	6.10	48.76	540.44	24.38	266	10.50	3/64
9.5	0.00	0.00	0.00	7.77	3.89	0.00	1.94	0.00	21.37	27.20	0.00	0.00	0.00	1.94	27.20	1.94	5.83	0.00	0.00	36.92	514.88	23.32	265	5.49	3/32
10.5	0.00	0.00	1.76	5.27	5.27	1.76	0.00	3.52	1.76	33.41	0.00	0.00	0.00	5.27	26.37	14.07	8.79	1.76	5.27	21.10	590.77	33.41	336	14.56	5/128
11.5	0.00	0.00	1.91	3.82	11.46	1.91	0.00	0.00	9.55	36.29	3.82	0.00	0.00	1.91	26.74	11.46	1.91	11.46	5.73	21.01	540.50	42.02	283	11.17	3/64
12.5	2.86	0.00	0.00	7.16	2.86	0.00	0.00	1.43	0.00	32.95	0.00	0.00	0.00	2.86	12.89	0.00	2.86	1.43	1.43	10.03	406.80	25.78	284	11.17	1/16
13.5	0.00	0.00	0.00	2.70	8.10	0.00	0.00	0.00	0.00	27.00	0.00	0.00	0.00	5.40	6.75	1.35	1.35	0.00	2.70	6.75	348.35	29.70	258	7.90	3/32
14.5	0.00	0.00	0.00	10.26	5.13	0.00	0.00	3.42	0.00	44.44	0.00	1.71	0.00	3.42	8.55	0.00	6.84	1.71	1.71	27.35	423.93	27.35	248	12.48	3/64
15.5	0.00	0.00	0.00	4.11	0.00	0.00	0.00	0.00	34.23	0.00	4.11	0.00	1.37	1.37	0.00	15.06	1.37	0.00	39.71	525.80	43.82	384	15.58	3/64	
16.5	0.00	0.00	0.00	4.96	4.96	0.00	0.00	0.00	0.00	39.69	0.00	3.31	0.00	0.00	9.92	3.31	9.92	0.00	3.31	14.88	489.51	29.77	296	12.90	3/64
17.5	1.34	0.00	0.00	6.71	2.68	0.00	0.00	0.00	0.00	48.32	0.00	0.00	0.00	4.03	1.34	4.03	6.71	1.34	6.71	437.58	42.95	326	11.92	1/16	
18.5	0.00	0.72	0.00	1.43	3.58	0.00	0.00	0.72	0.00	37.99	0.00	0.72	0.72	2.15	1.43	0.00	1.43	2.87	1.43	0.00	273.84	18.64	382	5.58	1/4

Table A 3.4 Paleontological data set of core SO136-147BX. All species are given in spec./g.

Table A 3.4 Paleontological data set of core SO136-147BX (continued). All species are given in spec./g.

0.5 depth (cm bsf)	<i>Heteroplea dumtemplei</i>																	
0.5	12.58	0.00	0.00	<i>Lagena globosa</i>														
1.5	8.02	0.00	8.02	0.00	0.00	<i>Lagena gracilis</i>												
2.5	7.13	0.00	2.85	0.00	0.00	0.00	<i>Lagena hispidula</i>											
3.5	4.22	2.11	2.11	0.00	0.00	0.00	<i>Lagena semilineata</i>											
4.5	6.50	0.00	3.25	0.00	0.00	0.00	<i>Lagena setigera</i>											
5.5	14.95	0.00	5.98	0.00	2.99	5.98	0.00	0.00	8.97	0.00	0.00	<i>Laticardina pauperata</i>						
6.5	6.32	0.00	12.65	1.58	0.00	0.00	0.00	0.00	3.16	0.00	1.58	<i>Lenticulina rotulata</i>						
7.5	11.13	0.00	5.57	0.00	0.00	0.00	0.00	0.00	16.70	0.00	0.00	<i>Melonis paleaeum</i>						
8.5	14.12	0.00	9.41	0.00	0.00	0.00	0.00	0.00	11.76	2.35	2.35	<i>Melonis pomphiloides</i>						
9.5	5.10	0.00	2.55	0.00	0.00	0.00	0.00	0.00	7.64	1.27	0.00	<i>Melonis zandami</i>						
10.5	3.60	0.00	3.60	1.80	0.00	0.00	0.00	1.80	5.41	1.80	3.60	<i>Miliammina arenacea</i>						
11.5	10.58	0.00	3.97	0.00	0.00	1.32	0.00	0.00	9.26	1.32	0.00	<i>Nodophthalidium tibia</i>						

Table A 3.4 Paleontological data set of core SO136-147BX (continued). All species are given in spec./g.

0.5 depth (cm bsf)	<i>Siphonotextularia rothauseni</i>																	
0.5	10.06	10.06	<i>Pulenia bulloides</i>															
1.5	14.04	2.01	5.03	0.00	<i>Pyrgo murinina</i>													
2.5	1.43	2.85	1.43	7.13	0.00	<i>Pyrgo oblonga</i>												
3.5	6.33	10.55	0.00	4.22	2.11	0.00	14.78	2.11	0.00	1.43	0.00	<i>Quinqueloculina</i> spp						
4.5	8.13	8.13	1.63	8.13	0.00	1.63	6.50	8.13	0.00	1.63	0.00	<i>Reusella</i> sp						
5.5	11.96	5.98	2.99	0.00	2.99	0.00	20.93	2.99	2.99	0.00	0.00	<i>Siphonotextularia rothauseni</i>						
6.5	11.07	6.32	1.58	4.74	1.58	1.58	7.91	1.58	4.74	0.00	0.00	<i>Suggrunda porosa</i>						
7.5	16.70	16.70	2.78	5.57	2.78	2.78	22.26	0.00	0.00	0.00	0.00	<i>Textularia truncata</i>						
8.5	0.00	4.71	0.00	9.41	9.41	0.00	18.82	2.35	7.06	0.00	0.00	<i>Trifarina angulosa</i>						
9.5	3.82	5.10	0.00	0.00	11.46	1.27	10.19	1.27	1.27	0.00	1.27	<i>Triloculina tricarinata</i>						
10.5	19.82	9.01	1.80	1.80	3.60	0.00	7.21	5.41	1.80	0.00	0.00	<i>Uvigerina auberiana</i>						
11.5	11.90	2.64	0.00	3.97	5.29	0.00	10.58	3.97	1.32	1.32	0.00	<i>Uvigerina peregrina</i>						
													Fragments of agglutinating spp.					
													372.33	All species (spec./g)	0.00	Clastic sediments / g	148	3.18
													268.67	0.00	134	3.99	1/8	
													218.18	1.43	153	5.61	1/8	
													236.41	0.00	112	3.79	1/8	
													221.14	1.63	136	4.92	1/8	
													26.92	2.99	113	5.35	1/16	
													337.94	5.98	113	5.35	1/16	
													237.44	3.16	167	5.06	1/8	
													246.03	3.16	125	5.75	1/16	
													347.83	2.78	118	6.8	1/16	
													277.65	2.35	163	6.28	1/8	
													207.64	1.27	162	4.44	1/8	
													291.89	0.00	174	6.05	1/8	
													230.08	7.93	174	6.05	1/8	

*Pseudorotalia gainardi**Parafissurina ovata**Oolina melo**Ornatosalis umbonatus**Osangularia culta**Nonionella indea**Nonionellina labradoricus**Nuttallides umbofer**Oolina caudigera**Oolina hexagona**Oridosalis sp**Parafissurina gainardi**Pseudorotalia gainardi*

Table A 3.5 Paleontological data set of core SO136-161BX. All species are given in spec./g.

depth (cm bs)	<i>Amphicyrta</i> sp	<i>Bolivina pacifica</i>	<i>Bulimina fossa</i>	<i>Bulimina aculeata</i>	<i>Caribinerella polystoma</i>	<i>Cassidulina laevigata</i>	<i>Cibicidoides fletcheri</i>	<i>Cibicidoides inawagensis</i>	<i>Cibicidoides lobatus</i>	<i>Cibicidoides mundulus</i>	<i>Cibicidoides wuellerstorfi</i>	<i>Cribostomoides subglobosum</i>	<i>Cruciloculina triangularis</i>	<i>Cyclammina trullissata</i>	<i>Dentalina baggi</i>	<i>Dentalina communialis</i>	<i>Dentalina inornata</i>	<i>Ehrenbergina glabra</i>	<i>Epistominella exigua</i>	<i>Fissurina abyssicola</i>	<i>Fissurina laevigata</i>	<i>Fissurina marginata</i>	<i>Fissurina orbigniana</i>	<i>Fissurina serrata</i>	<i>Fissurina wiesneri</i>	<i>Globocassidolina subglobosa</i>	<i>Gyroidina neosoldanii</i>	<i>Gyroides nipponicus</i>	<i>Haplophragmoides canariensis</i>	<i>Heteroplea dutemplei</i>	
0.5	0.00	2.20	0.00	0.00	0.00	0.00	0.00	0.00	2.20	0.00	0.00	0.00	0.00	0.00	0.00	0.00	0.00	0.00	0.00	0.00	0.00	0.00	0.00	0.00	0.00	0.00	0.00	0.00	0.00		
1.5	0.00	0.00	0.00	0.00	0.00	0.00	0.00	0.00	4.26	0.00	0.00	0.00	2.60	5.19	5.19	7.79	0.00	0.00	2.60	0.00	0.00	0.00	0.00	0.00	0.00	0.00	0.00	0.00	0.00		
2.5	0.00	2.60	0.00	0.00	0.00	0.00	0.00	0.00	0.00	2.60	5.19	5.19	7.79	0.00	0.00	2.60	0.00	0.00	2.61	2.61	2.61	91.21	0.00	5.21	2.61	2.61	0.00	0.00	5.19		
3.5	0.00	5.21	0.00	0.00	0.00	0.00	0.00	0.00	0.00	0.00	2.61	0.00	0.00	0.00	2.61	2.61	2.61	2.61	0.00	0.00	0.00	0.00	0.00	0.00	0.00	0.00	0.00	0.00	23.45		
4.5	2.08	2.08	0.00	0.00	0.00	0.00	0.00	0.00	0.00	2.08	10.42	4.17	4.17	0.00	0.00	0.00	0.00	0.00	0.00	0.00	0.00	0.00	0.00	0.00	0.00	0.00	0.00	0.00	10.42		
5.5	0.00	2.45	0.00	0.00	0.00	0.00	2.45	0.00	2.45	4.91	2.45	7.36	0.00	0.00	0.00	0.00	0.00	0.00	0.00	0.00	0.00	0.00	0.00	0.00	0.00	0.00	0.00	0.00	7.36		
6.5	0.00	0.00	0.00	0.00	0.00	0.00	0.00	0.00	0.00	6.12	10.20	6.12	0.00	0.00	0.00	0.00	0.00	0.00	0.00	0.00	0.00	0.00	0.00	0.00	0.00	0.00	0.00	0.00	20.41		
7.5	0.00	4.42	0.00	0.00	0.00	2.21	2.21	0.00	4.42	6.63	6.63	4.42	0.00	0.00	4.42	0.00	0.00	0.00	0.00	0.00	0.00	0.00	0.00	0.00	0.00	0.00	0.00	0.00	19.89		
8.5	5.13	0.00	1.28	0.00	0.00	0.00	2.56	0.00	2.56	6.41	11.54	2.56	0.00	0.00	1.28	0.00	0.00	0.00	52.56	2.56	1.28	1.28	3.85	0.00	5.13	3.85	2.56	0.00	16.67		
9.5	2.19	2.19	0.00	0.00	0.00	0.00	0.00	0.00	2.19	8.74	6.56	2.19	0.00	0.00	0.00	0.00	0.00	0.00	67.76	0.00	0.00	2.19	0.00	0.00	0.00	13.11	4.37	6.56	0.00	13.11	
10.5	5.25	3.50	0.00	0.00	0.00	0.00	1.75	0.00	1.75	3.50	5.25	3.50	0.00	0.00	0.00	0.00	0.00	0.00	78.69	1.75	1.75	1.75	0.00	0.00	6.99	3.50	0.00	0.00	13.99		
11.5	2.03	2.03	0.00	0.00	0.00	4.06	0.00	2.03	12.18	8.12	0.00	0.00	0.00	0.00	2.03	0.00	0.00	0.00	64.97	0.00	0.00	0.00	0.00	0.00	0.00	0.00	0.00	0.00	14.21		
12.5	5.11	0.00	0.00	1.70	0.00	3.40	0.00	0.00	3.40	6.81	1.70	1.70	0.00	0.00	1.70	0.00	0.00	0.00	73.19	0.00	0.00	0.00	1.70	1.70	0.00	11.91	1.70	0.00	0.00	32.34	
13.5	1.59	4.77	0.00	0.00	0.00	6.36	0.00	0.00	7.95	1.59	1.59	0.00	0.00	0.00	0.00	49.30	0.00	0.00	0.00	49.30	0.00	0.00	3.18	1.59	0.00	0.00	6.36	0.00	3.18	0.00	17.50
14.5	1.41	1.41	0.00	0.00	0.00	4.22	0.00	2.81	9.84	5.62	2.81	0.00	0.00	0.00	0.00	37.96	0.00	0.00	0.00	37.96	0.00	0.00	0.00	1.41	0.00	0.00	5.62	0.00	0.00	0.00	15.47
15.5	2.56	2.56	0.00	0.00	1.28	0.00	0.00	0.00	7.69	3.85	6.41	0.00	0.00	1.28	0.00	0.00	0.00	39.74	0.00	0.00	0.00	2.56	0.00	0.00	0.00	7.69	3.85	0.00	0.00	6.41	
16.5	1.69	0.00	0.00	1.69	0.00	1.69	0.00	0.00	8.47	11.86	0.00	0.00	0.00	1.69	0.00	0.00	0.00	62.71	0.00	3.39	5.08	0.00	0.00	0.00	0.00	6.78	0.00	1.69	0.00	13.56	
17.5	0.00	0.00	2.02	0.00	0.00	4.03	0.00	0.00	6.05	2.02	2.02	2.02	0.00	0.00	0.00	0.00	46.35	0.00	2.02	4.03	0.00	2.02	0.00	0.00	0.00	2.02	4.03	0.00	0.00	26.20	
18.5	4.89	0.00	0.00	1.63	0.00	1.63	0.00	0.00	1.63	3.26	0.00	0.00	0.00	0.00	0.00	0.00	0.00	47.30	0.00	0.00	6.52	6.52	0.00	0.00	13.05	3.26	1.63	0.00	11.42		
19.5	1.59	1.59	0.00	0.00	0.00	1.59	0.00	0.00	1.59	7.95	1.59	0.00	0.00	0.00	0.00	41.35	0.00	1.59	1.59	0.00	0.00	0.00	0.00	11.13	4.77	0.00	0.00	14.31			
20.5	1.33	1.33	0.00	0.00	0.00	1.33	0.00	0.00	7.97	1.33	5.32	1.33	0.00	2.66	0.00	0.00	1.33	45.18	0.00	0.00	3.99	3.99	0.00	0.00	11.96	2.66	2.66	3.99	21.26		
21.5	3.57	0.00	0.00	0.00	0.00	1.19	0.00	0.00	7.14	5.95	2.38	0.00	0.00	0.00	0.00	39.29	0.00	0.00	2.38	1.19	0.00	0.00	13.10	4.76	2.38	1.19	15.48				
22.5	1.01	1.01	0.00	0.00	0.00	2.02	0.00	0.00	6.05	3.02	2.02	0.00	0.00	0.00	0.00	40.30	0.00	0.00	1.01	0.00	0.00	0.00	0.00	15.11	1.01	3.02	0.00	9.07			
23.5	2.42	2.42	0.00	0.00	1.21	0.00	0.00	2.42	1.21	10.91	0.00	0.00	0.00	0.00	0.00	0.00	0.00	43.64	0.00	1.21	1.21	3.64	0.00	0.00	3.64	1.21	1.21	0.00	16.97		
24.5	0.00	1.58	0.00	0.00	0.00	3.17	0.00	1.58	3.17	4.75	0.00	0.00	0.00	0.00	0.00	0.00	0.00	3.17	52.28	0.00	1.58	1.58	0.00	0.00	0.00	7.92	6.34	1.58	1.58	15.84	
25.5	2.12	0.00	0.00	2.12	0.00	8.47	0.00	0.00	6.35	6.35	0.00	0.00	0.00	0.00	0.00	0.00	0.00	4.23	63.49	2.12	4.23	8.47	2.12	2.12	0.00	2.12	0.00	0.00	10.58		
26.5	2.37	4.74	0.00	0.00	0.00	4.74	2.37	0.00	4.74	4.74	0.00	2.37	0.00	0.00	0.00	0.00	45.04	0.00	2.37	7.11	2.37	0.00	0.00	0.00	14.22	0.00	2.37	0.00	23.70		
27.5	1.66	4.97	0.00	0.00	0.00	3.31	0.00	0.00	4.97	9.94	4.97	0.00	0.00	0.00	0.00	3.31	49.69	0.00	0.00	1.66	1.66	0.00	0.00	1.66	18.22	0.00	0.00	0.00	31.47		

Table A 3.5 Paleontological data set of core SO136-161BX (continued . All species are given in spec./g.

depth (cm bst)	<i>Lagenia gracilima</i>	<i>Lagenia gracilis</i>	<i>Lagenia hispidula</i>	<i>Lagenia semilineata</i>	<i>Lagenia setigera</i>	<i>Lagenia sp2</i>	<i>Lagenia striata</i>	<i>Lagenia substriata</i>	<i>Laticarinina pauperata</i>	<i>Lenticulina rotulata</i>	<i>Melonis baileanum</i>	<i>Melonis pomphiloides</i>	<i>Melonis zandami</i>	<i>Miliammina arenacea</i>	<i>Nodophthalidium tibia</i>	<i>Nonionella iridea</i>	<i>Nonionellina labradoricus</i>	<i>Nuttallides umbonifer</i>	<i>Oolina borealis</i>	<i>Oolina caudigera</i>	<i>Oolina hexagona</i>	<i>Oridosalis sp</i>	<i>Oridosalis umbonatus</i>	<i>Osangularia culta</i>	<i>Parafissurina ovata</i>	<i>Planulina ariminensis</i>	<i>Pseudorotalia gaimardi</i>	<i>Pulaniella asymmetrica</i>	<i>Pulenia bulboides</i>	<i>Pulenia quinqueloba</i>		
0.5	0.00	0.00	2.20	0.00	4.40	0.00	0.00	0.00	8.79	28.57	17.58	0.00	8.79	0.00	0.00	0.00	26.37	0.00	2.20	2.20	4.40	0.00	2.20	0.00	0.00	0.00	6.59	6.59	4.40			
1.5	0.00	4.26	0.00	0.00	2.13	0.00	0.00	0.00	4.26	34.04	31.91	14.89	2.13	0.00	0.00	0.00	0.00	12.77	0.00	2.13	0.00	8.51	12.77	0.00	0.00	0.00	0.00	0.00	8.51	4.26	4.26	
2.5	2.60	2.60	0.00	2.60	0.00	0.00	0.00	2.60	0.00	7.79	51.95	33.77	7.79	0.00	0.00	0.00	2.60	12.99	2.60	5.19	0.00	7.79	10.39	0.00	0.00	0.00	0.00	0.00	5.19	7.79	7.79	
3.5	0.00	2.61	2.61	2.61	0.00	0.00	0.00	2.61	0.00	7.82	41.69	23.45	2.61	0.00	0.00	0.00	0.00	28.66	0.00	7.82	0.00	5.21	10.42	0.00	2.61	0.00	0.00	5.21	2.61	2.61		
4.5	0.00	0.00	0.00	0.00	2.08	0.00	0.00	0.00	0.00	4.17	39.58	35.42	8.33	0.00	0.00	0.00	0.00	8.33	0.00	0.00	0.00	2.08	12.50	0.00	6.25	0.00	0.00	6.25	8.33	8.33		
5.5	0.00	0.00	2.45	0.00	0.00	0.00	0.00	0.00	0.00	4.91	26.99	29.45	0.00	4.91	0.00	0.00	2.45	0.00	12.27	0.00	4.91	0.00	4.91	19.63	0.00	4.91	0.00	0.00	12.27	12.27	7.36	
6.5	0.00	2.04	0.00	0.00	2.04	0.00	0.00	0.00	0.00	2.04	53.06	16.33	2.04	0.00	0.00	0.00	0.00	0.00	0.00	0.00	0.00	2.04	8.16	0.00	6.12	0.00	0.00	6.12	6.12	8.16		
7.5	0.00	0.00	0.00	4.42	0.00	0.00	0.00	0.00	0.00	2.21	30.94	26.52	0.00	0.00	0.00	0.00	0.00	2.21	19.89	0.00	4.42	0.00	2.21	11.05	0.00	0.00	0.00	0.00	0.00	4.42	6.63	2.21
8.5	0.00	1.28	0.00	1.28	0.00	0.00	0.00	0.00	0.00	6.41	21.79	2.56	1.28	0.00	1.28	0.00	0.00	0.00	7.69	0.00	5.13	0.00	0.00	3.85	3.85	0.00	2.56	0.00	0.00	3.85	5.13	2.56
9.5	0.00	2.19	0.00	0.00	2.19	0.00	0.00	0.00	0.00	6.56	24.04	17.49	2.19	0.00	0.00	0.00	2.19	0.00	15.30	0.00	8.74	0.00	0.00	8.74	0.00	4.37	0.00	0.00	13.11	10.93	2.19	
10.5	0.00	1.75	0.00	0.00	0.00	0.00	0.00	0.00	0.00	6.99	38.47	19.23	0.00	0.00	0.00	0.00	5.25	0.00	8.74	0.00	3.50	0.00	6.99	0.00	3.50	0.00	0.00	5.25	8.74	3.50		
11.5	0.00	0.00	0.00	0.00	0.00	0.00	0.00	0.00	0.00	2.03	30.46	20.30	0.00	0.00	0.00	0.00	2.03	0.00	8.12	0.00	0.00	0.00	0.00	10.15	0.00	2.03	0.00	0.00	6.09	8.12	2.03	
12.5	1.70	0.00	0.00	1.70	1.70	0.00	0.00	0.00	0.00	5.11	34.04	22.13	1.70	1.70	0.00	1.70	0.00	22.13	0.00	3.40	0.00	1.70	15.32	0.00	5.11	0.00	0.00	8.51	10.21	1.70		
13.5	0.00	0.00	0.00	3.18	0.00	0.00	0.00	0.00	0.00	1.59	36.58	23.86	1.59	3.18	0.00	0.00	0.00	9.54	0.00	0.00	0.00	7.95	12.72	0.00	1.59	1.59	0.00	6.36	7.95	0.00		
14.5	0.00	2.81	0.00	0.00	2.81	0.00	0.00	0.00	0.00	7.03	21.09	21.09	1.41	0.00	0.00	1.41	1.41	8.44	0.00	8.44	0.00	0.00	11.25	0.00	1.41	0.00	1.41	5.62	8.44	1.41		
15.5	0.00	1.28	0.00	0.00	1.28	0.00	0.00	0.00	0.00	1.28	24.36	17.95	2.56	1.28	0.00	0.00	5.13	2.56	0.00	1.28	1.28	0.00	8.97	0.00	1.28	0.00	0.00	7.69	6.41	2.56		
16.5	1.69	3.39	1.69	0.00	1.69	0.00	0.00	0.00	0.00	1.69	20.34	45.76	5.08	0.00	0.00	13.56	3.39	5.08	0.00	3.39	0.00	0.00	1.69	0.00	3.39	0.00	0.00	10.17	8.47	1.69		
17.5	0.00	0.00	0.00	0.00	0.00	0.00	0.00	0.00	0.00	4.03	34.26	32.24	2.02	0.00	0.00	6.05	0.00	20.15	0.00	4.03	0.00	0.00	10.08	0.00	2.02	0.00	0.00	10.08	10.08	0.00		
18.5	0.00	1.63	0.00	0.00	0.00	1.63	1.63	0.00	3.26	27.73	27.73	4.89	0.00	0.00	1.63	0.00	0.00	1.63	0.00	1.63	0.00	6.52	0.00	0.00	0.00	0.00	0.00	8.15	6.52	1.63		
19.5	0.00	0.00	0.00	0.00	0.00	0.00	0.00	0.00	1.59	0.00	0.00	27.04	31.81	3.18	0.00	0.00	4.77	0.00	1.59	0.00	4.77	0.00	4.77	14.31	0.00	4.77	0.00	0.00	7.95	9.54	0.00	
20.5	0.00	1.33	0.00	1.33	1.33	0.00	0.00	0.00	1.33	21.26	26.58	5.32	1.33	0.00	2.66	1.33	1.33	0.00	0.00	0.00	0.00	11.96	0.00	3.99	0.00	0.00	10.63	5.32	1.33			
21.5	0.00	2.38	0.00	0.00	0.00	0.00	0.00	1.19	1.19	2.38	28.57	39.29	7.14	4.76	0.00	4.76	0.00	9.52	0.00	0.00	0.00	0.00	5.95	0.00	3.57	0.00	0.00	5.95	10.71	0.00		
22.5	0.00	1.01	0.00	0.00	2.02	0.00	0.00	0.00	0.00	1.01	24.18	25.19	3.02	2.02	0.00	5.04	0.00	4.03	0.00	3.02	1.01	0.00	4.03	0.00	2.02	0.00	0.00	6.05	12.09	1.01		
23.5	0.00	0.00	0.00	1.21	1.21	0.00	0.00	1.21	0.00	0.00	36.36	27.88	1.21	3.64	0.00	4.85	0.00	4.85	0.00	1.21	0.00	0.00	6.06	0.00	2.42	0.00	0.00	1.21	9.70	0.00		
24.5	0.00	4.75	1.58	0.00	1.58	0.00	0.00	0.00	1.58	34.85	15.84	0.00	0.00	0.00	4.75	0.00	7.92	0.00	1.58	3.17	0.00	6.34	0.00	0.00	1.58	0.00	3.17	9.50	15.84			
25.5	0.00	6.35	0.00	4.23	0.00	0.00	0.00	0.00	0.00	19.05	23.28	0.00	2.12	0.00	2.12	0.00	2.12	0.00	2.12	0.00	0.00	6.35	2.12	0.00	0.00	0.00	0.00	0.00	19.05	12.70		
26.5	0.00	0.00	0.00	2.37	0.00	0.00	0.00	0.00	2.37	49.78	9.48	2.37	0.00	0.00	0.00	0.00	2.37	7.11	0.00	0.00	2.37	0.00	7.11	0.00	4.74	0.00	0.00	9.48	18.96	11.85		
27.5	0.00	1.66	0.00	4.97	0.00	0.00	0.00	0.00	0.00	36.44	6.63	1.66	0.00	0.00	1.66	3.31	3.31	0.00	3.31	0.00	1.66	0.00	8.28	0.00	3.31	0.00	0.00	9.94	19.88	1.66		

Table A 3.5 Paleontological data set of core SO135-161BX (continued). All species are given in spec./g.

depth (cm bsf)	Pygo murtinna	Pygo oblonga	Pygo rotalaria	Pyrolina cylindroides	Pyro serrata	Pyro spp.	Pyro micacaeus	Reophax spirifilifer	Reussella sp	Ehrenbergina mestayeri	Rutherfordia sp	Sigmolopsis schubumbergeri	Siphonotextularia rostratensis	Spiriloculina dispansis	Tectularia truncata	Tosala hanzawai	Trifarina angulosa	Trioculina tricantata	Uvigerina aubeariana	Uvigerina peregrina	Uvigerina pigmea	Furciferia contemplicata	All species (spec./g)	Clastic sediments (g)	Σ (counts)	Weight of sample (g)	factor of split				
0.5	0.00	8.79	4.40	4.40	15.38	0.00	4.40	0.00	0.00	8.79	0.00	0.00	2.20	0.00	0.00	2.20	15.38	0.00	0.00	10.99	30.77	4.40	0.00	285.71	654.95	8.79	298	1.82	1/4		
1.5	0.00	14.89	2.13	2.13	6.38	0.00	8.51	0.00	0.00	2.13	2.13	0.00	14.89	0.00	6.38	0.00	23.40	0.00	0.00	2.13	29.79	0.00	0.00	187.23	587.23	2.13	276	1.88	1/4		
2.5	0.00	5.19	5.19	0.00	10.39	0.00	7.79	0.00	0.00	12.99	0.00	0.00	5.19	5.19	2.60	0.00	10.39	0.00	7.79	23.38	38.96	2.60	0.00	135.06	594.81	5.19	229	3.08	1/8		
3.5	0.00	10.42	0.00	0.00	7.82	0.00	2.61	0.00	0.00	10.42	0.00	0.00	5.21	0.00	2.61	2.61	18.24	0.00	0.00	2.61	7.82	33.88	0.00	0.00	104.23	531.60	7.82	204	3.07	1/8	
4.5	0.00	10.42	2.08	0.00	8.33	0.00	14.58	6.25	0.00	6.25	0.00	0.00	10.42	0.00	0.00	0.00	27.08	2.08	0.00	10.42	27.08	6.25	0.00	222.92	629.17	0.00	302	1.92	1/4		
5.5	0.00	12.27	0.00	2.45	14.72	0.00	24.54	9.82	0.00	0.00	4.91	0.00	0.00	4.91	0.00	2.45	2.45	0.00	24.54	0.00	4.91	2.45	36.81	0.00	0.00	184.05	601.23	9.82	245	3.26	1/8
6.5	0.00	4.08	0.00	2.04	16.33	0.00	22.45	8.16	0.00	0.00	2.04	0.00	0.00	8.16	0.00	4.08	0.00	8.16	0.00	6.12	6.12	36.73	0.00	0.00	102.04	467.35	2.04	229	1.96	1/4	
7.5	0.00	11.05	4.42	2.21	8.84	0.00	8.84	2.21	0.00	0.00	0.00	0.00	0.00	8.84	4.42	0.00	0.00	0.00	0.00	2.21	0.00	24.31	0.00	0.00	68.51	400.00	15.47	181	3.62	1/8	
8.5	1.28	6.41	2.56	8.97	3.85	10.26	2.56	1.28	0.00	2.56	1.28	0.00	5.13	1.28	1.28	0.00	12.82	0.00	0.00	5.13	44.87	3.85	0.00	42.31	353.85	7.69	276	3.12	1/4		
9.5	0.00	2.19	4.37	0.00	6.56	4.37	8.74	0.00	0.00	0.00	0.00	0.00	6.56	2.19	2.19	0.00	15.30	0.00	6.56	0.00	54.64	0.00	0.00	63.39	428.42	2.19	196	3.66	1/8		
10.5	0.00	5.25	5.25	0.00	3.50	0.00	6.99	0.00	1.75	0.00	5.25	0.00	0.00	3.50	1.75	0.00	0.00	15.74	0.00	1.75	5.25	40.22	0.00	0.00	31.48	377.70	5.25	216	3.05	3/16	
11.5	4.06	4.06	2.03	2.03	12.18	12.18	8.12	0.00	2.03	0.00	0.00	0.00	6.09	0.00	0.00	0.00	22.34	0.00	4.06	6.09	40.61	0.00	0.00	46.70	389.85	32.49	192	3.94	1/8		
12.5	0.00	5.11	3.40	0.00	10.21	10.21	10.21	0.00	1.70	0.00	0.00	1.70	0.00	3.40	3.40	1.70	0.00	11.91	0.00	1.70	6.81	27.23	0.00	0.00	37.45	423.83	8.51	249	4.70	1/8	
13.5	0.00	1.59	1.59	4.77	11.13	1.59	6.36	1.59	0.00	0.00	4.77	0.00	0.00	0.00	0.00	0.00	0.00	19.09	1.59	0.00	1.59	41.35	0.00	0.00	41.35	361.03	7.95	227	5.03	1/8	
14.5	1.41	1.41	7.03	0.00	9.84	1.41	7.03	0.00	1.41	0.00	5.62	0.00	0.00	1.41	2.81	0.00	18.28	1.41	0.00	0.00	37.96	0.00	0.00	40.77	331.81	26.71	236	5.69	1/8		
15.5	1.28	0.00	0.00	1.28	3.85	1.28	3.85	0.00	1.28	0.00	6.41	0.00	0.00	3.85	2.56	2.56	0.00	8.97	0.00	0.00	3.85	28.21	1.28	0.00	26.92	270.51	8.97	211	4.16	3/16	
16.5	1.69	1.69	1.69	0.00	5.08	3.39	6.78	0.00	0.00	0.00	6.78	0.00	1.69	0.00	1.69	0.00	0.00	22.03	1.69	1.69	15.25	32.20	0.00	0.00	45.76	401.69	11.86	237	4.72	1/8	
17.5	2.02	2.02	0.00	0.00	10.08	6.05	10.08	2.02	0.00	0.00	2.02	0.00	0.00	4.03	0.00	0.00	0.00	20.15	2.02	4.03	12.09	40.30	0.00	6.05	16.12	378.84	6.05	188	3.97	1/8	
18.5	0.00	1.63	4.89	1.63	4.89	1.63	4.89	0.00	0.00	0.00	6.52	0.00	0.00	3.26	3.26	1.63	0.00	17.94	0.00	8.15	4.89	35.88	0.00	6.52	27.73	334.35	9.79	205	3.27	3/16	
19.5	0.00	1.59	3.18	0.00	3.18	1.59	4.77	0.00	0.00	0.00	3.18	0.00	0.00	1.59	0.00	0.00	0.00	6.36	0.00	1.59	3.18	20.68	0.00	1.59	39.76	299.01	14.31	188	5.03	1/8	
20.5	2.66	1.33	1.33	0.00	1.33	0.00	2.66	0.00	0.00	0.00	5.32	0.00	0.00	9.30	0.00	0.00	0.00	17.28	1.33	5.32	2.66	22.59	0.00	1.33	33.22	325.58	22.59	245	6.02	1/8	
21.5	0.00	3.57	2.38	0.00	1.19	1.19	3.57	0.00	0.00	0.00	3.57	0.00	0.00	3.57	1.19	0.00	0.00	9.52	0.00	1.19	5.95	20.24	3.57	1.19	34.52	323.81	15.48	272	3.36	1/4	
22.5	2.02	5.04	3.02	1.01	3.02	0.00	4.03	1.01	3.02	0.00	9.07	0.00	0.00	4.03	0.00	1.01	0.00	11.08	2.02	0.00	5.04	8.06	1.01	0.00	0.00	244.84	16.12	243	3.97	1/4	
23.5	2.42	1.21	9.70	0.00	4.85	1.21	3.64	0.00	1.21	0.00	7.27	1.21	0.00	4.85	0.00	0.00	0.00	9.70	1.21	121	8.48	13.33	0.00	1.21	15.76	284.85	6.06	235	4.40	3/16	
24.5	1.58	9.50	1.58	0.00	7.92	0.00	7.92	0.00	0.00	0.00	11.09	1.58	0.00	3.17	1.58	3.17	0.00	7.92	3.17	1.58	15.84	19.01	0.00	0.00	9.50	326.34	22.18	206	5.05	1/8	
25.5	0.00	6.35	4.23	0.00	4.23	0.00	6.35	0.00	0.00	0.00	12.70	2.12	0.00	6.35	0.00	2.12	0.00	19.05	2.12	0.00	0.00	25.40	0.00	0.00	16.93	340.74	31.75	161	3.78	1/8	
26.5	0.00	0.00	4.74	0.00	7.11	0.00	9.48	0.00	0.00	0.00	11.85	0.00	0.00	4.74	2.37	0.00	0.00	16.59	0.00	11.85	0.00	28.44	0.00	0.00	14.22	365.04	7.11	154	6.75	1/16	
27.5	1.66	11.59	3.31	1.66	4.97	0.00	8.28	0.00	0.00	0.00	9.94	0.00	0.00	4.97	0.00	0.00	0.00	19.88	1.66	1.66	6.63	4.97	0.00	6.63	4.97	337.89	21.53	204	4.83	1/8	

Table A 3.6 Paleontological data set of core SO136-165BX. All species are given in spec./g.

depth (cm bsf)	<i>Amphicoryna scalaris</i>	<i>Bagatella inconspicua</i>	<i>Bolivina pacifica</i>	<i>Bulimina alataensis</i>	<i>Caribicella polystoma</i>	<i>Cassidulina legulata</i>	<i>Cassidulina laevigata</i>	<i>Cibicidoides fletcheri</i>	<i>Cibicidoides inawagaensis</i>	<i>Cibicidoides lobatus</i>	<i>Cibicidoides mundulus</i>	<i>Cibicidoides sp</i>	<i>Cribrostomoides wuerstorfi</i>	<i>Cribrostomoides subglobosum</i>	<i>Crucilucina triangularia</i>	<i>Dentalina baggi</i>	<i>Dentalina communialis</i>	<i>Dentalina inornata</i>	<i>Dentalina sp1</i>	<i>Eggerella scabra</i>	<i>Ehrenbergina glabra</i>	<i>Ehrenbergina mestayeri</i>	<i>Epistominella exigua</i>	<i>Fissurina abyssicola</i>	<i>Fissurina laevigata</i>	<i>Fissurina marginata</i>	<i>Fissurina orbignyana</i>	<i>Fissurina serra</i>	<i>Fissurina wiessneri</i>
0.5	8.16	0.00	8.16	0.00	0.00	0.00	0.00	0.00	0.00	32.65	8.16	0.00	24.49	32.65	0.00	0.00	0.00	0.00	0.00	0.00	89.80	8.16	0.00	0.00	0.00	0.00	0.00		
1.5	8.16	0.00	0.00	0.00	0.00	0.00	0.00	24.49	0.00	32.65	0.00	0.00	73.47	32.65	0.00	0.00	0.00	0.00	14.29	0.00	7.14	50.00	14.29	0.00	7.14	0.00	0.00	0.00	
2.5	0.00	0.00	0.00	0.00	0.00	0.00	0.00	0.00	0.00	35.71	7.14	0.00	50.00	35.71	0.00	0.00	0.00	0.00	0.00	0.00	0.00	0.00	0.00	0.00	0.00	0.00	0.00	0.00	
3.5	0.00	0.00	0.00	0.00	0.00	0.00	0.00	0.00	0.00	49.12	0.00	0.00	56.14	42.11	0.00	0.00	0.00	0.00	14.04	0.00	0.00	0.00	77.19	0.00	0.00	0.00	0.00	0.00	
4.5	0.00	0.00	0.00	0.00	0.00	0.00	8.00	0.00	8.00	16.00	0.00	72.00	16.00	0.00	0.00	0.00	0.00	0.00	0.00	8.00	96.00	8.00	0.00	16.00	8.00	0.00	0.00	0.00	
5.5	0.00	0.00	0.00	0.00	0.00	0.00	0.00	0.00	0.00	80.00	13.33	0.00	53.33	40.00	0.00	0.00	0.00	0.00	0.00	6.67	13.33	26.67	13.33	0.00	13.33	0.00	0.00	0.00	
6.5	0.00	0.00	0.00	0.00	0.00	0.00	0.00	0.00	0.00	80.00	13.33	0.00	53.33	40.00	0.00	0.00	0.00	0.00	0.00	0.00	26.09	26.09	0.00	0.00	0.00	0.00	0.00	0.00	
7.5	0.00	0.00	0.00	0.00	0.00	0.00	0.00	0.00	0.00	34.78	26.09	8.70	0.00	60.87	95.65	0.00	0.00	0.00	0.00	0.00	0.00	0.00	0.00	0.00	0.00	0.00	0.00	0.00	0.00
8.5	0.00	0.00	0.00	0.00	0.00	0.00	0.00	0.00	0.00	5.23	0.00	62.75	0.00	0.00	52.29	52.29	0.00	15.68	0.00	0.00	0.00	0.00	0.00	0.00	0.00	0.00	0.00	0.00	
9.5	0.00	0.00	9.36	0.00	4.68	0.00	0.00	0.00	0.00	4.68	51.46	4.68	0.00	18.71	60.82	0.00	4.68	0.00	0.00	4.68	4.68	18.71	51.46	0.00	4.68	0.00	0.00	4.68	0.00
10.5	0.00	0.00	8.60	0.00	0.00	0.00	0.00	0.00	0.00	21.51	38.71	0.00	25.81	34.41	0.00	0.00	0.00	0.00	0.00	8.60	8.60	34.41	4.30	0.00	0.00	0.00	4.30	0.00	
11.5	0.00	0.00	0.00	0.00	0.00	0.00	3.81	0.00	0.00	34.29	7.62	0.00	30.48	38.10	0.00	6.25	0.00	0.00	0.00	0.00	3.81	19.05	53.33	3.81	0.00	0.00	7.62	0.00	0.00
12.5	0.00	0.00	11.43	0.00	0.00	0.00	0.00	3.81	0.00	3.81	3.81	0.00	45.71	26.67	0.00	0.00	0.00	0.00	0.00	3.81	68.57	0.00	0.00	15.24	7.62	0.00	0.00	0.00	
13.5	0.00	0.00	0.00	0.00	0.00	4.35	0.00	4.35	0.00	39.13	13.04	0.00	4.35	43.48	0.00	26.09	0.00	0.00	4.35	4.35	21.74	4.35	52.17	0.00	4.35	0.00	4.35	0.00	0.00
14.5	0.00	0.00	0.00	0.00	6.56	29.51	0.00	3.28	0.00	9.84	19.67	0.00	9.84	19.67	0.00	6.56	0.00	0.00	0.00	6.56	9.84	0.00	0.00	0.00	6.56	3.28	0.00	0.00	0.00
15.5	0.00	0.00	0.00	0.00	2.56	23.08	0.00	0.00	0.00	20.51	20.51	0.00	12.82	20.51	0.00	0.00	0.00	0.00	5.13	0.00	2.56	0.00	0.00	0.00	0.00	20.51	5.13	0.00	
16.5	0.00	0.00	0.00	0.00	0.00	10.81	0.00	5.41	0.00	5.41	8.11	0.00	24.32	29.73	2.70	0.00	0.00	2.70	0.00	0.00	2.70	0.00	2.70	0.00	2.70	0.00	8.11	5.41	0.00
17.5	0.00	0.00	2.96	0.00	0.00	2.96	0.00	2.96	0.00	5.93	20.74	0.00	8.89	20.74	0.00	0.00	2.96	0.00	0.00	0.00	11.85	26.67	8.89	0.00	0.00	2.96	0.00	0.00	0.00
18.5	0.00	0.00	0.00	2.76	2.76	0.00	8.29	8.29	0.00	2.76	11.05	0.00	19.34	13.82	0.00	0.00	5.53	0.00	0.00	0.00	0.00	24.87	0.00	0.00	8.29	5.53	0.00	0.00	0.00
19.5	0.00	2.82	0.00	0.00	0.00	5.63	0.00	8.45	5.63	0.00	14.08	16.90	0.00	2.82	0.00	0.00	0.00	0.00	0.00	8.45	25.35	2.82	0.00	2.82	8.45	2.82	0.00	0.00	0.00
20.5	0.00	0.00	0.00	0.00	0.00	17.65	0.00	0.00	23.53	11.76	5.88	2.94	14.71	0.00	0.00	0.00	0.00	2.94	0.00	2.94	20.59	5.88	2.94	0.00	5.88	0.00	0.00	0.00	
21.5	0.00	0.00	0.00	0.00	0.00	18.97	9.49	0.00	0.00	15.81	3.16	9.49	9.49	0.00	0.00	0.00	0.00	0.00	6.32	34.78	6.32	0.00	9.49	3.16	0.00	0.00	0.00		
22.5	0.00	0.00	3.00	0.00	0.00	0.00	8.99	0.00	0.00	8.99	11.99	3.00	8.99	3.00	0.00	0.00	0.00	0.00	0.00	3.00	17.98	0.00	3.00	14.98	8.99	0.00	0.00	0.00	
23.5	0.00	0.00	0.00	3.43	3.43	3.43	0.00	0.00	3.43	34.33	3.43	3.43	6.87	0.00	0.00	0.00	0.00	0.00	0.00	10.30	27.47	0.00	0.00	3.43	10.30	0.00	0.00	0.00	
24.5	0.00	3.76	0.00	0.00	0.00	3.76	7.51	0.00	0.00	7.51	3.76	0.00	18.78	7.51	0.00	0.00	0.00	0.00	0.00	0.00	11.27	45.07	0.00	0.00	0.00	3.76	0.00	0.00	0.00
25.5	0.00	0.00	6.81	0.00	0.00	0.00	4.54	0.00	15.89	13.62	0.00	9.08	6.81	0.00	0.00	0.00	0.00	0.00	0.00	9.08	20.43	0.00	0.00	15.89	2.27	0.00	0.00	0.00	
26.5	0.00	0.00	0.00	0.00	0.00	3.88	0.00	0.00	23.30	3.88	0.00	3.88	7.77	0.00	0.00	0.00	0.00	0.00	0.00	3.88	15.53	58.25	3.88	3.88	7.77	15.53	0.00	0.00	0.00

Table A 3.6 Paleontological data set of core SO136-165BX (continued). All species are given in spec./g.

depth (cm bsf)	<i>Fussonaria contempnata</i>	<i>Globocassidolina subglobosa</i>	<i>Gyrodina neosoldanii</i>	<i>Gyronoides nipponicus</i>	<i>Haplophragmoides canariensis</i>	<i>Heteroplaes du Templei</i>	<i>Lagena gracillima</i>	<i>Lagena gracilis</i>	<i>Lagena hispidula</i>	<i>Lagena semilineata</i>	<i>Lagena sericea</i>	<i>Melonis baileeanum</i>	<i>Melonis pomifera</i>	<i>Melonis zandami</i>	<i>Miliammina arenacea</i>	<i>Nanionella indea</i>	<i>Nuttallides labradoricus</i>	<i>Oolina caudigera</i>	<i>Oolina hexagona</i>	<i>Oridosalis sp</i>	<i>Oridosalis umbonatus</i>	<i>Osangularia culta</i>	<i>Parafissurina ovata</i>	<i>Puleria bulloides</i>	<i>Puleria quinquelobata</i>	<i>Pulenerella asymmetrica</i>	<i>Pyrgo murinina</i>						
0.5	0.00	16.33	8.16	0.00	8.16	155.10	0.00	16.33	16.33	0.00	16.33	0.00	8.16	8.16	0.00	16.33	0.00	163.27	57.14	8.16	0.00	146.94	24.49	0.00	97.96	8.16	114.29	81.63	8.16	16.33			
1.5	8.16	16.33	8.16	8.16	0.00	130.61	0.00	16.33	8.16	0.00	8.16	0.00	24.49	179.59	73.47	0.00	0.00	50.00	50.00	14.29	0.00	164.29	7.14	0.00	77.19	0.00	0.00	91.23	49.12	42.11	7.02		
2.5	0.00	28.57	0.00	0.00	14.29	92.86	0.00	14.29	14.29	0.00	7.14	0.00	0.00	200.00	50.00	50.00	161.40	49.12	14.04	0.00	0.00	126.32	14.04	0.00	0.00	120.00	0.00	0.00	96.00	32.00	8.00	8.00	
3.5	14.04	7.02	14.04	0.00	7.02	91.23	0.00	0.00	7.02	0.00	7.02	0.00	0.00	112.00	128.00	16.00	16.00	0.00	0.00	112.00	16.00	0.00	0.00	120.00	0.00	0.00	60.00	40.00	20.00	13.33			
4.5	16.00	16.00	24.00	16.00	8.00	88.00	0.00	8.00	0.00	0.00	8.00	0.00	8.00	8.00	0.00	17.39	8.70	191.30	26.09	8.70	8.70	0.00	0.00	173.91	0.00	0.00	121.74	0.00	0.00	69.57	60.87	17.39	17.39
5.5	6.67	20.00	0.00	13.33	0.00	66.67	0.00	6.67	6.67	0.00	0.00	0.00	6.67	14.00	46.67	6.67	6.67	0.00	0.00	93.33	0.00	0.00	0.00	0.00	0.00	0.00	0.00	0.00	0.00	0.00			
6.5	0.00	8.70	17.39	8.70	17.39	78.26	0.00	0.00	34.78	0.00	0.00	17.39	8.70	191.30	26.09	8.70	8.70	0.00	0.00	112.50	6.25	0.00	0.00	68.75	0.00	0.00	100.00	25.00	18.75	12.50			
7.5	0.00	25.00	25.00	6.25	0.00	31.25	0.00	0.00	31.25	0.00	0.00	0.00	31.25	156.25	43.75	25.00	37.50	0.00	0.00	112.50	6.25	0.00	0.00	52.29	0.00	0.00	73.20	26.14	10.46	20.92			
8.5	0.00	15.69	31.37	5.23	10.46	88.89	0.00	0.00	0.00	5.23	0.00	20.92	240.52	52.29	20.92	15.69	5.23	0.00	88.89	0.00	10.46	0.00	0.00	52.29	0.00	0.00	91.23	49.12	42.11	7.02			
9.5	23.39	14.04	18.71	4.68	18.71	56.14	0.00	0.00	9.36	0.00	4.68	0.00	18.71	177.78	65.50	9.36	18.71	0.00	0.00	56.14	28.07	0.00	0.00	51.46	0.00	4.68	70.18	28.07	37.43	4.68			
10.5	4.30	43.01	21.51	8.60	4.30	111.83	0.00	0.00	0.00	4.30	0.00	4.30	4.30	210.75	47.31	17.20	25.81	8.60	0.00	73.12	4.30	0.00	4.30	43.01	0.00	0.00	73.12	47.31	17.20	8.60			
11.5	7.62	30.48	7.62	7.62	7.62	19.05	0.00	0.00	3.81	0.00	0.00	0.00	11.43	156.19	102.86	26.67	11.43	0.00	3.81	49.52	26.67	0.00	3.81	45.71	0.00	3.81	34.29	7.62	0.00	3.81			
12.5	41.90	38.10	0.00	3.81	0.00	64.76	0.00	3.81	19.05	0.00	3.81	0.00	3.81	114.29	49.52	0.00	26.67	0.00	0.00	41.90	15.24	0.00	0.00	7.62	19.05	0.00	26.67	0.00	11.43	0.00			
13.5	39.13	13.04	0.00	0.00	0.00	47.83	0.00	0.00	8.70	0.00	4.35	0.00	0.00	134.78	34.78	13.04	13.04	30.43	4.35	21.74	4.35	0.00	4.35	52.17	4.35	8.70	26.09	0.00	26.09	0.00			
14.5	0.00	13.11	0.00	9.84	0.00	59.02	0.00	0.00	3.28	0.00	0.00	0.00	6.56	52.46	62.30	3.28	6.56	6.56	0.00	49.18	0.00	0.00	0.00	22.95	6.56	6.56	22.95	0.00	0.00	3.28			
15.5	43.59	30.77	0.00	25.64	0.00	15.38	0.00	0.00	10.26	2.56	2.56	0.00	10.26	117.95	25.64	5.13	10.26	23.08	5.13	38.46	0.00	0.00	0.00	56.41	0.00	10.26	30.77	0.00	17.95	0.00			
16.5	54.05	13.51	16.22	32.43	0.00	18.92	0.00	0.00	2.70	0.00	5.41	0.00	5.41	94.59	32.43	16.22	5.41	13.51	0.00	27.03	0.00	0.00	0.00	21.62	8.11	8.11	18.92	0.00	29.73	8.11			
17.5	56.30	8.89	0.00	5.93	0.00	14.81	0.00	0.00	11.85	0.00	0.00	0.00	2.96	88.89	11.85	23.70	17.78	0.00	17.78	26.67	0.00	2.96	2.96	32.59	0.00	11.85	14.81	2.96	20.74	8.89			
18.5	38.69	0.00	5.53	0.00	0.00	2.76	0.00	0.00	11.05	0.00	2.76	0.00	0.00	118.83	22.11	5.53	11.05	0.00	13.82	27.63	0.00	0.00	5.53	30.40	0.00	2.76	27.63	0.00	0.00	0.00			
19.5	33.80	2.82	0.00	5.63	0.00	16.90	0.00	0.00	5.63	0.00	0.00	0.00	0.00	104.23	25.35	5.63	5.63	11.27	5.63	33.80	0.00	0.00	0.00	16.90	0.00	0.00	22.54	0.00	8.45	0.00			
20.5	0.00	2.94	14.71	5.88	0.00	2.94	2.94	2.94	5.88	0.00	0.00	0.00	8.82	129.41	20.59	5.88	2.94	0.00	5.88	23.53	0.00	0.00	0.00	35.29	2.94	5.88	17.65	0.00	23.53	14.71			
21.5	37.94	15.81	0.00	12.65	0.00	22.13	0.00	3.16	6.32	0.00	0.00	0.00	0.00	88.54	15.81	9.49	0.00	0.00	9.49	12.65	0.00	0.00	3.16	25.30	0.00	0.00	37.94	0.00	15.81	12.65			
22.5	74.91	8.99	11.99	8.99	0.00	3.00	0.00	3.00	5.99	0.00	0.00	0.00	14.98	80.90	17.98	0.00	8.99	3.00	5.99	14.98	0.00	0.00	0.00	26.97	5.99	8.99	5.99	26.97	5.99	8.99	5.99		
23.5	85.84	24.03	17.17	3.43	3.43	24.03	0.00	0.00	3.43	0.00	0.00	0.00	0.00	68.67	20.60	10.30	0.00	0.00	6.87	13.73	0.00	0.00	0.00	34.33	0.00	3.43	17.17	0.00	6.87	3.43			
24.5	78.87	22.54	15.02	3.76	0.00	11.27	0.00	0.00	3.76	0.00	0.00	0.00	3.76	56.34	15.02	15.02	11.27	0.00	0.00	11.27	0.00	0.00	0.00	26.29	0.00	11.27	0.00	0.00	26.29	0.00	11.27	0.00	
25.5	68.09	15.89	15.89	0.00	6.81	0.00	0.00	0.00	6.81	0.00	6.81	0.00	6.81	68.09	24.96	4.54	4.54	11.35	0.00	11.35	0.00	0.00	0.00	22.70	0.00	0.00	29.50	0.00	13.62	2.27	0.00	0.00	0.00
26.5	93.20	3.88	0.00	7.77	0.00	23.30	0.00	0.00	0.00	0.00	0.00	0.00	0.00	135.92	7.77	11.65	11.65	3.88	3.88	23.30	0.00	0.00	11.65	11.65	3.88	0.00	11.65	0.00	7.77	11.65	0.00	0.00	0.00

Table A 3.6 Paleontological data set of core SO136-165BX (continued). All species are given in spec./g.

depth (cm bsf)	<i>Pyrgo oblonga</i>	<i>Pyrgo rotalaria</i>	<i>Pyrgo serrata</i>	<i>Pyrgo</i> spp	<i>Pyrgo tasmania</i>	<i>Pyrolina cylindroides</i>	<i>Quinqueloculina</i> spp	<i>Reophax micaceus</i>	<i>Reophax spiriculifer</i>	<i>Reussella</i> sp	<i>Rutherfordia</i> sp	<i>Siphonotextularia roshauseni</i>	<i>Spiraloculina disparilis</i>	<i>Sugrunda porosa</i>	<i>Tosaiia hanzawai</i>	<i>Tritania angulosa</i>	<i>Triloculina tricarinata</i>	<i>Uvigerina euberiaana</i>	<i>Uvigerina peregrina</i>	<i>Uvigerina pigmea</i>	<i>Uvigerina schwageri</i>	<i>Vasicostella craniomorpha</i>	Fragments of agglutinating spp.	All species / g	Calstic sediments / g	Σ (counts)	Weight of sample [g]	Factor of split
0.5	8.16	24.49	0.00	24.49	0.00	<i>Pyrolina cylindroides</i>																						
1.5	48.98	0.00	0.00	97.96	0.00																							
2.5	0.00	7.14	0.00	71.43	0.00																							
3.5	21.05	7.02	0.00	49.12	0.00	105.26	0.00	21.05	0.00	0.00	0.00	14.04	0.00	7.02	28.07	0.00	7.02	7.02	126.32	0.00	0.00	0.00	364.91	1775.44	28.07	253	0.57 1/4	
4.5	16.00	0.00	16.00	72.00	0.00	48.00	0.00	56.00	8.00	0.00	0.00	48.00	0.00	0.00	32.00	0.00	0.00	8.00	48.00	0.00	0.00	0.00	536.00	2000.00	32.00	250	0.5 1/4	
5.5	20.00	6.67	0.00	46.67	0.00	86.67	0.00	53.33	20.00	0.00	0.00	0.00	0.00	0.00	26.67	0.00	6.67	13.33	100.00	0.00	0.00	0.00	346.67	1540.00	26.67	231	0.6 1/4	
6.5	26.09	0.00	0.00	34.78	0.00	113.04	0.00	78.26	17.39	0.00	0.00	34.78	8.70	0.00	34.78	0.00	17.39	0.00	104.35	0.00	0.00	0.00	400.00	2069.57	0.00	238	0.46 1/4	
7.5	37.50	0.00	0.00	50.00	0.00	56.25	0.00	25.00	6.25	0.00	0.00	12.50	0.00	0.00	18.75	0.00	12.50	6.25	93.75	0.00	0.00	0.00	481.25	1943.75	12.50	311	0.64 1/4	
8.5	10.46	20.92	5.23	57.52	10.46	109.80	0.00	26.14	0.00	0.00	0.00	15.69	0.00	5.23	26.14	0.00	0.00	0.00	99.35	0.00	0.00	0.00	198.69	1683.66	15.69	322	0.51 3/8	
9.5	9.36	32.75	0.00	56.14	4.68	65.50	0.00	0.00	4.68	0.00	0.00	14.04	0.00	0.00	14.04	0.00	4.68	0.00	130.99	0.00	0.00	0.00	173.10	1478.36	0.00	316	0.57 3/8	
10.5	4.30	30.11	0.00	51.61	0.00	98.92	0.00	4.30	8.60	0.00	0.00	0.00	0.00	0.00	34.41	0.00	0.00	12.90	77.42	0.00	0.00	0.00	146.24	1445.16	12.90	336	0.62 3/8	
11.5	22.86	22.86	0.00	38.10	0.00	80.00	0.00	11.43	7.82	0.00	0.00	7.62	0.00	0.00	19.05	0.00	0.00	11.43	80.00	0.00	0.00	0.00	106.67	1180.95	7.62	310	0.6 7/16	
12.5	3.81	19.05	0.00	34.29	0.00	19.05	0.00	0.00	0.00	0.00	3.81	15.24	0.00	0.00	22.86	0.00	3.81	7.62	64.76	0.00	0.00	0.00	148.57	1024.76	22.86	269	1.4 3/16	
13.5	0.00	34.78	0.00	21.74	0.00	0.00	0.00	0.00	21.74	0.00	0.00	8.70	4.35	0.00	21.74	0.00	0.00	0.00	82.61	0.00	0.00	0.00	113.04	1030.43	13.04	237	0.92 1/4	
14.5	0.00	19.67	0.00	19.67	9.84	0.00	0.00	0.00	6.56	0.00	0.00	9.84	3.28	0.00	9.84	0.00	0.00	0.00	45.90	3.28	0.00	0.00	101.64	695.08	9.84	212	1.22 1/4	
15.5	0.00	15.38	0.00	35.90	0.00	0.00	0.00	0.00	0.00	0.00	0.00	10.26	0.00	0.00	38.46	0.00	0.00	0.00	79.49	0.00	0.00	0.00	115.38	910.26	5.13	355	1.56 1/4	
16.5	0.00	29.73	0.00	21.62	0.00	0.00	2.70	0.00	0.00	0.00	0.00	0.00	0.00	0.00	35.14	0.00	0.00	2.70	67.57	0.00	0.00	0.00	59.46	762.16	2.70	282	1.48 1/4	
17.5	0.00	23.70	0.00	17.78	0.00	0.00	0.00	0.00	0.00	0.00	0.00	5.93	0.00	2.96	23.70	2.96	0.00	5.93	41.48	0.00	0.00	2.96	47.41	678.52	1.00	229	1.8 3/16	
18.5	16.58	8.29	0.00	0.00	0.00	0.00	0.00	0.00	0.00	0.00	0.00	11.05	0.00	0.00	13.82	0.00	0.00	27.63	33.16	0.00	0.00	0.00	41.45	591.36	2.00	214	1.93 3/16	
19.5	14.08	2.82	0.00	11.27	0.00	0.00	8.45	0.00	0.00	0.00	0.00	5.63	0.00	0.00	19.72	0.00	0.00	8.45	25.35	0.00	2.82	0.00	33.80	549.30	0.00	195	1.42 1/4	
20.5	0.00	0.00	17.65	0.00	0.00	2.94	0.00	0.00	0.00	0.00	0.00	5.88	0.00	0.00	20.59	0.00	0.00	2.94	20.59	0.00	0.00	0.00	0.00	523.53	5.88	178	2.72 1/8	
21.5	3.16	0.00	0.00	15.81	0.00	0.00	0.00	0.00	0.00	0.00	0.00	3.16	0.00	0.00	22.13	0.00	0.00	3.16	18.97	0.00	0.00	3.16	47.43	572.33	3.16	181	2.53 1/8	
22.5	0.00	14.98	0.00	8.99	0.00	0.00	0.00	0.00	0.00	0.00	0.00	3.00	0.00	0.00	53.93	0.00	0.00	3.00	11.99	0.00	0.00	0.00	14.98	551.31	8.99	184	2.67 1/8	
23.5	0.00	6.87	0.00	10.30	0.00	0.00	0.00	0.00	0.00	0.00	0.00	13.73	3.43	0.00	6.87	0.00	0.00	3.43	13.73	10.30	0.00	0.00	13.73	542.49	17.17	158	2.33 1/8	
24.5	0.00	7.51	0.00	15.02	0.00	0.00	3.76	0.00	0.00	0.00	0.00	11.27	0.00	0.00	18.78	0.00	3.76	0.00	11.27	3.76	0.00	0.00	30.05	514.55	11.27	137	2.13 1/8	
25.5	0.00	11.35	0.00	13.62	0.00	0.00	2.27	0.00	0.00	0.00	0.00	4.54	0.00	0.00	20.43	0.00	2.27	0.00	24.96	0.00	0.00	0.00	40.85	553.76	6.81	244	2.35 3/16	
26.5	11.65	7.77	0.00	15.53	3.88	0.00	0.00	0.00	7.77	0.00	0.00	31.07	0.00	0.00	0.00	42.72	3.88	0.00	0.00	69.90	737.86	0.00	190	2.06 1/8				

A4 Q-MODE FACTOR ANALYSIS DATA SET

Table A 4.1 Varimax factor loading of core SO136-019BX.

No.	Depth (cm bsf)	Comm.	1	2	3	4
1	0.5	0.983	0.231	0.951	0.160	-0.002
2	1.5	0.987	0.162	0.969	0.143	-0.020
3	2.5	0.986	0.300	0.933	0.155	0.009
4	3.5	0.982	0.164	0.953	0.216	-0.013
5	4.5	0.968	0.407	0.855	0.266	-0.022
6	5.5	0.957	0.290	0.672	0.625	-0.173
7	6.5	0.917	0.228	0.433	0.817	-0.100
8	7.5	0.949	0.662	0.482	0.525	-0.050
9	8.5	0.949	0.507	-0.029	0.769	0.314
10	9.5	0.929	0.548	0.220	0.745	0.159
11	10.5	0.968	0.484	0.365	0.757	-0.169
12	11.5	0.940	0.339	0.575	0.704	0.008
13	12.5	0.933	0.636	0.335	0.644	0.052
14	13.5	0.951	0.488	0.478	0.687	-0.116
15	14.5	0.966	0.660	0.644	0.338	0.031
16	15.5	0.929	0.677	0.434	0.520	0.112
17	16.5	0.953	0.602	0.668	0.347	0.154
18	17.5	0.962	0.516	0.753	0.353	0.069
19	18.5	0.962	0.684	0.574	0.372	0.164
20	19.5	0.960	0.776	0.500	0.319	0.082
21	20.5	0.942	0.592	0.578	0.499	0.093
22	21.5	0.964	0.758	0.505	0.365	-0.033
23	22.5	0.937	0.780	0.314	0.480	-0.018
24	23.5	0.945	0.846	0.255	0.403	-0.046
25	24.5	0.977	0.750	0.573	0.293	0.025
26	25.5	0.981	0.858	0.412	0.274	0.030
27	26.5	0.980	0.844	0.385	0.347	0.004
28	27.5	0.966	0.826	0.409	0.327	-0.097
29	28.5	0.959	0.822	0.449	0.277	0.075
30	29.5	0.988	0.724	0.635	0.247	0.010
31	30.5	0.985	0.869	0.419	0.224	0.060
32	31.5	0.985	0.927	0.242	0.257	0.033
33	32.5	0.969	0.916	0.142	0.331	-0.012
34	33.5	0.978	0.948	0.151	0.237	-0.007
35	34.5	0.969	0.888	0.283	0.315	-0.010
36	35.5	0.973	0.902	0.270	0.294	0.014
37	36.5	0.988	0.947	0.081	0.290	-0.003
VARIANCE			46.134	29.417	19.845	0.870
CUM. VAR			46.134	75.551	95.397	96.267

Table A 4.2: Varimax factor scores matrix of core SO136-019BX. Species of ecological relevance are bold.

1 VAR.	2 VAR.	3 VAR.	4 VAR.
0.940 <i>Nuttallides umbonifer</i>	0.479 <i>Globocassidolina subglobosum</i>	0.519 <i>Fissurina orbignyana</i>	0.687 <i>Heteroplea dutemplei</i>
0.128 <i>Ehrenbergina mestayeri</i>	0.425 <i>Siphonotularia rolshauseni</i>	0.382 <i>Epistominella exigua</i>	0.301 <i>Pulenia bulloides</i>
0.071 <i>Trifarina angulosa</i>	0.408 <i>Epistominella exigua</i>	0.197 <i>Lagena gracilis</i>	0.196 <i>Fissurina marginata</i>
0.060 <i>Fissurina laevigata</i>	0.294 <i>Pulenia bulloides</i>	0.187 <i>Nuttallides umbonifer</i>	0.166 <i>Miliammina arenaca</i>
0.059 <i>Cibicidoides inawagaensis</i>	0.224 <i>Ehrenbergina mestayeri</i>	0.159 <i>Lagena hispidula</i>	0.102 <i>Tosala hanzawai</i>
0.053 <i>Oolina caudigera</i>	0.212 <i>Heteroplea dutemplei</i>	0.150 <i>Pulenia bulloides</i>	0.101 <i>Cassidulina laevigata</i>
0.041 <i>Cibicidoides wuellerstorffii</i>	0.176 <i>Nuttallides umbonifer</i>	0.132 <i>Quinqueloculina spp</i>	0.094 <i>Cibicidoides mundulus</i>
0.032 <i>Fissurina marginata</i>	0.175 <i>Tosala hanzawai</i>	0.101 <i>Psammosphaera fusca</i>	0.094 <i>Cibicidoides wuellerstorffii</i>
0.023 <i>Globocassidolina subglobosum</i>	0.142 <i>Oridosalis umbunatus</i>	0.085 <i>Lagena setigera</i>	0.088 <i>Fissurina laevigata</i>
0.022 <i>Melonis pomphiloides</i>	0.141 <i>Pyrgo oblonga</i>	0.063 <i>Dentalina baggi</i>	0.087 <i>Pyrgo spp</i>
0.021 <i>Cibicidoides lobatulus</i>	0.135 <i>Lagena gracilis</i>	0.060 <i>Fissurina laevigata</i>	0.085 <i>Melonis pomphiloides</i>
0.018 <i>Lagena globosa</i>	0.122 <i>Melonis balearum</i>	0.056 <i>Melonis pomphiloides</i>	0.076 <i>Cibicidoides lobatulus</i>
0.011 <i>Lenticulina rotulata</i>	0.119 <i>Fissurina marginata</i>	0.048 <i>Sigmolopsis schlumbergeri</i>	0.065 <i>Ehrenbergina glabra</i>
0.011 <i>Reusella sp</i>	0.114 <i>Parafissurina ovata</i>	0.047 <i>Pulenia quinqueloba</i>	0.056 <i>Nuttallides umbonifer</i>
0.007 <i>Fissurina serra</i>	0.109 <i>Pulenia quinqueloba</i>	0.045 <i>Melonis balearum</i>	0.056 <i>Sigmolopsis schlumbergeri</i>
0.006 <i>Suggrunda porosa</i>	0.097 <i>Ehrenbergina glabra</i>	0.042 <i>Pyrgo oblonga</i>	0.053 <i>Pyrgo rotalaria</i>
0.005 <i>Ehrenbergina glabra</i>	0.094 <i>Cibicidoides wuellerstorffii</i>	0.041 <i>Pyrgo rotalaria</i>	0.051 <i>Lagena globosa</i>
0.004 <i>Dentalina baggi</i>	0.081 <i>Pyrgo spp</i>	0.041 <i>Cibicidoides lobatulus</i>	0.041 <i>Oolina caudigera</i>
0.001 <i>Lagena substriata</i>	0.080 <i>Cibicidoides mundulus</i>	0.033 <i>Lagena substriata</i>	0.023 <i>Cibicidoides inawagaensis</i>
-0.004 <i>Sigmolopsis schlumbergeri</i>	0.077 <i>Lagena setigera</i>	0.032 <i>Pyrgo spp</i>	0.022 <i>Cibicidoides fletcheri</i>
-0.010 <i>Oridosalis umbunatus</i>	0.076 <i>Trifarina angulosa</i>	0.026 <i>Fissurina serra</i>	0.007 <i>Epistominella exigua</i>
-0.015 <i>Cibicidoides fletcheri</i>	0.070 <i>Cassidulina laevigata</i>	0.026 <i>Lagena globosa</i>	0.007 <i>Trifarina angulosa</i>
-0.015 <i>Pyrgo rotalaria</i>	0.065 <i>Quinqueloculina spp</i>	0.019 <i>Parafissurina ovata</i>	0.006 <i>Parafissurina ovata</i>
-0.018 <i>Lagena hispidula</i>	0.064 <i>Lagena substriata</i>	0.012 <i>Lenticulina rotulata</i>	0.003 <i>Fissurina serra</i>
-0.018 <i>Miliammina arenaca</i>	0.056 <i>Fissurina orbignyana</i>	0.007 <i>Suggrunda porosa</i>	0.002 <i>Lagena hispidula</i>
-0.021 <i>Psammosphaera fusca</i>	0.041 <i>Melonis pomphiloides</i>	0.005 <i>Fissurina marginata</i>	-0.007 <i>Lenticulina rotulata</i>
-0.023 <i>Lagena gracilis</i>	0.039 <i>Miliammina arenaca</i>	0.000 <i>Siphonotularia rolshauseni</i>	-0.014 <i>Dentalina baggi</i>
-0.023 <i>Pyrgo spp</i>	0.037 <i>Cibicidoides fletcheri</i>	0.000 <i>Tosala hanzawai</i>	-0.020 <i>Melonis balearum</i>
-0.024 <i>Lagena setigera</i>	0.030 <i>Lagena hispidula</i>	0.000 <i>Cibicidoides fletcheri</i>	-0.025 <i>Psammosphaera fusca</i>
-0.024 <i>Parafissurina ovata</i>	0.028 <i>Psammosphaera fusca</i>	-0.015 <i>Oridosalis umbunatus</i>	-0.027 <i>Suggrunda porosa</i>
-0.030 <i>Cassidulina laevigata</i>	0.027 <i>Fissurina serra</i>	-0.017 <i>Miliammina arenaca</i>	-0.028 <i>Lagena gracilis</i>
-0.031 <i>Quinqueloculina spp</i>	0.025 <i>Pyrgo rotalaria</i>	-0.029 <i>Reusella sp</i>	-0.041 <i>Oridosalis umbunatus</i>
-0.033 <i>Cibicidoides mundulus</i>	0.019 <i>Cibicidoides lobatulus</i>	-0.037 <i>Cibicidoides mundulus</i>	-0.045 <i>Reusella sp</i>
-0.036 <i>Fissurina orbignyana</i>	0.014 <i>Lenticulina rotulata</i>	-0.056 <i>Cassidulina laevigata</i>	-0.070 <i>Lagena setigera</i>
-0.039 <i>Melonis balearum</i>	0.014 <i>Dentalina baggi</i>	-0.069 <i>Cibicidoides wuellerstorffii</i>	-0.073 <i>Siphonotularia rolshauseni</i>
-0.042 <i>Heteroplea dutemplei</i>	0.012 <i>Reusella sp</i>	-0.078 <i>Oolina caudigera</i>	-0.081 <i>Fissurina orbignyana</i>
-0.042 <i>Pulenia quinqueloba</i>	0.007 <i>Cibicidoides inawagaensis</i>	-0.082 <i>Cibicidoides inawagaensis</i>	-0.099 <i>Pulenia quinqueloba</i>
-0.045 <i>Pyrgo oblonga</i>	0.002 <i>Suggrunda porosa</i>	-0.129 <i>Ehrenbergina glabra</i>	-0.115 <i>Lagena substriata</i>
-0.071 <i>Tosala hanzawai</i>	0.000 <i>Oolina caudigera</i>	-0.197 <i>Trifarina angulosa</i>	-0.116 <i>Quinqueloculina spp</i>
-0.100 <i>Pulenia bulloides</i>	-0.002 <i>Fissurina laevigata</i>	-0.239 <i>Heteroplea dutemplei</i>	-0.127 <i>Pyrgo oblonga</i>
-0.139 <i>Epistominella exigua</i>	-0.007 <i>Sigmolopsis schlumbergeri</i>	-0.321 <i>Globocassidolina subglobosum</i>	-0.154 <i>Ehrenbergina mestayeri</i>
-0.177 <i>Siphonotularia rolshauseni</i>	-0.012 <i>Lagena globosa</i>	-0.405 <i>Ehrenbergina mestayeri</i>	-0.431 <i>Globocassidolina subglobosum</i>

Table A 4.3: Varimax factor loading matrix of core SO136-025BX

No.	depth (cm bsf)	Comm.	1	2	3	4
1	0.5	0.773	0.865	-0.094	-0.074	0.100
2	1.5	0.780	0.625	-0.287	0.546	-0.094
3	2.5	0.456	0.597	-0.102	0.186	0.235
4	3.5	0.940	0.198	-0.176	0.150	0.920
5	4.5	0.737	0.132	-0.780	0.239	0.232
6	5.5	0.903	0.057	-0.123	0.920	0.197
7	6.5	0.846	0.143	-0.908	0.027	0.034
VARIANCE			22.508	22.575	18.065	14.492
CUM. VAR			22.508	45.083	63.148	77.640

Table A 4.4 Varimax factor scores matrix of core SO136-025BX

1 VAR.	2 VAR.	3 VAR.	4
0.559 <i>Epistominella exigua</i>	0.083 <i>Cibicidoides</i> sp	0.427 <i>Heteroplea dutemplei</i>	0.614 <i>Ehrenbergina mestayeri</i>
0.457 <i>Pyrgo rotalaria</i>	0.071 <i>Cibicidoides fletcheri</i>	0.407 <i>Pyrgo murrhina</i>	0.463 <i>Quinqueloculina</i> spp
0.371 <i>Gyroidinoides orbicularis</i>	0.067 <i>Cibicidoides inawagaensis</i>	0.402 <i>Cibicidoides</i> sp	0.330 <i>Cibicidoides inawagaensis</i>
0.303 <i>Pyrgo</i> spp	0.066 <i>Pyrgo tasmania</i>	0.340 <i>Cibicidoides wuellerstorffii</i>	0.255 <i>Uvigerina auberiana</i>
0.272 <i>Pyrgo tasmania</i>	0.066 <i>Fissurina orbignyana</i>	0.286 <i>Trifarina angulosa</i>	0.191 <i>Fissurina orbignyana</i>
0.179 <i>Dentalina baggi</i>	0.051 <i>Gyroidinoides orbicularis</i>	0.262 <i>Pyrgo</i> spp	0.174 <i>Cibicidoides lobatus</i>
0.150 <i>Cibicidoides inawagaensis</i>	0.048 <i>Pyrgo rotalaria</i>	0.188 <i>Ehrenbergina glabra</i>	0.166 <i>Pyrgo tasmania</i>
0.147 <i>Lenticulina rotulata</i>	0.040 <i>Cibicidoides lobatus</i>	0.164 <i>Gyroidinoides neosoldanii</i>	0.148 <i>Nuttallides umboniferus</i>
0.117 <i>Fissurina orbignyana</i>	0.040 <i>Nuttallides umboniferus</i>	0.152 <i>Nuttallides umboniferus</i>	0.141 <i>Pyrgo</i> spp
0.086 <i>Cibicidoides lobatus</i>	0.039 <i>Pyrgo serrata</i>	0.138 <i>Dentalina baggi</i>	0.120 <i>Planulina ariminensis</i>
0.078 <i>Pyrgo serrata</i>	0.035 <i>Uvigerina auberiana</i>	0.108 <i>Ehrenbergina mestayeri</i>	0.097 <i>Globocassidolina subglobosum</i>
0.074 <i>Globocassidolina subglobosum</i>	0.033 <i>Ehrenbergina glabra</i>	0.104 <i>Planulina ariminensis</i>	0.073 <i>Cibicidoides</i> sp
0.069 <i>Gyroidinoides neosoldanii</i>	0.030 <i>Dentalina baggi</i>	0.072 <i>Pyrgo serrata</i>	0.057 <i>Melonis balearum</i>
0.067 <i>Ehrenbergina glabra</i>	0.025 <i>Pulenia bulloides</i>	0.072 <i>Cruciloculina triangularia</i>	0.032 <i>Pyrgo oblonga</i>
0.065 <i>Trifarina angulosa</i>	0.014 <i>Siphonotextularia rolshauseni</i>	0.072 <i>Lagena substriata</i>	0.024 <i>Pyrgo oblonga</i>
0.062 <i>Uvigerina peregrina</i>	0.011 <i>Cruciloculina triangularia</i>	0.066 <i>Lenticulina rotulata</i>	0.019 <i>Pyrgo murrhina</i>
0.062 <i>Uvigerina pigmea</i>	0.011 <i>Lagena substriata</i>	0.061 <i>Tosaya hanzawai</i>	0.018 <i>Lagena hispidula</i>
0.055 <i>Cibicidoides wuellerstorffii</i>	0.009 <i>Uvigerina peregrina</i>	0.057 <i>Fissurina orbignyana</i>	0.017 <i>Pulenia bulloides</i>
0.047 <i>Siphonotextularia rolshauseni</i>	0.009 <i>Uvigerina pigmea</i>	0.027 <i>Epistominella exigua</i>	0.015 <i>Siphonotextularia rolshauseni</i>
0.033 <i>Uvigerina auberiana</i>	0.008 <i>Gyroidinoides neosoldanii</i>	0.002 <i>Lagena hispidula</i>	0.009 <i>Cibicidoides mundulus</i>
0.031 <i>Pulenia bulloides</i>	0.005 <i>Lenticulina rotulata</i>	0.001 <i>Pyrgo oblonga</i>	0.009 <i>Gyronoides nipponicus</i>
0.029 <i>Pyrgo oblonga</i>	0.004 <i>Pyrgo</i> spp	0.001 <i>Cibicidoides mundulus</i>	0.009 <i>Stilostomella lepidula</i>
0.018 <i>Cibicidoides fletcheri</i>	-0.006 <i>Pyrgo murrhina</i>	0.001 <i>Gyronoides nipponicus</i>	0.006 <i>Tosaya hanzawai</i>
-0.008 <i>Tosaya hanzawai</i>	-0.007 <i>Trifarina angulosa</i>	0.001 <i>Stilostomella lepidula</i>	0.005 <i>Lagena gracilis</i>
-0.008 <i>Fissurina laevigata</i>	-0.021 <i>Heteroplea dutemplei</i>	0.000 <i>Siphonotextularia rolshauseni</i>	0.002 <i>Cruciloculina triangularia</i>
-0.008 <i>Heteroplea dutemplei</i>	-0.036 <i>Quinqueloculina</i> spp	-0.001 <i>Cibicidoides fletcheri</i>	0.002 <i>Lagena substriata</i>
-0.008 <i>Parafissurina ventricosa</i>	-0.049 <i>Ehrenbergina mestayeri</i>	-0.004 <i>Melonis balearum</i>	0.000 <i>Trifarina angulosa</i>
-0.016 <i>Cruciloculina triangularia</i>	-0.057 <i>Pyrgo oblonga</i>	-0.015 <i>Cibicidoides lobatus</i>	-0.003 <i>Uvigerina peregrina</i>
-0.016 <i>Lagena substriata</i>	-0.066 <i>Melonis balearum</i>	-0.022 <i>Fissurina laevigata</i>	-0.003 <i>Uvigerina pigmea</i>
-0.018 <i>Cibicidoides mundulus</i>	-0.071 <i>Cibicidoides mundulus</i>	-0.022 <i>Parafissurina ventricosa</i>	-0.006 <i>Fissurina marginata</i>
-0.018 <i>Gyronoides nipponicus</i>	-0.071 <i>Gyronoides nipponicus</i>	-0.023 <i>Oridosalis umbunatus</i>	-0.009 <i>Cibicidoides fletcheri</i>
-0.018 <i>Stilostomella lepidula</i>	-0.071 <i>Stilostomella lepidula</i>	-0.025 <i>Uvigerina auberiana</i>	-0.016 <i>Gyroidinoides orbicularis</i>
-0.019 <i>Planulina ariminensis</i>	-0.079 <i>Fissurina laevigata</i>	-0.026 <i>Uvigerina peregrina</i>	-0.017 <i>Fissurina laevigata</i>
-0.021 <i>Melonis balearum</i>	-0.079 <i>Parafissurina ventricosa</i>	-0.026 <i>Uvigerina pigmea</i>	-0.017 <i>Parafissurina ventricosa</i>
-0.023 <i>Lagena gracilis</i>	-0.118 <i>Planulina ariminensis</i>	-0.041 <i>Cibicidoides inawagaensis</i>	-0.019 <i>Oridosalis umbunatus</i>
-0.036 <i>Quinqueloculina</i> spp	-0.141 <i>Lagena hispidula</i>	-0.053 <i>Fissurina marginata</i>	-0.043 <i>Ehrenbergina glabra</i>
-0.037 <i>Lagena hispidula</i>	-0.194 <i>Lagena gracilis</i>	-0.061 <i>Lagena gracilis</i>	-0.050 <i>Epistominella exigua</i>
-0.046 <i>Nuttallides umboniferus</i>	-0.232 <i>Cibicidoides wuellerstorffii</i>	-0.062 <i>Pyrgo rotalaria</i>	-0.072 <i>Heteroplea dutemplei</i>
-0.047 <i>Cibicidoides</i> sp	-0.233 <i>Epistominella exigua</i>	-0.073 <i>Quinqueloculina</i> spp	-0.075 <i>Dentalina baggi</i>
-0.051 <i>Oridosalis umbunatus</i>	-0.301 <i>Oridosalis umbunatus</i>	-0.092 <i>Pyrgo tasmania</i>	-0.088 <i>Gyroidinoides neosoldanii</i>
-0.061 <i>Ehrenbergina mestayeri</i>	-0.437 <i>Tosaya hanzawai</i>	-0.108 <i>Globocassidolina subglobosum</i>	-0.092 <i>Lenticulina rotulata</i>
-0.094 <i>Fissurina marginata</i>	-0.479 <i>Globocassidolina subglobosum</i>	-0.154 <i>Gyroidinoides orbicularis</i>	-0.105 <i>Pyrgo rotalaria</i>
-0.109 <i>Pyrgo murrhina</i>	-0.480 <i>Fissurina marginata</i>		-0.136 <i>Cibicidoides wuellerstorffii</i>

Table A 4.5 Varimax factor loading matix of core SO136-037BX.

No.	Depth (cm bsf)	Comm.	1	2	3	4
1	0.5	0.986	0.562	0.224	0.237	0.751
2	1.5	0.972	0.802	0.412	0.242	0.318
3	2.5	0.983	0.741	0.464	0.380	0.271
4	3.5	0.953	0.821	0.351	0.302	0.255
5	4.5	0.948	0.717	0.406	0.410	0.317
6	5.5	0.969	0.770	0.320	0.371	0.368
7	6.5	0.963	0.745	0.459	0.234	0.377
8	7.5	0.886	0.646	0.134	0.470	0.480
9	8.5	0.979	0.551	0.444	0.363	0.589
10	9.5	0.937	0.706	0.299	0.308	0.504
11	10.5	0.956	0.665	0.413	0.449	0.376
12	11.5	0.950	0.652	0.548	0.261	0.396
13	12.5	0.928	0.639	0.485	0.425	0.321
14	13.5	0.906	0.494	0.591	0.490	0.270
15	14.5	0.961	0.371	0.541	0.530	0.501
16	15.5	0.859	0.535	0.379	0.461	0.466
17	16.5	0.980	0.392	0.371	0.785	0.268
18	17.5	0.942	0.252	0.731	0.554	0.192
19	18.5	0.984	0.348	0.894	0.171	0.186
VARIANCE			38.659	22.643	17.343	16.307
CUM. VAR			38.659	61.302	78.645	94.952

Table A.4.6 Varimax factor scores matrix of core SO136-037BX. Species of ecological relevance are bold.

1 VAR.	2 VAR.	3 VAR.	4 VAR.
0.863 <i>Ehrenbergina mestayeri</i>	0.572 <i>Trifarina angulosa</i>	0.830 <i>Pyrgo</i> spp	0.611 <i>Tosaia hanzawai</i>
0.236 <i>Uvigerina peregrina</i>	0.512 <i>Epistominella exigua</i>	0.278 <i>Trifarina angulosa</i>	0.424 <i>Epistominella exigua</i>
0.218 <i>Pyrgo</i> spp	0.310 <i>Ehrenbergina glabra</i>	0.276 <i>Epistominella exigua</i>	0.420 <i>Pyrgo oblonga</i>
0.190 <i>Tosaia hanzawai</i>	0.261 <i>Ehrenbergina mestayeri</i>	0.207 <i>Tosaia hanzawai</i>	0.221 <i>Uvigerina peregrina</i>
0.128 <i>Textularia truncata</i>	0.140 <i>Pyrgo oblonga</i>	0.135 <i>Uvigerina schwageri</i>	0.111 <i>Textularia truncata</i>
0.125 <i>Cibicidoides fletcheri</i>	0.126 <i>Eggerellina brevis</i>	0.117 <i>Dentalina inorta</i>	0.094 <i>Heteroplea dutemplei</i>
0.098 <i>Fissurina orbignyana</i>	0.114 <i>Melonis balearum</i>	0.099 <i>Cibicidoides lobatus</i>	0.084 <i>Cibicidoides wuellerstorfi</i>
0.096 <i>Melonis balearum</i>	0.103 <i>Cibicidoides wuellerstorfi</i>	0.081 <i>Ehrenbergina glabra</i>	0.075 <i>Bulimina aculeata</i>
0.095 <i>Parafissurina ovata</i>	0.094 <i>Heteroplea dutemplei</i>	0.054 <i>Sigmoilopsis schlumbergerii</i>	0.069 <i>Parafissurina ovata</i>
0.078 <i>Fissurina marginata</i>	0.079 <i>Oolina melo</i>	0.041 <i>Fissurina marginata</i>	0.051 <i>Siphonotextularia rolshauseni</i>
0.077 <i>Cibicidoides wuellerstorfi</i>	0.071 <i>Siphonotextularia rolshauseni</i>	0.038 <i>Pyrgo oblonga</i>	0.049 <i>Cibicidoides lobatus</i>
0.069 <i>Quinqueloculina</i> spp	0.063 <i>Pulenia bulloides</i>	0.032 <i>Pyrgo rotalaria</i>	0.045 <i>Kariella siphonella</i>
0.065 <i>Cibicidoides inawagaensis</i>	0.053 <i>Cibicidoides mundulus</i>	0.031 <i>Eggerellina brevis</i>	0.030 <i>Globocassidolina subglobosa</i>
0.049 <i>Oridosalis umbunatus</i>	0.051 <i>Oridosalis umbunatus</i>	0.031 <i>Fissurina orbignyana</i>	0.018 <i>Cibicidoides inawagaensis</i>
0.047 <i>Pyrgo rotalaria</i>	0.047 <i>Parafissurina ovata</i>	0.017 <i>Cibicidoides fletcheri</i>	0.003 <i>Ehrenbergina glabra</i>
0.034 <i>Pulenia bulloides</i>	0.044 <i>Cibicidoides fletcheri</i>	0.014 <i>Bulimina aculeata</i>	-0.026 <i>Sigmoilopsis schlumbergerii</i>
0.033 <i>Bulimina aculeata</i>	0.042 <i>Globocassidolina subglobosa</i>	0.013 <i>Melonis balearum</i>	-0.028 <i>Uvigerina pigmea</i>
0.033 <i>Uvigerina pigmea</i>	0.030 <i>Sigmoilopsis schlumbergerii</i>	0.013 <i>Globocassidolina subglobosa</i>	-0.037 <i>Cibicidoides fletcheri</i>
0.026 <i>Dentalina inorta</i>	0.010 <i>Kariella siphonella</i>	0.012 <i>Cibicidoides mundulus</i>	-0.038 <i>Fissurina marginata</i>
0.018 <i>Cibicidoides mundulus</i>	0.008 <i>Fissurina orbignyana</i>	0.011 <i>Kariella siphonella</i>	-0.039 <i>Pulenia bulloides</i>
0.009 <i>Sigmoilopsis schlumbergerii</i>	0.007 <i>Uvigerina pigmea</i>	0.009 <i>Uvigerina pigmea</i>	-0.039 <i>Oridosalis umbunatus</i>
0.008 <i>Ehrenbergina glabra</i>	0.003 <i>Cibicidoides lobatus</i>	-0.001 <i>Cibicidoides inawagaensis</i>	-0.045 <i>Oolina melo</i>
0.004 <i>Oolina melo</i>	-0.013 <i>Uvigerina schwageri</i>	-0.002 <i>Siphonotextularia rolshauseni</i>	-0.055 <i>Eggerellina brevis</i>
0.003 <i>Kariella siphonella</i>	-0.017 <i>Pyrgo rotalaria</i>	-0.006 <i>Quinqueloculina</i> spp	-0.057 <i>Quinqueloculina</i> spp
-0.003 <i>Cibicidoides lobatus</i>	-0.031 <i>Quinqueloculina</i> spp	-0.010 <i>Oolina melo</i>	-0.059 <i>Melonis balearum</i>
-0.005 <i>Uvigerina schwageri</i>	-0.034 <i>Fissurina marginata</i>	-0.010 <i>Pulenia bulloides</i>	-0.074 <i>Cibicidoides mundulus</i>
-0.007 <i>Heteroplea dutemplei</i>	-0.034 <i>Cibicidoides inawagaensis</i>	-0.032 <i>Cibicidoides wuellerstorfi</i>	-0.085 <i>Uvigerina schwageri</i>
-0.008 <i>Globocassidolina subglobosa</i>	-0.041 <i>Dentalina inorta</i>	-0.033 <i>Oridosalis umbunatus</i>	-0.094 <i>Pyrgo rotalaria</i>
-0.012 <i>Pyrgo oblonga</i>	-0.046 <i>Bulimina aculeata</i>	-0.063 <i>Uvigerina peregrina</i>	-0.099 <i>Ehrenbergina mestayeri</i>
-0.022 <i>Siphonotextularia rolshauseni</i>	-0.061 <i>Textularia truncata</i>	-0.076 <i>Heteroplea dutemplei</i>	-0.141 <i>Fissurina orbignyana</i>
-0.061 <i>Eggerellina brevis</i>	-0.082 <i>Uvigerina peregrina</i>	-0.084 <i>Textularia truncata</i>	-0.145 <i>Dentalina inorta</i>
-0.086 <i>Trifarina angulosa</i>	-0.228 <i>Tosaia hanzawai</i>	-0.114 <i>Parafissurina ovata</i>	-0.161 <i>Pyrgo</i> spp
-0.119 <i>Epistominella exigua</i>	-0.283 <i>Pyrgo</i> spp	-0.157 <i>Ehrenbergina mestayeri</i>	-0.239 <i>Trifarina angulosa</i>

Table A 4.7 Varimax factor loading matrix fo core SO136-147BX.

No.	Depth (cm bsf)	Comm.	1	2	3	4
1	0.5	0.957	0.347	-0.749	0.385	-0.356
2	1.5	0.970	0.296	-0.838	0.299	-0.299
3	2.5	0.909	0.305	-0.411	0.685	-0.421
4	3.5	0.926	0.544	-0.378	0.326	-0.618
5	4.5	0.902	0.321	-0.368	0.438	-0.686
6	5.5	0.906	0.363	-0.531	0.312	-0.629
7	6.5	0.917	0.634	-0.515	0.453	-0.211
8	7.5	0.910	0.614	-0.289	0.445	-0.501
9	8.5	0.916	0.434	-0.381	0.701	-0.302
10	9.5	0.910	0.371	-0.523	0.607	-0.361
11	10.5	0.976	0.798	-0.344	0.288	-0.371
12	11.5	0.932	0.434	-0.645	0.350	-0.453
VARIANCE			23.025	27.455	21.424	20.839
CUM. VAR			23.025	50.480	71.904	92.742

Table A 4.8 Varimax factor scores matrix of core SO136-147BX. Species of ecological relevance are bold.

1 VAR.	2 VAR.	3 VAR.	4 VAR.
0.519 <i>Siphonotularia rolshauseni</i>	0.542 <i>Epistominella exigua</i>	0.717 <i>Bulimina aculeata</i>	0.424 <i>Pyrgo</i> spp
0.458 <i>Ehrenbergina glabra</i>	0.419 <i>Pulenia bulloides</i>	0.477 <i>Epistominella exigua</i>	0.314 <i>Laticarinina pauperata</i>
0.373 <i>Bulimina aculeata</i>	0.336 <i>Siphonotularia rolshauseni</i>	0.210 <i>Oridosalis</i> sp	0.287 <i>Pyrgo rotalaria</i>
0.189 <i>Pulenia quinqueloba</i>	0.210 <i>Globocassidolina subglobosa</i>	0.159 <i>Pyrgo</i> spp	0.259 <i>Globocassidolina subglobosa</i>
0.187 <i>Tosaia hanzawai</i>	0.181 <i>Triloculina tricarinata</i>	0.153 <i>Cibicidoides wuellerstorfi</i>	0.247 <i>Heteroplea dutemplei</i>
0.141 <i>Pyrgo</i> spp	0.172 <i>Tosaia hanzawai</i>	0.151 <i>Pulenia bulloides</i>	0.237 <i>Oolina caudigera</i>
0.128 <i>Cibicidoides mundulus</i>	0.171 <i>Cibicidoides wuellerstorfi</i>	0.119 <i>Cibicidoides fletcheri</i>	0.218 <i>Cibicidoides fletcheri</i>
0.125 <i>Parafissurina ovata</i>	0.163 <i>Lagena gracilis</i>	0.110 <i>Cruciloculina triangularia</i>	0.199 <i>Cibicidoides wuellerstorfi</i>
0.124 <i>Pulenia bulloides</i>	0.155 <i>Ehrenbergina glabra</i>	0.108 <i>Pyrgo tasmania</i>	0.197 <i>Pyrgo oblonga</i>
0.114 <i>Globocassidolina subglobosa</i>	0.150 <i>Pulenia quinqueloba</i>	0.102 <i>Heteroplea dutemplei</i>	0.166 <i>Tosaia hanzawai</i>
0.083 <i>Gyronoides nipponicus</i>	0.116 <i>Fissurina marginata</i>	0.100 <i>Fissurina marginata</i>	0.159 <i>Oridosalis umbunatus</i>
0.080 <i>Laticarinina pauperata</i>	0.115 <i>Nonionella iridea</i>	0.088 <i>Oridosalis umbunatus</i>	0.154 <i>Textularia truncata</i>
0.078 <i>Heteroplea dutemplei</i>	0.085 <i>Cibicidoides mundulus</i>	0.073 <i>Lagena gracilis</i>	0.143 <i>Triloculina tricarinata</i>
0.077 <i>Pyrgo tasmania</i>	0.072 <i>Parafissurina ovata</i>	0.069 <i>Suggrunda porosa</i>	0.133 <i>Epistominella exigua</i>
0.075 <i>Uvigerina peregrina</i>	0.055 <i>Gyronoides nipponicus</i>	0.041 <i>Cibicidoides mundulus</i>	0.133 <i>Pyrolina cylindroides</i>
0.073 <i>Cibicidoides fletcheri</i>	0.044 <i>Oridosalis</i> sp	0.026 <i>Gyronoides nipponicus</i>	0.115 <i>Uvigerina peregrina</i>
0.051 <i>Nonionella iridea</i>	0.038 <i>Oolina caudigera</i>	0.021 <i>Fissurina orbignyana</i>	0.092 <i>Siphonotularia rolshauseni</i>
0.036 <i>Pyrgo oblonga</i>	0.033 <i>Textularia truncata</i>	0.014 <i>Triloculina</i> sp	0.086 <i>Lagena gracilis</i>
0.028 <i>Fissurina orbignyana</i>	0.033 <i>Pyrolina cylindroides</i>	0.010 <i>Parafissurina ovata</i>	0.064 <i>Suggrunda porosa</i>
0.010 <i>Oolina caudigera</i>	0.025 <i>Oridosalis umbunatus</i>	0.009 <i>Nonionella iridea</i>	0.060 <i>Triloculina</i> sp
-0.014 <i>Suggrunda porosa</i>	0.017 <i>Pyrgo tasmania</i>	0.007 <i>Pyrgo oblonga</i>	0.053 <i>Fissurina marginata</i>
-0.021 <i>Triloculina</i> sp	0.003 <i>Cruciloculina triangularia</i>	0.001 <i>Pyrolina cylindroides</i>	0.034 <i>Pulenia quinqueloba</i>
-0.027 <i>Cruciloculina triangularia</i>	-0.008 <i>Fissurina orbignyana</i>	-0.017 <i>Uvigerina peregrina</i>	0.030 <i>Fissurina orbignyana</i>
-0.033 <i>Textularia truncata</i>	-0.013 <i>Suggrunda porosa</i>	-0.045 <i>Pyrgo rotalaria</i>	0.015 <i>Oridosalis</i> sp
-0.044 <i>Triloculina tricarinata</i>	-0.024 <i>Pyrgo rotalaria</i>	-0.055 <i>Laticarinina pauperata</i>	-0.010 <i>Ehrenbergina glabra</i>
-0.057 <i>Pyrgo rotalaria</i>	-0.026 <i>Uvigerina peregrina</i>	-0.065 <i>Textularia truncata</i>	-0.014 <i>Cibicidoides mundulus</i>
-0.068 <i>Oridosalis</i> sp	-0.034 <i>Triloculina</i> sp	-0.073 <i>Tosaia hanzawai</i>	-0.069 <i>Cruciloculina triangularia</i>
-0.076 <i>Oridosalis umbunatus</i>	-0.037 <i>Laticarinina pauperata</i>	-0.075 <i>Ehrenbergina glabra</i>	-0.072 <i>Parafissurina ovata</i>
-0.087 <i>Pyrolina cylindroides</i>	-0.062 <i>Pyrgo oblonga</i>	-0.079 <i>Globocassidolina subglobosa</i>	-0.074 <i>Bulimina aculeata</i>
-0.125 <i>Lagena gracilis</i>	-0.100 <i>Heteroplea dutemplei</i>	-0.084 <i>Pulenia quinqueloba</i>	-0.079 <i>Gyronoides nipponicus</i>
-0.138 <i>Fissurina marginata</i>	-0.109 <i>Cibicidoides fletcheri</i>	-0.086 <i>Oolina caudigera</i>	-0.086 <i>Nonionella iridea</i>
-0.196 <i>Cibicidoides wuellerstorfi</i>	-0.158 <i>Pyrgo</i> spp	-0.100 <i>Siphonotularia rolshauseni</i>	-0.104 <i>Pyrgo tasmania</i>
-0.301 <i>Epistominella exigua</i>	-0.324 <i>Bulimina aculeata</i>	-0.111 <i>Triloculina tricarinata</i>	-0.338 <i>Pulenia bulloides</i>

Table A 4.9 Varimax factor score matrix of core SO136-161BX.

No.	Depth (cm bsf)	Comm.	1	2	3	4
1	0.5	0.989	0.152	-0.981	-0.064	0.005
2	1.5	0.992	0.312	-0.939	-0.095	0.064
3	2.5	0.973	0.496	-0.839	-0.139	0.052
4	3.5	0.964	0.560	-0.788	-0.174	0.001
5	4.5	0.992	0.268	-0.955	-0.067	0.059
6	5.5	0.984	0.286	-0.937	-0.144	0.056
7	6.5	0.974	0.527	-0.810	-0.191	-0.059
8	7.5	0.960	0.618	-0.748	-0.126	0.053
9	8.5	0.969	0.633	-0.593	-0.457	-0.088
10	9.5	0.974	0.606	-0.657	-0.414	0.056
11	10.5	0.966	0.813	-0.459	-0.308	0.001
12	11.5	0.976	0.699	-0.591	-0.368	0.052
13	12.5	0.949	0.810	-0.505	-0.195	0.000
14	13.5	0.973	0.726	-0.560	-0.350	0.100
15	14.5	0.964	0.642	-0.609	-0.400	0.142
16	15.5	0.966	0.747	-0.540	-0.318	0.126
17	16.5	0.961	0.710	-0.563	-0.213	0.308
18	17.5	0.935	0.825	-0.318	-0.351	0.173
19	18.5	0.970	0.780	-0.470	-0.320	0.195
20	19.5	0.972	0.715	-0.623	-0.127	0.239
21	20.5	0.951	0.755	-0.547	-0.202	0.202
22	21.5	0.982	0.755	-0.557	-0.087	0.307
23	22.5	0.974	0.955	-0.162	0.000	0.187
24	23.5	0.954	0.893	-0.370	-0.043	0.134
25	24.5	0.949	0.917	-0.297	-0.121	-0.068
26	25.5	0.893	0.840	-0.359	-0.235	0.056
27	26.5	0.928	0.886	-0.286	-0.207	-0.139
28	27.5	0.950	0.938	-0.205	0.029	-0.165
VARIANCE			49.757	38.891	5.800	1.935
CUM. VAR			49.757	88.648	94.448	96.383

Table A 4.10 Varimax factor scores matrix of core SO136-161BX. Species of ecological relevance are bold.

1 VAR.	2 VAR.	3 VAR.	4 VAR.
0.886 <i>Uvigerina peregrina</i>	0.657 <i>Melonis balearum</i>	0.187 <i>Heteroplea dutemplei</i>	0.094 <i>Pyrgo</i> spp.
0.201 <i>Tosaia hanzawai</i>	0.484 <i>Heteroplea dutemplei</i>	0.176 <i>Globocassidolina subglobosa</i>	0.088 <i>Pulenia quinqueloba</i>
0.158 <i>Epistominella exigua</i>	0.266 <i>Pulenia bulloides</i>	0.109 <i>Pulenia bulloides</i>	0.075 <i>Pyrolina cylindroides</i>
0.136 <i>Pyrgo</i> spp.	0.255 <i>Globocassidolina subglobosa</i>	0.087 <i>Pulaniella asymetrica</i>	0.050 <i>Pyrgo oblonga</i>
0.117 <i>Cibicidoides mundulus</i>	0.163 <i>Epistominella exigua</i>	0.082 <i>Uvigerina peregrina</i>	0.049 <i>Nuttallides umbonifer</i>
0.114 <i>Pyrolina cylindroides</i>	0.154 <i>Ehrenbergina mestayeri</i>	0.071 <i>Triloculina tricarinata</i>	0.047 <i>Lenticulina rotulata</i>
0.112 <i>Heteroplea dutemplei</i>	0.098 <i>Pulenia quinqueloba</i>	0.063 <i>Furstenkonia contemplata</i>	0.030 <i>Nonionellina labradoricus</i>
0.101 <i>Melonis balearum</i>	0.091 <i>Pyrolina cylindroides</i>	0.062 <i>Melonis pompilioides</i>	0.010 <i>Triloculina tricarinata</i>
0.100 <i>Pulaniella asymetrica</i>	0.082 <i>Cibicidoides wuellerstorfi</i>	0.057 <i>Cibicidoides mundulus</i>	0.006 <i>Pyrgo tasmania</i>
0.091 <i>Oridosalis umbunatus</i>	0.072 <i>Triloculina tricarinata</i>	0.048 <i>Melonis balearum</i>	-0.001 <i>Uvigerina peregrina</i>
0.090 <i>Lenticulina rotulata</i>	0.068 <i>Pyrgo oblonga</i>	0.032 <i>Oridosalis umbunatus</i>	-0.001 <i>Cibicidoides fletcheri</i>
0.084 <i>Pyrgo tasmania</i>	0.058 <i>Oridosalis umbunatus</i>	0.031 <i>Cibicidoides fletcheri</i>	-0.009 <i>Gyronoides nipponicus</i>
0.072 <i>Triloculina tricarinata</i>	0.055 <i>Furstenkonia contemplata</i>	0.031 <i>Tosaia hanzawai</i>	-0.016 <i>Siphonotextularia rolshauseni</i>
0.052 <i>Nonionellina labradoricus</i>	0.053 <i>Pyrgo rotalaria</i>	0.028 <i>Nonionella iridea</i>	-0.027 <i>Furstenkonia contemplata</i>
0.042 <i>Cibicidoides fletcheri</i>	0.052 <i>Pyrgo</i> spp.	0.027 <i>Pyrgo rotalaria</i>	-0.029 <i>Oolina caudigera</i>
0.034 <i>Oolina caudigera</i>	0.050 <i>Pulaniella asymetrica</i>	0.027 <i>Pyrgo tasmania</i>	-0.030 <i>Cibicidoides wuellerstorfi</i>
0.027 <i>Gyronoides nipponicus</i>	0.041 <i>Cibicidoides fletcheri</i>	0.024 <i>Fissurina marginata</i>	-0.037 <i>Heteroplea dutemplei</i>
0.025 <i>Nuttallides umbonifer</i>	0.037 <i>Uvigerina auberiana</i>	0.023 <i>Nonionellina labradoricus</i>	-0.043 <i>Fissurina marginata</i>
0.023 <i>Fissurina marginata</i>	0.033 <i>Siphonotextularia rolshauseni</i>	0.000 <i>Gyronoides nipponicus</i>	-0.045 <i>Pyrgo rotalaria</i>
0.021 <i>Cibicidoides wuellerstorfi</i>	0.026 <i>Nonionellina labradoricus</i>	-0.006 <i>Melonis zandami</i>	-0.065 <i>Ehrenbergina mestayeri</i>
0.009 <i>Furstenkonia contemplata</i>	0.023 <i>Tosaia hanzawai</i>	-0.007 <i>Cibicidoides wuellerstorfi</i>	-0.076 <i>Cibicidoides mundulus</i>
0.003 <i>Pyrgo rotalaria</i>	0.016 <i>Fissurina marginata</i>	-0.009 <i>Oolina caudigera</i>	-0.082 <i>Uvigerina auberiana</i>
-0.006 <i>Pulenia bulloides</i>	0.005 <i>Nuttallides umbonifer</i>	-0.014 <i>Ehrenbergina mestayeri</i>	-0.093 <i>Oridosalis umbunatus</i>
-0.020 <i>Siphonotextularia rolshauseni</i>	0.000 <i>Gyronoides nipponicus</i>	-0.051 <i>Pyrolina cylindroides</i>	-0.094 <i>Pulaniella asymetrica</i>
-0.026 <i>Pulenia quinqueloba</i>	-0.019 <i>Cibicidoides mundulus</i>	-0.053 <i>Lenticulina rotulata</i>	-0.104 <i>Pulenia bulloides</i>
-0.027 <i>Globocassidolina subglobosa</i>	-0.020 <i>Oolina caudigera</i>	-0.067 <i>Pyrgo</i> spp.	-0.125 <i>Melonis balearum</i>
-0.036 <i>Melonis zandami</i>	-0.021 <i>Pyrgo tasmania</i>	-0.081 <i>Siphonotextularia rolshauseni</i>	-0.130 <i>Melonis zandami</i>
-0.038 <i>Nonionella iridea</i>	-0.031 <i>Nonionella iridea</i>	-0.111 <i>Pulenia quinqueloba</i>	-0.147 <i>Tosaia hanzawai</i>
-0.066 <i>Melonis pompilioides</i>	-0.038 <i>Lenticulina rotulata</i>	-0.114 <i>Uvigerina auberiana</i>	-0.147 <i>Nonionella iridea</i>
-0.076 <i>Ehrenbergina mestayeri</i>	-0.046 <i>Melonis zandami</i>	-0.215 <i>Pyrgo oblonga</i>	-0.174 <i>Globocassidolina subglobosa</i>
-0.093 <i>Uvigerina auberiana</i>	-0.187 <i>Uvigerina peregrina</i>	-0.220 <i>Nuttallides umbonifer</i>	-0.194 <i>Epistominella exigua</i>
-0.108 <i>Pyrgo oblonga</i>	-0.230 <i>Melonis pompilioides</i>	-0.864 <i>Epistominella exigua</i>	-0.879 <i>Melonis pompilioides</i>

Table A 4.11 Varimax factor loading matrix of core SO136-165BX.

No.	Depth (cm bsf)	Comm.	1	2	3	4
1	0.5	0.969	0.179	-0.968	-0.014	-0.007
2	1.5	0.975	0.261	-0.940	-0.138	0.063
3	2.5	0.979	0.265	-0.938	-0.160	0.058
4	3.5	0.977	0.319	-0.893	-0.267	0.084
5	4.5	0.961	0.270	-0.941	-0.044	0.040
6	5.5	0.960	0.263	-0.910	-0.231	0.094
7	6.5	0.953	0.279	-0.889	-0.285	0.057
8	7.5	0.962	0.280	-0.925	-0.167	0.029
9	8.5	0.964	0.423	-0.692	-0.540	0.118
10	9.5	0.955	0.468	-0.678	-0.469	0.239
11	10.5	0.915	0.455	-0.622	-0.537	0.181
12	11.5	0.897	0.466	-0.581	-0.550	0.198
13	12.5	0.924	0.555	-0.723	-0.256	0.164
14	13.5	0.910	0.599	-0.576	-0.385	0.267
15	14.5	0.925	0.328	-0.742	-0.239	0.458
16	15.5	0.926	0.611	-0.600	-0.309	0.312
17	16.5	0.933	0.704	-0.430	-0.321	0.386
18	17.5	0.943	0.801	-0.407	-0.322	0.178
19	18.5	0.926	0.727	-0.367	-0.511	-0.007
20	19.5	0.959	0.736	-0.381	-0.519	0.063
21	20.5	0.942	0.595	-0.140	-0.753	0.022
22	21.5	0.933	0.778	-0.438	-0.369	0.012
23	22.5	0.920	0.920	-0.151	-0.224	0.034
24	23.5	0.910	0.928	-0.155	-0.115	0.108
25	24.5	0.940	0.926	-0.285	-0.046	-0.010
26	25.5	0.962	0.882	-0.362	-0.164	0.160
27	26.5	0.929	0.832	-0.392	-0.289	-0.017
VARIANCE			36.089	42.738	12.466	2.970
CUM. VAR			36.089	78.828	91.294	94.264

Table A 4.12 Varimax factor scores matrix of core SO136-165BX. Species of ecological relevance are bold.

1 VAR.	2 VAR.	3 VAR.	4 VAR.
0.480 <i>Nuttallides umbonifer</i>	0.149 <i>Pyrolina cylindroides</i>	0.316 <i>Furstenkonia contemplata</i>	0.460 <i>Uvigerina peregrina</i>
0.349 <i>Pyrolina cylindroides</i>	0.061 <i>Pulenia quinqueloba</i>	0.294 <i>Heteroplea dutemplei</i>	0.366 <i>Melonis pomphiloides</i>
0.334 <i>Heteroplea dutemplei</i>	0.052 <i>Nuttallides umbonifer</i>	0.200 <i>Epistominella exigua</i>	0.297 <i>Pyrgo rotalaria</i>
0.268 <i>Melonis balearum</i>	0.017 <i>Heteroplea dutemplei</i>	0.175 <i>Melonis pomphiloides</i>	0.288 <i>Cassidella tegulata</i>
0.267 <i>Pulenia bulloides</i>	0.017 <i>Cibicidoides lobatulus</i>	0.156 <i>Nuttallides umbonifer</i>	0.249 <i>Heteroplea dutemplei</i>
0.244 <i>Uvigerina peregrina</i>	0.013 <i>Oolina caudigera</i>	0.133 <i>Globocassidolina subglobosum</i>	0.189 <i>Gyronoides nipponicus</i>
0.222 <i>Epistominella exigua</i>	0.010 <i>Dentalina baggi</i>	0.124 <i>Pulenia bulloides</i>	0.189 <i>Nonionella iridea</i>
0.214 <i>Cibicidoides wuellerstorffii</i>	0.009 <i>Ehrenbergina glabra</i>	0.120 <i>Cibicidoides wuellerstorffii</i>	0.145 <i>Cibicidoides mundulus</i>
0.211 <i>Oridosalis umbunatus</i>	0.007 <i>Cassidella tegulata</i>	0.112 <i>Siphonotularia rolshauseni</i>	0.119 <i>Globocassidolina subglobosum</i>
0.201 <i>Pulenia quinqueloba</i>	0.005 <i>Uvigerina peregrina</i>	0.090 <i>Oridosalis umbunatus</i>	0.116 <i>Pyrgo spp</i>
0.178 <i>Melonis pomphiloides</i>	0.001 <i>Pyrgo oblonga</i>	0.057 <i>Pulenia quinqueloba</i>	0.075 <i>Ehrenbergina glabra</i>
0.163 <i>Pyrgo spp</i>	-0.001 <i>Amphicoryna scalaris</i>	0.052 <i>Cassidella tegulata</i>	0.075 <i>Pulaniella asymmetrica</i>
0.108 <i>Cibicidoides lobatulus</i>	-0.017 <i>Nonionella iridea</i>	0.050 <i>Pyrgo spp</i>	0.072 <i>Dentalina baggi</i>
0.085 <i>Pyrgo oblonga</i>	-0.019 <i>Uvigerina auberiana</i>	0.044 <i>Cibicidoides mundulus</i>	0.069 <i>Tosaia hanzawai</i>
0.063 <i>Siphonotularia rolshauseni</i>	-0.019 <i>Pyrgo murrhina</i>	0.041 <i>Gyroidina neosoldanii</i>	0.054 <i>Oridosalis umbunatus</i>
0.058 <i>Oolina caudigera</i>	-0.035 <i>Pyrgo spp</i>	0.035 <i>Oolina caudigera</i>	0.050 <i>Fissurina marginata</i>
0.031 <i>Uvigerina auberiana</i>	-0.042 <i>Cibicidoides wuellerstorffii</i>	0.029 <i>Ehrenbergina mestayeri</i>	0.016 <i>Miliammina arenaca</i>
0.027 <i>Globocassidolina subglobosum</i>	-0.056 <i>Miliammina arenaca</i>	0.022 <i>Fissurina marginata</i>	0.009 <i>Cibicidoides lobatulus</i>
0.024 <i>Gyroidina neosoldanii</i>	-0.056 <i>Fissurina marginata</i>	-0.007 <i>Fissurina orbignyana</i>	0.008 <i>Ehrenbergina mestayeri</i>
0.024 <i>Ehrenbergina mestayeri</i>	-0.059 <i>Ehrenbergina mestayeri</i>	-0.008 <i>Miliammina arenaca</i>	0.008 <i>Fissurina orbignyana</i>
0.023 <i>Melonis zandami</i>	-0.059 <i>Cassidulina laevigata</i>	-0.010 <i>Amphicoryna scalaris</i>	0.007 <i>Nuttallides umbonifer</i>
0.023 <i>Pyrgo murrhina</i>	-0.059 <i>Pyrgo rotalaria</i>	-0.010 <i>Gyronoides nipponicus</i>	0.003 <i>Amphicoryna scalaris</i>
0.022 <i>Miliammina arenaca</i>	-0.060 <i>Siphonotularia rolshauseni</i>	-0.014 <i>Pyrgo rotalaria</i>	-0.003 <i>Melonis zandami</i>
0.006 <i>Tosaia hanzawai</i>	-0.060 <i>Gyronoides nipponicus</i>	-0.017 <i>Melonis zandami</i>	-0.007 <i>Oolina caudigera</i>
0.001 <i>Pulaniella asymmetrica</i>	-0.062 <i>Fissurina orbignyana</i>	-0.018 <i>Ehrenbergina glabra</i>	-0.009 <i>Siphonotularia rolshauseni</i>
-0.001 <i>Fissurina marginata</i>	-0.064 <i>Melonis pomphiloides</i>	-0.024 <i>Dentalina baggi</i>	-0.009 <i>Melonis balearum</i>
-0.003 <i>Dentalina baggi</i>	-0.068 <i>Melonis zandami</i>	-0.035 <i>Pyrgo oblonga</i>	-0.016 <i>Furstenkonia contemplata</i>
-0.004 <i>Ehrenbergina glabra</i>	-0.072 <i>Pulaniella asymmetrica</i>	-0.042 <i>Tosaia hanzawai</i>	-0.037 <i>Pyrgo murrhina</i>
-0.007 <i>Amphicoryna scalaris</i>	-0.087 <i>Gyroidina neosoldanii</i>	-0.045 <i>Nonionella iridea</i>	-0.057 <i>Gyroidina neosoldanii</i>
-0.018 <i>Cassidulina laevigata</i>	-0.115 <i>Cibicidoides mundulus</i>	-0.047 <i>Uvigerina auberiana</i>	-0.065 <i>Uvigerina auberiana</i>
-0.018 <i>Fissurina orbignyana</i>	-0.122 <i>Globocassidolina subglobosum</i>	-0.065 <i>Pyrolina cylindroides</i>	-0.092 <i>Cassidulina laevigata</i>
-0.027 <i>Cibicidoides mundulus</i>	-0.124 <i>Oridosalis umbunatus</i>	-0.068 <i>Pyrgo murrhina</i>	-0.109 <i>Cibicidoides wuellerstorffii</i>
-0.031 <i>Cassidella tegulata</i>	-0.125 <i>Pulenia bulloides</i>	-0.071 <i>Cassidulina laevigata</i>	-0.117 <i>Pulenia bulloides</i>
-0.039 <i>Pyrgo rotalaria</i>	-0.183 <i>Tosaia hanzawai</i>	-0.098 <i>Pulaniella asymmetrica</i>	-0.128 <i>Pulenia quinqueloba</i>
-0.041 <i>Gyronoides nipponicus</i>	-0.270 <i>Epistominella exigua</i>	-0.166 <i>Uvigerina peregrina</i>	-0.129 <i>Pyrgo oblonga</i>
-0.044 <i>Nonionella iridea</i>	-0.456 <i>Melonis balearum</i>	-0.174 <i>Cibicidoides lobatulus</i>	-0.228 <i>Pyrolina cylindroides</i>
-0.237 <i>Furstenkonia contemplata</i>	-0.737 <i>Furstenkonia contemplata</i>	-0.739 <i>Melonis balearum</i>	-0.381 <i>Epistominella exigua</i>

A5 DATA SET OF PHYSICAL AND PHYSICOCHEMICAL SEDIMENT PROPERTIES

Table A 5.1 Physical and physicochemical sediment properties of core SO136-019BX

Depth (cm bsf)	Water content (wt%)	Grain fraction >63 (wt%)	Grain fraction >150 (µm / >63µm)	TC (wt%)	TOC (wt%)	CaCO ₃ (wt%)	CaCO ₃ (wt%) shipboard	TN (wt%)	C/N	Photosp (SO) 400 vvm	Photosp (SO) 700 vvm	Photosp (SO) L* - value	G. bulloides δ ¹³ O (‰ vs PDB)	G. bulloides δ ¹³ C (‰ vs PDB)	C. wuellestorffii δ ¹³ O (‰ vs PDB)	C. wuellestorffii δ ¹³ C (‰ vs PDB)	DBD (g/cm ³)	WBD (g/cm ³)		
0.5	44.45	48.11	23.95	0.50	7.16	0.20	57.97	53.00	0.02	8.26	12.12	31.87	54.77	2.60	0.64					
1.5	45.71	46.30	25.16	0.54	7.51	0.18	61.02		0.02	9.22	12.12	31.87	54.77	2.72	0.05	1.85	-0.55	0.59	1.06	
2.5	45.86	46.40	25.79	0.56	7.83	0.13	64.07		0.01	9.99	14.69	36.53	59.26	2.59	0.41	2.21	-0.28	0.59	1.06	
3.5	45.84	48.97	29.23	0.60	8.15	0.12	66.85		0.01	12.40	15.12	36.69	59.39	2.82	0.28					
4.5	46.01	48.55	29.07	0.60	8.35	0.13	68.53		0.01	9.48	15.40	38.65	60.53	2.53	0.54		3.88	-0.03	0.59	1.06
5.5	46.97	49.71	30.40	0.61	8.74	0.13	71.73		0.02	7.96	14.90	38.16	59.88	2.82	0.20		2.74	-0.47	0.58	1.06
6.5	47.82	46.26	28.10	0.61	8.54	0.09	70.43	37.00	0.01	6.79	14.33	37.10	58.87	2.86	0.19		3.46	0.17	0.57	1.06
7.5	48.05	45.34	27.08	0.60	8.26	0.07	68.20		0.01	5.00	12.98	36.29	57.70	3.03	0.36		3.65	0.17	0.57	1.06
8.5	48.01	46.15	27.67	0.60	8.19	0.08	67.57		0.03	2.85	12.71	35.63	57.30	2.96	0.41		3.75	0.07	0.57	1.06
9.5	48.21	46.23	27.10	0.59	8.00	0.09	65.86	61.00	0.03	2.60	13.11	35.37	57.43	3.08	0.23		1.11	-0.79	0.57	1.06
10.5	47.81	51.45	32.53	0.63	7.89	0.08	65.09		0.04	1.89	11.68	33.58	55.66	3.05	0.21		-0.75	-1.33	0.57	1.06
11.5	47.35	51.17	32.00	0.63	7.53	0.07	62.17		0.03	2.46	13.54	37.66	59.34	3.20	0.40		4.12	-0.26	0.58	1.06
12.5	48.06	55.26	35.93	0.65	6.77	0.08	55.75		0.03	2.76	12.29	34.03	56.27	3.22	0.28		5.23	0.29	0.57	1.06
13.5	47.71	46.98	30.10	0.64	6.55	0.07	53.96		0.03	2.45	11.34	31.75	54.21	3.12	0.35		4.01	-0.24	0.57	1.06
14.5	46.56	47.76	31.29	0.66	5.77	0.08	47.33		0.03	3.07	10.30	28.96	52.08	3.22	0.32		2.91	-0.53	0.58	1.06
15.5	44.66	45.79	29.84	0.65	4.83	0.08	39.54		0.03	2.93	10.32	29.42	52.45	3.19	0.55		3.73	-0.72	0.60	1.06
16.5	43.21	49.95	33.18	0.66	4.36	0.10	35.46		0.03	3.95	9.61	27.24	50.67	3.00	-0.01			0.62	1.06	
17.5	42.60	48.41	31.54	0.65	4.04	0.07	33.08		0.03	2.43	9.60	25.87	50.00	3.38	0.57		4.69	0.15	0.62	1.06
18.5	42.12	49.31	33.41	0.68	4.19	0.08	34.22		0.03	2.51	9.42	24.40	49.01	3.45	0.56		3.47	-0.48	0.63	1.06
19.5	44.00	49.42	33.73	0.68	5.57	0.07	45.74	36.00	0.02	3.62	10.34	26.64	50.90	3.08	0.29		3.78	-0.29	0.61	1.06
20.5	44.69	49.87	34.27	0.69	5.72	0.07	47.06		0.02	4.34	10.32	25.98	51.24	3.34	0.60		4.82	0.59	0.60	1.06
21.5	43.25	61.22	44.47	0.73	5.98	0.04	49.48		0.02	2.51	10.69	26.95	52.20	2.99	0.56		1.96	-0.26	0.62	1.06
22.5	45.12	67.53	51.70	0.77	6.61	0.07	54.48		0.01	6.79	10.64	27.55	52.00	3.31	0.28		3.30	0.02	0.60	1.06
23.5	43.72	65.78	49.58	0.75	5.52	0.02	45.82		0.01	1.79	10.99	26.94	51.57	3.21	0.43		3.76	-0.09	0.61	1.06
24.5	39.16	61.48	60.44	0.98	3.95	0.05	32.50		0.04	1.23	11.82	29.30	53.35	3.32	0.42			0.66	1.06	
25.5	35.59	67.97	54.16	0.80	3.78	0.08	30.83		0.03	3.01	10.53	25.48	49.00	3.11	0.48		1.36	-1.00	0.70	1.06
26.5	32.45	74.55	60.43	0.81	3.47	0.06	28.44		0.04	1.42	10.53	25.48	50.34	3.15	0.67		3.35	-0.02	0.73	1.06
27.5	32.27	74.41	61.72	0.83	3.33	0.08	27.08		0.04	2.13	10.75	24.45	49.51	2.95	0.26		3.36	-0.10	0.73	1.06
28.5	32.49	81.03	68.04	0.84	3.17	0.05	25.98	24.50	0.04	1.35	9.65	19.80	45.43	3.09	0.91		3.04	-0.09	0.73	1.06
29.5	31.75	88.18	76.53	0.87	3.08	0.07	25.03		0.04	2.01	12.95	21.33	48.37	3.28	0.68			0.74	1.06	
30.5	35.43	82.88	70.65	0.85	4.26	0.06	35.02		0.03	1.88	11.22	24.94	49.61	2.86	0.94		2.89	0.14	0.70	1.06
31.5	38.81	83.32	70.73	0.85	4.81	0.05	39.62		0.27	0.19	8.88	18.58	43.68	3.06	0.86		2.84	-0.02	0.66	1.06
32.5	40.47	79.80	64.79	0.81	5.18	0.04	42.83		0.03	1.70	11.54	24.70	49.74	2.69	0.68		3.26	0.13	0.65	1.06
33.5	41.56	72.82	57.12	0.78	5.75	0.03	47.72		0.03	0.91	12.49	31.53	54.23	2.93	0.98		2.84	0.12	0.63	1.06
34.5	36.55	79.66	66.53	0.84	4.54	0.07	37.19		0.04	1.72	11.52	28.87	52.51	3.00	0.86		3.51	-0.23	0.69	1.06
35.5	34.49	83.91	72.05	0.86	3.87	0.05	31.77	34.00	0.04	1.45	10.98	24.06	49.49	3.02	0.97		4.24	-0.46	0.71	1.06
36.5	31.83	83.21	68.36	0.82	3.58	0.05	29.38		0.04	1.43	10.98	24.06	49.49	3.04	0.97		3.87	-0.55	0.73	1.06

overlapping sampled

Table A 5.2 Physical and physicochemical sediment properties of core SO136-025BX

Depth (cm bsf)	Water content (wt%)	Grain fraction >63 (wt%)	Grain fraction >150 (wt%)	>150μm / >63μm	TC (wt%)	TOC (wt%)	CaCO ₃ (wt%)	CaCO ₃ (wt%) shipboard	TN (wt%)	C/N	Photosp (SO) 400 vvm	Photosp (SO) 700 vvm	Photosp (SO) L* - value	G.bulloides δ¹³C (‰ vs PDB)	G.bulloides δ¹³C (‰ vs PDB)	C.wuellerstorff δ¹³C (‰ vs PDB)	WBD (g/cm³)
0.5	51.41	91.65	86.53	0.94	10.41	0.11	85.54	87.00	0.01	15.47	21.92	40.97	63.55	3.03	0.04	3.35	-0.14 0.53 1.06
1.5	46.30	81.39	67.12	0.82	9.63	0.11	79.24		0.01	11.38	21.92	40.97	63.55	2.63	0.40	no forams	0.59 0.93
2.5	52.55	72.88	55.95	0.77	9.99	0.04	82.91		0.01	3.87	19.42	40.32	62.44	2.76	0.17	3.92	0.14 0.52 1.06
3.5	36.74	75.39	57.55	0.78	10.098	0.04	83.76		0.01	5.56	20.20	41.94	63.44	2.84	0.14	3.53	0.19 0.68 1.06
4.5	45.45	77.72	62.65	0.81	9.995	0.03	82.99	73.00	0.00	6.51	20.88	42.46	63.49	2.48	0.00	4.37	-0.01 0.59 1.06
5.5	50.55	72.62	56.53	0.81	7.878	0.02	65.54		0.01	2.96	15.67	39.10	61.01	3.31	-0.04	4.38	-0.34 0.54 1.06
6.5	62.97	31.99	17.75	0.55	1.534	0.02	12.65		0.01	1.52	10.15	35.53	58.66	3.31	0.46	no forams	0.42 1.06
7.5	67.78	19.01	3.45	0.19	0.176	0.02	1.27		0.01	2.49	9.49	29.49	54.22	3.18	0.34	no forams	0.37 1.06
8.5	67.99	15.01	2.46	0.16	0.123	0.03	0.75		0.01	3.12	8.46	33.48	56.39	3.04	0.10	no forams	0.36 1.06
9.5	68.01	13.92	2.01	0.14	0.059	0.04	0.17	1.00	0.01	4.21	9.98	32.54	56.36	3.91	0.17	no forams	0.36 0.96
10.5	68.34	13.87	1.38	0.10	0.068	0.03	0.30		0.01	3.08	9.70	31.50	55.64	1.89	-0.22	no forams	0.38 0.96
11.5	68.57	11.60	1.17	0.10	0.052	0.04	0.09		0.01	4.80	9.70	31.50	55.64	2.26	0.28	no forams	0.36 1.06

amount of planktic forams decreases downcore
3 plankt. Forams in the whole sample

Table A 5.3 Physical and physicochemical sediment properties of core SO136-037BX

Depth (cm bsf)	Water content (wt%)	Grain fraction >63 (wt%)	Grain fraction >150 (wt%)	>150μm / >63μm	TC (wt%)	TOC (wt%)	CaCO ₃ (wt%)	CaCO ₃ (wt%) shipboard	TN (wt%)	C/N	Photosp (SO) 400 vvm	Photosp (SO) 700 vvm	Photosp (SO) L* - value	G.bulloides δ¹³C (‰ vs PDB)	G.bulloides δ¹³C (‰ vs PDB)	C.wuellerstorff δ¹³C (‰ vs PDB)	WBD (g/cm³)		
0.5	47.40	65.16	35.72	0.55	11.31	0.47	90.31	86.50	0.03	18.34	31.30	53.09	73.49	2.39	0.21	3.09	0.54 0.57 1.06		
1.5	46.05	60.77	33.19	0.55	11.32	0.35	91.41		0.03	13.64	31.31	53.09	73.49	2.33	0.69	2.67	0.84 0.59 1.06		
2.5	45.38	60.74	33.70	0.55	11.52	0.30	93.43		0.02	18.46	31.30	53.09	73.49	2.47	0.61	2.84	0.88 0.60 1.06		
3.5	44.53	60.52	32.54	0.54	11.37	0.16	93.36		0.02	7.55	29.48	52.30	72.53	2.46	0.42	2.78	0.88 0.60 1.06		
4.5	44.53	61.78	35.00	0.57	11.38	0.12	93.83	88.00	0.10	59.0	0.12	87.25	0.14	0.81	29.81	52.63	72.84	2.46 0.22 2.72	
5.5	43.49	60.38	33.46	0.55	11.43	0.17	93.77		0.02	10.19	33.76	55.96	75.51	2.27	0.52	2.84	0.87 0.61 1.06		
6.5	42.90	60.29	31.18	0.52	11.51	0.15	94.61		0.01	22.88	33.53	56.38	75.73	2.22	0.55	2.78	0.70 0.62 1.06		
7.5	43.62	61.03	33.23	0.54	11.42	0.23	93.16		0.02	12.84	37.28	57.98	77.39	2.54	0.56	2.60	0.73 0.61 1.06		
8.5	43.31	61.61	32.59	0.53	11.46	0.16	94.15		0.01	11.52	38.38	57.16	77.31	2.59	0.33	2.69	0.95 0.62 1.06		
9.5	43.00	60.44	30.50	0.50	11.43	0.16	93.87	88.00	0.01	10.77	37.27	57.05	76.97	2.42	0.39	2.72	0.91 0.62 1.06		
10.5	42.87	64.47	36.05	0.56	11.55	0.13	95.12		0.01	18.10	39.72	59.94	78.60	2.81	0.26	2.91	0.78 0.62 1.06		
11.5	43.26	63.13	35.08	0.56	11.54	0.17	94.70		0.01	31.56	37.89	56.61	76.95	2.40	0.42	2.68	0.92 0.62 1.06		
12.5	42.83	62.46	34.45	0.55	11.32	0.14	93.08		0.02	8.92	35.78	53.46	75.24	2.47	0.60	2.99	0.78 0.62 1.06		
13.5	42.23	63.90	36.99	0.58	11.40	0.09	94.22		0.02	5.70	38.60	55.94	77.05	2.44	0.38	2.90	0.52 0.63 1.06		
14.5	41.79	63.52	37.29	0.59	11.55	0.09	95.42	10.65	0.09	87.93	0.01	8.04	40.24	57.48	77.99	2.79	0.50	2.67	0.79 0.63 1.06
15.5	42.27	65.48	40.40	0.62	11.34	0.16	93.15		0.01	20.57	39.60	56.14	77.81	2.66	0.38	2.74	0.89 0.63 1.06		
16.5	41.82	66.80	39.73	0.59	11.42	0.13	94.05		0.01	16.43	35.58	51.90	75.18	2.58	0.43	1.46	-1.04 0.63 1.06		
17.5	41.23	64.50	36.82	0.57	11.44	0.11	94.33	87.50	0.02	5.91	37.74	53.02	76.52	2.06	0.42	3.04	0.69 0.64 1.06		
18.5	41.44	64.49	35.01	0.54	11.44	0.15	94.08		0.01	13.92	36.05	51.03	75.00	2.58	0.29	Analyser failure	Analyser failure 0.64 1.06		

Table A 5.4 Physical and physicochemical sediment properties of core SO136-147BX

Depth (cm bsf)	Water content (wt%)	Grain fraction >63 (wt%)										Grain fraction >150 (wt%)										>150µm / >63µm									
		TC (wt%)	TOC (wt%)	CaCO ₃ (wt%)	CaCO ₃ (wt%) shipboard	L	LECO TC (wt%)	LECO Corg (wt%)	LECO CaCO ₃ (wt%)	TN (wt%)	C/N	Photosp (SO) 400 vvm	Photosp (SO) 700 vvm	L* - value	G.bulloides	δ ₁₈ O (‰ vs PDB)	G.bulloides	δ ₁₃ C (‰ vs PDB)	C.wuellerstorffii	δ ₁₃ C (‰ vs PDB)	DBD (g/cm ³)	WBD (g/cm ³)	Trend of (C/N)/(LECO)								
0.5	45.70	43.10	15.73	0.37	11.29	0.45	90.28	91.00	10.91	0.14	89.68	0.07	2.11	32.01	53.51	73.51	2.16	0.29	3.80	0.20	0.59	1.06	1.01								
1.5	43.76	39.14	14.00	0.36	11.35	0.22	92.73		11.06	0.11	91.19	0.06	2.04	32.01	53.51	73.51	2.60	0.30	2.81	0.47	0.61	1.06	1.02								
2.5	42.57	39.43	14.14	0.36	11.37	0.14	93.49		11.15	0.09	92.13	0.06	1.43	32.01	53.51	73.51	2.26	0.31	2.34	0.60	0.62	1.06	1.01								
3.5	42.52	36.98	13.20	0.36	11.32	0.18	92.80		10.82	0.11	89.24	0.12	0.86	31.56	51.24	72.33	2.00	0.13	Analyser failure	Analyser failure	0.62	1.06	1.04								
4.5	42.22	38.51	13.97	0.36	11.45	0.08	94.74	90.50	10.93	0.11	90.13	0.02	5.21	34.25	57.02	75.35	2.83	0.16	3.08	-0.30	0.63	1.06	1.05								
5.5	42.19	39.72	15.19	0.38	11.49	0.15	94.48		11.17	0.11	92.14	0.03	3.66	33.30	56.02	74.72	1.57	-0.01	3.18	0.45	0.63	1.06	1.03								
6.5	41.57	40.46	14.88	0.37	11.53	0.25	94.00		11.01	0.09	90.95	0.03	3.34	33.36	57.11	75.00	2.45	0.09	2.56	0.35	0.63	1.06	1.03								
7.5	41.20	40.69	16.12	0.40	11.49	0.10	94.83		11.00	0.09	90.85	0.03	3.44	34.79	58.31	75.83	1.83	0.06	2.51	-0.14	0.64	1.06	1.04								
8.5	40.79	42.66	17.64	0.41	11.47	0.36	92.53		10.96	0.08	90.61	0.03	2.98	32.78	55.67	74.17	2.25	0.03	2.63	0.31	0.64	1.06	1.02								
9.5	41.02	40.55	16.86	0.42	11.41	0.41	91.68	90.50	10.84	0.12	89.31	0.16	0.72	36.96	61.82	77.36	2.35	0.37	3.04	0.19	0.64	1.06	1.03								
10.5	40.52	41.09	16.59	0.40	11.44	0.11	94.36		10.77	0.10	88.89	0.02	5.27	34.76	59.93	75.84	3.04	0.10	1.96	0.17	0.65	1.06	1.06								
11.5	39.91	40.46	17.29	0.43	11.69	0.08	96.68		10.98	0.08	90.79	0.01	10.23	34.90	61.03	76.49	2.33	0.18	2.53	0.27	0.65	1.06	1.06								

Table A 5.5 Physical and physicochemical sediment properties of core SO136-161BX

Table A 5.6 Physical and physicochemical sediment properties of core SO136-165BX

Depth (cm bs)	Water content (wt%)	Grain fraction >63 (wt%)	Grain fraction >150 (wt%)	>150µm / >63µm	TC (wt%)	TOC (wt%)	CaCO ₃ (wt%)	CaCO ₃ (wt%) shipboard	TN (wt%)	C/N	Photosp (SO) 400 v/m	Photosp (SO) 700 v/m	Photosp (SO) L* - value	G.bullaoides	δ ¹⁸ O (‰ vs PDB)	G.bullaoides	δ ¹³ C (‰ vs PDB)	C. wuellerstorffii	δ ¹³ C (‰ vs PDB)	δ ¹⁸ O (‰ vs PDB)	DBD (g/cm ³)	WBD (g/cm ³)
0.5 53.13	6.02	2.46	0.41	9.36	0.39	74.73	not measured	0.07	5.39	17.18	41.54	62.66	1.85	0.89			2.59		0.14	0.52	1.06	ca. 90% fragments of foraminifera
1.5 50.97	5.47	2.11	0.39	9.48	0.33	76.15		0.05	6.31	17.18	41.54	62.66	0.83	-0.24			2.74		0.15	0.54	1.06	tests disintegrate when touched
2.5 50.49	5.85	2.24	0.38	9.52	0.32	76.58		0.05	6.89	17.09	40.45	62.14	1.29	-0.05			2.64		0.45	0.54	1.06	
3.5 48.75	5.58	2.21	0.40	9.45	0.27	76.45		0.04	6.43	16.99	42.35	62.98	1.93	-0.01			2.72		0.36	0.56	1.06	
4.5 48.48	5.54	2.05	0.37	9.52	0.28	77.03		0.04	6.86	18.68	43.65	64.23	1.50	0.37			2.51		0.50	0.56	1.06	
5.5 47.67	4.77	1.73	0.36	9.50	0.31	76.57		0.04	8.37	18.42	34.72	59.36	1.84	0.18			2.71		-0.01	0.57	1.06	
6.5 47.48	5.20	1.83	0.35	9.52	0.32	76.68		0.04	8.09	17.22	41.14	62.50	1.04	-0.50			2.69		0.29	0.57	1.06	
7.5 47.14	5.12	1.77	0.35	9.53	0.29	76.91		0.04	7.29	18.20	42.38	63.34	0.84	-0.30			2.95		0.16	0.58	1.06	
8.5 46.15	4.99	1.65	0.33	9.62	0.27	77.87		0.03	7.80	18.19	43.14	63.78	1.36	-0.05			2.83		0.53	0.59	1.06	
9.5 45.53	5.36	1.81	0.34	9.73	0.26	78.86		0.02	15.43	17.84	43.60	63.80	1.20	-0.44			2.77		0.11	0.59	1.06	
10.5 45.35	5.53	2.06	0.37	9.68	0.21	78.91		0.02	11.46	18.45	43.49	63.85	1.59	-0.12			2.76		0.04	0.60	1.06	
11.5 45.08	6.47	2.44	0.38	9.70	0.20	79.11		0.02	9.12	18.08	43.36	63.66	1.38	-0.09			3.34		-0.09	0.60	1.06	
12.5 45.15	7.15	2.66	0.37	9.62	0.19	78.55		0.02	10.16	18.96	44.41	64.66	1.81	0.01			2.91		0.46	0.60	1.06	
13.5 45.42	8.36	3.37	0.40	9.68	0.28	78.25		0.03	11.09	19.18	45.43	65.09	1.00	-0.34			0.45		0.33	0.60	1.06	
14.5 45.67	8.72	3.68	0.42	9.69	0.16	79.37		0.02	9.63	18.36	45.54	64.81	2.48	0.21			2.46		0.46	0.59	1.06	
15.5 45.44	9.01	3.97	0.44	9.66	0.25	78.34		0.02	14.28	18.28	45.56	64.80	1.67	0.47			2.72		0.24	0.59	1.06	
16.5 46.06	10.17	4.48	0.44	9.64	0.16	78.92		0.01	12.39	19.05	45.82	65.17	1.35	-0.47			2.75		0.44	0.59	1.06	
17.5 46.48	10.77	4.97	0.46	9.54	0.15	78.27		0.02	8.74	17.41	43.08	63.43	1.74	-0.17	Analyser failure	Analyser failure	0.58	1.06				
18.5 47.70	11.10	5.03	0.45	9.56	0.16	78.34		0.01	12.96	19.02	44.41	64.52	1.63	-0.08			2.99		0.46	0.57	1.06	
19.5 47.67	12.23	6.07	0.50	9.51	0.20	77.51		0.04	5.12	21.68	45.40	65.83	2.17	0.31			3.47		-0.05	0.57	1.06	
20.5 47.45	14.87	7.60	0.51	9.48	0.21	77.24		0.03	7.30	17.42	43.72	63.85	1.19	-0.84			4.05		-0.29	0.57	1.06	
21.5 47.53	14.61	7.72	0.53	9.62	0.19	78.57		0.03	5.63	18.35	43.33	63.85	1.01	-0.50			3.31		-0.15	0.57	1.06	
22.5 47.76	16.16	8.40	0.52	9.66	0.20	78.81		0.03	6.29	18.83	45.38	65.26	1.66	-0.46			3.82		-0.45	0.57	1.06	
23.5 47.88	15.14	8.34	0.55	9.63	0.21	78.47		0.03	7.37	18.56	44.66	64.60	1.43	-0.61			3.49		-0.70	0.57	1.06	
24.5 48.38	14.89	8.17	0.55	9.66	0.21	78.68		0.02	8.75	17.71	44.11	64.18	1.26	-0.59			3.90		-0.32	0.56	1.06	
25.5 49.47	15.94	8.57	0.54	9.74	0.17	79.66		0.03	6.30	18.29	45.22	64.87	1.71	-0.20			3.24		0.26	0.55	1.06	
26.5 49.43	15.73	8.57	0.54	9.64	0.27	78.09		0.02	15.57	18.75	45.94	65.31	1.68	-0.26			2.29		-0.21	0.55	1.06	

A6 AMS ¹⁴C RADIOCARBON DATA**Table A 6.1** Conventional AMS ¹⁴C ages

Core	Depth (cm bsf)	Weight of C (mg)	Corrected pMC (%)	Conventional age (a BP)	$\delta^{13}\text{C}$ (‰ vs. PDB)
SO136-147BX	4.5	1.2	41.01 ± 0.28	7160 ± 55	1.73 ± 0.14
SO136-147BX	9.5	1.2	37.19 ± 0.32	7950 ± 70	2.00 ± 0.11
SO136-161BX	7.5	1.1	58.10 ± 0.27	4360 ± 40	1.58 ± 0.18
SO136-161BX	22.5	1.1	29.06 ± 0.20	9925 ± 55	0.47 ± 0.14
SO136-165BX	13.5	1.1	40.60 ± 0.47	7240 ± 90	1.21 ± 0.13
SO136-165BX	21.5	1.0	28.23 ± 0.19	10160 ± 55	0.88 ± 0.14

Table A 6.2 Correction of conventional ¹⁴C ages

UNIVERSITY OF WASHINGTON
QUATERNARY ISOTOPE LAB
RADIOCARBON CALIBRATION PROGRAM REV 4.1.2

Calibration file: marine98.14c, 100.0% marine carbon

SO136-147BX depth: 4.5

Radiocarbon Age BP 7160 +/- 55

Reservoir corrected age BP 6758 +/- 55

Reference: STUIVER *et al.*,

(1998a)

Calibrated age(s) cal BP 7616

cal BP age ranges obtained from intercepts (Method A): two Sigma* cal BP 7716 - 7547

Summary of above:

Maximum of cal age ranges (cal ages) minimum of cal age ranges:

2 sigma cal BP 7717 (7616) 7548

SO136-147BX depth: 9.5

Radiocarbon Age BP 7950 +/- 70

Reservoir corrected age BP 7548 +/- 70

Reference: STUIVER *et al.*, (1998a)

Calibrated age(s) cal BP 8387

cal BP age ranges obtained from intercepts (Method A): two Sigma* cal BP 8567 - 8281

Summary of above:

Maximum of cal age ranges (cal ages) minimum of cal age ranges:

2 sigma cal BP 8568 (8387) 8282

SO136-161BX depth: 13.5

Radiocarbon Age BP 7240 +/- 90

Reservoir corrected age BP 6838 +/- 90

Reference: STUIVER *et al.*, (1998a)

Calibrated age(s) cal BP 7678

cal BP age ranges obtained from intercepts (Method A): two Sigma* cal BP 7867 - 7553

Summary of above:

Maximum of cal age ranges (cal ages) minimum of cal age ranges:

2 sigma cal BP 7868 (7678) 7554

SO136-161BX depth: 10160

Radiocarbon Age BP 10160 +/- 55

Reservoir corrected age BP 9758 +/- 55

Reference: STUIVER *et al.*, (1998a)

Calibrated age(s) cal BP 11116, [10963], [10857]

cal BP age ranges obtained from intercepts (Method A):

two Sigma* cal BP 11603 - 11495 11329 - 11242

11220 - [10926] [10898]- 10821

10693 - 10640 10569 - 10569

Summary of above:

Maximum of cal age ranges (cal ages) minimum of cal age ranges:

2 sigma cal BP 11604 (11116, [10963], [10857]) 10570

SO136-165BX depth: 7.5

Radiocarbon Age BP 4360 +/- 40

Reservoir corrected age BP 3958 +/- 40

Reference: STUIVER *et al.*, (1998a)

Calibrated age(s) cal BP 4497

cal BP age ranges obtained from intercepts (Method A): two Sigma* cal BP 4600 - 4397

Summary of above:

Maximum of cal age ranges (cal ages) minimum of cal age ranges:

2 sigma cal BP 4600 (4497) 4397

SO136-165BX depth: 22.5

Radiocarbon Age BP 9925 +/- 55

Reservoir corrected age BP 9523 +/- 55

Reference: STUIVER *et al.*, (1998a)

Calibrated age(s) cal BP 10795

cal BP age ranges obtained from intercepts (Method A):

two Sigma* cal BP 11162 – [10955] [10870] - 10331

Summary of above:

Maximum of cal age ranges (cal ages) minimum of cal age ranges:

2 sigma cal BP 11163 (10795) 10322

Comments:

* 2 sigma = $2 \times \sqrt{\text{sample std. dev.}^2 + \Delta R \text{ uncertainty}^2}$ where $\wedge 2$ = quantity squared.

[] = Calibrated with an uncertain region or a linear extension to the calibration curve

A7 PHOTOS OF EACH CORE

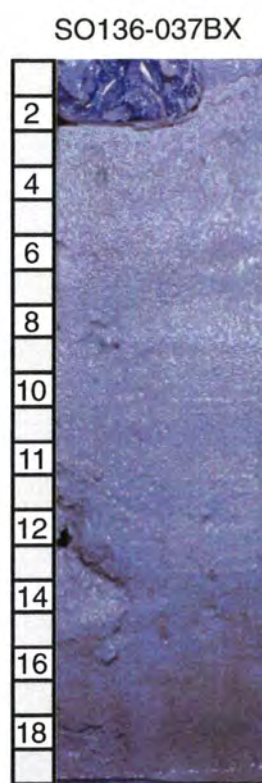
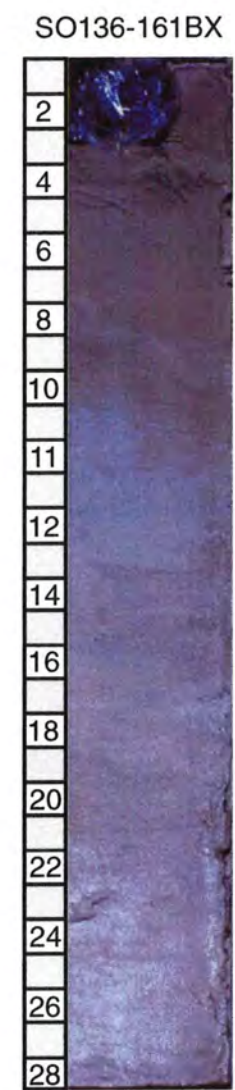
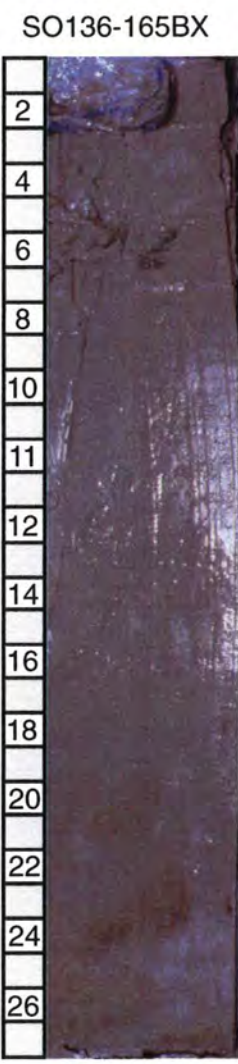


Photo A 7 The sampled boxcores. Core SO136-019BX is compounded of two photos

A8 VISUAL CORE DESCRIPTIONS

Table A 7.1 Visual core description of SO136-019BX

METRES		BIOIRRIGATION INTENSITY	PHYSICAL STRUCTURES ACCESSORIES ICHOFOSSILS FOSSILS	COLOUR	REMARKS
-0.1		Mn - Ø	Mn - Ø	It br GY	0 - 0.5 Sandy foram ooze with dark grains (Mn), single burrows Colour: 2.5Y 6/2 (light brownish gray)
-0.2		Ø Ø	Ø Ø	It GY	0.05 - 0.07 Sandy foram ooze with interbedded lenses of finer material and different colour (2.5Y 7/1: light gray).
-0.2		Ø Ø	Ø Ø	It br GY	0.07 - 0.10 Foram sand with high QZ-content Colour: 2.5Y 6/2 (light brownish gray).
-0.2		Ø Ø	Ø Ø	It ol BR	0.10 - 0.20 Sandy foram ooze, burrows filled with fine material, mottled Colour: 2.5Y 5/3 (light olive brown).
-0.2		Ø Ø	Ø Ø	pal YE	0.20 - 0.23 Fine sand, very Qz-rich, colour: 2.5Y 7/3 (pale yellow).
-0.2		Ø Ø	Ø Ø	gy BR	0.23 - 0.30 Sandy ooze, Qz-rich, mixed with dark grains (Mn). Colour: 2.5Y 5/2 (grayish brown).
-0.2		Ø Ø	Ø Ø	It ol BR	0.30 - 0.38 Fine sand, very qtz-rich, Colour: 2.5Y 5/4 (light olive brown).
0.38		Mn			

Table A 7.2 Visual core description of SO136-025-BX

METRES		BIOIRRIGATION INTENSITY	PHYSICAL STRUCTURES ACCESSORIES ICHOFOSSILS FOSSILS	COLOUR	REMARKS
-0.1		Ø Ø	Ø Ø	It GY	Forams look well preserved, without large-scale corrosion. 0.00-0.06 Silt - fine sand, well sorted. Foram sand (90% forams), low clay content, blackened forams Accessories: black clasts, volcanic glass (light brown), brown iron minerals, dropstones with manganese crust. Colour: 2.5Y 7/1 (light grey).
-0.12		Ø Ø	Ø Ø	It ye BR	0.06: Undulating erosional surface. 0.06 - 0.19: Fine silt, well sorted, with black streaks. Colour: 2.5Y 6/4 (light yellowish brown).

Table A 7.3 Visual core description of SO136-037-BX

METRES		BIOIRRIGATION INTENSITY	PHYSICAL STRUCTURES ACCESSORIES ICHOFOSSILS FOSSILS	COLOUR	REMARKS
-0.1		Ø Ø	Ø Ø	Vpl BR	0-0.07: Fine sandy foram ooze, strong bioturbation, colour: 10YR 8/2 (very pale brown). 0.07-0.12: Fine sandy foram ooze, darker patch (3cm, 10YR 7/2: light gray), colour: 10YR 8/1 (white), several burrows.
-0.19		Ø Ø	Ø Ø	WH	0.12-0.17: Fine sandy foram ooze, colour: 5Y 8/1 (white), big burrow (4cm) on boundary (12.5cm, 10YR 7/3: very pale brown), strongly bioturbated. 0.12-0.19: Fine sandy foram ooze, colour: 5Y 8/1 (white), dark patches and burrows with darker infill.

Table A 7.4 Visual core description of SO136-147-BX

METRES		BIOBURBATION INTENSITY	PHYSICAL STRUCTURES	ACCESSORIES	ICHNOFOSSILS	FOSSILS	COLOUR	REMARKS
0.1							WH pal YE	<p>0.00-0.02: Fine to very fine foram sand with silt fraction, colour: 2.5Y 8/1 (white).</p> <p>0.02-0.18: Well sorted (coarsening up) fine silty foram sand, colour 2.5Y 6/2 (pale yellow). Very fine sandy, angular black grains throughout entire box-core.</p> <p>0.08-0.15: Large burrow, colour: 2.5Y 7/1 (light gray).</p>

Table A 7.5 Visual core description of SO136-161BX

METRES		BIOBURBATION INTENSITY	PHYSICAL STRUCTURES	ACCESSORIES	ICHNOFOSSILS	FOSSILS	COLOUR	REMARKS
0.1							vpl BR il GY	<p>0.00-0.005: Fine to very fine foram sand, colour: 10YR 8/2 (very pale brown).</p> <p>0.005-0.34: Coarse silty foram ooze with some angular black grains.</p> <p>Colours: 0.005-0.055: 10 YR 8/3 (very pale brown).</p> <p>0.055-0.255: 10YR 7/2 (light gray).</p> <p>0.095-0.255: Mixture of all core colours due to heavy bioturbation.</p> <p>0.255-0.34: 10YR 6/2 (light brownish gray).</p>
0.2							il GY vpl BR lt br GY	

Table 3.7 Visual core description of SO136-165-BX

METRES		BIOBURBATION INTENSITY	PHYSICAL STRUCTURES	ACCESSORIES	ICHNOFOSSILS	FOSSILS	COLOUR	REMARKS
0.1							pal YE	<p>0.00-0.03: Present-day layer (fluff).</p> <p>0.03-0.46: Foram ooze with varying % of forams.</p> <p>Fining upwards cycle.</p> <p>All boundaries are bioturbated.</p> <p>0.00-0.16: Colour: 2.5Y 8/2 (pale yellow).</p>
0.2							lt ye BR	<p>0.16-0.24: Light yellowish brown (2.5Y 6/3) burrowed interval with large burrows. burrow infill is material from above and below (5G 8/1, light greenish gray).</p>
0.27							gy BR	<p>0.24-0.30: Grayish brown (2.5Y 5/2) layer with parallel bedded burrows, some with clear halos. Dark brown layer intercalated (diagenesis horizon).</p>